University of Newcastle upon Tyne

Department of Civil Engineering

AN INVESTIGATION INTO THE MECHANICAL CUTTING OF ROCK MATERIALS WITH PARTICULAR REFERENCE TO FRACTURE MECHANICS

BY

MASOUD CHERAGHI SEIFABAD (M.Sc.)

This thesis is submitted for the degree of

Doctor of Philosophy in the Faculty of Engineering

June, 1992

ACKNOWLEDGMENTS

I would like to express my appreciation to Dr E.K.S.Passaris, lecturer in Geotechnical Engineering, for providing the opportunity to carry out the research and in particular I wish to thank him for providing the appropriate academic environment in which I pursued effectively the specific concepts and ideas which were pertinent to the subject under investigation.

I would also like to express my appreciation to Mr M.E.Mckenna, chief technician, for his cheerful assistance and especially the preparation of specimens for the fracture tests.

I would like to thank Dr M.Jamalbastami, Mr A.Tountas, Mr N.Boussoulas and also Mr W.E.Short, J.T.Moore, L.Moore, F.Beadle for their contribution in parts of my work.

Furthermore, I wish to express my sincere appreciation to my family especially my wife and my daughter Yasamin, for their understanding, patience, assistance and also my brother Saeed who helped me at the initial steps at my work.

ABSTRACT

A comprehensive series of laboratory rock cutting tests were carried out on both core specimens and large blocks of different rock material. Five types of rock were used, Springwell sandstone, Matlock limestone, Welton chalk, Pennant sandstone and Teesdale Whinstone. As part of the investigations the influence of physical and mechanical properties of rock materials on their cuttability has been assessed during the early part of the research programme. Furthermore, a study was undertaken to investigate the influence of rock discontinuities on cutting parameters employing different degrees of saturation.

The Finite Element Method has been used to identify the optimum geometric configuration for rock cutting experiments. Furthermore, it was used to model rock cutting operations and was proven that it is possible to simulate the failure conditions existing in rock cutting experiments by using Finite Element analysis.

Rock fracture toughness as a rock property was found to have a good correlation with cutting parameters. ISRM suggested methods, short rod and three point test (Chevron Bend Test) were used in determining rock fracture toughness. In addition, rock fracture toughness was also compared with other characteristics of rock such as uniaxial compressive strength, tensile strength, shore hardness and NCB cone indenter index.

CONTENTS

Chapter 1

INTRODUCTION

There is a general increase in the level of underground mechanical excavation activities both in mining and civil engineering tunnelling projects. Furthermore, this trend indicates that such activities will increase considerably in the future.

Essentially there are two ways of excavating underground openings in rock, by conventional drill and blast methods or by mechanical excavation techniques. Mechanical excavation of rock during tunnelling is generally achieved by one of the two principal methods : a) by of selective cutting, as with roadheaders whose boom mounted cutting head is usually equipped with drag (cutter) picks or b) by of excavating the entire cross section, as with tunnel boring machines (TBM). TBMs and roadheaders have enjoyed wide popularity.

Excavation of rock by tunnelling machines has steadily increased in popularity as improvements in design have gradually extended the applicablity of such machines to cutting rocks of greater strength. This in turn has allowed successful tunnelling in geologically disturbed areas under difficult geotechnical conditions.

Roadheaders became significant during the 1940s in Europe, and important developments with boom cutting machines during the 1950s in the USSR led to the introduction of the Russian PK3 roadheader in U.K. in 1961.

Considerable attention has been focussed in recent years on increasing the capacity of roadheader type of machines in order to increase tunnelling rates and to excavate harder rocks. These developments resulted in an appreciable increase in the weight of such machines.

Roadheaders have played a major role in the drivages of roadways in coal mines and soft rocks in the UK , but when applied in stronger strata, with a uniaxial compressive strength (UCS) greater than 70 MPa, the limitations of earlier designs became apparent. Cutting in stronger strata resulted in excessive pick consumption, high maintenance costs and frequent breakdowns which often rendered the use of earlier machines uneconomic. The development of heavier duty roadheaders has greatly extended the range of rock conditions which could be excavated by this type of tunnelling machines.

The basic design of a roadheader is that of a boom, usually mounted on a tracked base, equipped with a revolving head where the cutting tools are fixed. Mucking of the excavated rock is achieved by gathering arms or by an encircling flight conveyor.

The excavated rock, normally piles against the tunnel face and is continuously picked up and forwarded by conveyance through the machine to the main rock debris disposal system.

The main design features of the roadheaders are those of flexibility in operation, the ability to cut a range of roadway/tunnel shapes and its manoeuvrability for cutting mine roadway junctions. The earlier lighter machines (of 25 tonnes or less) experienced limited success when cutting strong rock (more than 70 MPa UCS), with resulting machine vibrations causing damage to the picks and often to the machine itself.

The heavy duty types of roadheader (of around 90 tonnes or more) have resulted in substantially greater machine stiffness with corresponding improvements in structural and power transmission aspects. Wider bodied machines have been adapted in British mines for reasons of increased rigidity and greater consistency in application of the cutting tools to the rock face. Heavy duty machines have resulted in improved reliability in terms of decreased machine down time, coupled with the ability to economically cut stronger types.

McFeat-Smith (1982) has presented a comparison between three types of excavation, drill and blast, roadheader, and TBMs (Table 1.1). Muirhead (1984) indicated, as a very rough guide, that tunnels less than 2 km in length do not individually justify the use of a TBM.

The main difference between tunnelling machines and drill and blast techniques is the reliability of the latter. As a result where costs are about the same, the greater reliability of drill and blast in coping with difficult conditions is often the deciding factor in its favour. On the other hand, tunnelling machines are selected because they offer better progress and lower costs in reasonable tunnelling conditions. Since it is unlikely that any machine can cope with all possible ground conditions, the range of ground to be excavated and supported on any project must be clearly defined so that machine manufactures can design accordingly.

Table 1.1 Shift analysis, utilization and progress data for drill and blast, roadheader and TBM excavated tunnels (After McFeat-Smith, 1982)

Excavation method		Drill and blast		Roadheader				Full-face TBM			
Machine type		Pneumatic rotary percussion drills + rocker shovel		Light weight	Medium weight	Medium weight	Heavy weight	Single disc	Single disc	Triple disc	Triple disc
Rock type		Fresh granite	Weathered granite	Sandstone Mudstone	Soft sandstone	Siltstone	Hard sandstone	Mudstone	Sandstone	Limestone	Dolerite
Tunnel diameter, m (or equivalent)		5.7	5.7	4.4	4.4	4.4	4.4	3.5	3.5	3.5	3.5
Shift analysis	Non-essential stoppages, %	10.1	13.8	19.3	22.1	17.1	19.3	24.0	20.6	11.5	19.1
	Essential stoppages, %	6.6	5.2	9.1	17.1	13.9	12.0	12.7	20.0	23.2	23.9
	Support, %	–	20.0	20.6	2.2	12.6	15.3	17.7	6.9	1.0	0.1
	Mucking, %	44.5	32.9	8.8	12.0	–	–	9.6	17.5	8.2	9.0
	Utilization, %	38.8	28.1	42.2	46.6	56.4	53.4	36.0	35.0	56.1	47.9
	Cutting rate, m^3/h	13.8	18.5	11.0	23.2	15.5	13.0	28.0	36.0	13.5	5.8
Progress data	Weekly progress, m/120 h	25	24	37	85	69	55	126	158	95	35

The basic operations involved in the associated cutting process are to force the available cutting tools into the rock and to break out fragments of the rock surface. The available rock cutting tools comprise drag picks, disc cutters, roller cutters and button cutters. Drag picks are the most efficient and versatile cutting tools, basically in chisel and conical forms. These plough into the rock surface, and the rock fragments are formed in front of them. The drag bits are essentially used in coal and soft rocks, however, their applications in hard and abrasive rocks are limited due to the high wear rate of the drag picks.

The work described in this thesis refers to rock cutting experimental investigation using drag picks.

The aim of the research was to find out whether operational parameters in chisel pick (cutting speed, cutting depth, tool spacing), tool geometry (rake angle) and also rock conditions (presense of discontinuities) can affect rock cutting parameters (cutting forces, specific energy). Special attention was paid to rock under water saturated conditions. Furthermore an effort was made to correlate certain rock cutting parameters with the fracture toughness of the tested rocks.

In this work five types of rock were used, Matlock limestone, Teesdale Whinstone, Welton chalk, Springwell sandstone and Pennant sandstone.

The thesis is organized in two parts. Part 1, has nine chapters, and part 2 comprises a series of Appendices with the experimental results and details of some important cutting theories.

The review of previous relevant work in rock cutting is presented in chapter 2.

Chapter 3 deals with the design of the experimental work.

Chapter 4 presents details of the physical and mechanical properties of the tested rocks. This chapter gives experimental details and

results from the following tests : UCS, triaxial compressive strength, Shore scleroscope hardness, Shore plasticity, NCB cone indenter and CERCHAR abrasivity.

Chapter 5 deals with the methods and the experimental equipment for rock cutting and rock fracture tests. The finite element method was used here to investigate the optimum geometry for the clamping devices employed in the rock cutting experiments.

Chapter 6 consists of eight parts that deal with the effect of different conditions on rock cutting parameters. The conditions investigated were : discontinuities, different saturation conditions, subsurface damage, cutting speed, rake angle, wear, cutting depth and cutting tool spacing. Furthermore finite element analysis was used to simulate rock cutting experiments.

In chapter 7, the results of fracture mechanics tests according to the ISRM suggested methods (short rod, chevron bend) are presented.

Chapter 8 deals with the relationship between rock fracture and rock cutting parameters. Furthermore the results of boundary element analysis of fracture tests are also presented in this chapter.

Finally general conclusions and recommendations are given in chapter 9.

Chapter 2

PREVIOUS WORK IN ROCK CUTTING

The performance of drag bit cutting depends on two factors, the rock itself and the cutting parameters. The cutting parameters refer to the tool geometry, and tool speed and the rock characteristics refer amongst others to the presence of discontinuities and the moisture conditions.

Since the work in this thesis deals with the above topics, this chapter presents a review of the previous work on these topics.

2.1 Rock discontinuities

George (1975) has investigated the effect of discontinuities on cutting performance parameters using rock blocks 200 x 200 x 200 mm, with discontinuity spacings ranging between 30 mm and 80 mm. The results of his work has been shown that there is little difference in rock cutting parameters. Young and Fowell (1978) quantified the properties of rock mass to allow for more accurate prediction of tunnelling machine performance. From many rock mass characteristics, discontinuity intensity has been shown to be one of the major influences on the cutting and ripping performance of the machine. The relationship between excavation rate ($CR_{f)}$ and the average number of discontinuities per meter (λ) was investigated and was found to satisfy the relationship shown in Fig (2.1). The investigated rock formation was mudstone.

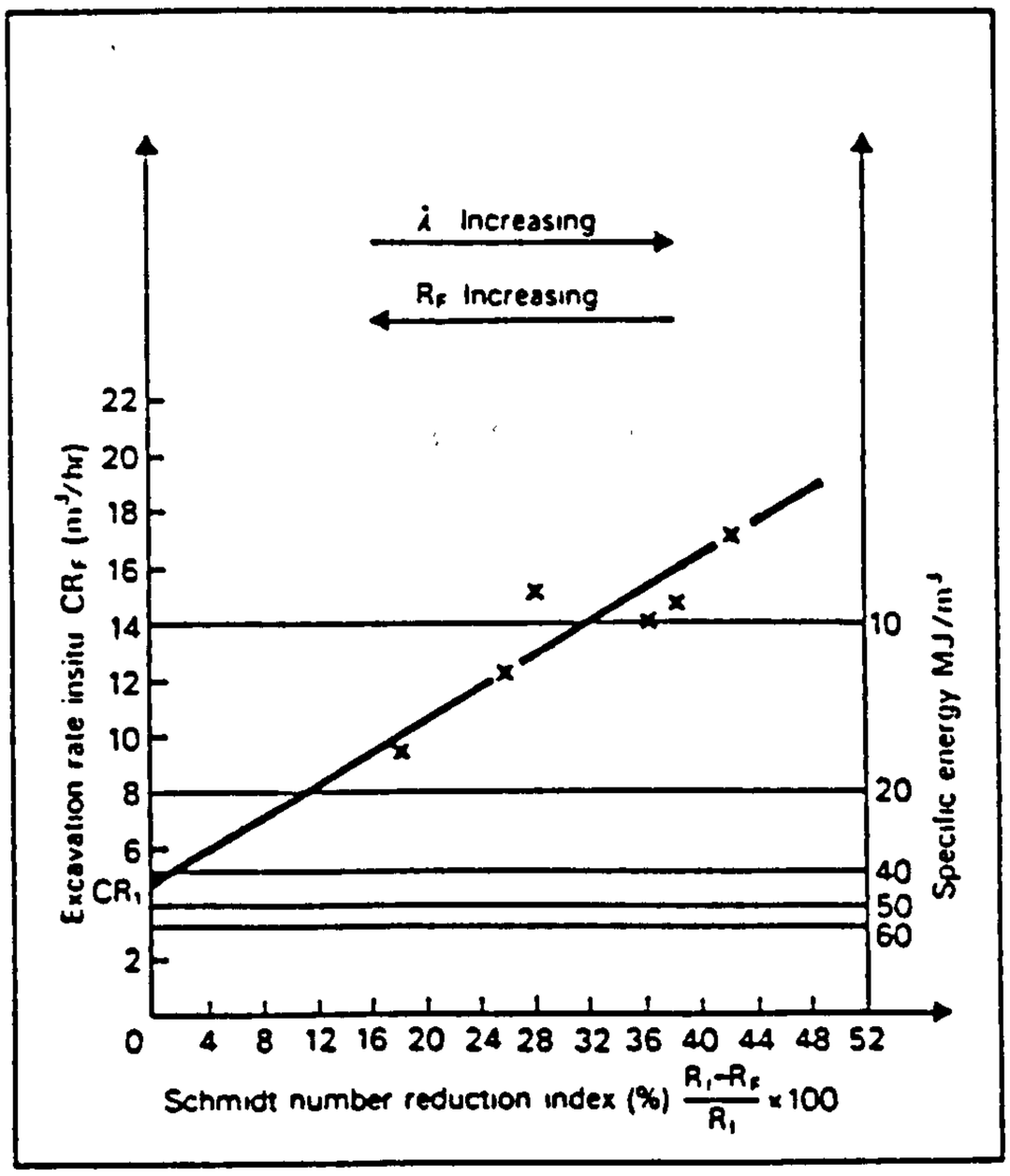

Fig 2.1 Relationship between excavation rate and the average number of discontinuities (after Young and Fowell, 1978)

Fowell and McFeat-Smith (1976) having recognised the important role played by rock mass properties in rock excavation mechanics, decided to seek one rapid and simple method of quantifying the presence of breaks in the rock mass under in situ conditions. They decided to use the break index which was defined as an average number of weakness planes intersecting horizontal and vertical scan lines per metre for each bed under consideration. Using this method they recorded the planes present on the face prior to the excavation including joints, bedding planes, fissures, and other significant planes of weakness present at the time of measurement. By combining the results from in situ, a wide range of break index values was obtained and plotted against two primary parameters of cutting performance;

namely, specific energy and cutting rate, so that the influence of break in strata on performance could be determined. Their results have shown that there was a rapid decrease in specific energy values with an increase in breakage from massive condition. Furthermore, the value of the specific energy was found depending on the cutting mode, undercutting being the most efficient and sumping the least efficient operation in the same rock material. The small changes of the break index from the massive condition resulted in a rapid increase in cutting rate (Figs 2.2, 2.3).

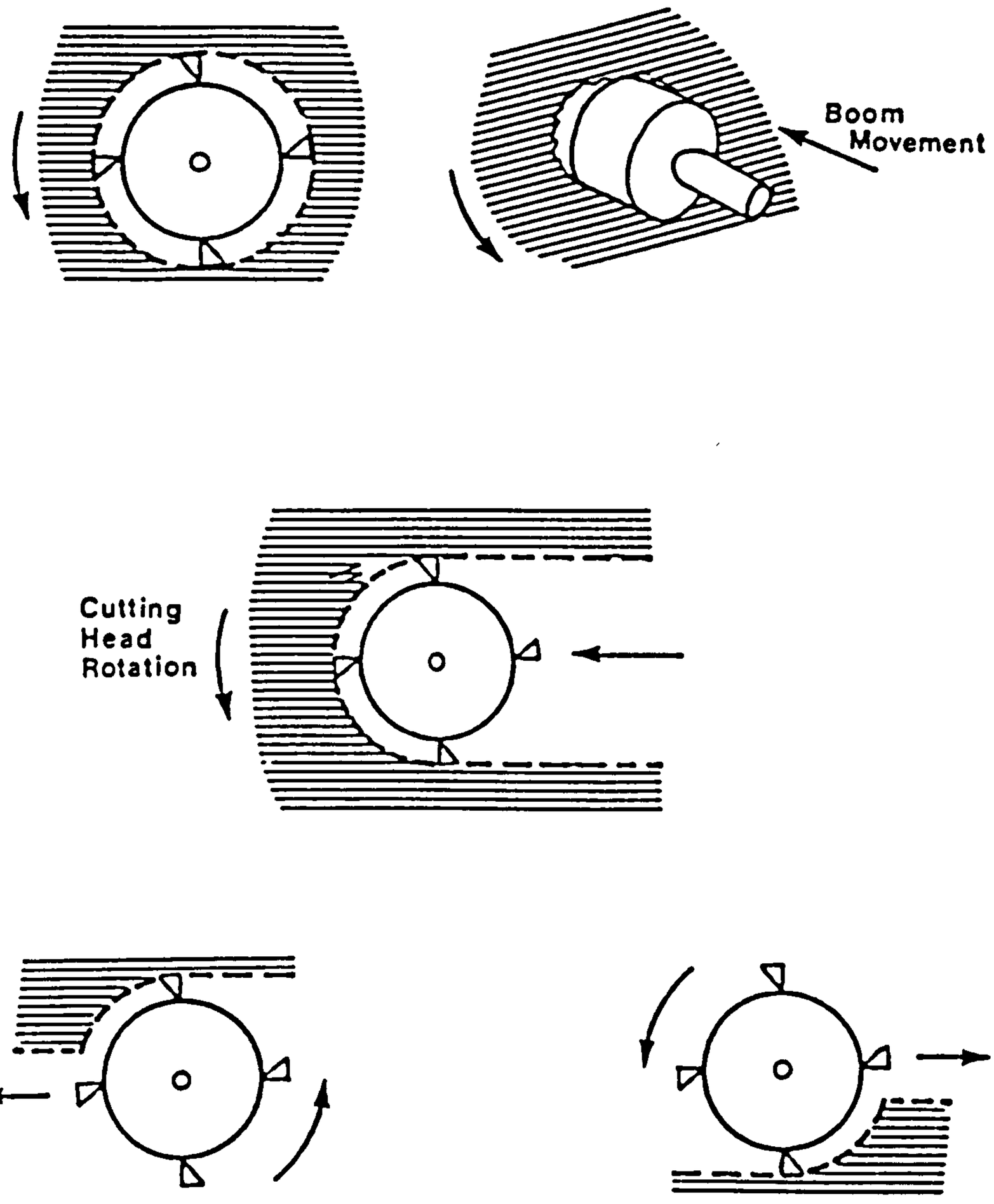

Fig 2.2 Upper:sumping; center:traversing; lower:undercutting (left), overcutting (right), after Fowell and McFeat-Smith (1976)

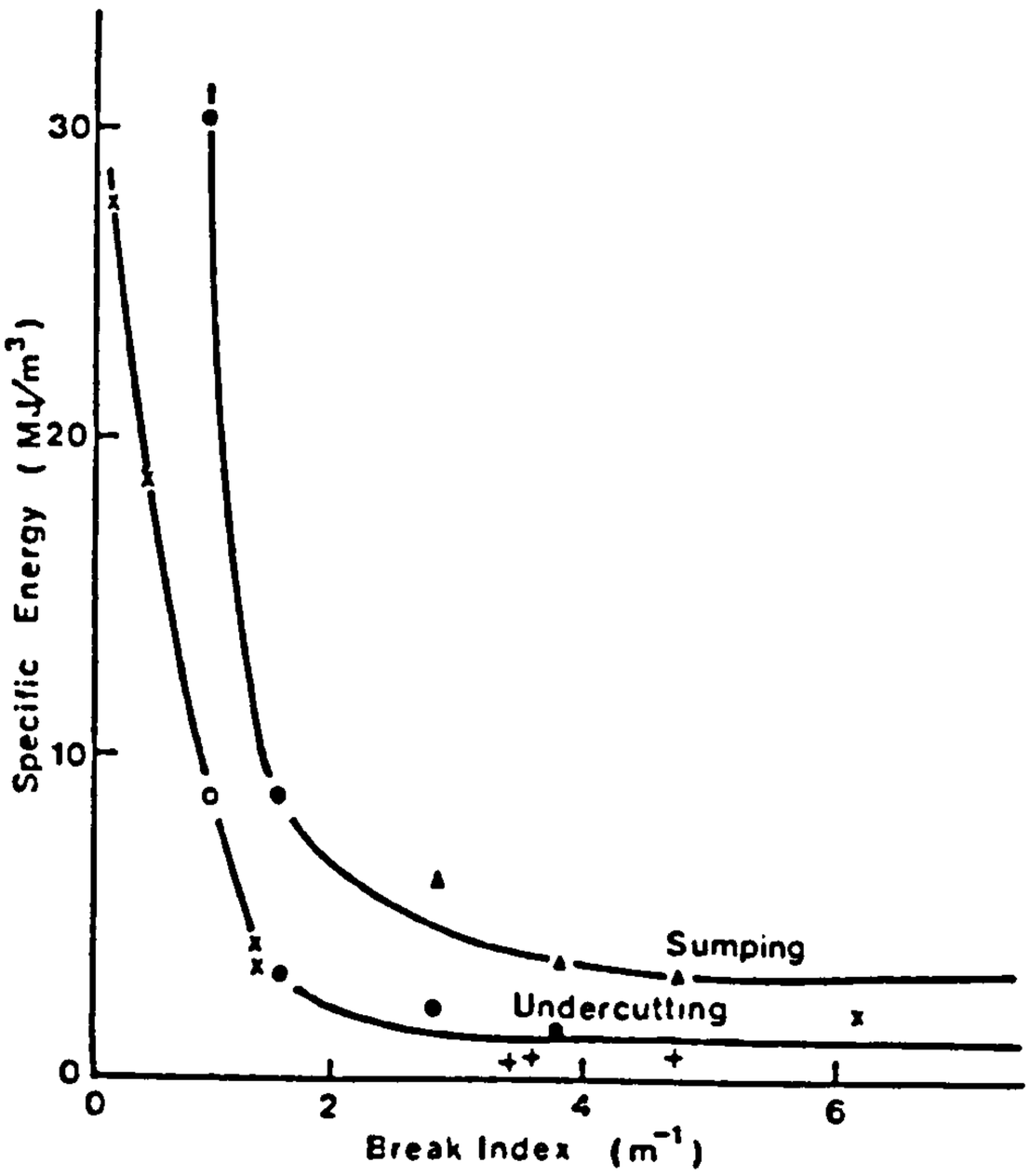

Fig 2.3 Influence of break index on specific energy in mudstone (after McFeat-Smith 1976)

Aleman (1983) has found for rock in a highly fractured state, that the influence of intact rock strength is of little consequence and hence only an assessment of rock structure is necessary. He introduced an index known as the 'A value':

A= microcracks/m+(100-RQD)

where RQD is the Rock Quality Designation (Goodman, 1989)

typical 'A values' are :

hard strata-'A value' <10

medium strata-'A value' 10 to 200

weak strata-'A value' >200

By classifying the strata according to the A value, instead of using the UCS prediction, the equation can be improved.

McFeat-Smith (1975) has investigated the effect of joints on rock cutting parameter, by using Bunter sandstone cores with different spacing, 50 mm, 75 mm, 100 mm, 150 mm. It was found that the specific energy of joint spacing of 50 mm is less than others. The tests were carried out with the discontinuities set at an angle of 90° (with respect to core axis). Jamalbastami (1990) used different angles for the orientation of discontinuities in his thesis (0°, 45°, 90°) and he found at 90° the efficiency of cutting parameters improved by 10% compared with 0° and 45°.

2.2 Moisture content

There appears, to be a reduction in tensile strength when the moisture content increases, and Vutukuri (1974) using ring tests (diametrical compression of a disc with a small central hole) with limestone material gave the following reasoning for the reduction in tensile strength.

The tensile strength is directly related to the $\sqrt{\sigma}$ where σ is the surface free energy of the material.

Since free surface energy of the saturated rock is a function of the properties of liquid (such as surface tension, dielectric constant), the liquid can influence the strength of the rock.

Obert and Duvall (1967) studied the effect of moisture on different types of rock and found that the effect is less pronounced. The effect of moisture content was investigated by Colback and Widd (1965), who identified a 50% reduction of UCS under saturated conditions for shale and sandstone. In general UCS decreases with increase in moisture content. Other researchers Broch (1979) and Vutukuri (1974), have shown rock is weaker under saturation conditions. Brook and Ojo (1990) have shown that moisture substantially reduces the UCS of rocks. Rock can be expected to exhibit lower strength during rainy periods than during snowy periods. Brook

and Ojo (1990) recommended to ISRM that the classification of rock strength should be based on minimum strength attained at maximum saturation. The only problem for this suggestion is that some rocks such as shale deteriorate in water. The other conclusion from their work is that oven drying of rock specimens leads to spuriously high strength values. Most rocks have different moisture contents ranging from less than 1% for evaporitic minerals to over 35% for porous sandstone.

Roxborough and Phillips (1975) carried out cutting tests in both 'dry' and 'wet' states using Bunter sandstone. All forces increased by 20% in wet conditions, which is contrary to results from strength tests. Later Roxborough (1990) hypothesized this to be due to pore water dissipating high localised stress concentrations. Rambanda (1984) carried out cutting test with nine materials in dry and wet conditions: four sandstones, chalk, marble, gypsum, and concrete.

Howarth et al (1986) made a TBM model to investigate the effect of moisture on the cuttability of rock on four types of sandstone and two types of marble. The model had an overall diameter of 106 mm and was fitted with six tungsten carbide tipped square faced drag bits of dimensions 9.5 x 9.5 mm and a spacing between adjacent cutters of 7.5 mm. They found that when UCS decreases as a result of increased moisture content, the penetration rate was more. It was suggested that porosity (pores, voids) is likely to assist the formation of fracture paths and this phenomenon is likely to assist the breakdown of the structure and hence production rates.

McFeat-Smith (1975) studied the effect of moisture on cuttability of Bunter sandstone and found that there is a reduction in specific energy and cutting forces, from the dry to the saturated state.

Cutting speed

There is great interest in the effect of cutting speed on tool forces. The importance of speed is connected with wear, since at high speeds temperature will increase , thus causing an increase in the rate of wear of the cutting tool. Because the hardness of the tungsten carbide chip decreases noticeably as the temperature increases, the higher the tool velocity, the shorter will be the tool life. The effect of tool velocity in rock cutting is most important in this respect. Kenny and Johnson (1976) found that the tool wear did not increase until a critical speed was reached. Nishimatsu (1979) has indicated that crack velocity is 100 times greater than the tool velocity, therefore it may be concluded that the tool velocity does not give any substantial effect on the cutting force, since the tool velocity could not have any relevant effect on the crack velocity. O'Dogherty (1963) found that cutting speeds between 1-3 m/s do not affect mean cutting forces in coal. Roxborough (1973) showed for anhydrite, that tool forces do not change significantly when cutting speed varies between 0.15 to 0.57 m/s. Later using Bunter sandstone, Roxborough and Phillips (1975) found similar results, and indicated that in non-abrasive rocks, cutting speed within the range of 0-5 m/s has no influence on tool performance.

Hood (1983) employed a series of high speed films to photograph cutting operations using a special rotating camera, with a film speed of 1000 frames per second. From the films the crack propagation was found to be of the order of 80 m/s. Evenden and Edwards (1985) reported that cutting speed had no measurable effect on the mean cutting force, and using high speed films the velocity of crack propagation in Barnsley Hards was estimated to be in excess of 500 m/s. Fowell and Johnson (1984) have also shown that cutting speed has no influence on cutting forces. In hard rock

cutting ,Demou et al (1983) indicated that tool forces did not change significantly relative to cutting speed, Fig (2.4).

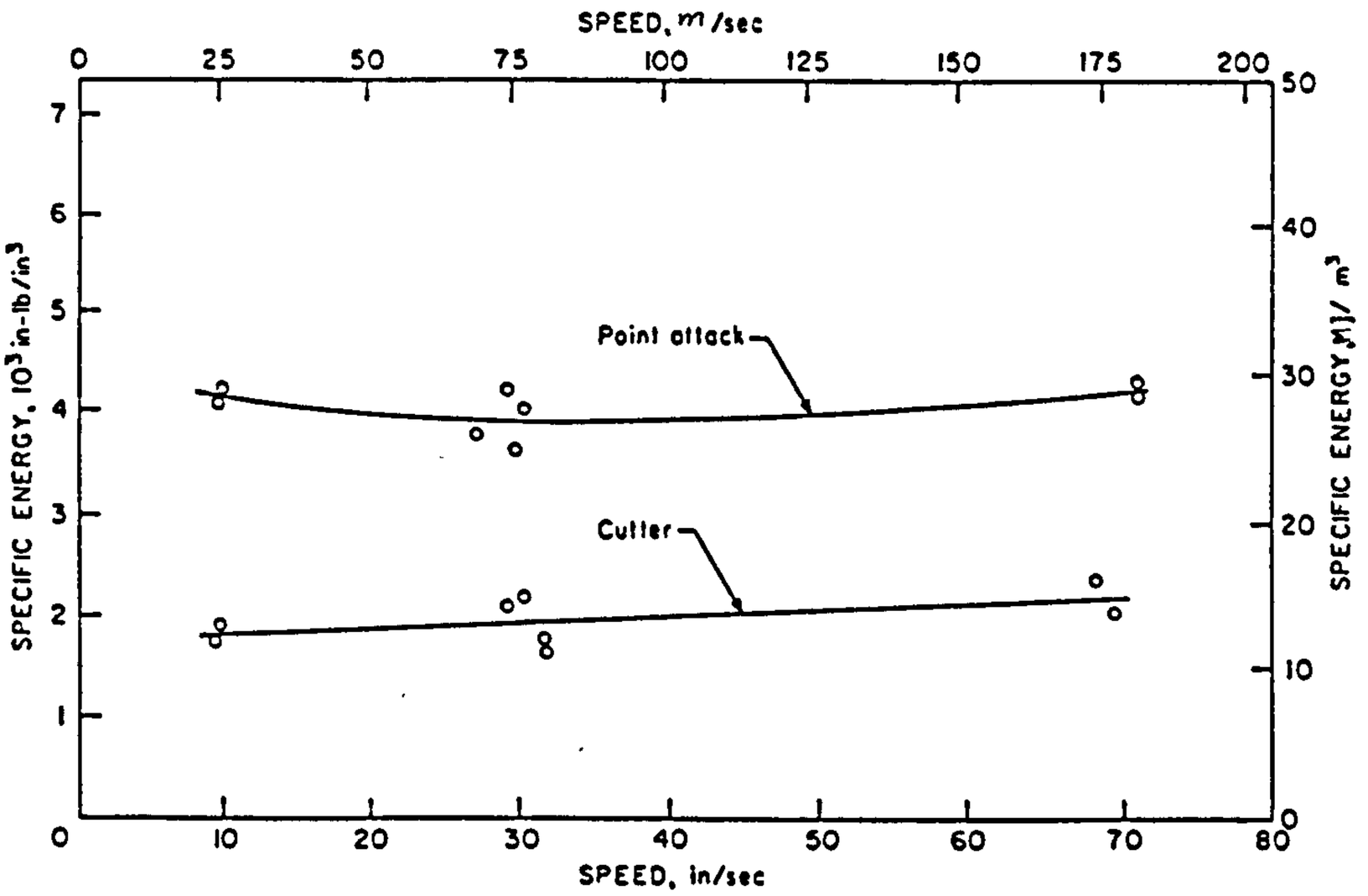

Fig 2.4 Specific Energy v Cutting speed (after Demou et al, 1983)

Ip (1986) investigated Dumfries sandstone, Grindleford sandstone, Penrith sandstone, and Middleton limestone with cutting speeds from 0.27 m/s to 1.10 m/s. Because at high speeds wear increases, care was taken to use cutting tools which have been subjected to the same wear. For Dumfries sandstone and Middleton limestone there was no change but in the case of Grindleford and Penrith sandstones normal force increased and this may be attributed to the quartz content of the various mineral components.

2.4 Cutting tool spacing

The relative positions of the cutting picks is extremely important in the design of machines used for the mechanical cutting of rocks. If the picks are well positioned relative to one another, the machine stands a good chance of producing material in a desirable size range , with economic use of power and minimum production of fines. If the picks are badly positioned, an

excessive amount of power will be used and a super-abundance of fines produced. If the picks are positioned close together, then the attacked rock surface between the picks is certainly broken down, but such a configuration leads to more picks than necessary. Somewhere between the two extremes there is an optimum distance of separation at which the rock material between channels is simply broken. This is the regime of maximum efficiency in cutting, with economy in picks and used power. Evans (1972,1981) has indicated that the optimum spacing is 3-4 times the pick width, for picks of simple chisel shape. Roxborough (1973) has confirmed the same trend.

2.5 Rake angle of cutting tool

The effect of rake angle has been widely investigated by many researchers. Bilgin (1977) carried out a series of tests with different rake angles for limestone, graywacke, granite and anhydrite. Since specific energy and tool forces decrease with increasing rake angle, consideration should be given on the balance between rake angle and tool strength. Phillips (1975) has investigated the effect of rake angle on cutting parameters for Bunter sandstone. The observed trends supported the relationship between specific energy and rake angle.

2.6 Subsurface damage

Zuech et al (1983) carried out a series of single-cutter drag-bit tests on specimens of Tennessee marble and Westerly granite. In parallel with the experimental studies, finite element analyses of the cutting process were implemented. A worn cutter configuration was specified in the analyses, using a rake angle of -20°. Two meshes were used, one in which the rock surface was flat (see Fig 2.5), and were where the presence of a groove was

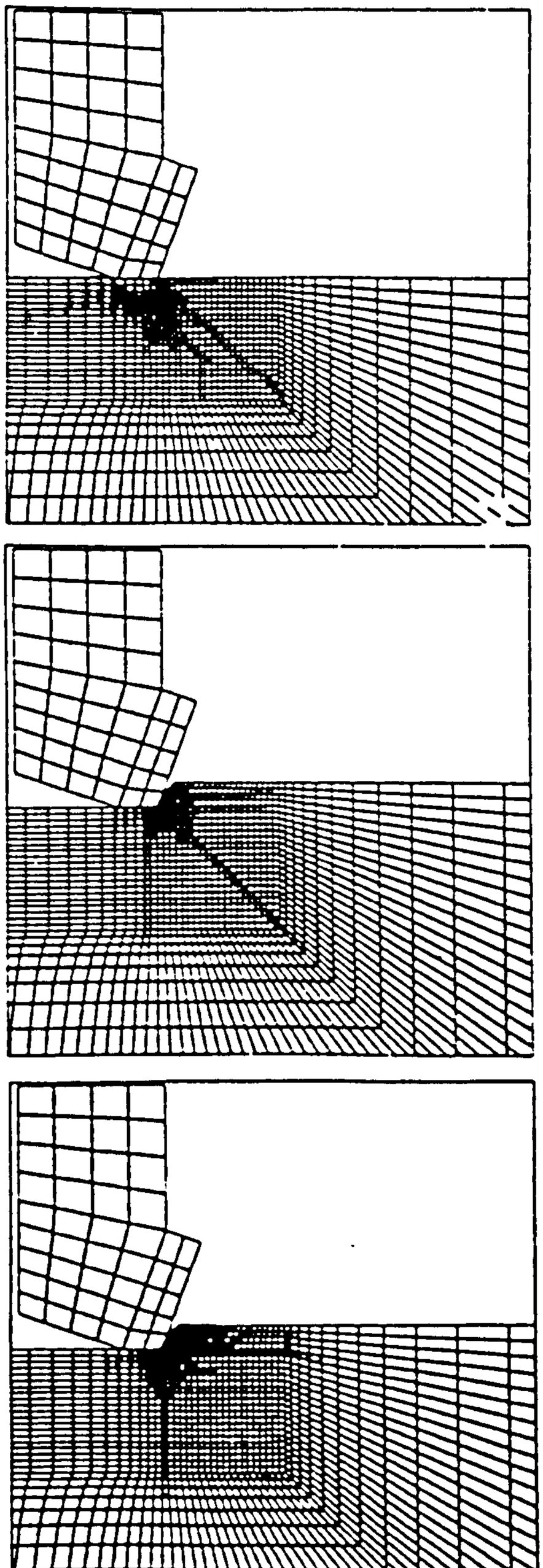

Figs 2.5, 2.6, 2.7 Process of subsurface damage (after Zuech et al 1983)

excessive amount of power will be used and a super- was displaced 0.05 mm downward (Fig 2.6). The downward displacement is sufficient to cause fracturing and chip formation ahead of the cutter and considerable damage under the cutter. Figs 2.6 and 2.7 show the calculated fracture patterns for Berea sandstone and Tennessee marble from which three observations can be made. First, the fractures extend ahead of the cutter in a manner that would be expected to form a rather flat chip. Second, there is a tensile fracture dipping at approximately 45° in the direction of cutter displacement. And third, there is considerable damage locally under the cutter. Preliminary tests indicate that the presence of subsurface damage produced by prior cuts has little influence on the strength of the rock.

Hekimoglu (1984) studied trimmed surface areas, and found that the forces varied with s/d (s=spacing between tools, d=depth of cut) in such a manner that they first increased gradually and then levelled out.

2.7 Rock Cutting under uniaxial compressive Loading

Dunn (1977) used blocks of Bunter sandstone and Lower chalk and applied a uniaxial compressive stress perpendicular to the direction of the cutting tool. The maximum applied stress was approximately 20 MPa. He used the following configuration :

Rock type	Applied stress (MPa)	depth of cut (mm)
Bunter sandstone	0, 9.84, 19.68	3, 6, 9
Lower chalk	0, 5	3, 6, 9

He found there was no change in rock cutting parameters (cutting forces, specific energy).

2.8 Specific energy

Taele (1965) suggested that specific energy (SE) is the basic factor which relates to the mechanical properties of rock. Because UCS and SE are both functions of rock strength, it was thought there must be some kind of relationship between them. Aleman (1981) has shown that the UCS is not a reliable indicator, instead he proposed an in-situ strength index that could offer an accurate indication of the cutting performance of the machine.

Farmer (1986) has considered the limitation of UCS by examining two types of rock: limestone and phyllite shale. Limestone has a medium UCS (σ_{cf1}) and high modulus of elasticity, shale has a low UCS (σ_{cf2}) , and a low modulus. In terms of energy required to fracture the rock they have equal resistance (Fig 2.8 illustrates stress-strain curve).

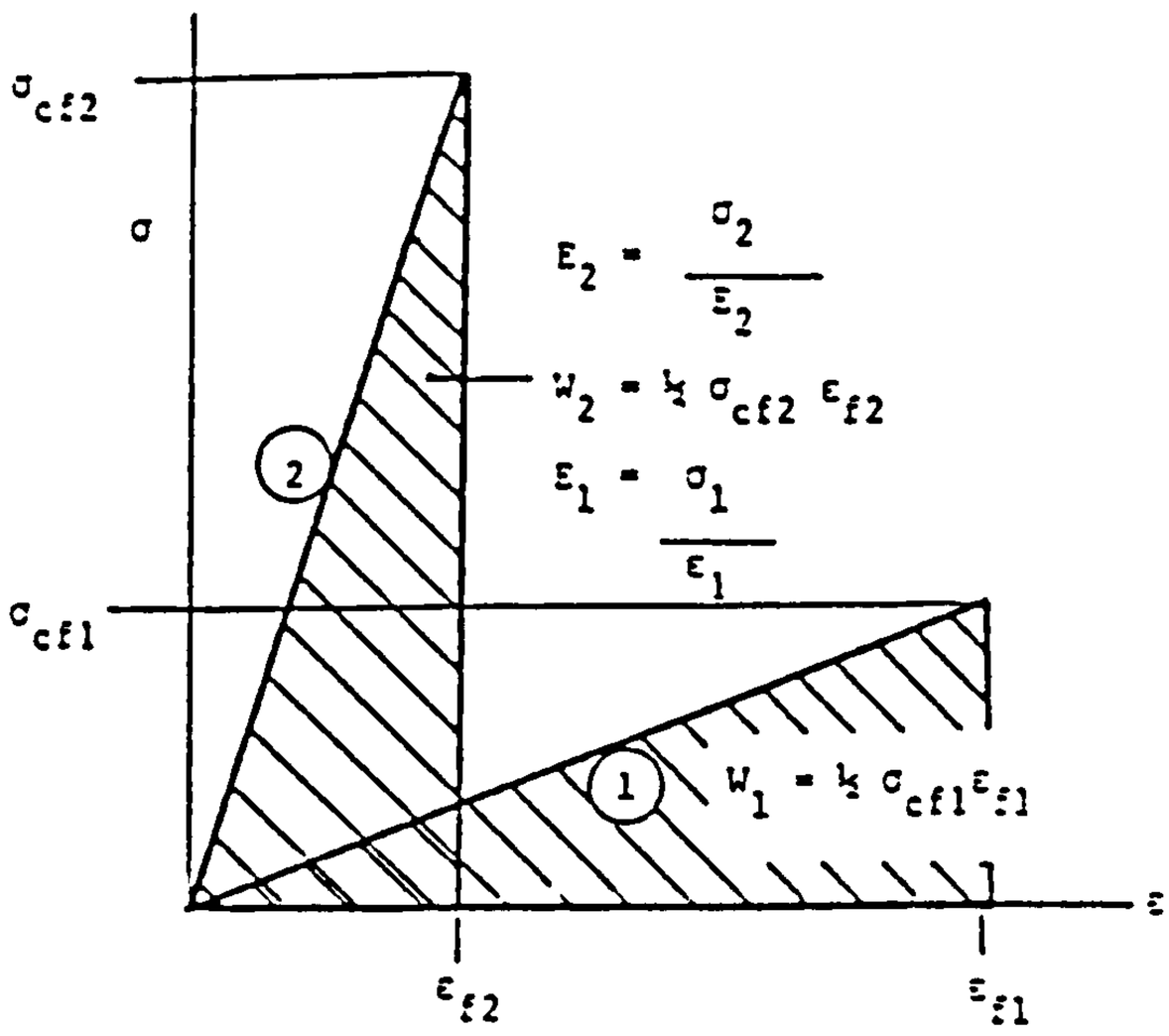

Fig 2.8 Rocks requiring similar strain energy to induce fracture (after Farmer, 1986)

2.9 Prediction of tunnelling machine performance

Fowell and Johnson (1984) have shown that statistical, rather empirical, procedures using rock material, rock mass and machine parameters are more useful in predicting tunnelling machine performance .

For the heavyweight class of boom tunnelling machines, Fowell and Johnson (1982) have indicated that a relationship exists between the Rock Mass Rating (RMR) geomechanics classification and cutting rates (Fig 2.9).

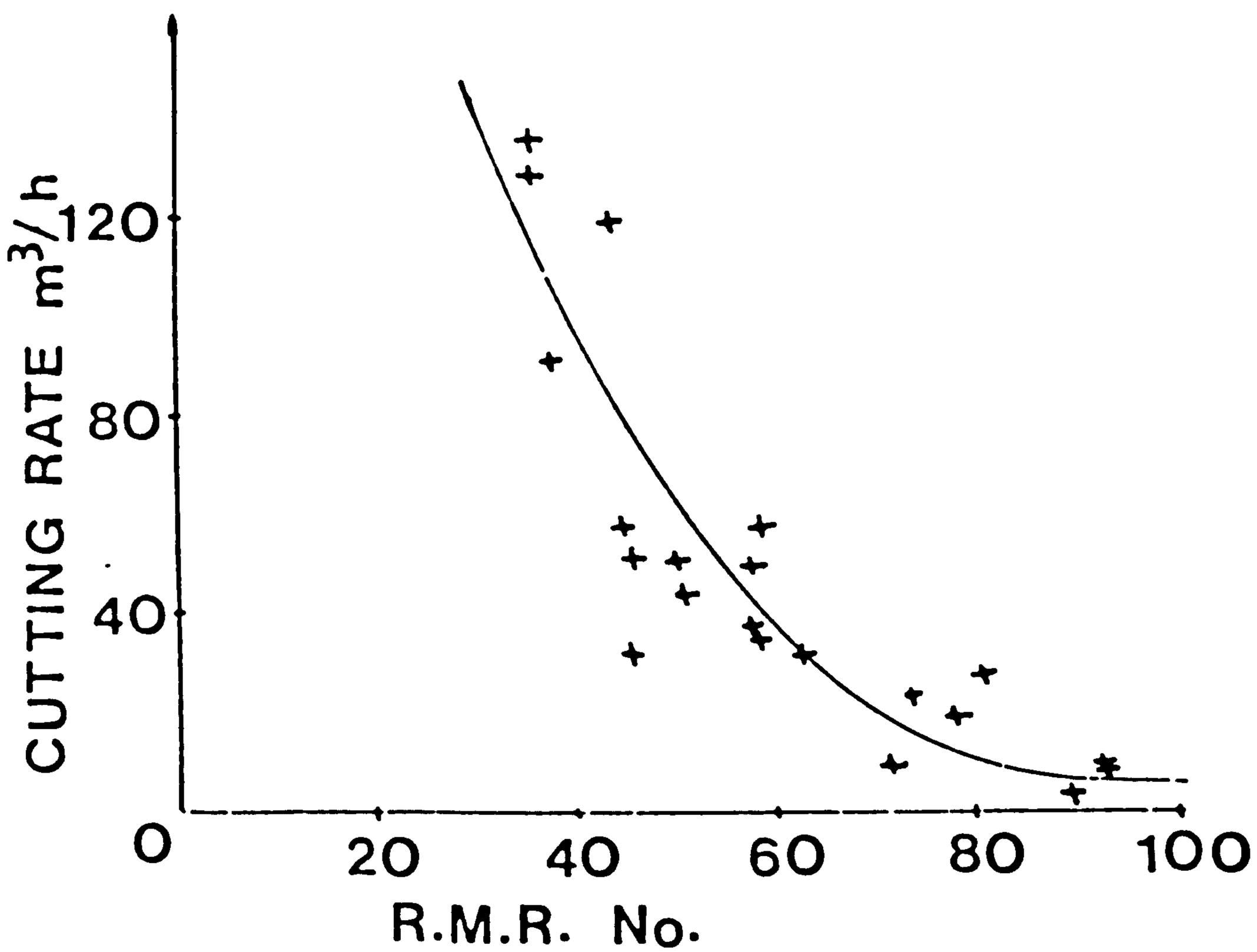

Fig 2.9 Cutting rate v RMR (after Fowell and Johnson, 1982)

Sandback (1985) has demonstrated that a good relationship exists between geomechanical rock classification system of rock mass (RMR) and roadheader performance. Farmer (1986) has shown that the rock toughness ινδεξ, defined as σ_c^2/E (σ_c=UCS, E=Young's modulus) can be a useful tool to predict roadheader performance (Fig 2.10). He used σ_c^2/E, cone indenter hardness, natural discontinuities frequency, and face structure as a base for the prediction of machine performance. The same data used by Farmer (1986) may be presented in a more conventional way by weighting the factors according to the degree to which they influence operations. By summing the weightings for particular face conditions a useful insight into potential operation performance can be gained. A sum of 10 or above indicates that partial face machines are very well suited to these rocks. Consequently, good excavation rates and low pick wear may be expected. Values between 5 and 10 indicate generally satisfactory operation and drivage rates. Pick wear and energy requirements may be significant in some circumstances.

Fig 2.10 Toughness index v Volume excavation rate (after Farmer, 1986)

2.10 Fracture mechanics related to rock cutting

Nelson et al (1985) have shown a good relationship between critical energy release rate and field penetration index (field penetration index, is the ratio of the average net thrust per cutter to the penetration per cutterhead revolution, used normally for evaluating TBM performance). Guo et al (1988) have investigated the mode of fracture in a drag bit by using strain energy release rate . It was shown that a sharp bit is able to provide much more strain energy for crack development than a blunt bit. Deliac (1988) suggested two fundamental chipping modes called mode A and mode B. Mode A is typical of shear fracture of the rock, while Mode B is a fracture propagation mode. Mode A is predominant when the pick is wide, the rock is not very brittle, or when the depth of cut is high. Mode B is predominant when the pick is sharp and when the rock is brittle.

To measure fracture toughness Deliac (1986) used the double torsion test, short rod and three point bend test, unfortunately these tests do not comply with the ISRM suggested methods for fracture testing.

2.11 Rock fracture toughness as a parameter for prediction of cutting performance

Rock cutting machinery requires capital investment, especially for large scale machines such as a roadheader. Production is highly depended on performance and stability of the system. It is therefore very important to determine the most suitable cutting machine, and to assess the performance of the machine for particular rocks. An excavating process is influenced by many factors such as rock properties, machine operating parameter, i.e. thrust, torque, RPM etc. As a result, prediction or assessment

of cutting performance of a rock cutting machine should be based on these factors.

In the search for a suitable measure of rock properties to assess rock cutting performance of rock cutting, many parameters have been proposed, of which the UCS has been the most widely used

The SE (specific energy) is proposed by Teale (1965) as a parameter for measuring the relative efficiency of various cutting tools, machines and cutting processes in a given rock. It has also been used by many investigators to assess the relative resistance of various rocks to a given tool or machine. A number of indentation probes have also been proposed, which normally involve an indenter, with some kind of configuration, being forced into the surface of the rock. A typical example of such a device is the NCB cone indenter (the NCB cone indenter, 1977).

Rock cutting with drag bits, is characterized by the penetration of the cutting tool into the rock, which results in crushing the rock around the tool. As the penetration continues, cracks are developing and propagation of such cracks result in rock fragments, which are removed by further movement of the cutting tool. This fracture mechanism suggests that rock cutting performance should be related to rock fracture properties, i.e, rock fracture toughness.

Cherepanov (1986) proposed a mode II fracture mechanism as being the typical mode for rock cutting action. By introducing N and T as the normal and cutting forces; respectively in the elastic stationary regime of cutting, the following equations were proposed (Fig 2.11):

$T=h\sigma_s hH\sin a$ $T=\mu N$

h=depth of cut H=sample thickness (normal to drawing)

σ_s=tensile strength of rock

a=angle of bending to the surface of the cutter

h,μ= coefficients depending on depth and shape of the cutter

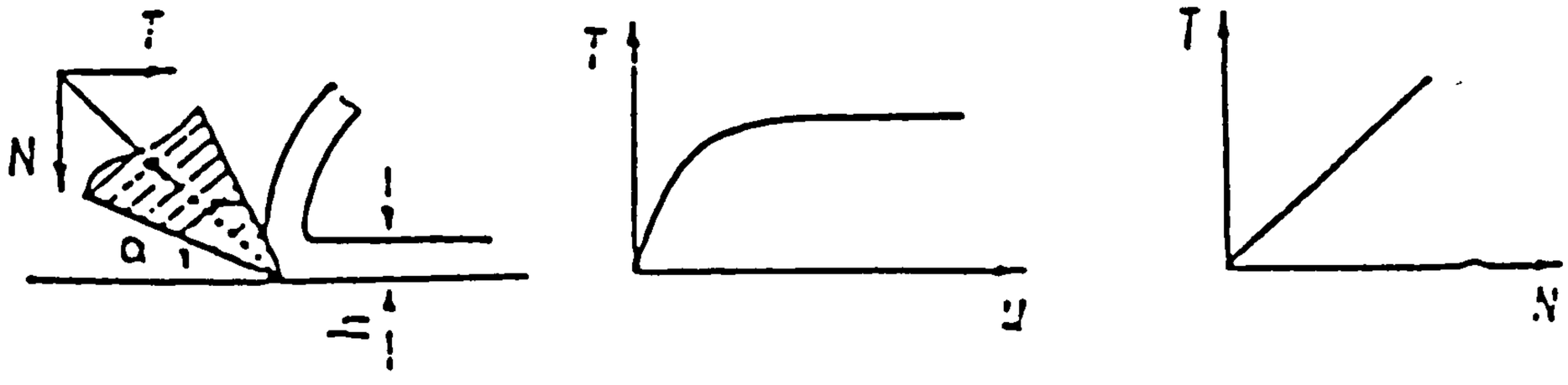

Fig 2.11 Rock cutting according to Cherapanov (1986)

Fig (2.12) shows a typical oscillograph of the cutting force against displacement, where one may observe the stick-slip movements of cutter. T_{max} and T_{min} are roughly proportional to the normal force applied to the cutter.

$$T_{max}=\mu_{max} N \quad ; \quad T_{min}=\mu_{min} N$$

In addition the sharpness of cutter can affect rock cutting forces.

The following formula are suggested for a brittle regime of cutting of rock in a state of plane-strain (stress intensity factor)

$$T_{max}=H K_{IIc} \sqrt{2h}$$

The mechanism of cutting is modelled by using a spring analogue. The cutter is considered as a point mass m, which moves along the rock surface

The mechanism of cutting is modelled by using a spring analogue. The cutter is considered as a point mass m, which moves along the rock surface and is pressed against it by force N. The rock sample is stable and the cutter is connected to a thick elastic body (a base), whose movement results in the movement of the cutter. Thus it is possible to calculate the maximum cutting force by using a relationship between Mode II fracture toughness and fracture energy.

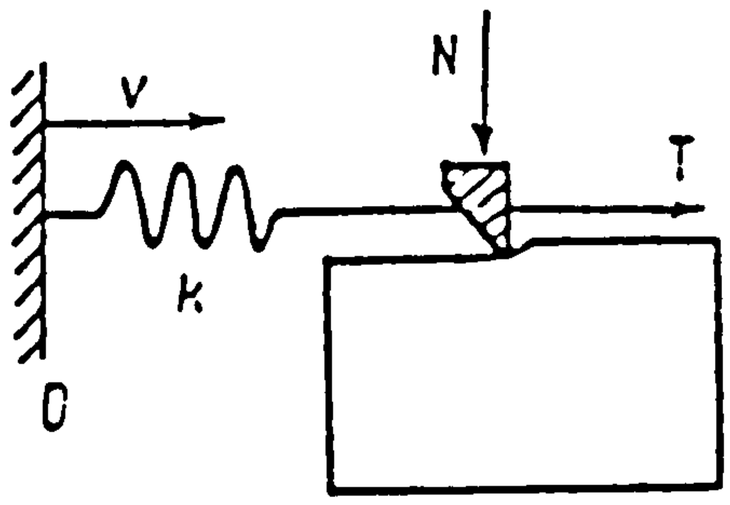

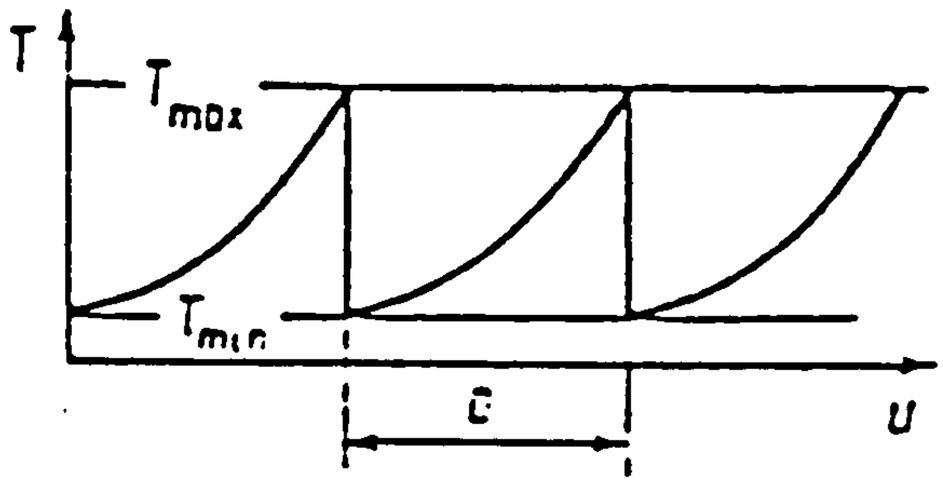

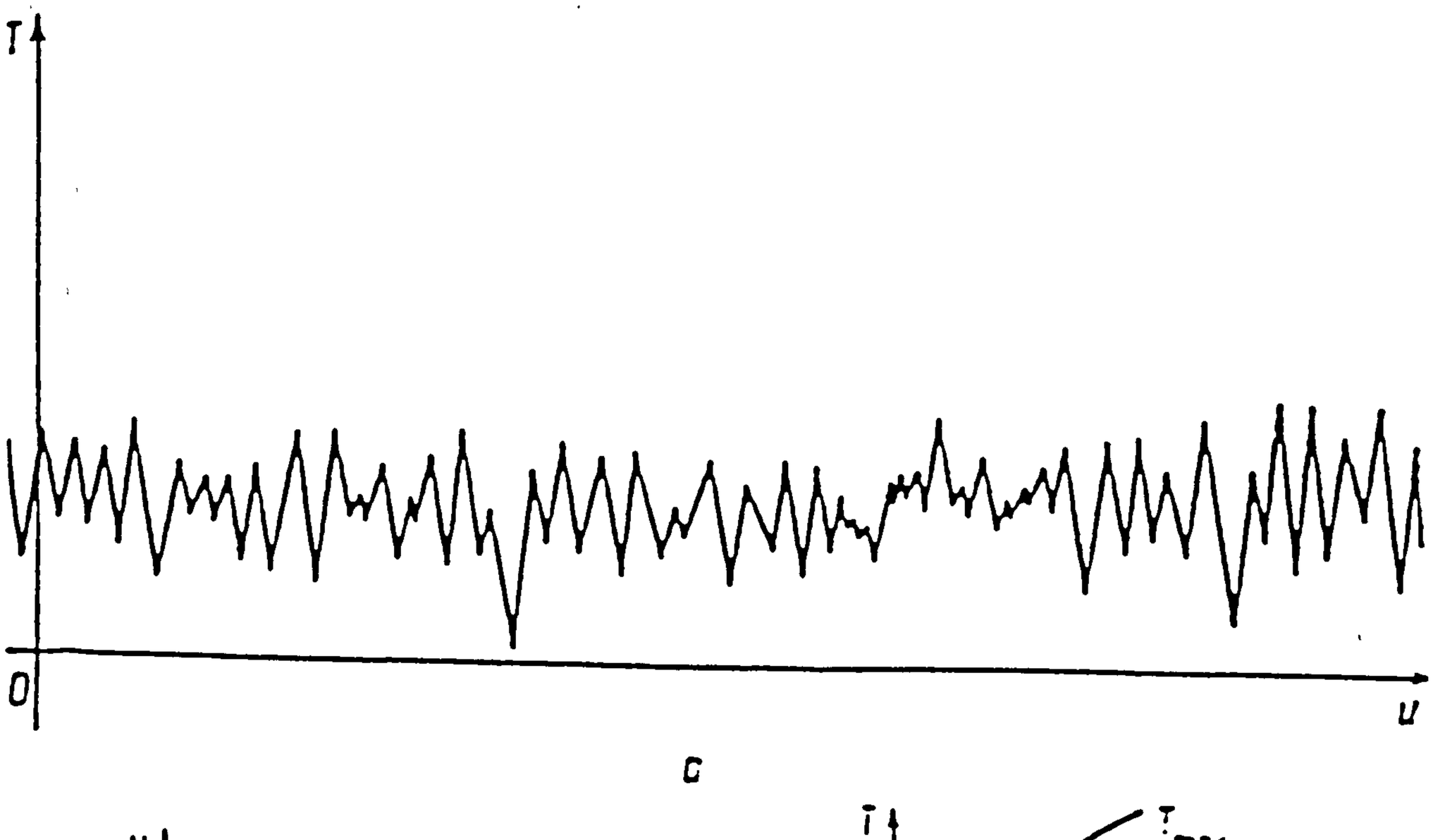

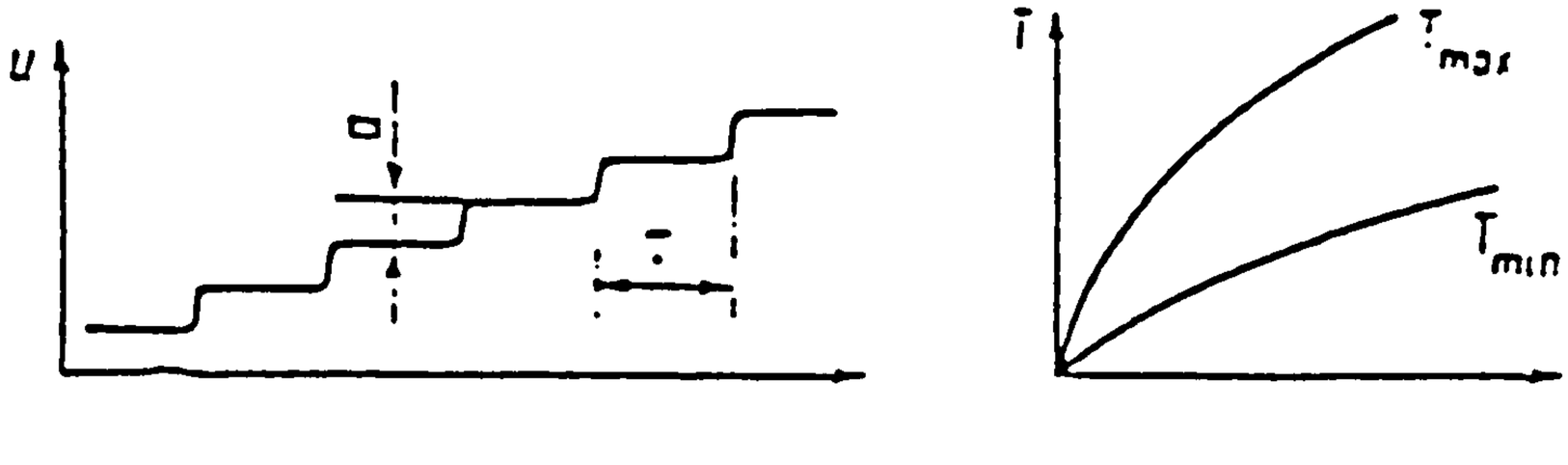

Fig 2.12 Typical oscillograph cutting force v Displacement (after Cherapanov, 1986)

$$K_{IIc}=\sqrt{E\Gamma_c}$$

this formula can be converted to : $\Gamma_c=\frac{K_{IIc}^2}{E}$

which is similar to the critical energy release rate in mode II in the state of plane stress.

It is shown from experimental results that fracture energy is a good estimation for rock cutting. However there are certain differences between the conditions referred to the work by Cherapanov (1986) and the situation characterizing the work described in this thesis : the type of bit is not tungsten carbide which normally is used in rock cutting : the thickness of sample is not usually important in rock cutting and only marble was used to develop this theory.

Chapter 3

DESIGN OF EXPERIMENTAL WORK

Rock parameters such as rock mass properties (discontinuities), environment (water) and intact properties, may influence machine performance. Therefore there is a need to investigate these parameters by means of specific investigations. Five different rocks (Teesdale Whinstone, Pennant sandstone, Springwell sandstone, Matlock limestone and Welton chalk) were chosen to investigate the relationship between rock properties and rock cutting parameters. The response of some of these rocks was influenced by the water (Springwell sandstone) while for others (Teesdale Whinstone) water content had very little influenced on their characteristics.

Discontinuities at different angles (15°, 30°, 45°, 60° relative to core axis) and different spacing (120 mm, 80 mm, 60 mm) may affect rock cutting parameters, for this reason their characteristics where investigated for different moisture contents.

Sometimes a discontinuity contains filling material, so the effect of chalk and clay filling on a Springwell sandstone specimen containing a discontinuity was also investigated.

Different rake angles may have different effects on rock cutting parameters. Consequently, rake angles of +16°, 0°,-10° were chosen to assess which angle is advantageous when cutting water saturated rock specimens.

Although cutting speed may affect rock cutting parameters, because of equipment limitations it was not possible to use relatively high speeds to investigate its influence on the rock cutting parameters. Consequently rock cutting parameters were investigated by using cutting speeds in the range of 0.100 m/s to 0.125 m/s.

To find out if the forces induced by drag bit affect the structure of the rock below the depth of the cut (subsurface damage), depths of cut of 4 mm, 6 mm and 8 mm were investigated using saturated rock specimens.

In addition different depths of cut (4 mm, 6 mm, 8 mm) in combination with different spacings were used to investigate their combined effect on the rock cutting parameters of saturated rock specimens.

Since, tool consumption may restrict the use of machines in certain types of rocks, the tool wear, was investigated using both ambient and saturated moisture content conditions.

Because under in situ conditions rock is subjected to stresses, there is a need to investigate rock cutting parameters while a static loading is applied to the rock specimens. Full details of the results are represented in Appendix 2.

The fracture mechanics approach appears to be a useful tool that may be used in correlating rock properties with rock cutting parameters. The test procedures used to determine the rock fracture toughness conformed with the ISRM (1989,1988) suggestions.

The experimental work was supplemented by using a 2D and 3D boundary element analysis.

To find out which geometry is suitable for the clamping device used in the cutting tests, a 2D finite element analysis was used.

In assessing the variations, trends and apparent relations between the investigated parameters there is a need to conduct an appropriate statistical analysis. For this reason it was decided to employ the statistical package Minitab which runs on IBM compatible personal computers. Chart 1 represents the plan for the experimental investigations carried out as part of the Ph.D research presented in this thesis.

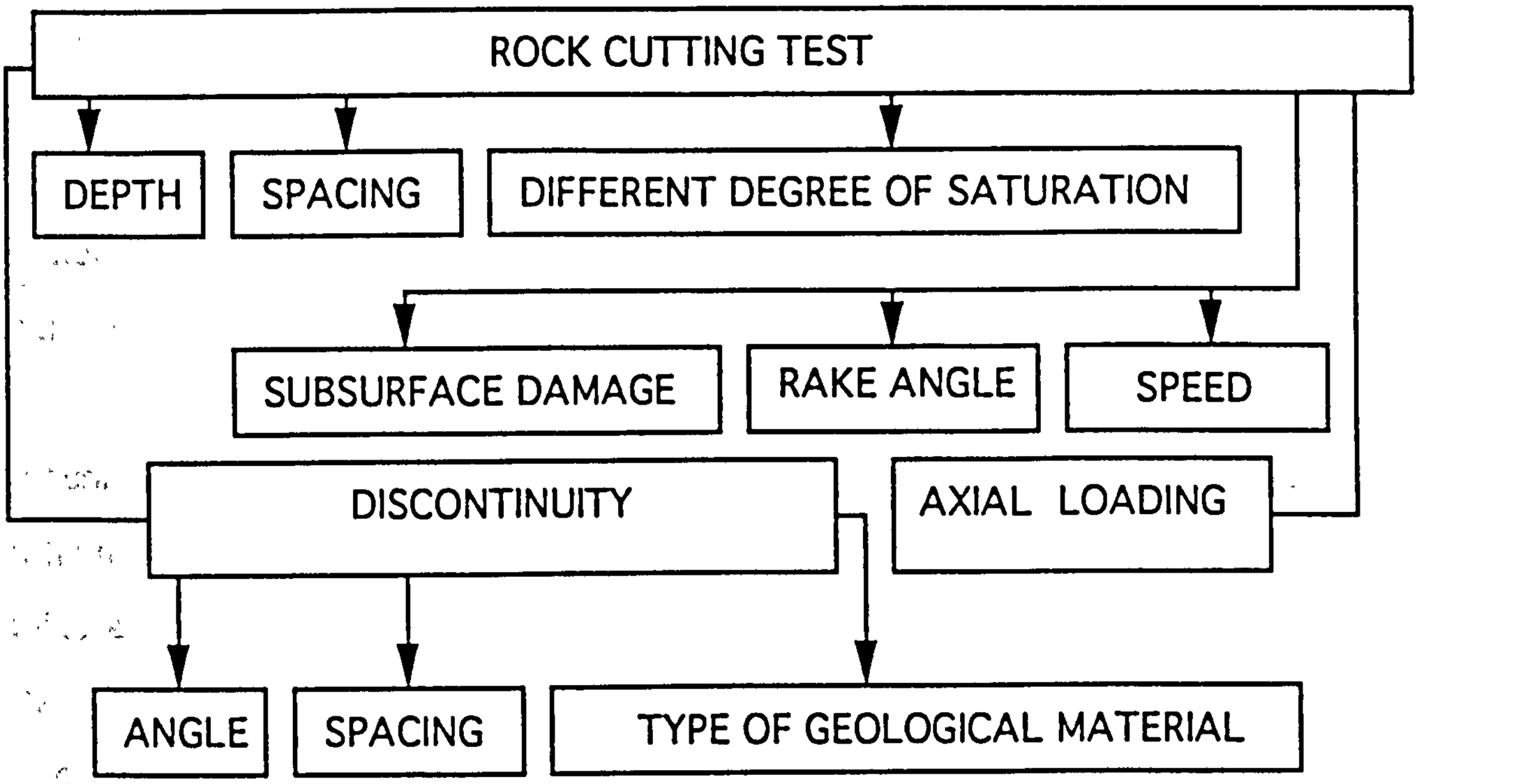

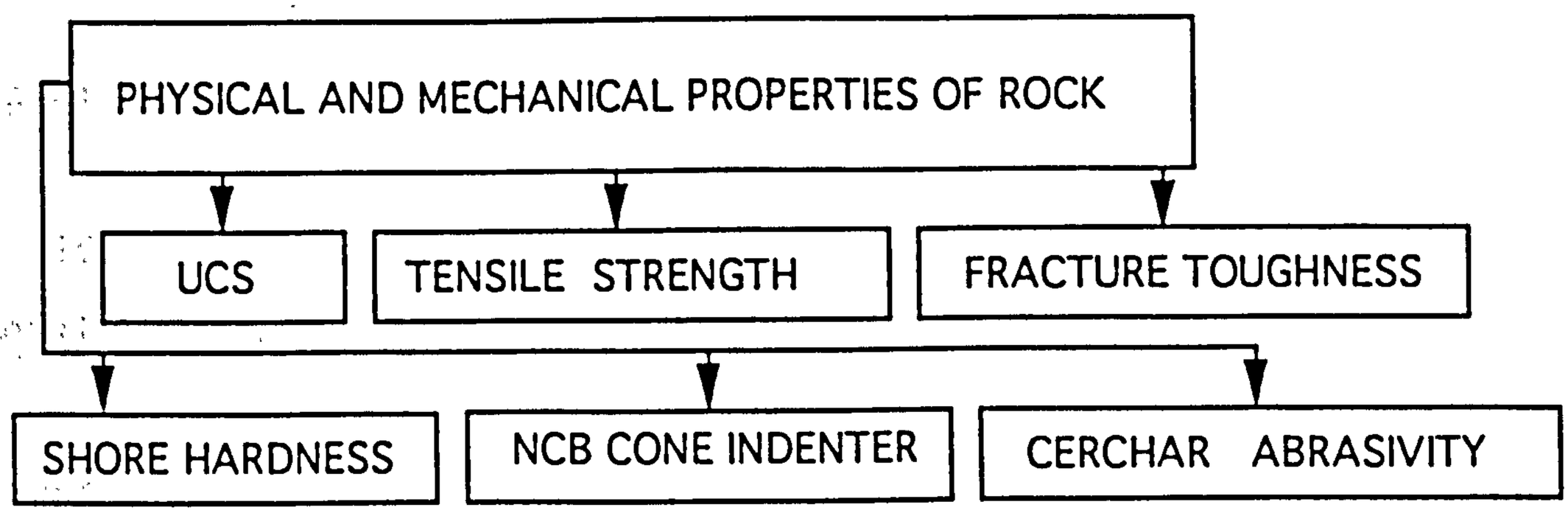

Chart 1 Experimental plan

Chapter 4

PHYSICAL AND MECHANICAL PROPERTIES OF TESTED ROCKS

There is a need not only to determine the rock properties of the materials used, but also to assess how these rock properties may affect rock cutting parameters (cutting forces, specific energy).

Laboratory investigations into the performance of tunnelling machines involves both rock cutting tests and the determination of rock material properties. On the other hand, it is equally essential to study the mineralogical structure of the rocks. Consequently for each type of rock, two thin sections were produced and studied under the microscope. The mineralogical composition, quartz content, grain size and shape and cement coefficient were determined.

Generally, the rock characterization tests may be divided into two classes:

1-Petrographical and physical properties such as bulk density, porosity and P-wave velocity

2-Mechanical characteristics such as : UCS , strength under triaxial compression, tensile strength, Shore scleroscope hardness, NCB cone indenter hardness and CERCHAR abrasivity

In many underground workings the rock contains water in the form of pore water and water dripping or flowing along joints and fractures. The presence of water in rock can affect its properties in many ways; in Bunter sandstone a reduction of 30% to 40% on tensile strength and a reduction of 17% on UCS have been identified by Roxborough and Phillips (1975). Therefore, for the tests reported here the laboratory testing was carried out on both dry and water saturated specimens. Rock samples were collected from the rock blocks used in the cutting tests, and subjected to

certain testing procedures following guide-lines prescribed in ISRM suggested methods (Brown, 1981).

4.1 Petrographical analysis and origin

4.1.1 Springwell sandstone

This sandstone is lightly yellow brown and is uniformly fine grained and well sorted with clay and micaeous (muscovite) partings. No particular bedding does occur but very thin laminations may be observed. Macroscopic examination of the blocks used did not show any discontinuities. Hydrochloric acid was also employed to identify calcite particles, but no reaction occured. The quartz grains are mainly monocrystaline and partly polycrystaline typified by a subrounded to subangular shape. The mineralogical composition is quartz 69%, clay minerals 17%, mica (muscovite) 1%, feldspars 0.5 % and badly squashed (mainly quartz) rock fragments about 5%, plus 7.5% voids. Cement coefficient is 7 (the quartz grains are cemented by a combination of clay matrix with precipitated quartz grains, Table 4.1).

Table 4.1 Cement coefficient (after McFeat-Smith, 1977)

1 Non cemented rocks or those having greater than 20 per cent voids.
2 Ferruginous cement.
3 Ferruginous and Clay cement.
4 Clay cement.
5 Clay and calcite cement.
6 Calcite (or Halite) cement.
7 Silt; Clay or Calcite with quartz overgrowths.
8 Silt with quartz overgrowths.
9 Quartz cement, quartz mozaic cements.
10 Quartz cement with less than 2 per cent voids.

The location of origin is Springwell village, SE of Gateshead, North East England (Plate 4.1).

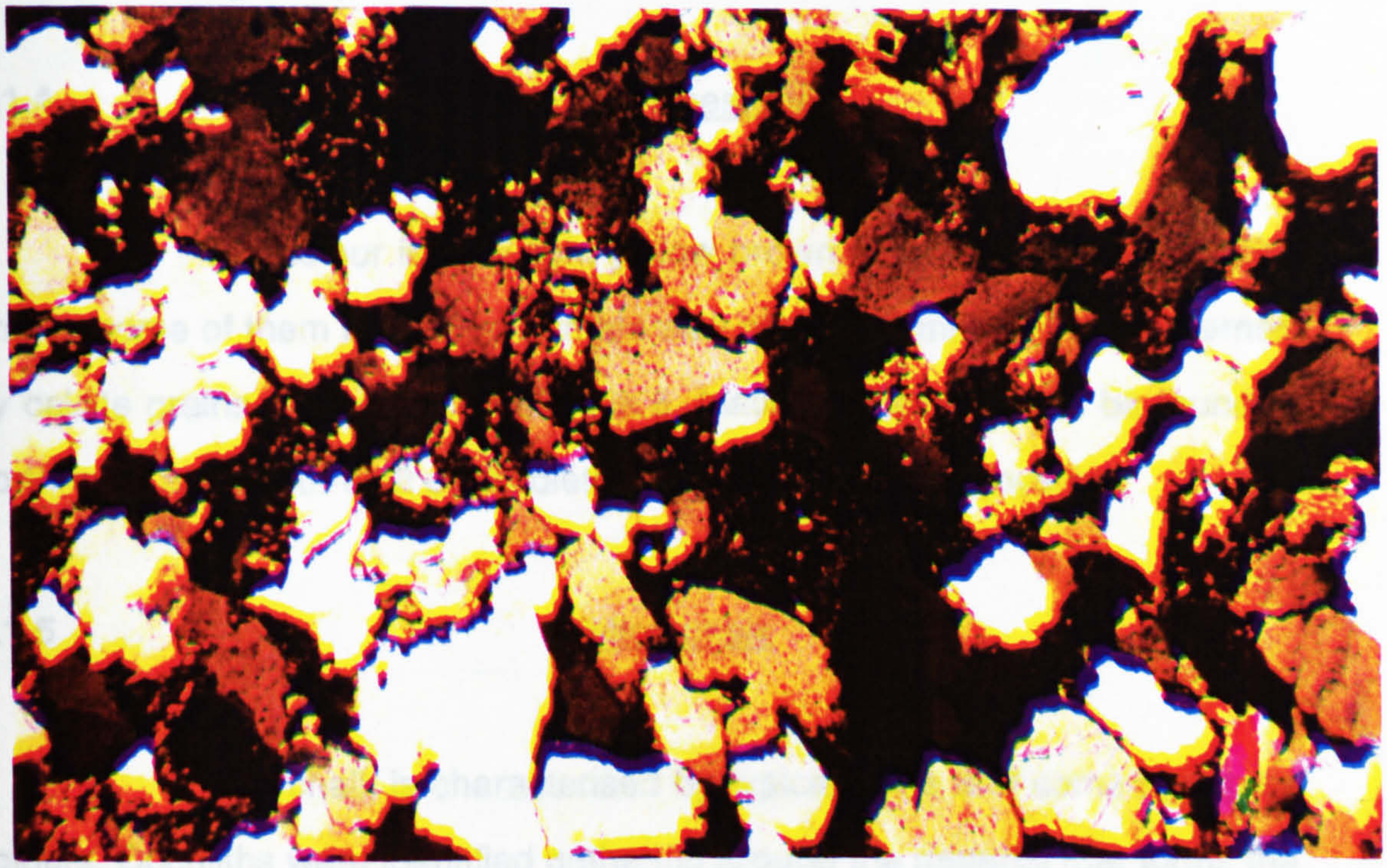

Plate 4.1 Specimen from Springwell sandstone ;magnification x 125

4.1.2 Pennant sandstone

It is a well sorted sandstone containing quartz grains mainly monocrystaline and subrounded to subangular. The mineralogical composition is quartz 64%, clay minerals 20%, mica 3%, feldspars 3%, rock fragments 3 % and the rest is voids. Cement coefficient is 8. Pennant sandstone originates from South Wales.

4.1.3 Teesdale Whinstone

Most of the rock is supported by the feldspar framework. The feldspars are supported by other smaller size grains of feldspar and mica grains. Grain size is between 0.2-0.8 mm. The mineralogical composition is feldspar 76%, quartz 13%, mica 9% and other 2%. Cement coefficient is 10.

Whinstone originates from the Great Whin Sill in Upper Teesdale, Co. Durham.

4.1.4 Matlock limestone

The colour is very light yellow brown. It is dominated by calcite grains, some of them have approximate size of up to 5 mm and are governed by calcite grains. Cement coefficient is 6. Matlock limestone can be found in north-west and south-east of Middleton Mine which is in Derbyshire.

4.1.5 Welton chalk

This chalk is characterised by typical white and some light grey colours. Cocoliths were identified gathering around the material that forms the rock. Cement coefficient is 6. Welton chalk is located in the south shore of river Humber.

4.2 Physical properties

The bulk density and porosity of specimens (1981) were measured according to ISRM and the results for the various rocks are as follows (Table 4.2):

Table 4.2 Porosity and density

Rock	porosity(%)	density (Mg/m^3)
Springwell sandstone	12	2.30
Pennant sandstone	0.14	2.66
Teesdale Whinstone	0.18	2.95
Welton chalk	1.05	2.30
Matlock limestone	6.9	2.46

4.3 Mechanical properties

4.3.1 Uniaxial compressive strength

Most theories of rock cutting predict a correlation between rock material strength and productivity. This relationship has been used by a number of researchers to predict roadheader performance.

A suitable arrangement (Plate 4.2) satisfying ISRM recommendations was used for applying and measuring axial load to the specimens. Steel platens were placed at the cylindrical specimens' ends which had nominal dimensions height=150mm and diameter=75mm. LVDTs (linear variable differential transformers) were used for measuring the axial and lateral deformation. Load on the specimens was applied continuously at a constant stress rate of 3 MPa/min (according to ISRM, 1981).

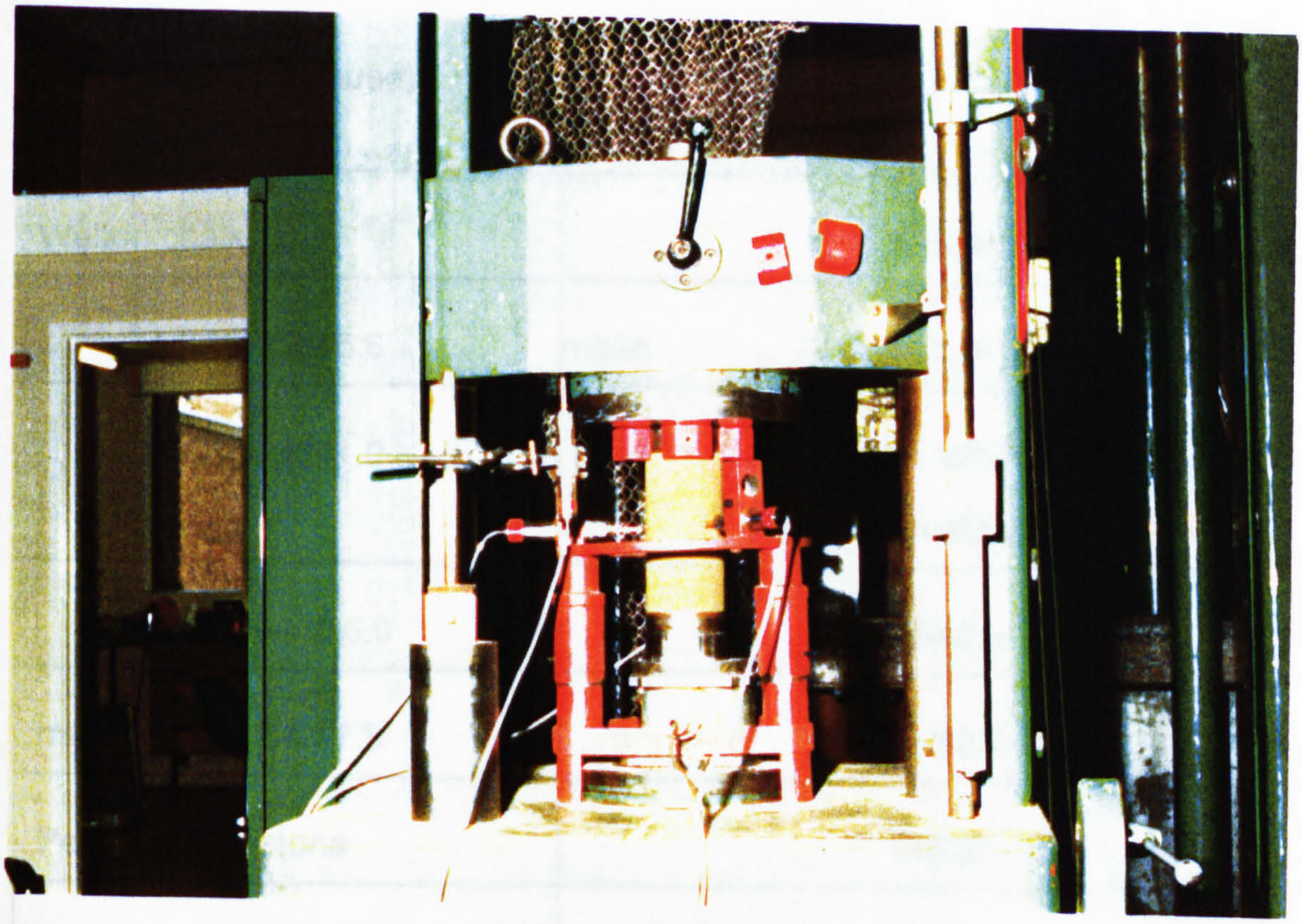

Plate 4.2 Uniaxial compressive strength test apparatus

The results are given in Table 4.3.

Table 4.3 Uniaxial compressive strength (MPa)

fully saturated/ambient moisture content	
Springwell sandstone	Matlock Limestone (after Jamalbastami, 1989)
37.8/44.6	120.5/———
35.0/44.5	124.5/———
33.6/42.3	121.0/———
36.3/44.1	119.0/———
mean 35.7/43.9	122.0/———

Table 4.3 (continued)

Welton chalk			125.0/———
45.0/45.6		mean	122.0/———
39.8/41.0			Teesdale Whinstone (after Jamalbastami, 1989)
———/56.0			150.0/———
mean	42.4/47.5		142.0/———
Pennant sandstone			146.0/———
147.6/78.1			138.0/———
139.6/104.1			152.0/———
165.3/103.8			———/———
160.7/———			———/———
116.4/———			———/———
mean	145.92/95.33	mean	145.6/———

4.3.2 Triaxial compression test

This test was used to determine the strength characteristics of cylindrical rock specimens containing an artificial joint. A 2 MPa confining pressure was applied during the triaxial tests.

The apparatus consists of three parts : a triaxial cell, a loading device, and a device for generating a constant confining pressure. The triaxial

cell used was the Hoek cell type which allowed rapid testing. The confining pressure was generated by an electrical pump fitted with a pressure gauge for measuring the pressure at the required value.

A specimen of diameter 75 mm and length of 150 mm, containing an artificial discontinuity, was placed inside the impervious polyurethene rubber jacket and the ends were brought into contact with the respective loading platens. The cell was then positioned in the testing machine and the axial load and confining pressure were increased simultaneously in equal steps until a confining pressure of 2 MPa was reached. Subsequently, the confining pressure was kept constant while the axial load was increased continuously at a constant strain rate (0.25 %/min) until the material failure or shear failure along the discontinuity occurred.

It can be seen that there is a relationship between joint strength and moisture state (Fig4.1, Fig4.2 and Fig4.3).

4.3.3 Tensile strength

The Brazil disc test was used to measure indirectly the uniaxial tensile strength of rock specimens.

A cylindrical specimen of diameter 60 mm and thickness 30 mm (ratio 2:1) was compressed diametrically between two platens. A constant loading rate was applied so that failure occurred within 20-25 s of loading (Plate 4.3).

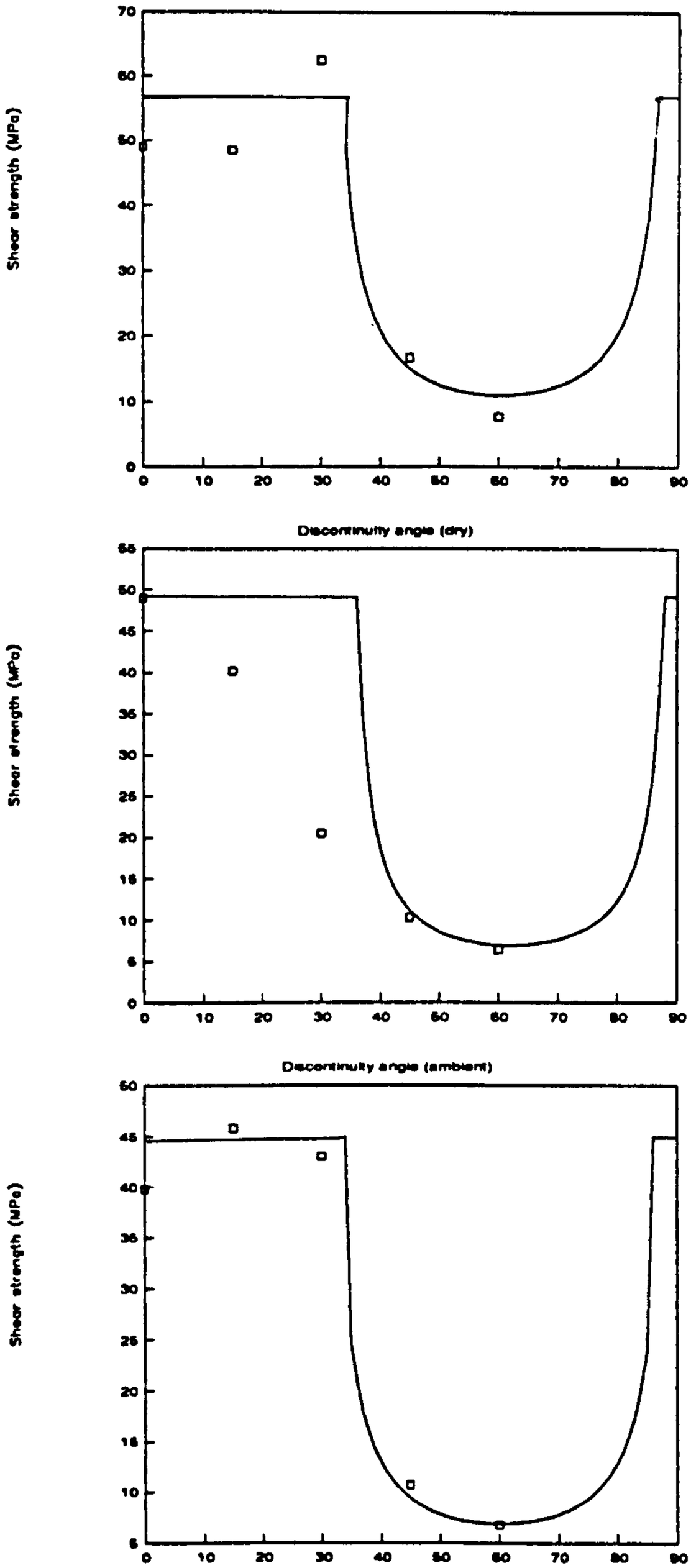

Figs 4.1, 4.2, 4.3 Shear strength v Discontinuity angle in different environment states (dry, ambient, saturated)

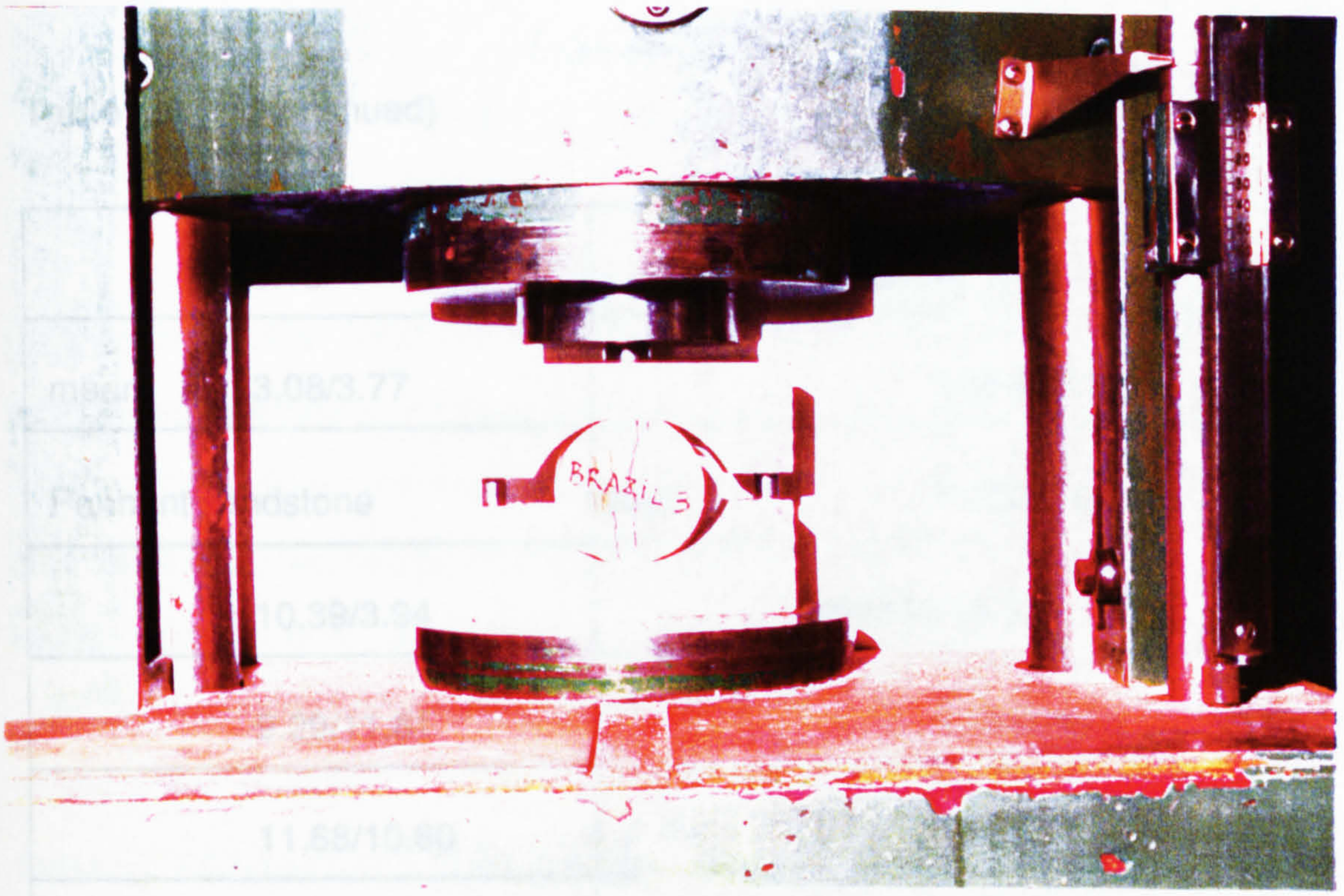

Plate 4.3 Brazilian test for tensile strength

The results for fully saturated and ambient moisture content rock samples are given in Table 4.4:.

Table 4.4 Tensile strength (MPa)

fully saturated/ambient moisture content	
Springwell sandstone	Matlock limestone
3.06/4.18	3.97/6.04
3.01/3.45	3.64/5.15
2.86/3.33	5.14/4.82
3.29/4.13	4.45/5.23

Table 4.4 (continued)

3.16/———	4.60/4.88
mean 3.08/3.77	4.54/5.25
Pennant sandstone	mean 4.39/5.23
10.39/3.94	Welton chalk
9.29/11.81	3.82/3.85
11.68/10.60	2.68/3.86
8.40/10.78	3.66/4.70
8.35/11.80	3.39/2.29
8.81/8.76	2.61/2.93
mean 9.49/11.28	3.59/———
Teesdale Whinstone	3.48/———
17.25/19.01	2.42/———
21.54/19.31	2.94/———
20.30/19.27	3.12/———
20.58/19.22	mean 3.17/4.41
20.09/18.44	———/———
21.31/19.90	———/———
mean 20.8/19.19	———/———

4.3.4 Shore scleroscope hardness

This method determines an index of hardness of rock minerals as an average of readings taken at random on individual mineral grains and reflects a measure of rock mineralogy, elasticity and cementation.

The instrument consists of a vertically mounted barrel containing a precision bored glass tube through which a diamond tipped cone is dropped from a set height and rebounds within the glass tube. A scale graded from 0 to 140, is set behind the barrel and is visible through the glass tube (Plate 4.4a).

Plate 4.4 Shore hardness and NCB cone indenter (shore hardness Fig 4.4a right, NCB cone indenter Fig 4.4b left)

To perform the test (according to ISRM, 1981) a core specimen with a flat ground surface is marked off in small squares of 10 mm sides and

the instrument is positioned vertically with the bottom of the barrel in firm contact with the specimen, and normal to its surface. The hammer is brought up to the elevated position by squeezing a rubber bulb, and then allowed to fall to strike the test surface. The rebound height on the first bounce is observed and recorded as the hardness of the sample. Only one test at the same spot is made by spacing the indentation at least 5 mm apart. The test is repeated another 19 (R20) times and the average over these 20 reading is taken as the Shore scleroscope hardness. Michalopoulos et al (1976) have investigated the influence of water on the hardness of some rocks. Saturated specimens show less hardness than air-dried ones. The trend agrees with the UCS of rocks. Rabia and Brook (1979) have studied the influence of size and moisture content on shore hardness. It was found that a reliable value for the volume of the specimen should be 0.00004 m^3 and Shore hardness for some rocks such as Markfield granite did not change at all. The results of the conducted tests are given in Table 4.5.

Table 4.5 Shore scleroscope hardness

fully saturated/moisture ambient content	
Springwell sandstone	Pennant sandstone
40.50/46.85	65.80/70.3
Welton chalk	Matlock limestone
39.7/38.65	38.60/41.8
Teesdale Whinstone .	
82.12/88.0	

4.3.5 Shore plasticity

If the scleroscope test is carried out at one location on the surface of the specimen a 'work hardened' surface is altered into a fine homogeneous powder. A ratio of the change in rebound values during this test to the final hardness provides a convenient relative measure of the plasticity of the rock specimen.

The 'coefficient of plasticity' of the rock types was obtained from the formula defined as (k %) :

$$k = \frac{H_{20} - H_1}{H_{20}}$$

Where H_1 and H_{20} are the first and final rebound values for the rock samples.

In the studies of the mechanics of cutting picks, it was found by McFeat-Smith (1975) that the difficulty of cutting intact samples of sedimentary rocks increases with :

a: the square root of the standard cone indenter hardness

b: the cube root of the coefficient of plasticity

Thus the cutting action of picks is primarily an indention action implying that a quantity of energy is also absorbed during the plastic deformation of non-brittle rocks. This may explain why anomalously high energies are required to excavate some soft, low strength evaporate rocks.

The Shore plasticity of the investigated rock types is given in

Table 4.6:

Table 4.6		Shore plasticity (%)
Springwell	sandstone	32
Matlock	limestone	50
Welton	chalk	49
Pennant	sandstone	6
Teesdale	Whinstone	9

Tests were also carried out in water saturated state but are not include here, because it has been accepted that shore plasticity is valid for rocks under ambient moisture content.

4.3.6 Cone indenter hardness

The NCB cone indenter is used to determine the indentation hardness of the specimen. The hardness of the specimen is determined by measuring its resistance to indentation by a hardened tungsten carbide cone under a standard load (the NCB cone indenter, 1977). The cone indenter comprises of a steel strip clamped to a steel frame at its ends, a dial gauge to measure the central deflection of the steel strip and a cone attached to the spindle of a micrometer (Plate 4.4b).

A specimen not larger than 12 mm x 12 mm x 6 mm is placed on the steel strip at its midspan and the cone is lowered by turning the micrometer until the tip of the cone touches the specimen. The screw is rotated and the advance is read as the difference between the first and second (R2-R1) readings. The deflection of the thin spring bond is measured by the gauge and is directly related to the force on the specimen. The test is carried out 20 times on each rock type. The cone indenter (CI) hardness is then calculated as :

CI=0.635/(average(R2-R1)-0.635)

The cone indenter test results for the investigated rocks are given in Table 4.7 :

Table 4.7	NCB cone indenter
fully saturated/ambient moisture content	
Springwell sandstone	
1.36/1.74	
Welton chalk	
1.74/1.74	
Matlock limestone	
1.74/1.74	
Pennant sandstone	
2.15/2.82	
Teesdale Whinstone	
1.77/3.85	

4.3.7 CERCHAR abrasivity

This is done by a simple scratch (10mm) on a plate of rock specimen by the CERCHAR machine (Plate 4.5). The measurement of abrasivity being in terms of the wear flat diameter in 1/10 mm units. The wear flat is measured under a microscope with a micrometer. A travelling microscope with an eyepiece micrometer is used to measure the wear flat in two orthogonal directions. They are allowed to coincide at one edge and the first reading R1 recorded from the micrometer. Then the other line is moved to other edge of the wear flat and reading R2 is recorded. The difference, R2-

R1 is then computed. The tests is repeated on each sample 5 times, (West, 1989), Fig 4.4. The results are given in Table 4.8 :

Table 4.8 CERCHAR abrasivity
saturated/ambient
Springwell sandstone
1.10/1.33
Welton chalk
0.33/0.32
Matlock limestone
0.64/0.79
Pennant sandstone
1.98/1.58
Teesdale Whinstone
1.65/1.54

The magnitudes of abrasivity for chalk and Pennant sandstone and Teesdale Whinstone for water saturated state show an abnormal pattern. These rocks are not porous rocks the same as Springwell sandstone and also Pennant and Whinstone are very strong materials. These experiments show that the CERCHAR abrasivity test is not suitable for strong material and less porous rock in saturated state.

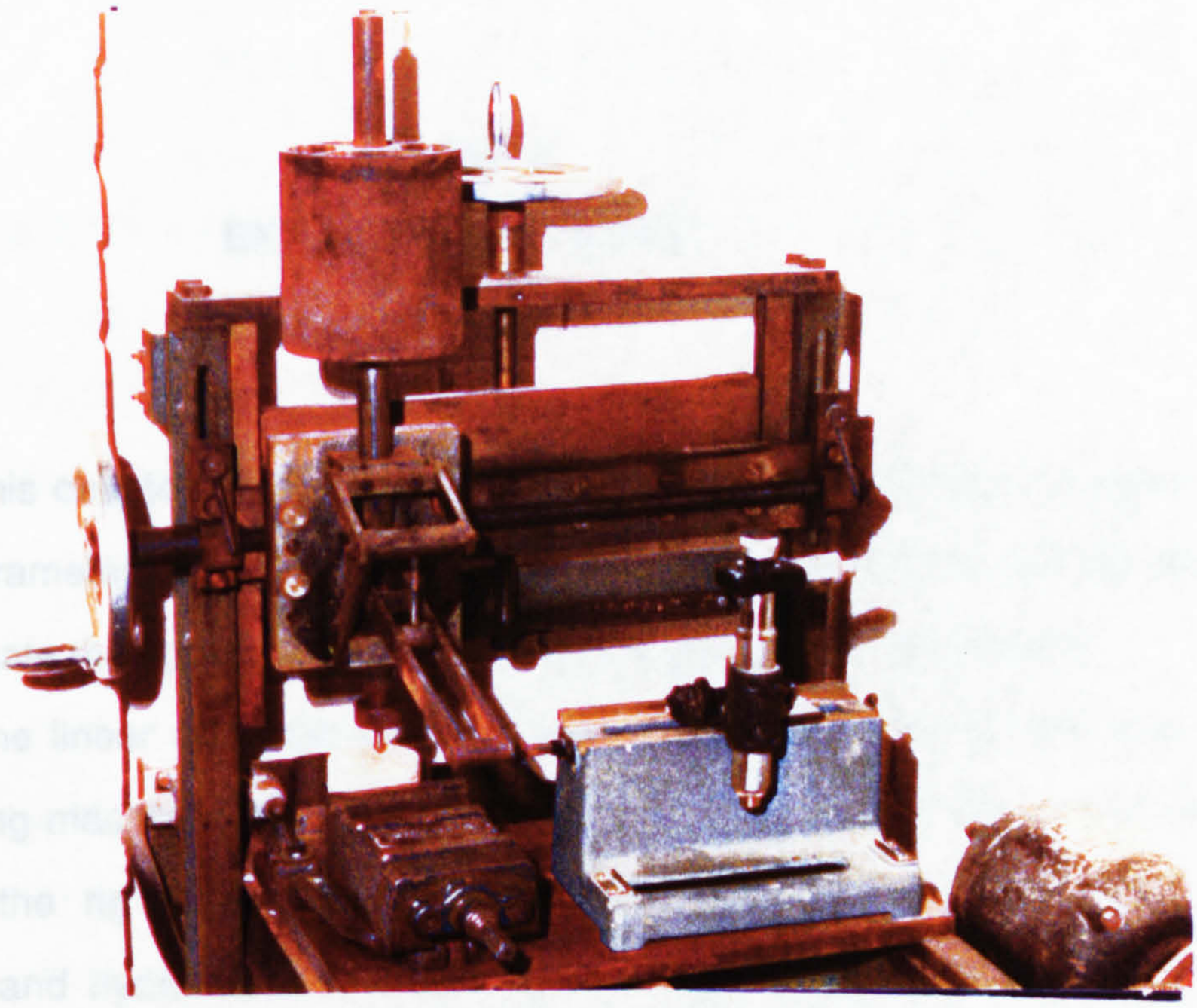

Plate 4.5 CERCHAR abrasivity test

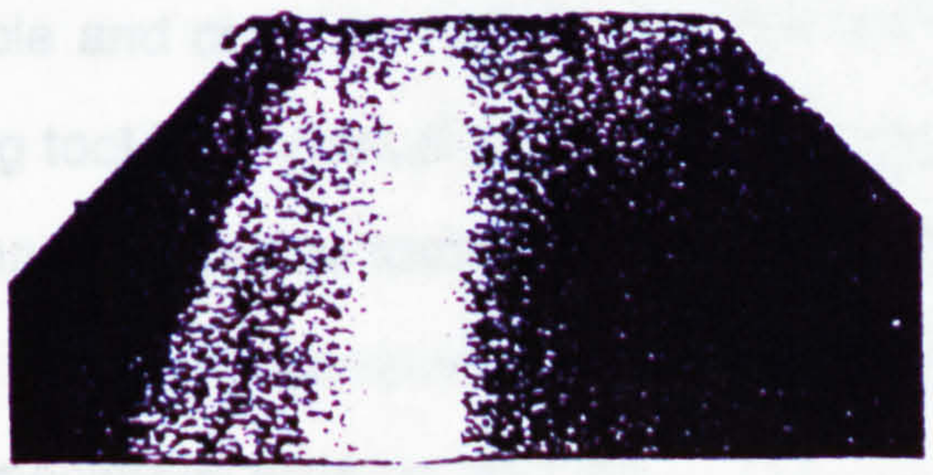

Fig 4.4 View of tip of CERCHAR test (after West, 1989)

Chapter 5

EXPERIMENTAL WORK

5.1 Rock cutting rig

This chapter deals with the methods which were used to measure rock cutting parameters and rock fracture tests. The finite element method was used to investigate the optimum geometry for the rock cutting experiments.

The linear rock cutting rig employed for these experiments was a modified shaping machine with a maximum cutting stroke of 800 mm . A further modification of the rig was the replacement of the normal driving mechanism by a power pack and hydraulic ram providing a maximum in-line force of 50 kN. Hydraulic power was supplied by a 7.5 kW swash plate pump capable of generating a cutting speed of up to 200 mm/s. Block rock specimens of dimensions 500 mm square and 300 mm high can be accommodated on the machine table and could be raised, lowered and laterally traversed with respect to the cutting tool by a manual screw feed. During cutting, the bed or table where the specimen rests can be locked in position to avoid any undesirable deflection.

Curved clamping jaws were specially designed to keep the cylindrical specimens firmly in position.

Fitted to the head mounting plate is the dynamometer and bearing rollings in horizontal rails on the upper steel welded frame, for additional support of the tool. The tool holder carrying the pick is bolted to the dynamometer.

5.2 Force measuring system

The force measuring system monitors the components of force acting on the rock cutting tool during a cutting stroke and consists of :

1-Triaxial dynamometer

2-Ultra-Violet (UV) chart recorder

5.2.1 Triaxial dynamometer

A triaxial dynamometer has been developed (Roxborough, 1969) to resolve the force acting on the cutting tool into three mutually orthogonal components. The cutting, lateral and normal forces, are each measured by a strain gauged bridge circuit. The strain imposed upon a set of electrical resistance strain gauges arranged in three bridges is used to resolve the forces acting upon the tool whilst cutting. The tool is placed within a tool holder which transmits the strains from the tool to the strain gauges. The dynamometer resolves the forces into three components, the normal force acting vertically on the tool, the horizontal cutting force acting in the direction of cut, and, the side force acting on the side of the tool, Fig (5.1).

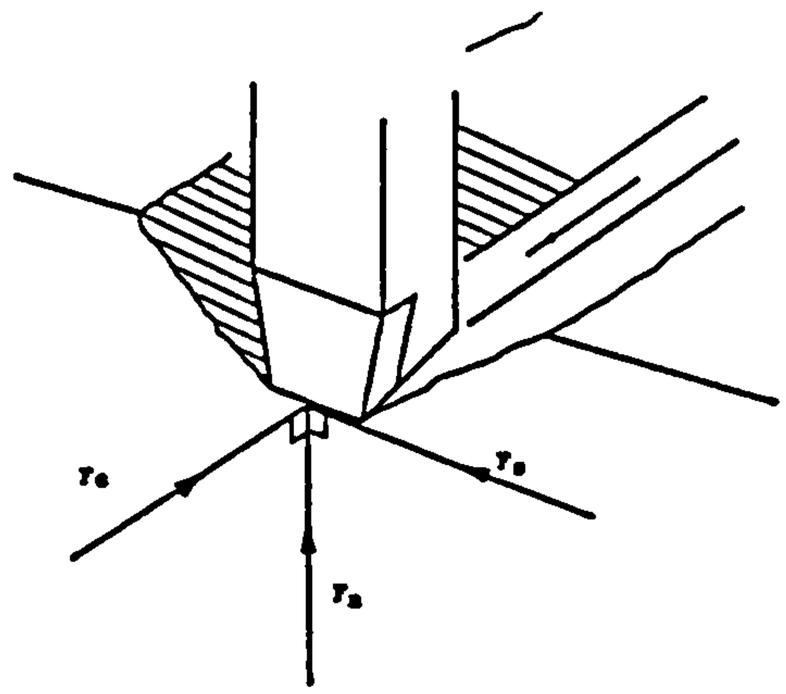

Fc : cutting force Fn : normal force Fs : side force

Fig 5.1 The components of tool forces (after Hurt, 1980)

The outputs of the cutting forces are amplified and fed continuously to a UV recorder, the signals being integrated simultaneously and also sent to the UV recorder.

5.2.2 UV chart recorder

Continuous recording is facilitated by the use of a SE4000 carrier amplifier system. The analogue outputs from each of the amplifier dynamometer signals and the start and stop pulses are provided in the front of unit, so that the information can be recorded on an UV recorder. The system carries three amplifying channels and three integrating channels for the three mutually orthogonal components. The amplified and integrated signals are then fed to the UV chart recorder fitted with photo-sensitive paper chart moving at selected constant speed to give a measure of peak and mean values of the forces during the cutting operation.

The UV charts obtained from these experiments show the instantaneous peak and integrated mean values of the three components of force throughout a cut. The chart usually shows seven traces, three for the instantaneous forces, three for the integrated forces, and one for the time datum line. A typical UV recorder trace with only four traces (side forces were not recorded during the tests), used in this research programme, is shown in Fig (5.2). The magnitude of the peak forces is shown on the UV trace as the displacement of the instantaneous trace from its original position. The magnitude of the mean forces is given by the slope of the integrated trace. The actual value of the forces is obtained by multiplying displacements and slope by scale factors derived through a calibration process.

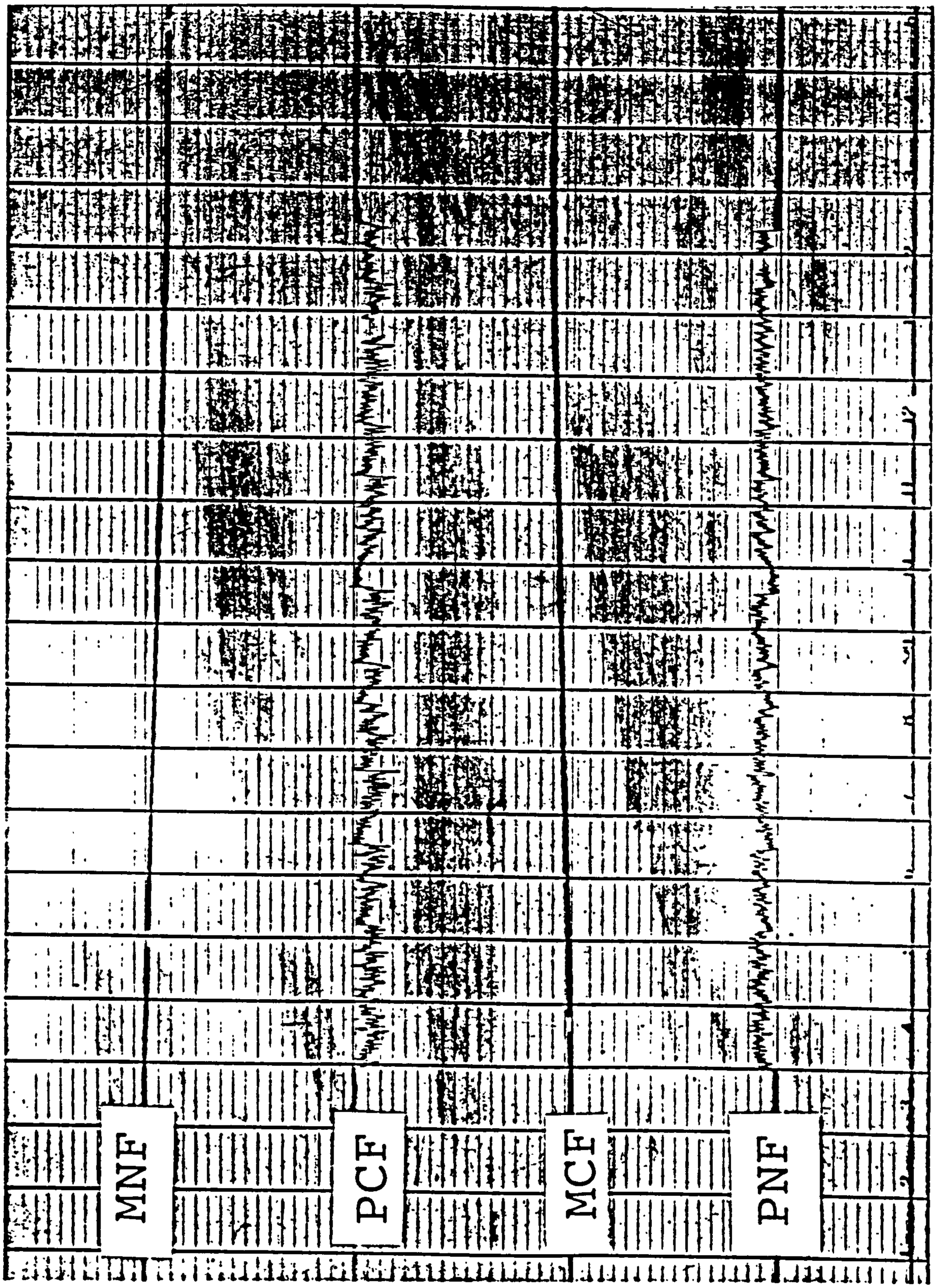

Fig 5.2 UV chart recorder

5.2.3 Calibration of dynamometer

Calibration of the dynamometer is carried out to enable the output obtained on the UV to be quoted in units of force. It is necessary to know what load in kN corresponds to a unit displacement and a unit slope.

A P-3500 digital strain indicator manufactured by Measurements Group Inc was used in conjunction with a load cell, type 405 in a simple calibration test for the load cell and corresponding strain values recorded by the strain indicator. From this test a calibration constant of 0.039 (kN/mV) was determined for the load cell.

Each channel carries various amplification and integration settings which allow a range of force to be monitored by this channel. Amplifier and integrator settings of 0.05 and 9 for cutting force (channel 1) and 0.05 and 8 for the normal force (channel 2) were chosen as adequate for the range of forces anticipated to be encountered during the cutting tests. The arrangements for the cutting force is the ball fixed (Plate5.1) to the pyramidal plate to ensure horizontal directional loading at the dynamometer. A spirit level is used to check for horizontal alignment. Known loads (as indicated by the strain gauge reading) are applied to the dynamometer and the peak and integrated traces are recorded.

After checking that the system is balanced and that there is no drift in the bright spots of the UV recorder, tests can then be carried out. From the measured displacements and slope of these traces, calibration constants can be determined for that channel setting. The loading and measuring procedures are repeated three times for each amplification setting and a mean value taken as the calibration constant:

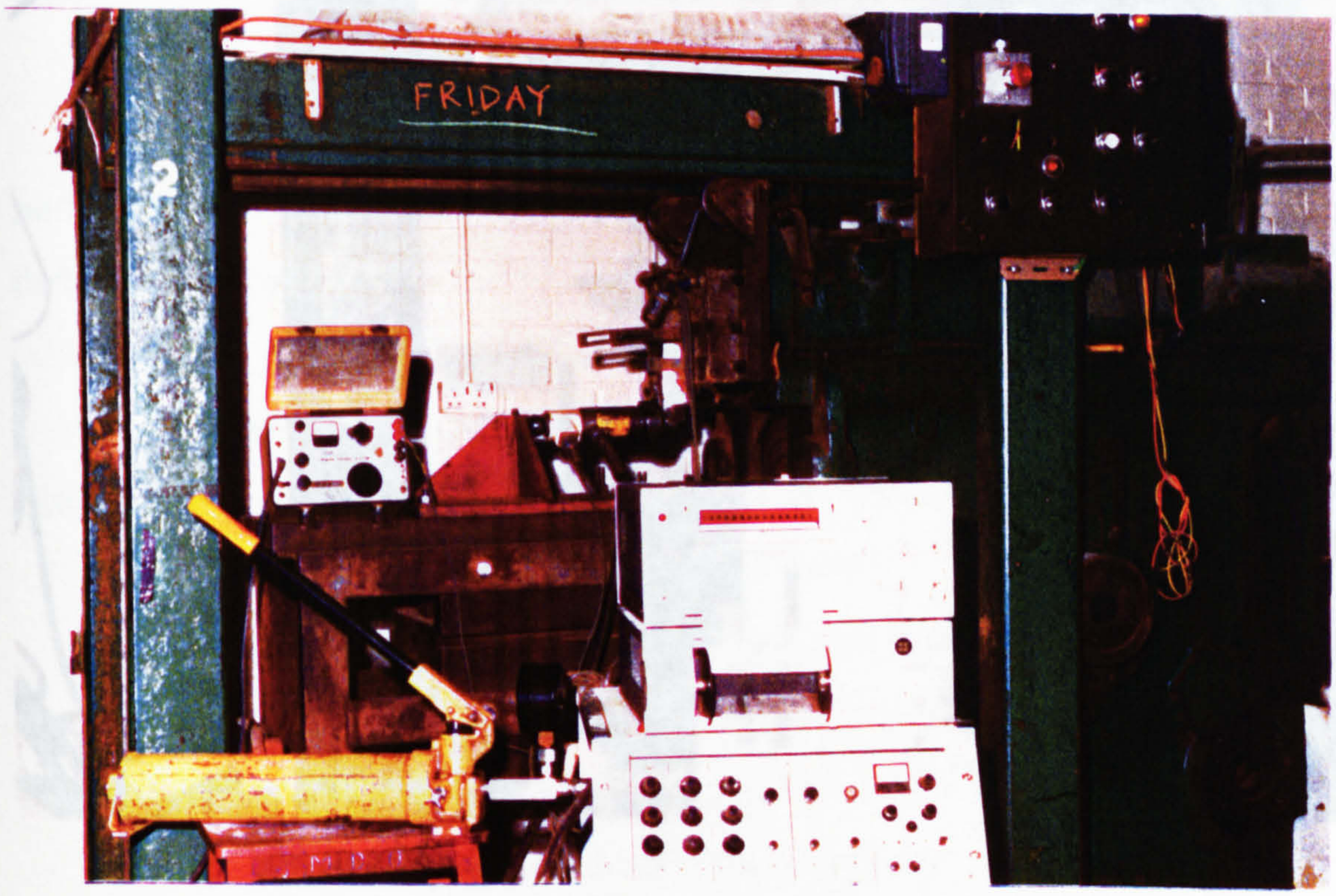

Plate 5.1 Cutting force calibration and UV recorder

The calibration arrangements for normal force are followed in the same manner except that the settings are located in the vertical plane (Plate 5.2).

The calibration constants in kN/mm were found to be as follows:

	calibration constant (kN/mm)
Mean Cutting Force(MCF)	0.493884
Peak Cutting Force(PCF)	0.245563
Mean Normal Force(MNF)	0.375655
Peak Normal Force(PNF)	0.340535

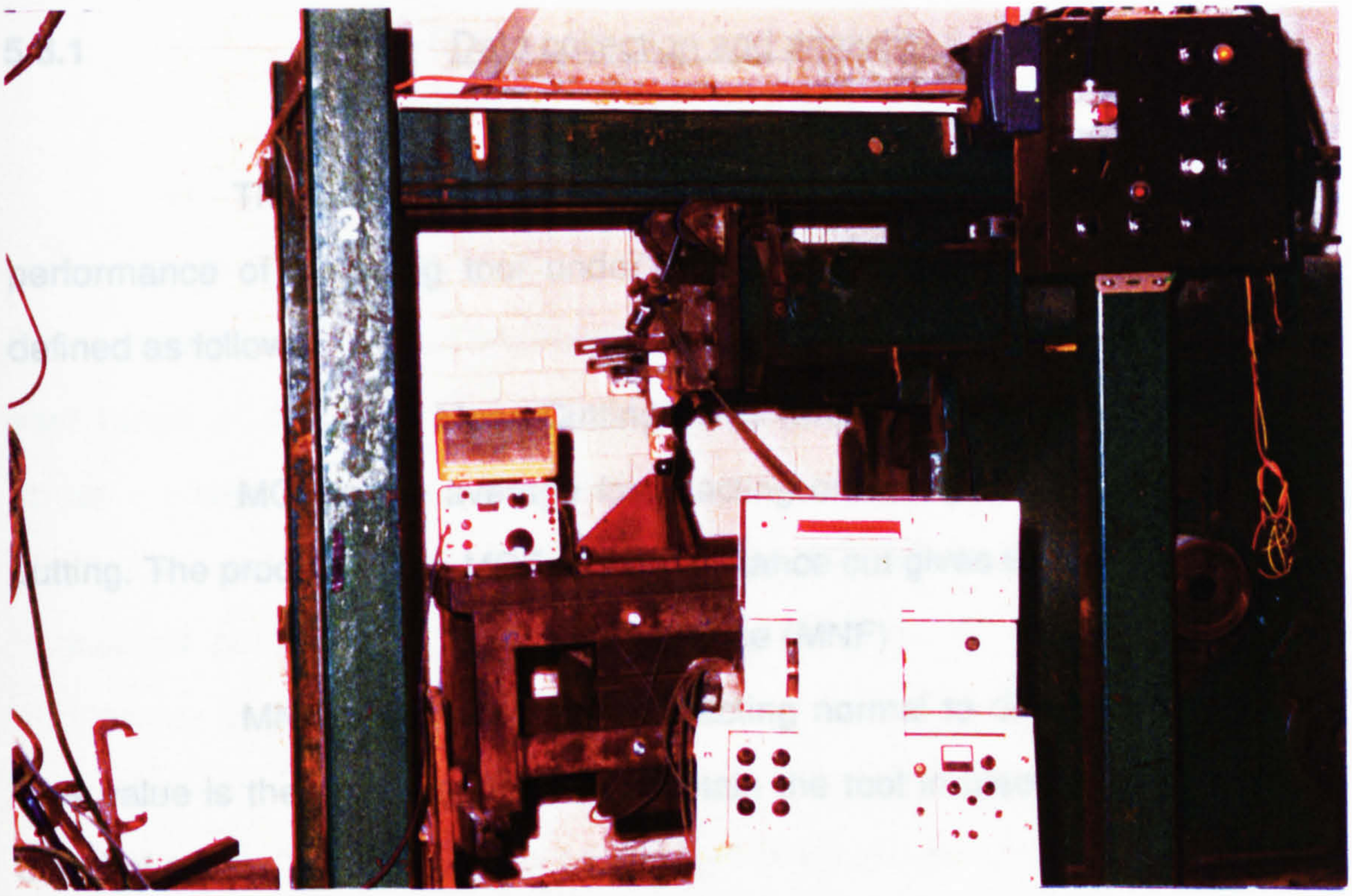

Plate 5.2 Normal force calibration

5.3 Mechanical cutting

A core grooving test developed in the University of Newcastle upon Tyne (Roxborough, 1975) is used extensively in the assessment of the machineability of rock for roadheaders and other drag tool equipped machines.

The test may be carried out on either core samples or block samples of rock. Four cuts are normally made in the rock sample at a constant depth of 5 mm with a tungsten carbide tool 12.7 mm wide, chisel-edged, with a -5° front rake and +5° back clearance angle. This tool is mounted on an instrumented shaping machine (Plate 5.3). If there is a need to apply an axial compressive loading during cutting a modified cell can be used that exercises uniaxial compressive stress parallel to the direction of cutting (Plate 5.4).

5.3.1 Data collection and analysis

The following parameters are used in assessing the performance of a cutting tool under different cutting conditions. They are defined as follows:

Mean Cutting Force (MCF)

MCF is the average force acting on the tool in the direction of cutting. The product of the MCF and the distance cut gives the work done.

Mean Normal Force (MNF)

MNF is the average force acting normal to direction of cutting. This value is the thrust required to maintain the tool in place at the required depth of cut.

Mean Peak Cutting Force (MPCF)

MPCF is the average of the maximum values of the cutting force and varies greatly as chips form. MPCF shows the lowest force that has to be applied to the tool to cut the rock.

Mean Peak Normal Force (MPNF)

MPNF is the average of the maximum forces generated during cutting to keep the tool in the rock.

Yield, (Q)

This is the mass of rock cut by the pick per unit length of cut and is expressed in m^3/m.

Specific Energy, (SE)

This is defined as the work done to cut a unit volume of rock and is expressed in MJ/m^3. It is obtained by dividing the mean cutting force component by the yield, the latter being expressed as the volume of material cut per unit distance cut.

PAGE NUMBERING AS ORIGINAL

5.4 Finite Element analysis of clamping jaws

In the most general terms the finite element method is a technique for the solution of partial differential equations by discretisation in their space dimensions. In engineering, this technique has been applied to a vast range of problems including structural analysis, linear and non-linear stress analysis, heat transfer, fluid dynamics, electromagnetism, electrochemical problems and acoustics. The present work its application is concerned purely with linear elastic stress analysis. In the finite element method the continuum is modelled as an assemblage of subdivisions termed finite elements which are considered to be interconnected at specific points termed nodes. The nodes may be thought of as nut-and-bolt devices, which secure adjacent finite elements through their ends or corners and hold them together. It is the finite character of the structural connectivity which makes possible the analysis by means of simultaneous algebraic equations, and which distinguishes a structural system from problems of continuum mechanics.

The purpose of the finite element method of stress analysis as used in this part of the thesis assesses stresses generated, and the extent to which the distribution of these stresses in the rock influence the cutting tool performance. The PAFEC-FE computer program is available at Newcastle University and was used in the finite element stress analysis.

PAFEC-FE stands for Program for Automatic Finite Element Calculations, and it has been designed so that users may input the data in a very straightforward manner (PAFEC-FE manual).

Tecen (1984) used PAFEC-FE to find out stress distribution around a cutting bit. Sauma et al (1984),Fig 5.3, and Ingraffea (1987), Fig 5.4 attempted to use the finite element to solve the problem of discrete crack modelling of rock cutting using fracture mechanics principles.

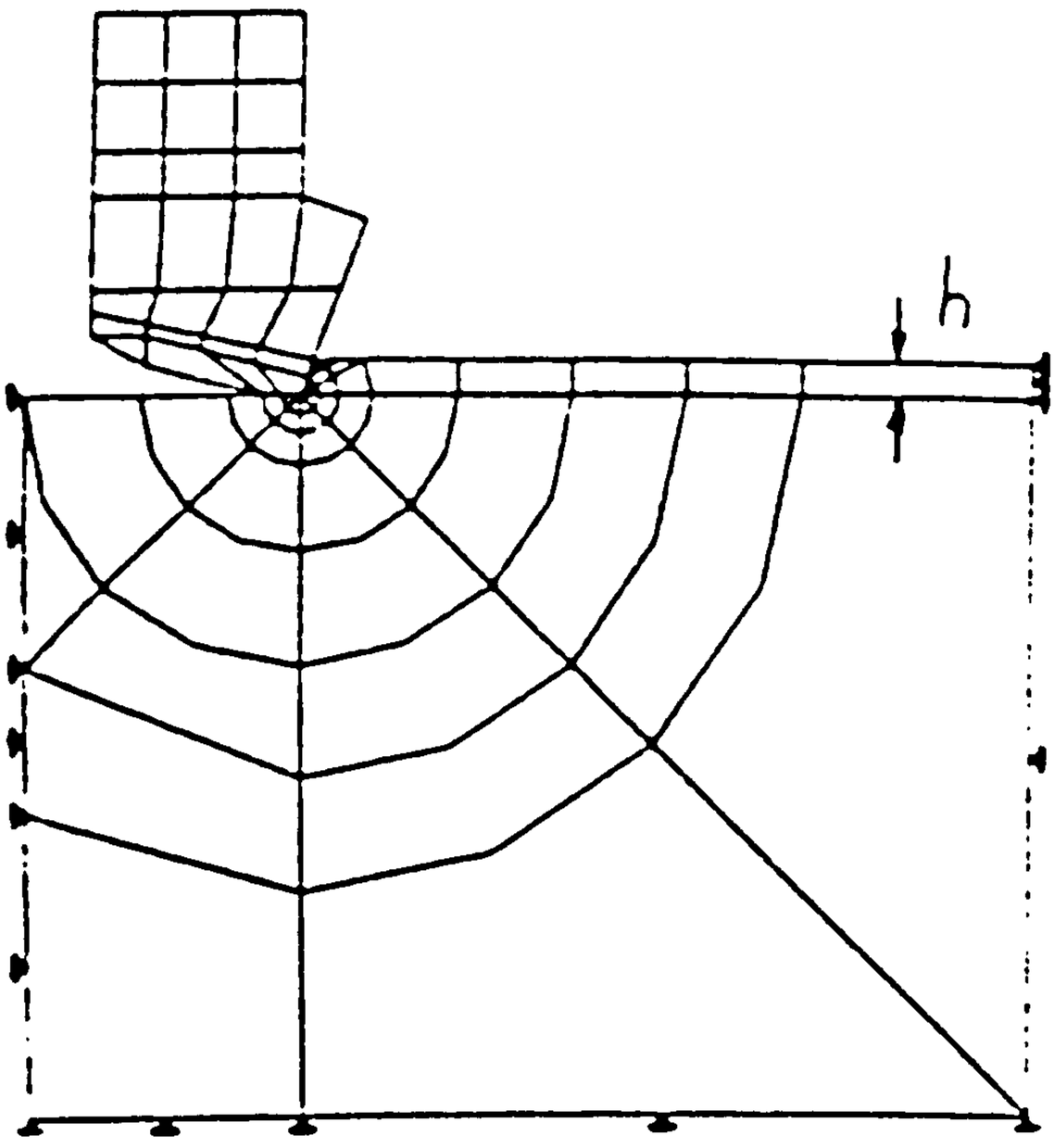

Fig 5.3 Sauma's finite element mesh

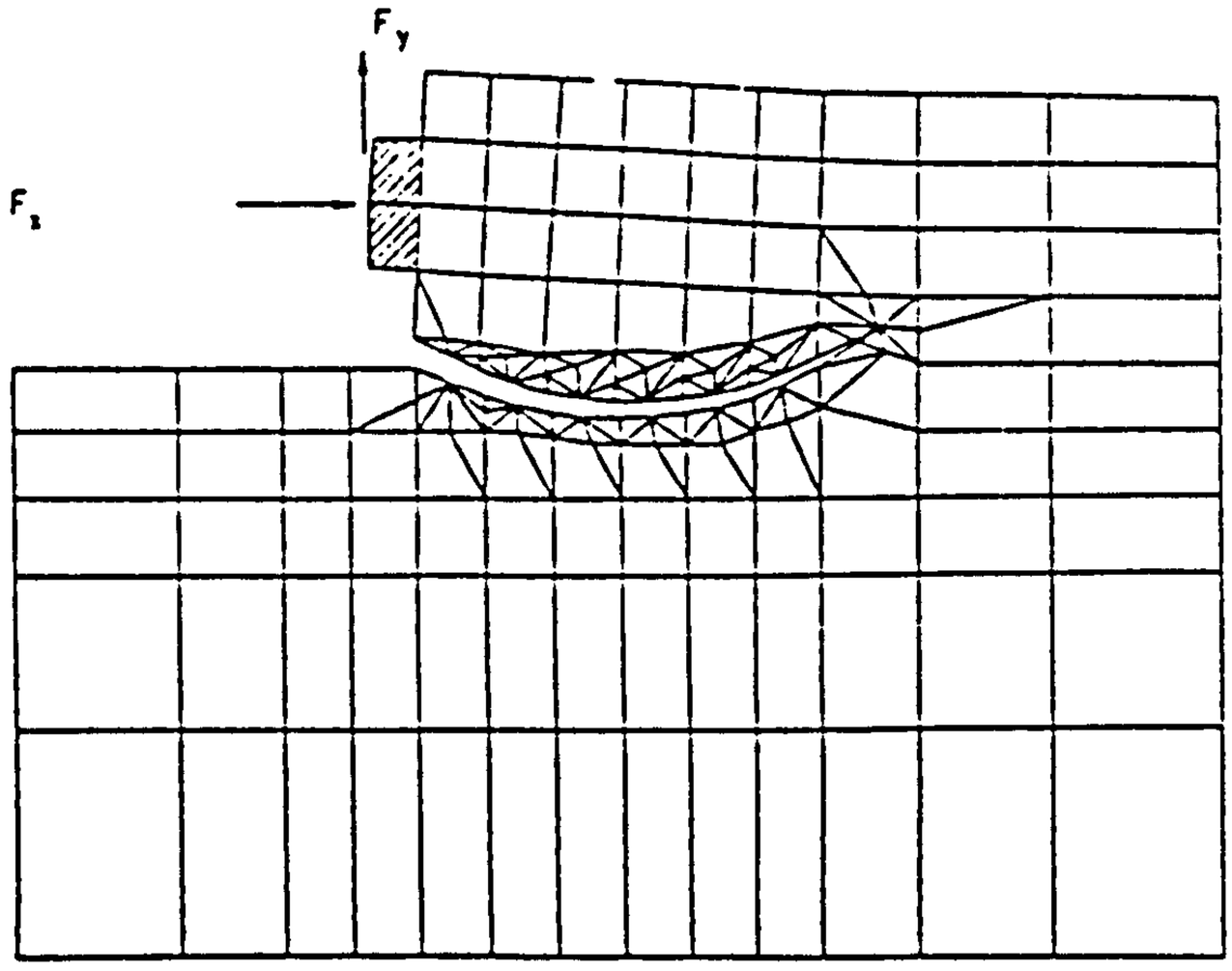

Fig 5.4 Ingraffea's finite element mesh

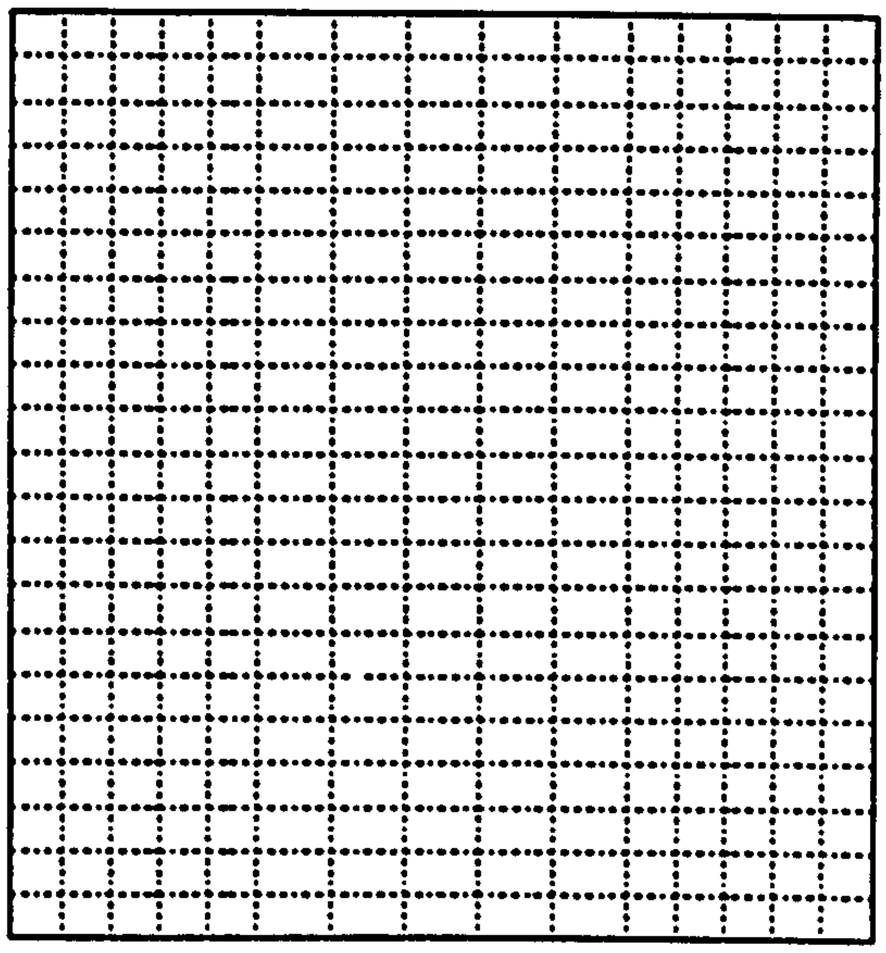

Fig 5.5 Finite Element idealization of block specimen

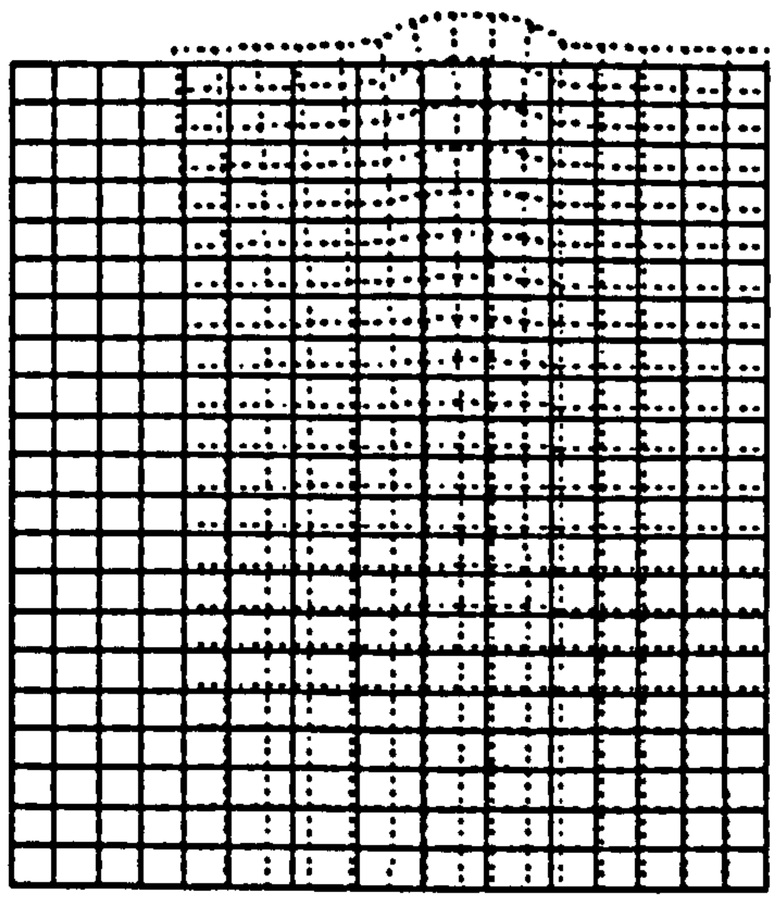

Fig 5.6 Deformed shape of block specimen

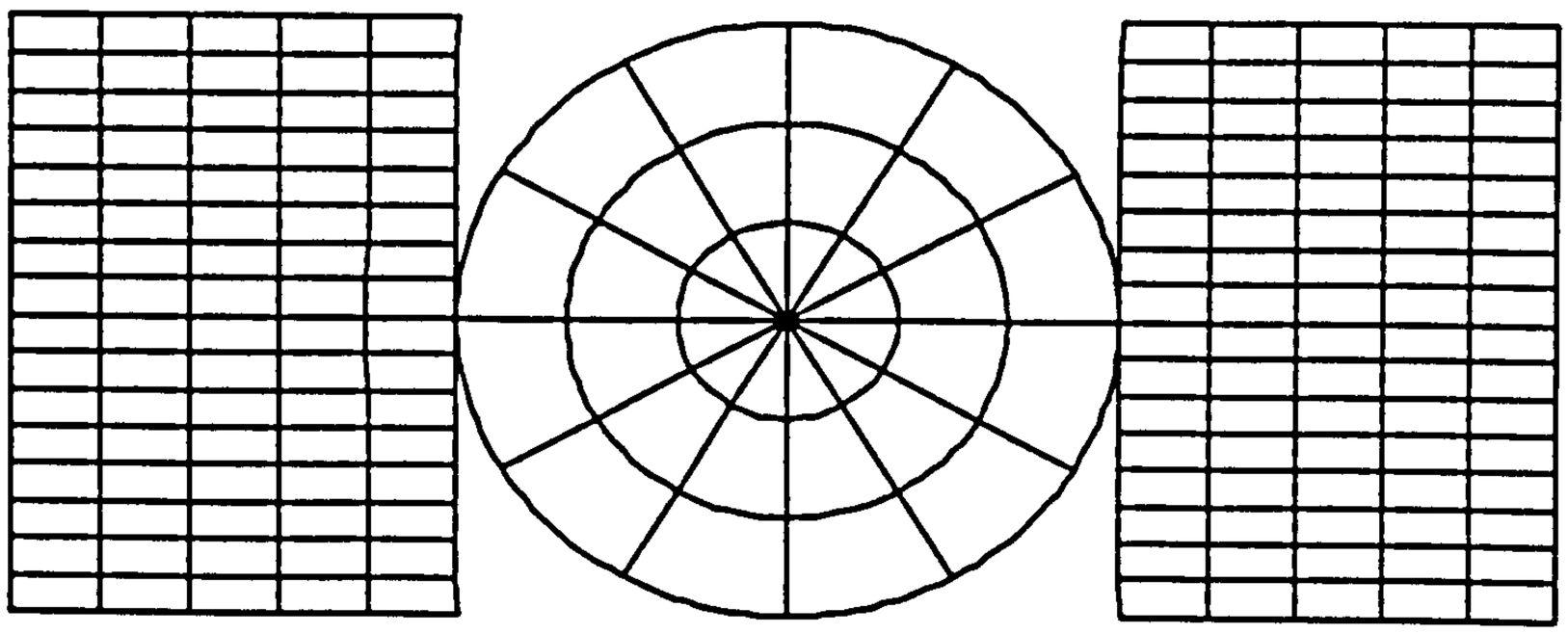

Fig 5.7 Finite Element idealization of a core specimen clamped by a vice

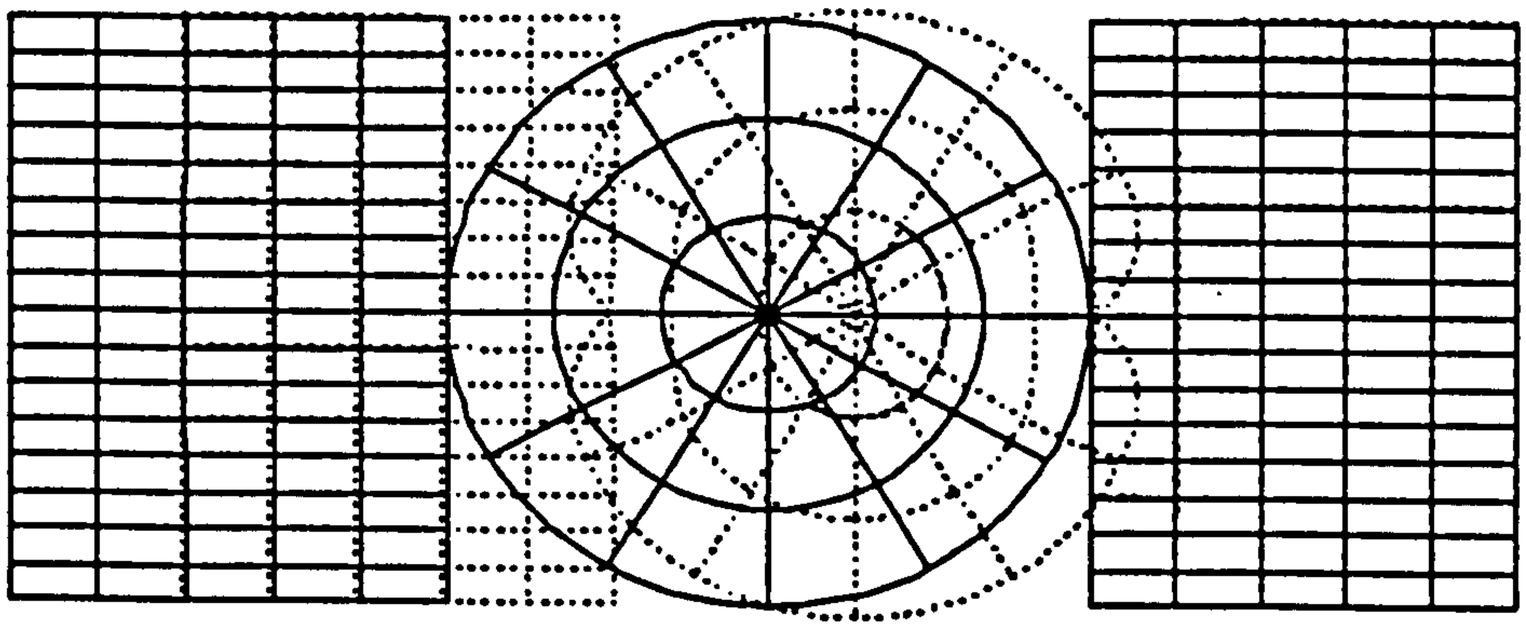

Fig 5.8 Deformed shape of a core specimen clamped by a vice

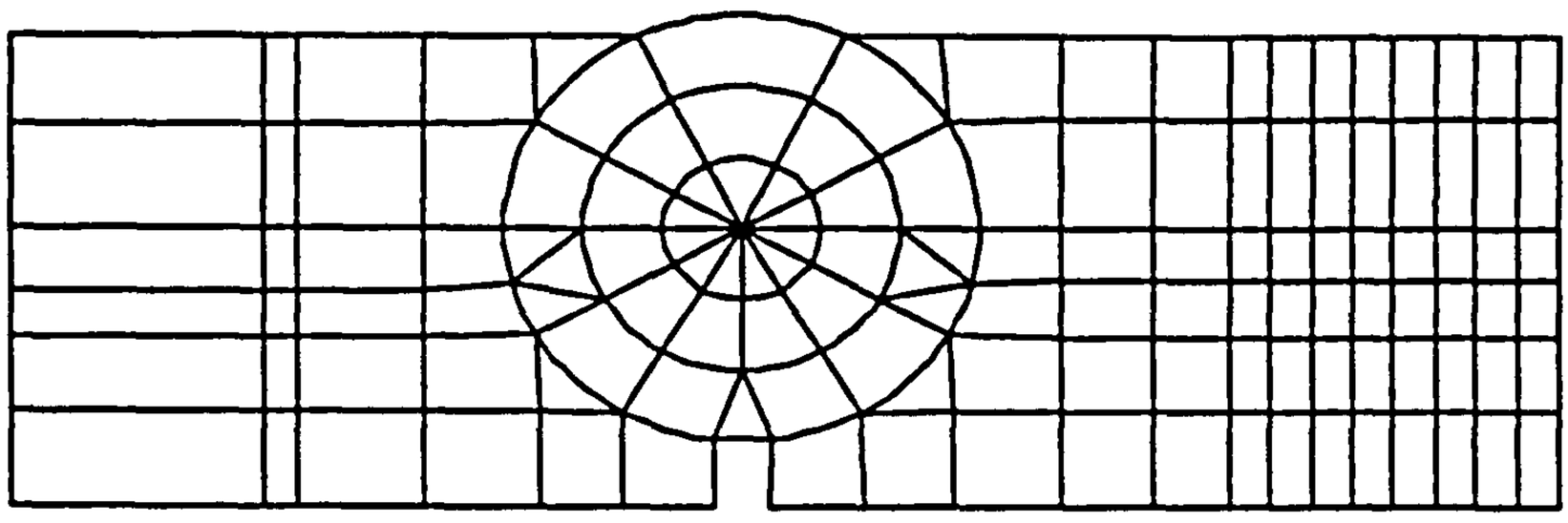

Fig 5.9 Finite Element idealization of a specimen clamped by curved jaws

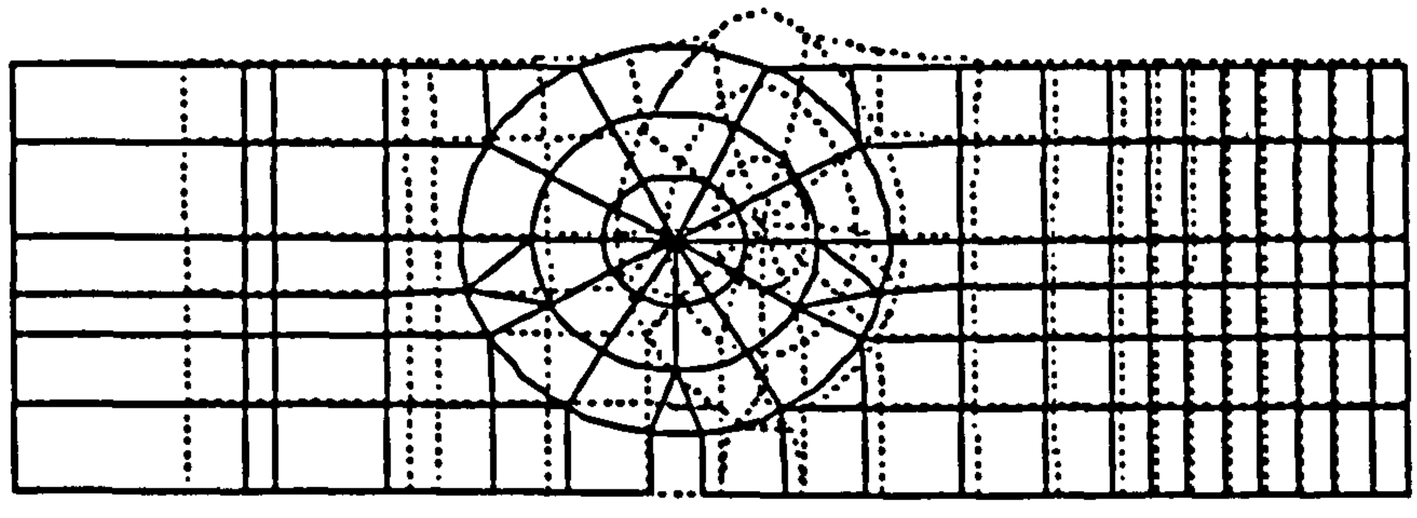

Fig 5.10 Deformed shape of a specimen clamped by curved jaws

Xiang et al (1988) investigated failure of rock during drag bit cutting by using the finite element method and they found for a sharp bit, that the rock was failing in shear.

There are normally two types of rock specimen geometry employed in rock cutting tests : cores or rectangular blocks. In this part of the work, the effect of different confinements on the samples with respect to those two geometries were investigated. For block specimens only a plate shape frame is required to keep the specimen in position. On the other hand cores can be held either with the flat clamping jaws or with cylindrically shaped clamping jaws. To consider which geometry is more suitable for rock cutting three different geometry models were investigated (see Figs 5.5, 5.6, 5.7, 5.8, 5.9, 5.10). When specimens are secured in clamping only a limited stress is applied. Therefore there was no need to use high confining stresses in the model. Consequently 0.35 MPa and 3.5 MPa were chosen as typical values of lateral pressure.

Three configurations was examined :

I-core with jaws

1-test 53 lateral pressure 0.35 MPa

2-test 54 lateral pressure 3.5 MPa

II-core with frame

1-test 36 lateral pressure 0.35 MPa

2-test 37 lateral pressure 3.5 MPa

III-block with frame

1-test 21 lateral pressure 0.35 MPa

2-test 22 lateral pressure 3.5 MPa

The stress distribution (of the principal stress components) was plotted against vertical axis from top to bottom of the specimen (diameter =75 mm) to show which geometry is favourable (Figs 5.11, 5.12 and 5.13). The results show both case I, and III are acceptable, and case I is better than

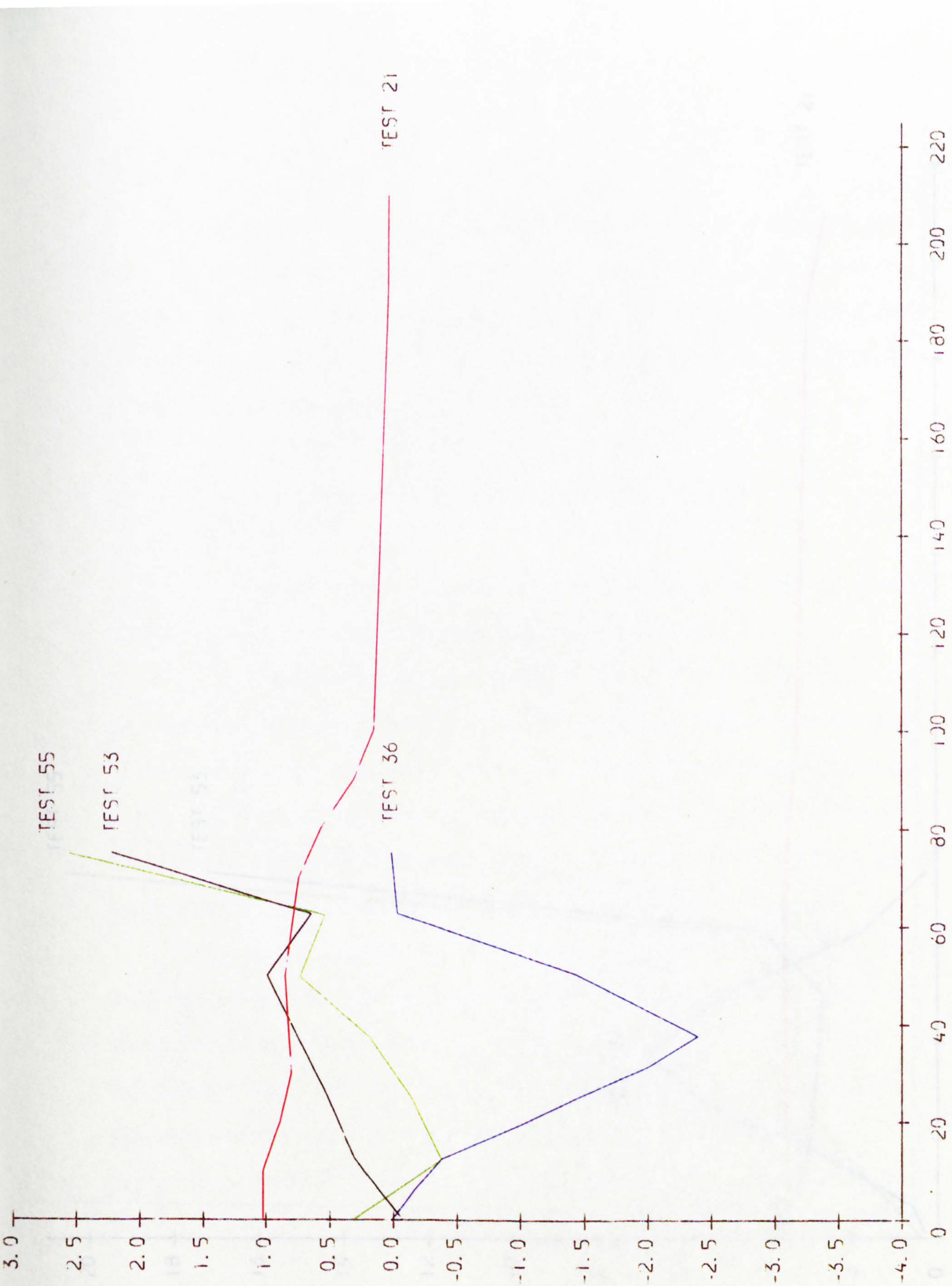

Fig 5.11 Principal stresses v Vertical distance from top of specimen

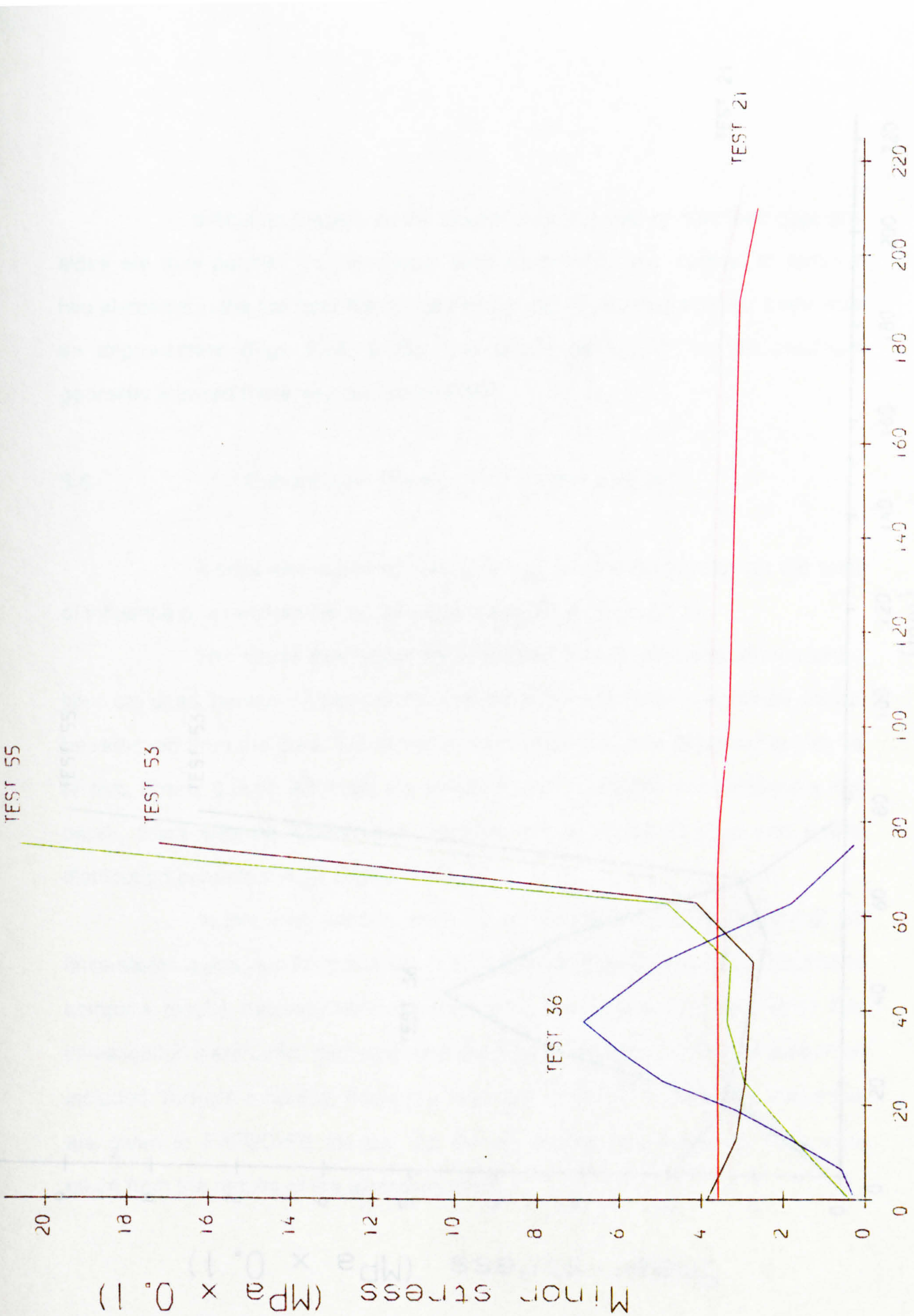

Fig 5.12 Minor principal stresses v Vertical distance from top of specimen

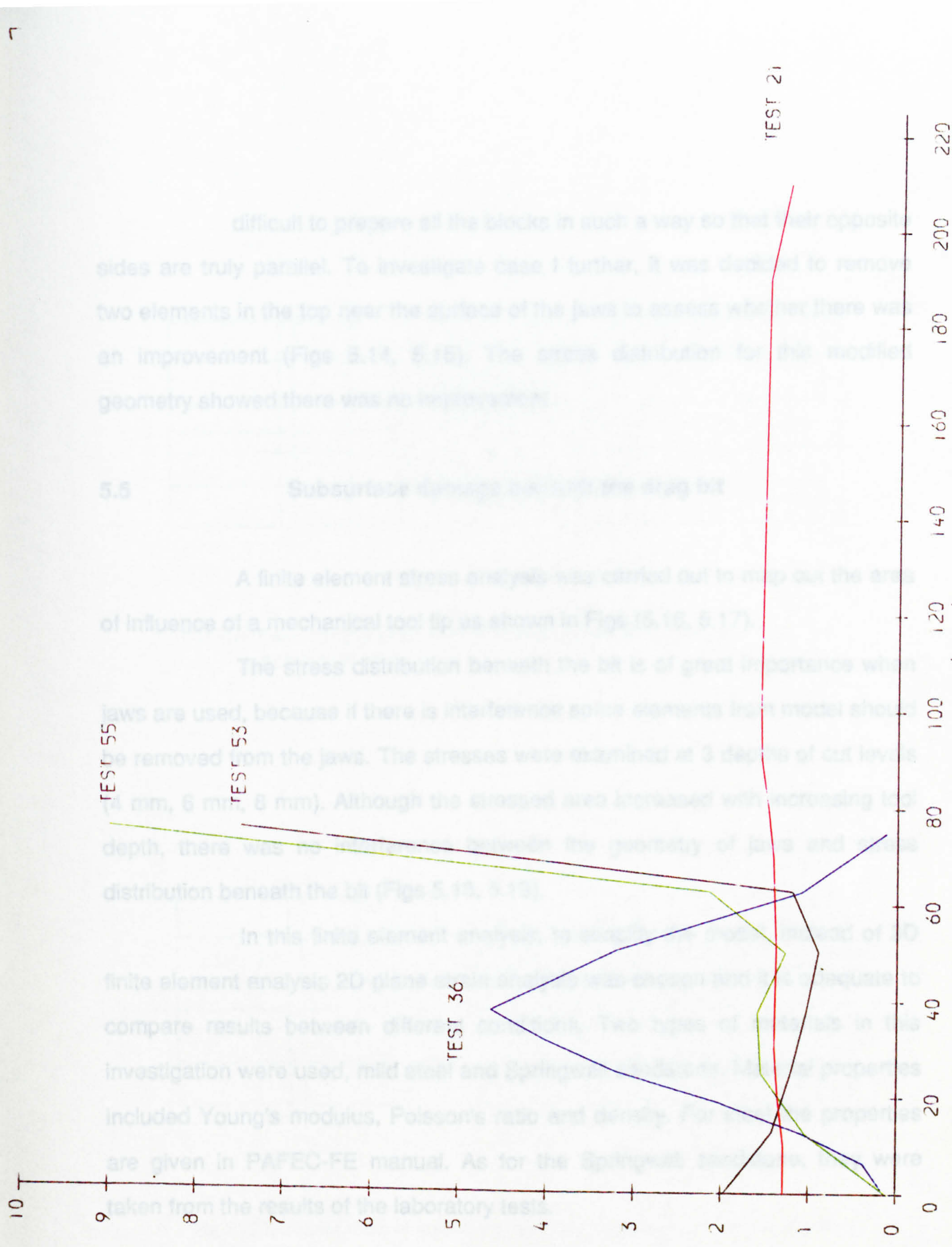

Fig 5.13 Shear stresses v Vertical distance from top of specimen

difficult to prepare all the blocks in such a way so that their opposite sides are truly parallel. To investigate case I further, it was decided to remove two elements in the top near the surface of the jaws to assess whether there was an improvement (Figs 5.14, 5.15). The stress distribution for this modified geometry showed there was no improvement.

5.5 Subsurface damage beneath the drag bit

A finite element stress analysis was carried out to map out the area of influence of a mechanical tool tip as shown in Figs (5.16, 5.17).

The stress distribution beneath the bit is of great importance when jaws are used, because if there is interference some elements from model should be removed from the jaws. The stresses were examined at 3 depths of cut levels (4 mm, 6 mm, 8 mm). Although the stressed area increased with increasing tool depth, there was no interference between the geometry of jaws and stress distribution beneath the bit (Figs 5.18, 5.19).

In this finite element analysis, to simplify the model, instead of 3D finite element analysis 2D plane strain analysis was chosen and it is adequate to compare results between different conditions. Two types of materials in this investigation were used, mild steel and Springwell sandstone. Material properties included Young's modulus, Poisson's ratio and density. For steel the properties are given in PAFEC-FE manual. As for the Springwell sandstone, they were taken from the results of the laboratory tests.

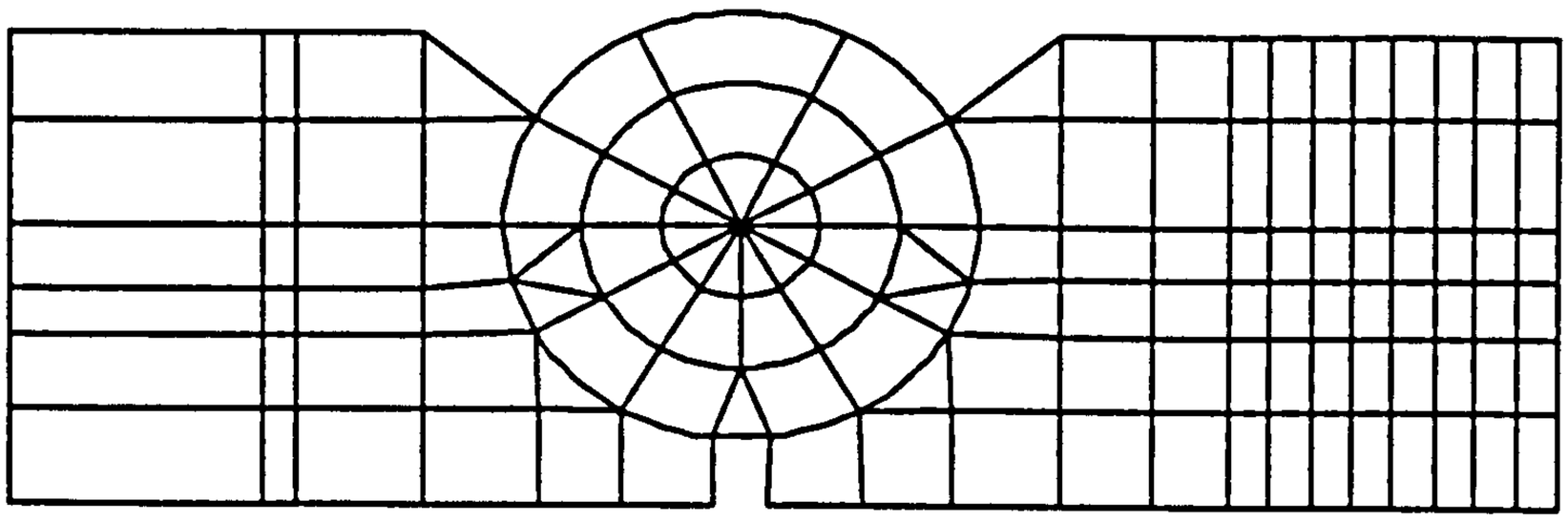

F ig 5.14 Finite Element idealization of assembly of specimen clamped by modified curved jaws

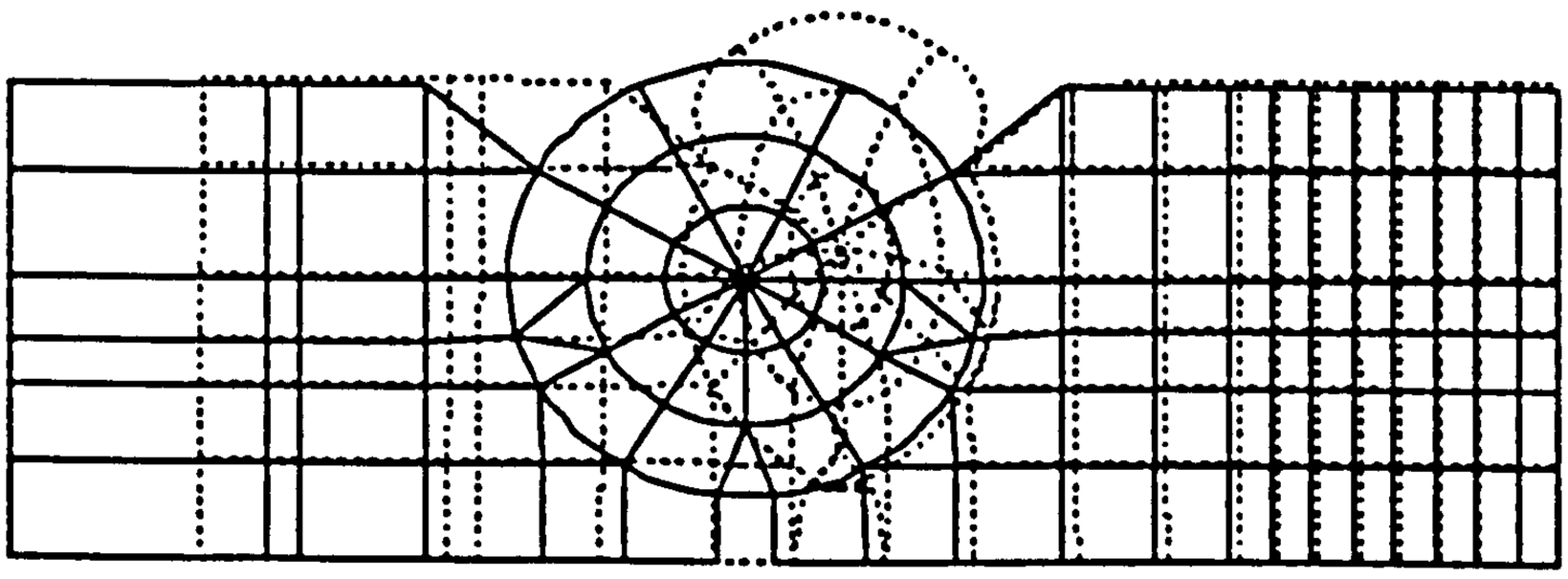

Fig 5.15 Deformed shape of assembly of specimen clamped by modified curved jaws

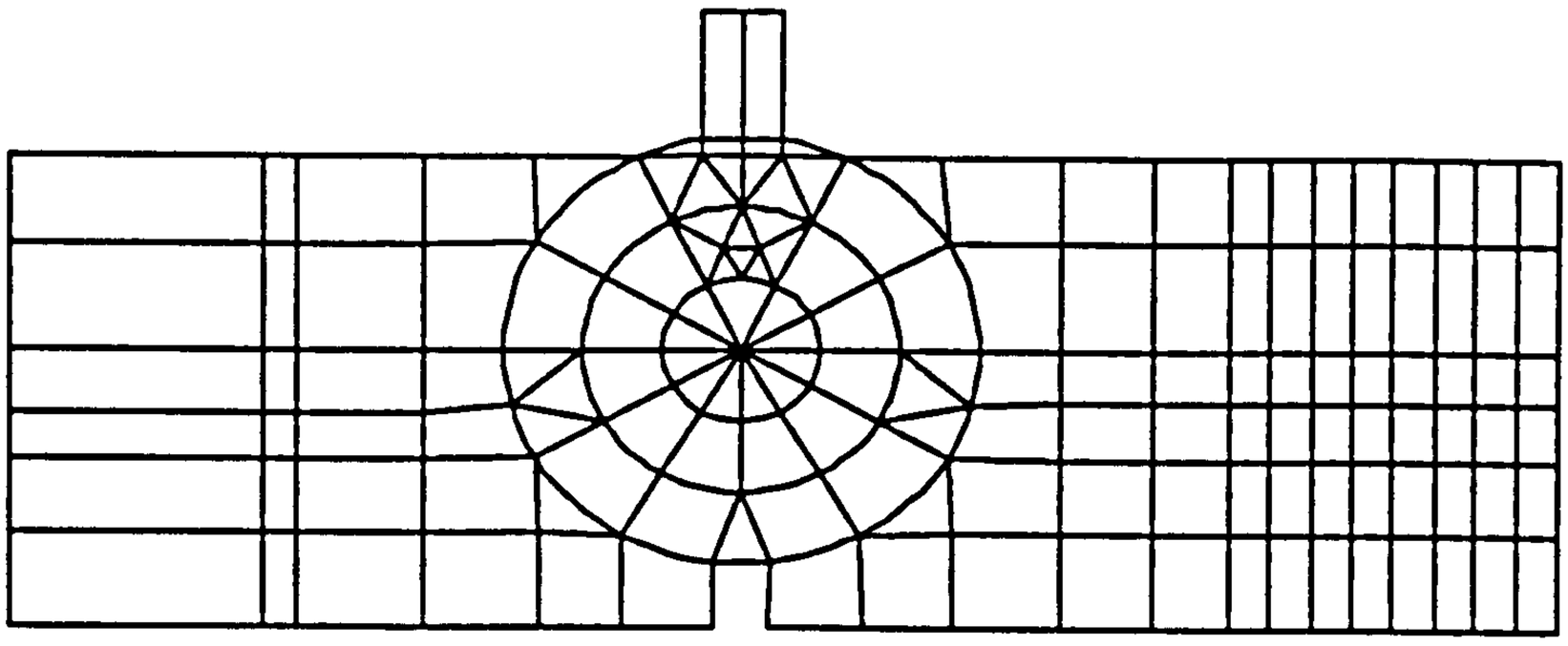

Fig 5.16 Finite Element idealization of a bit cutting a core specimen clamped by curved jaws

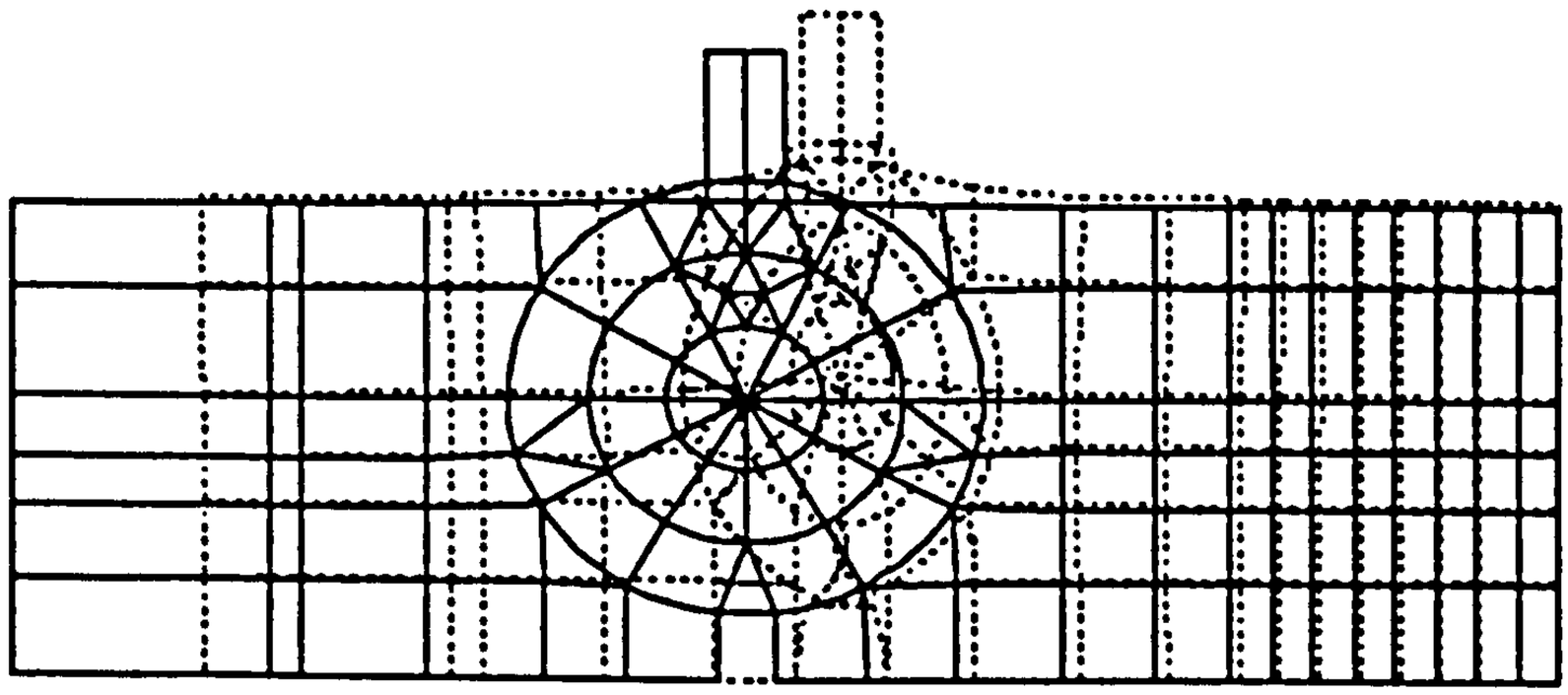

Fig 5.17 Deformed shape of a bit cutting a core specimen clamped by curved jaws

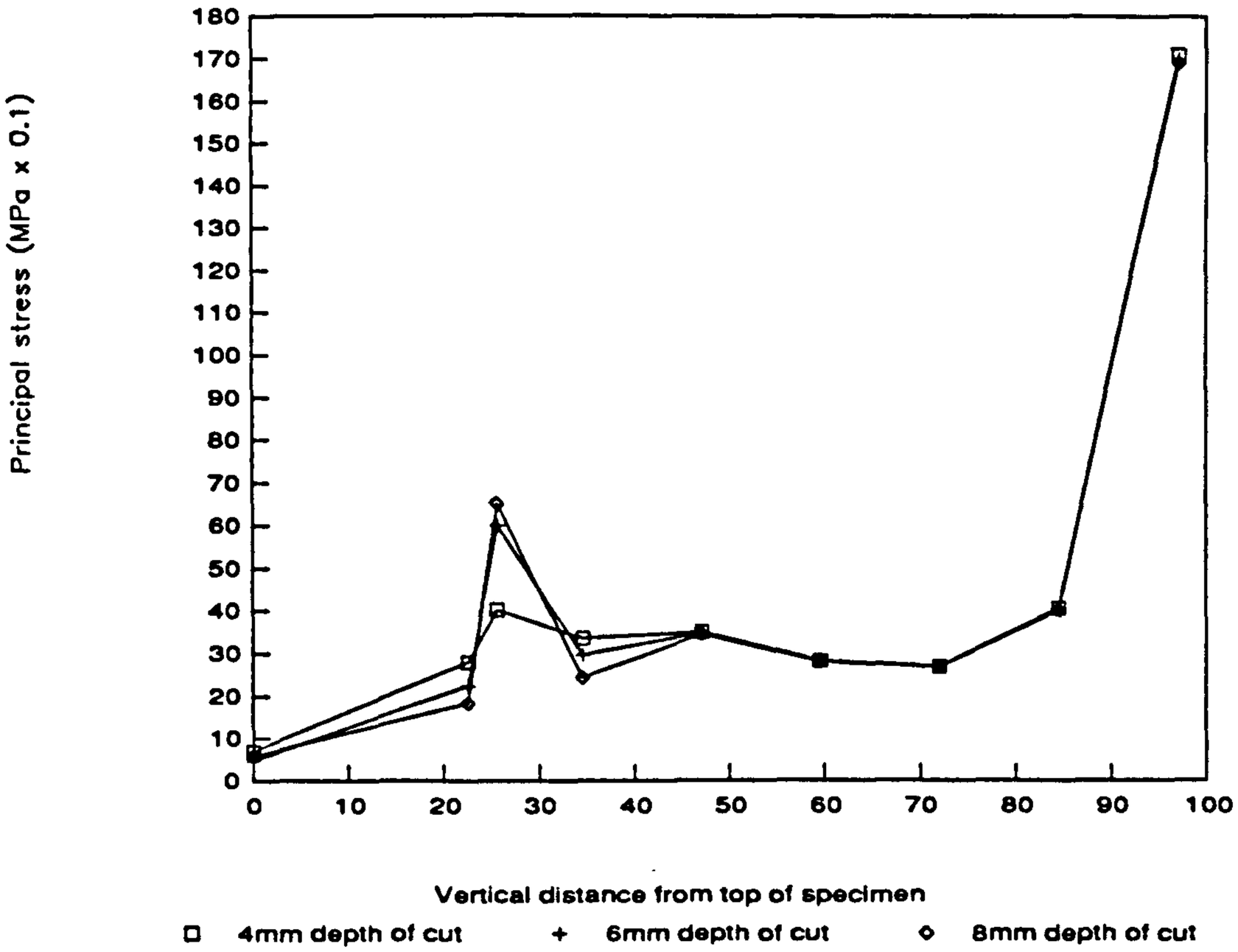

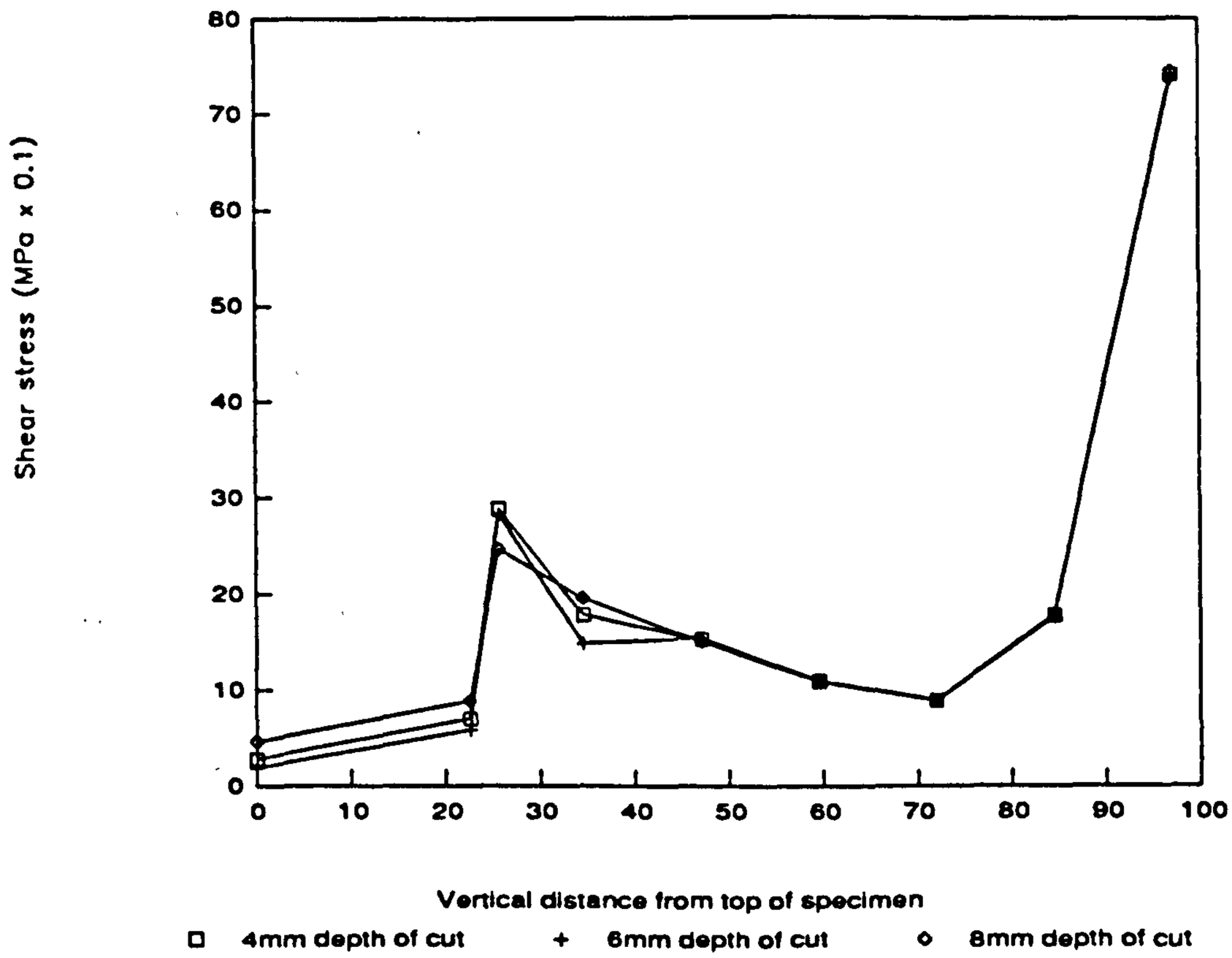

Figs 5.18, 5.19 Stress distribution of cutting bit

For each geometrical configuration the number of elements, number of nodes and degrees of freedom are:

	Test No				
	21	36	53	55	82
number of elements	3	36	87	86	106
number of nodes	7	83	150	137	153
degrees of freedom	39	34	35	34	38

The type of elements used are 8-noded and 6-noded isoparametric plate elements. The material properties employed were:

	Young's modulus (GPa)	Poisson's ratio ———	density (kg/m^3)
steel	209	0.3	7800
sandstone	15	0.25	2210.6

Full details of finite element graphics output are presented in Appendix 7.

5.6 Fracture mechanics tests

The fracture mechanics principles and the calculation of fracture toughness are examined later in chapter 7.

From the methods for measuring fracture toughness, ISRM has suggested the following two:

1-three point bend test

2-short rod test

These two methods are based on mode I fracture mechanics and there are two levels, level I that is employing load controled and level II that uses displacement controled. The main difference between level II and level I is time and accuracy. The available testing facilities were not suitable

for measuring fracture toughness at level II. Therefore in this investigation level I has been adopted for both types of test with a loading rate of 20.3 kN/min.

The tests were carried out on a 50 kN servo-hydraulic, closed loop testing machine. The load was read by a load ring-shaped transducer and recorded by a data logger using an LVDT. One LVDT and one clip gauge were used to measure the displacements. The LVDT was used for measurement of loading point deformation, the clip gauge was manufactured in the University on the basis of the ASTM E399-78 drawings (Fig 5.20) and it was calibrated to the nearest 0.0025 mm. A pair of knife edges that support the gauges'arms and serve as displacement reference points, were attached to the specimens using adhesive prior to testing.

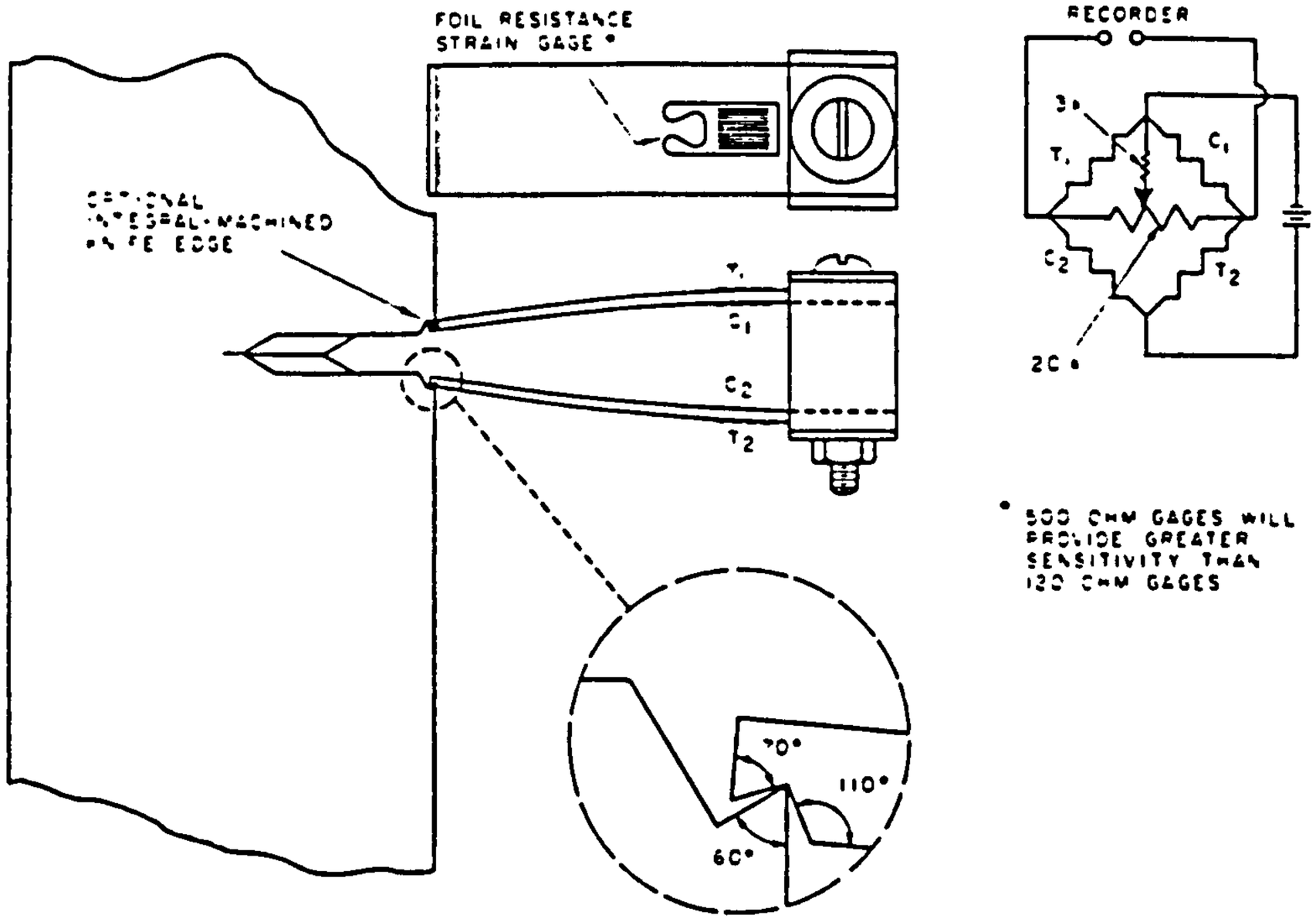

Fig 5.20 Clip gauge and its attachment to the specimen

All the data, which included the load, the point displacement, and crack open displacement, were monitored using a data logger (Plates 5.5, 5.6).

5.6.1 Three Point Bend Test

One of the methods introduced by ISRM is the chevron notched three point bend test. A core based specimen with a chevron-notch is illustrated in Fig 5.21. Loading at three points causes the chevron-notch to start crack propagation at the crack tip and proceed to the core axis in a stable fashion until the point where the fracture toughness is evaluated. The specimen dimensions are given in Table (5.1).

Table 5.1 Specimen and notch for 3 point bend test

geometry parameter	value	tolerance
specimen diameter (mm)	D	>10xgrain size
specimen length (mm)	4 D	>3.5 D
support span, S (mm)	3.33 D	±1.0
subtended chevron angle, θ°	90	±1.0
chevron v tip position, a_0 (mm)		0.15 D
notch width, t (mm)		<0.03 D or 1 mm

Using the geometry guidelines given in Table 5.5 the following geometry was implemented :

D=61 mm , s=200, a_0=9 mm and a=200 (according to Ouchterlony, 1988), see Fig 5.22.

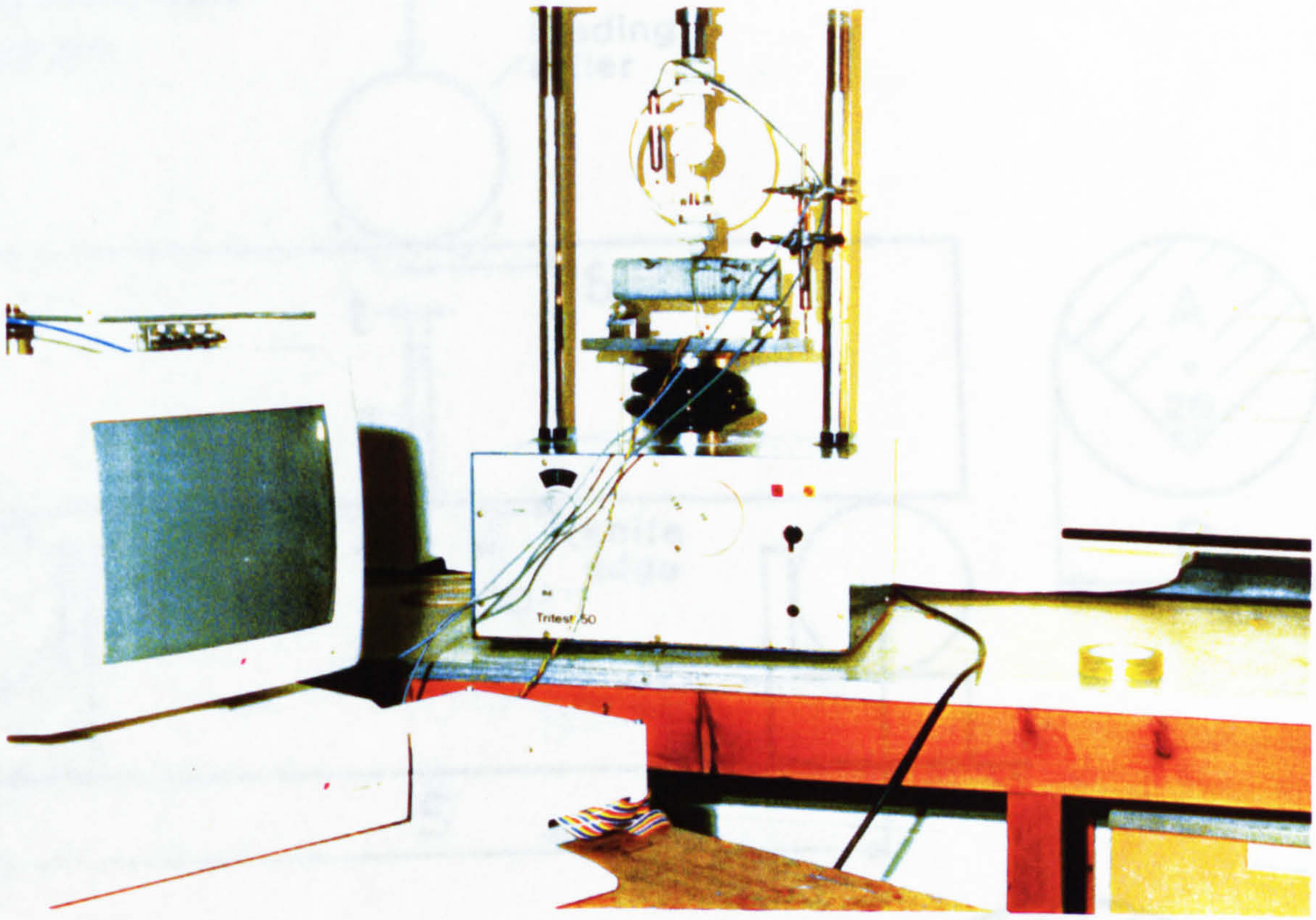

Plate 5.5 Setup for chevron bend test

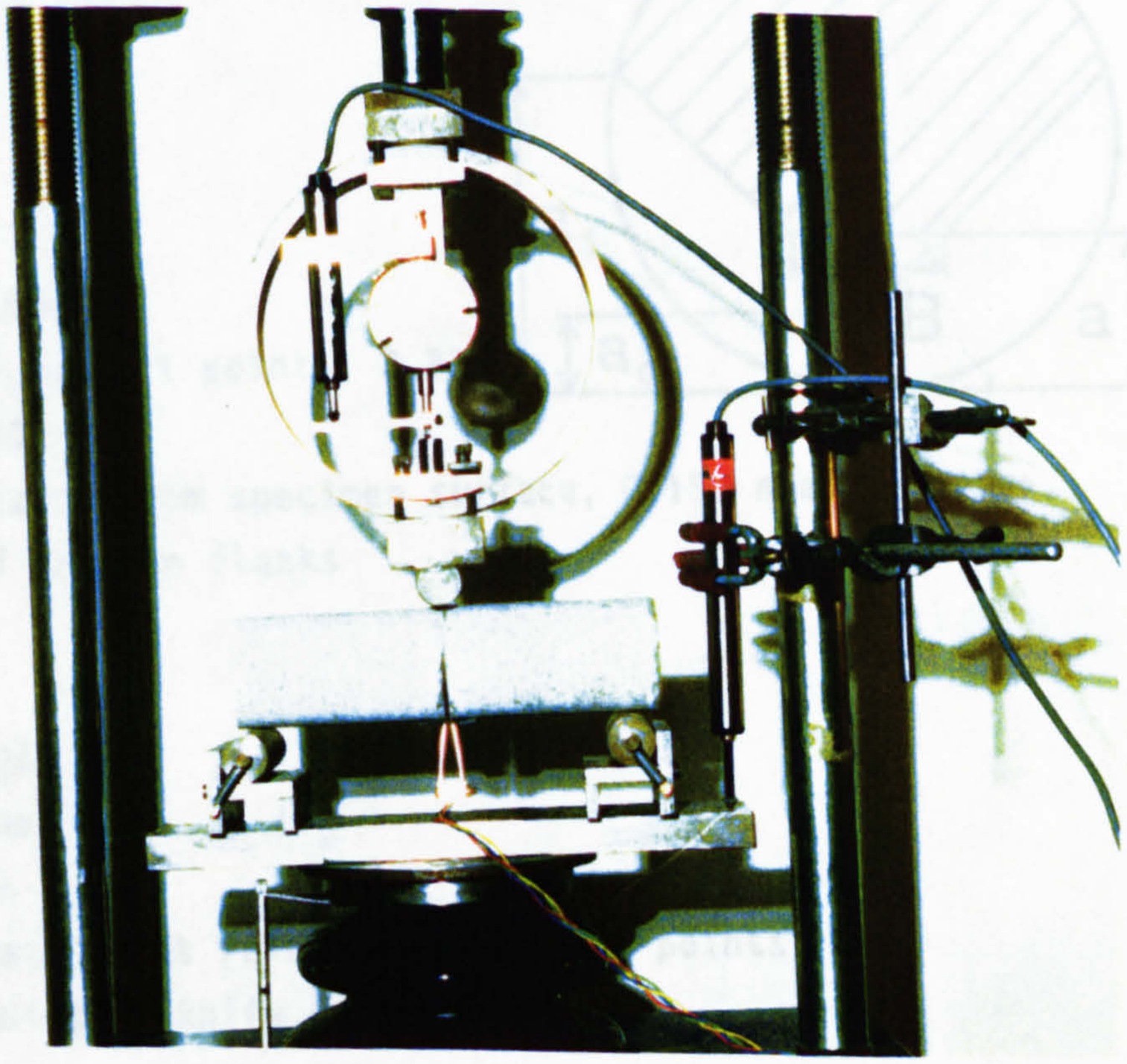

Plate 5.6 The load-displacement arrangements for chevron bend specimens

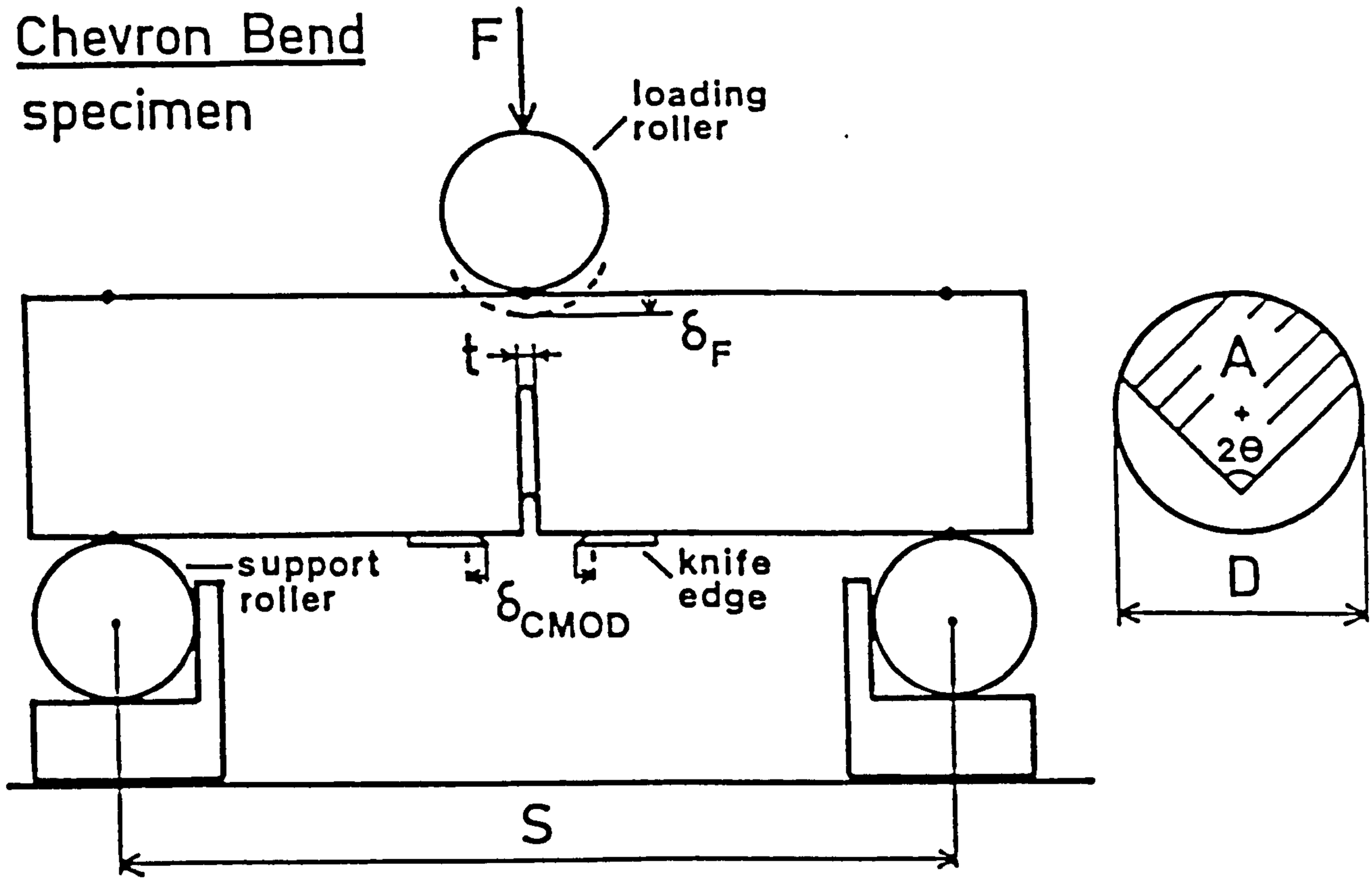

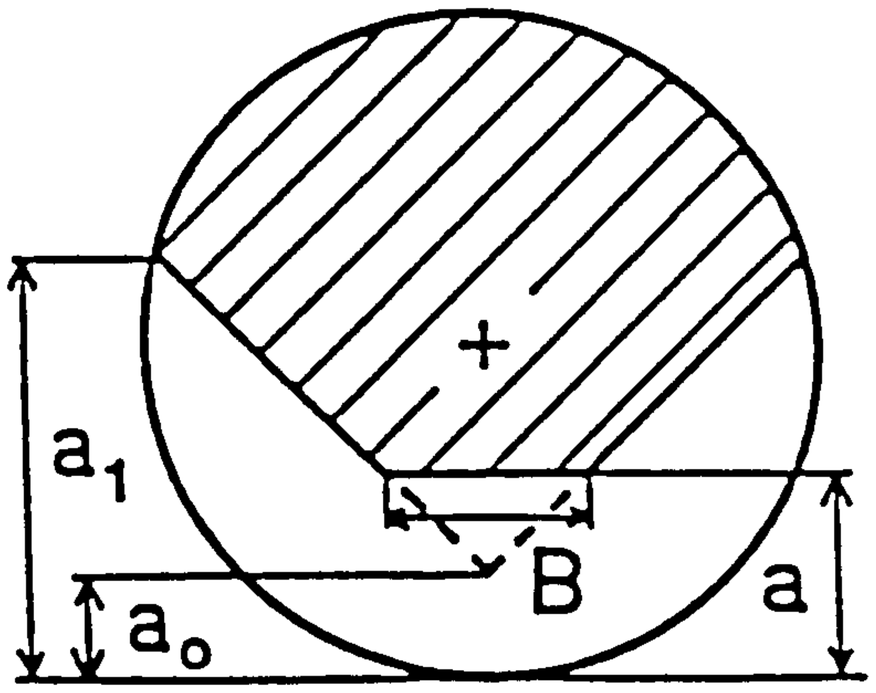

Basic notation:

D = diameter of specimen
S = distance between support points, 3.33D
2θ = chevron angle, 90°
a_o = chevron tip distance from specimen surface, 0.15D nominal value
a_1 = maximum depth of chevron flanks
t = notch width
a = crack length
B = crack front length
A = projected ligament area
F = load on specimen
δ_F = deflection of load point relative to support points, LPD
δ_{CMOD} = relative opening of knife edges, CMOD

Fig 5.21 Chevron bend test (Ouchterlony, 1989)

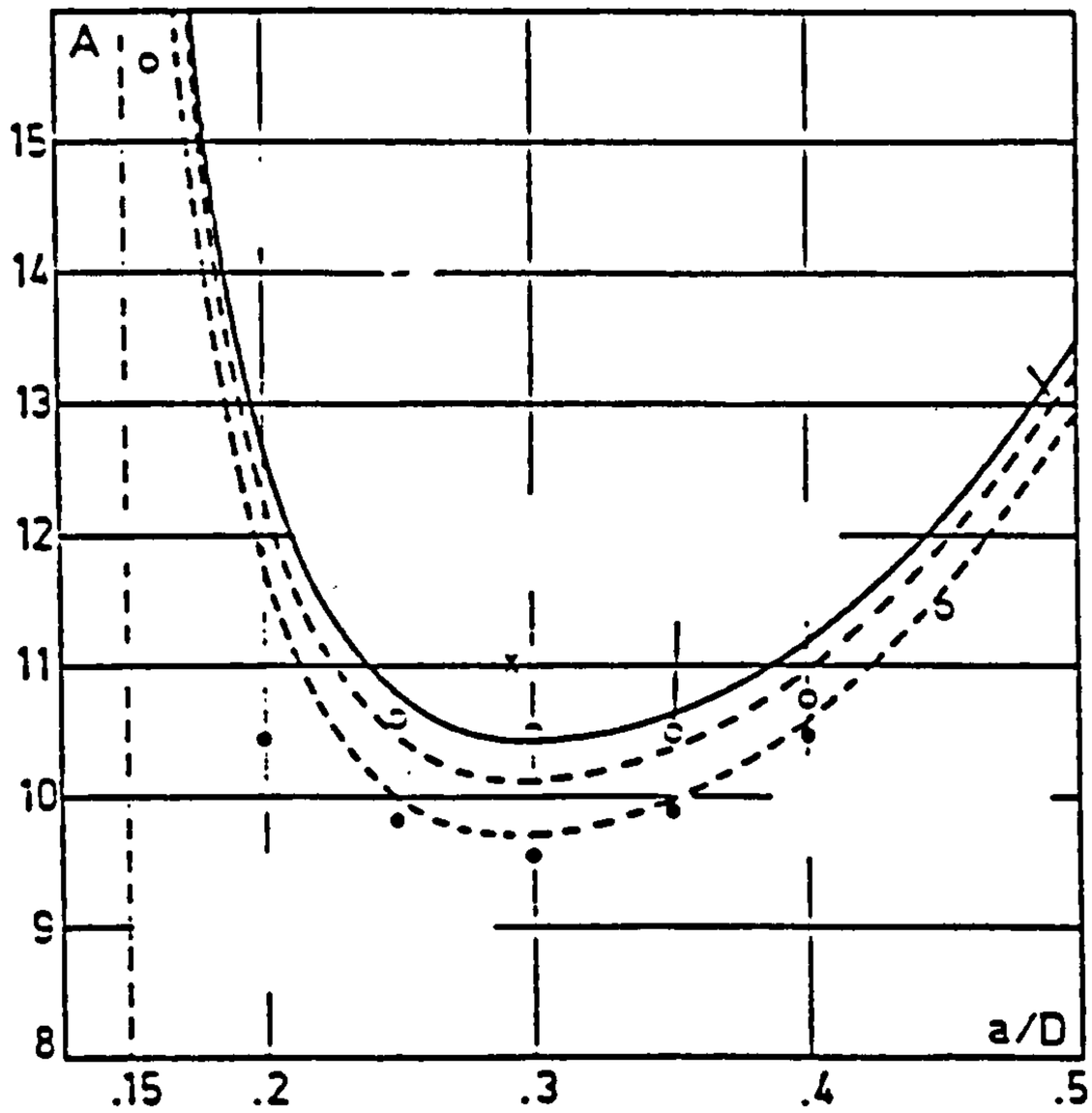

Fig 5.22 Normalised stress intensity factor curves
(after Ouchterlony, 1988)

In this type of test Springwell sandstone, Pennant sandstone, Teesdale Whinstone, Welton chalk and Matlock limestone were used characterised by the following grain size (Plate 5.7):

Springwell sandstone	0.5 mm to 0.75 mm
Pennant sandstone	up to 1.0 mm
Teesdale Whinstone	0.2 mm to 1.0 mm

Welton chalk and Matlock limestone are characterized by an amorphous mineral structure consequently grain size identification is not relevant.

The process followed requires a cylindrical specimen of diameter approximately 61 mm, length 220 mm notched with milling machine using a 100 mm diameter diamond wheel saw cut. The notch should be

placed at equal distances from the ends of the face. When the specimen is placed in the vice , first of all the distance between the saw blade and the specimen should be zeroed position, then the specimen should be cut to a depth of 0.25 D, which is 15 mm. After this cut, the specimen is rotated 90° with the aid of the fixture and cut again to the same depth as in the first cut.

Special alignment aids that facilitate accurate positioning of the specimen in the load fixture should be used in this method. First, it is used to centre the support rollers with respect to the upper (loading) roller and to give an exact support span length. Second, it is used aligning the specimen axis perpendicular to the rollers. Third the guide ensures that accurate centring of the notch between support rollers is achieved. The fixture as shown in Plate (5.8), has been used to set up three point bent test specimens. Once the load roller and two support rollers are fixed to parallel position, this set up should be suitable for all of the tests and there is no need for any movement. Another alignment aid which can be used is a metal plate which has a spirit level whose reference plane is the base of the testing machine. The direction of loading can be checked by inserting this plate into the notch. If this angle is unsatisfactory the specimen can easily be notched into the correct position. This metal plate can be used to identify the axis of span which is perpendicular to two support rollers.

5.6.2 Short Rod Test

The geometry of the short rod specimens is illustrated in Fig (5.23). The specimen dimensions for this method suggested by ISRM are given in Table (5.2).

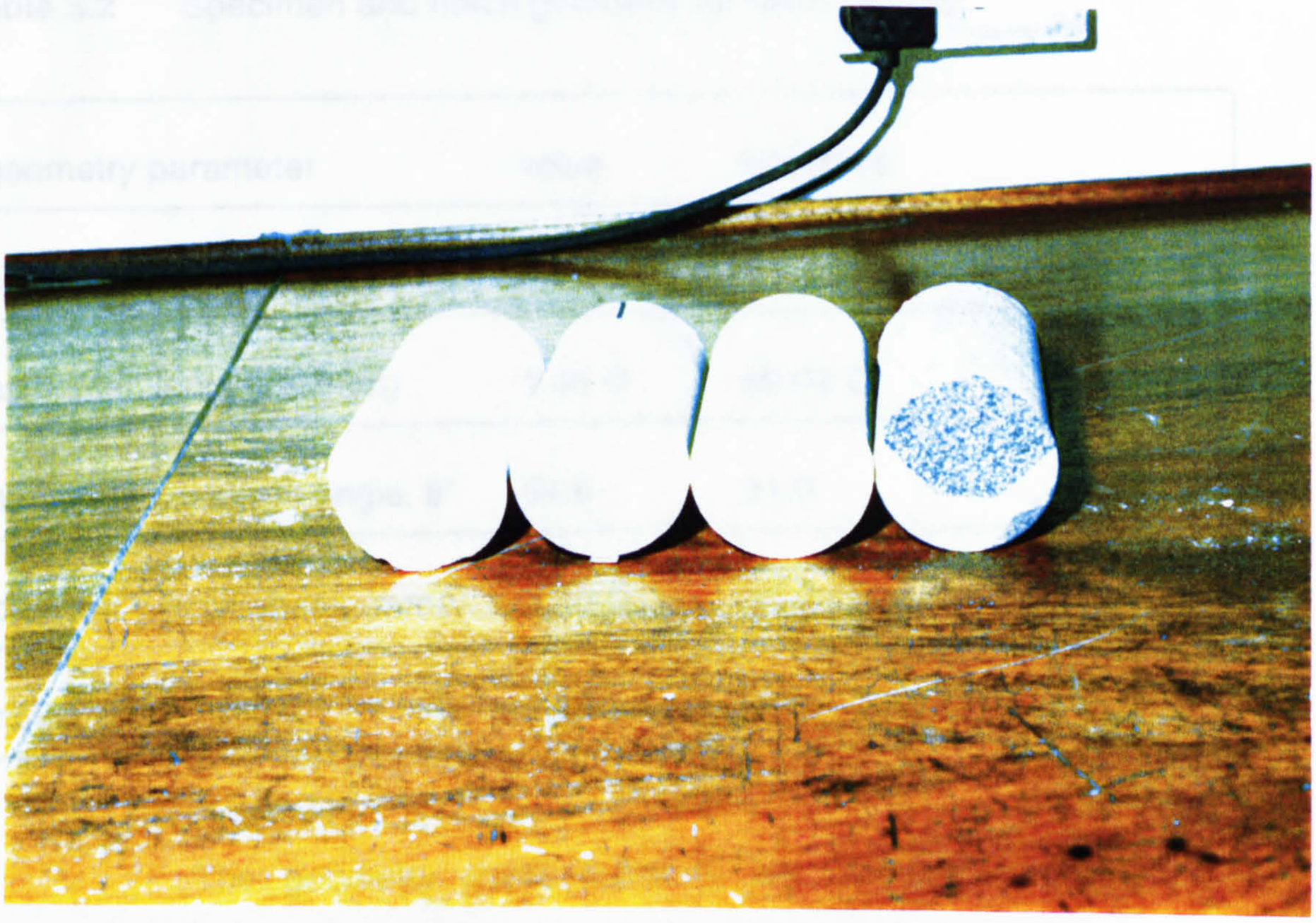

Plate 5.7 The chevron bend specimen

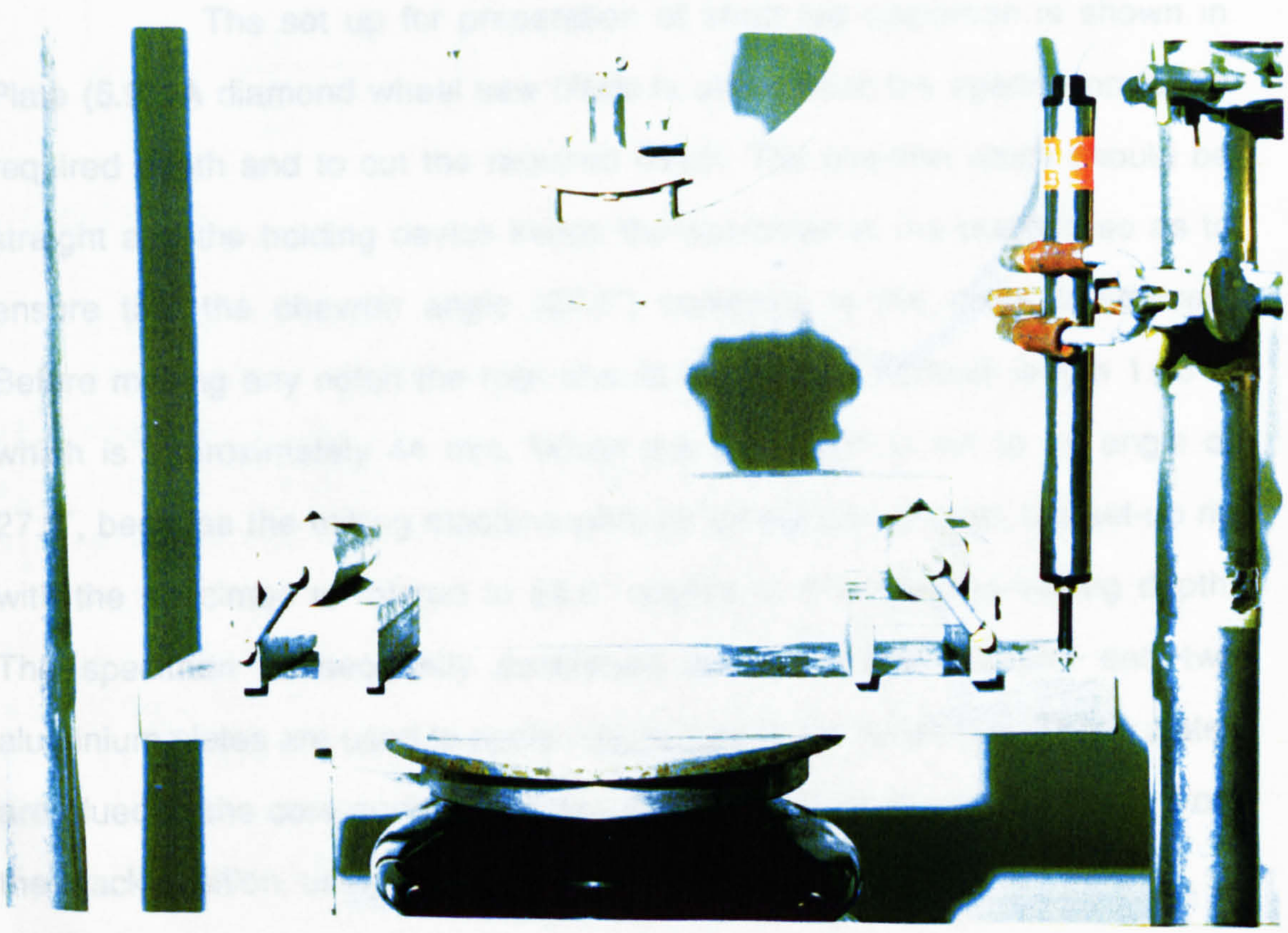

Plate 5.8 Diagram of alignment fixture for chevron bend specimens

Table 5.2 Specimen and notch geometry for short rod test

geometry parameter	value	tolerance
specimen diameter (mm)	D	>10 x grain size
specimen length, w (mm)	1.45 D	±0.02 D
subtended chevron angle, θ°	54.6	±1.0
chevron v position, a_o (mm)	0.48 D	±0.02 D
notch width, t (mm)		<0.03 D or 1 mm

The geometry used, following the guidelines of Table 5.2 resulted in a D=44 mm, a_o=21 mm and a=30 mm (Ingraffea, 1982)

The set up for preparation of short rod specimen is shown in Plate (5.9). A diamond wheel saw blade is used to cut the specimens to the required depth and to cut the required notch. The chevron notch should be straight and the holding device keeps the specimen in the position so as to ensure that the chevron angle (27.3°) conforms to the given tolerances. Before making any notch the rock should be cut to a nominal length 1.45 D which is approximately 44 mm. When the first notch is cut to an angle of 27.3°, because the milling machine with the saw blade is fixed, the set-up rig with the specimen is rotated to 54.6° degree to the required cutting depth. The specimen subsequently positioned in the testing machine and two aluminium plates are used to apply tensile load to the specimen. These plates are glued to the core surface and are set parallel and at equal distance from the crack position, using a space bar with a stem in the middle.

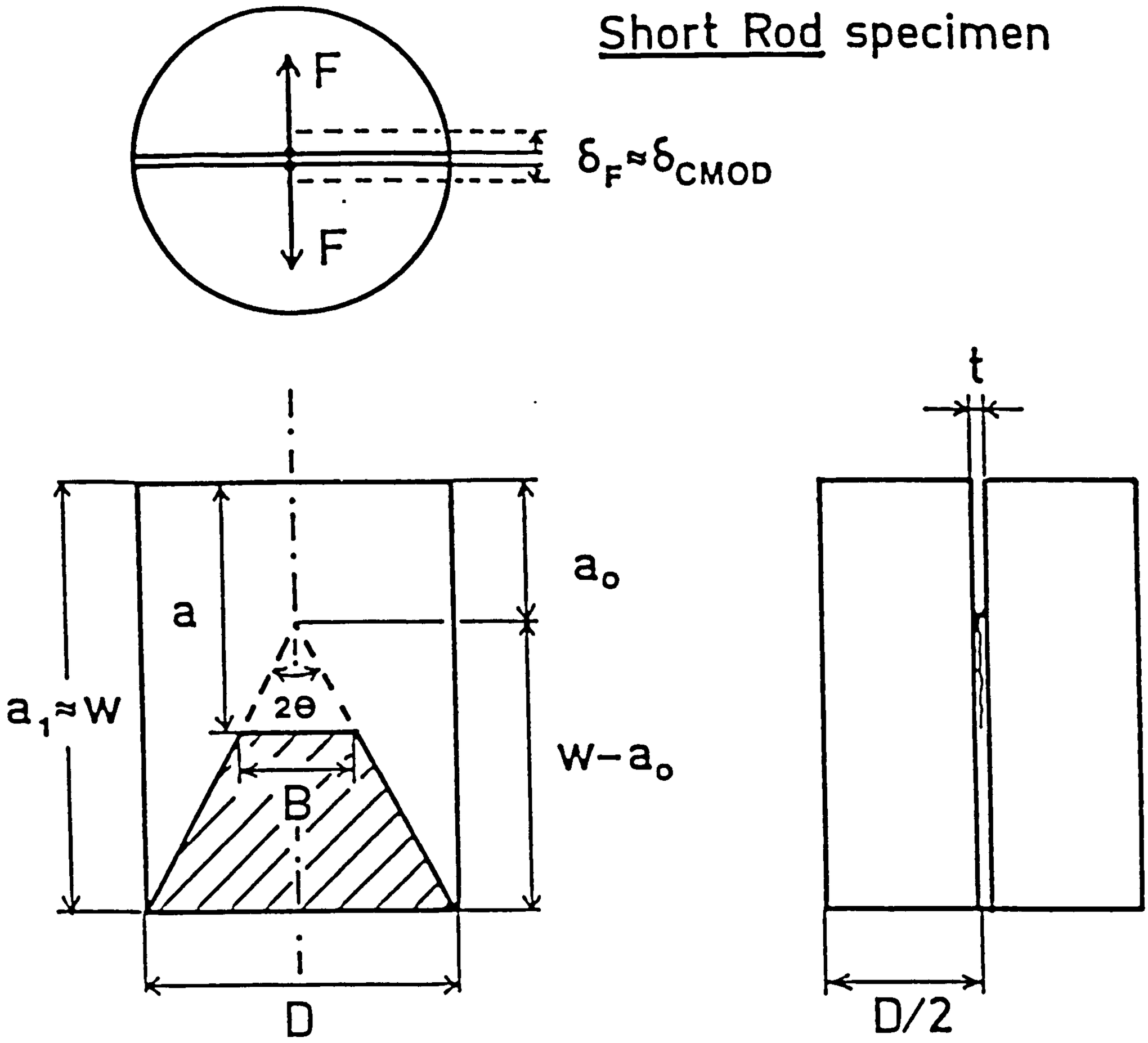

Basic notation:

D = diameter of short rod specimen
w = length of specimen, 1.45D
2θ = chevron angle, 54.6°
a_o = chevron tip distance from load line, 0.48D
a_1 = maximum depth of chevron flanks, in practice not necessarily equal to w.
t = notch width
a = crack length
B = crack front length
F = load on specimen
δ_F = load line displacement, LPD
δ_{CMOD} = crack mouth opening displacement, CMOD ≈ LPD

Fig 5.23 Short Rod test (Ouchterlony, 1989)

Short rod testing requires a tensile load to be applied to the specimen to be tested. A fixture is shown in Plates (5.10, 5.11) has been used to record the maximum load failure in level I testing as described before. The clip gauge measures the relative displacement of two precisely located gauge positions spanning the notch mouth with a pair of accurately machined knife edges that support the gauge arms and serve as displacement reference points.

If necessary a sling is used to hold the specimen firmly in the testing rig. A stem can apply load corresponding to a displacement with a constant rate of 4.8 mm/min.

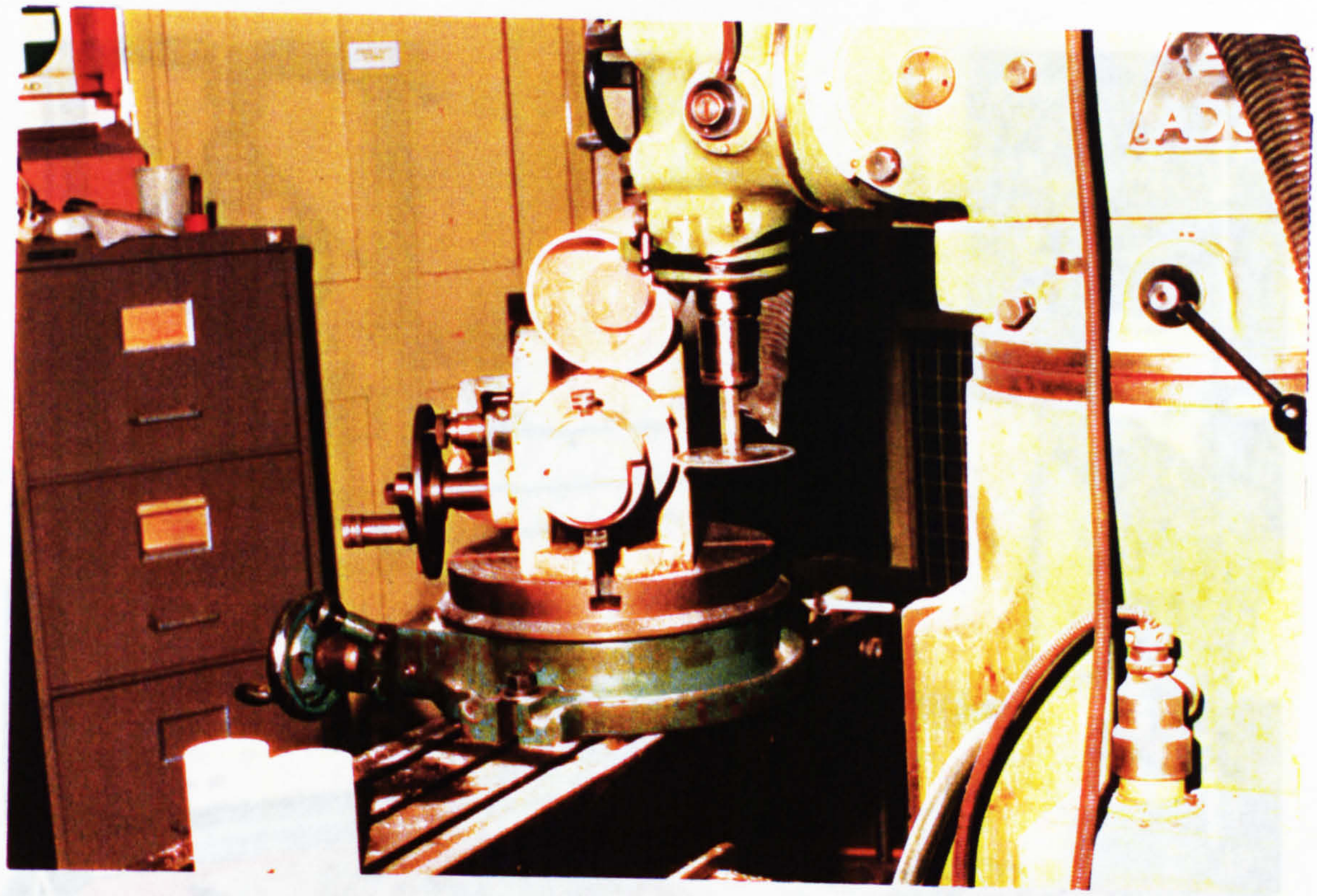

Plate 5.9 Preparation of short rod specimen

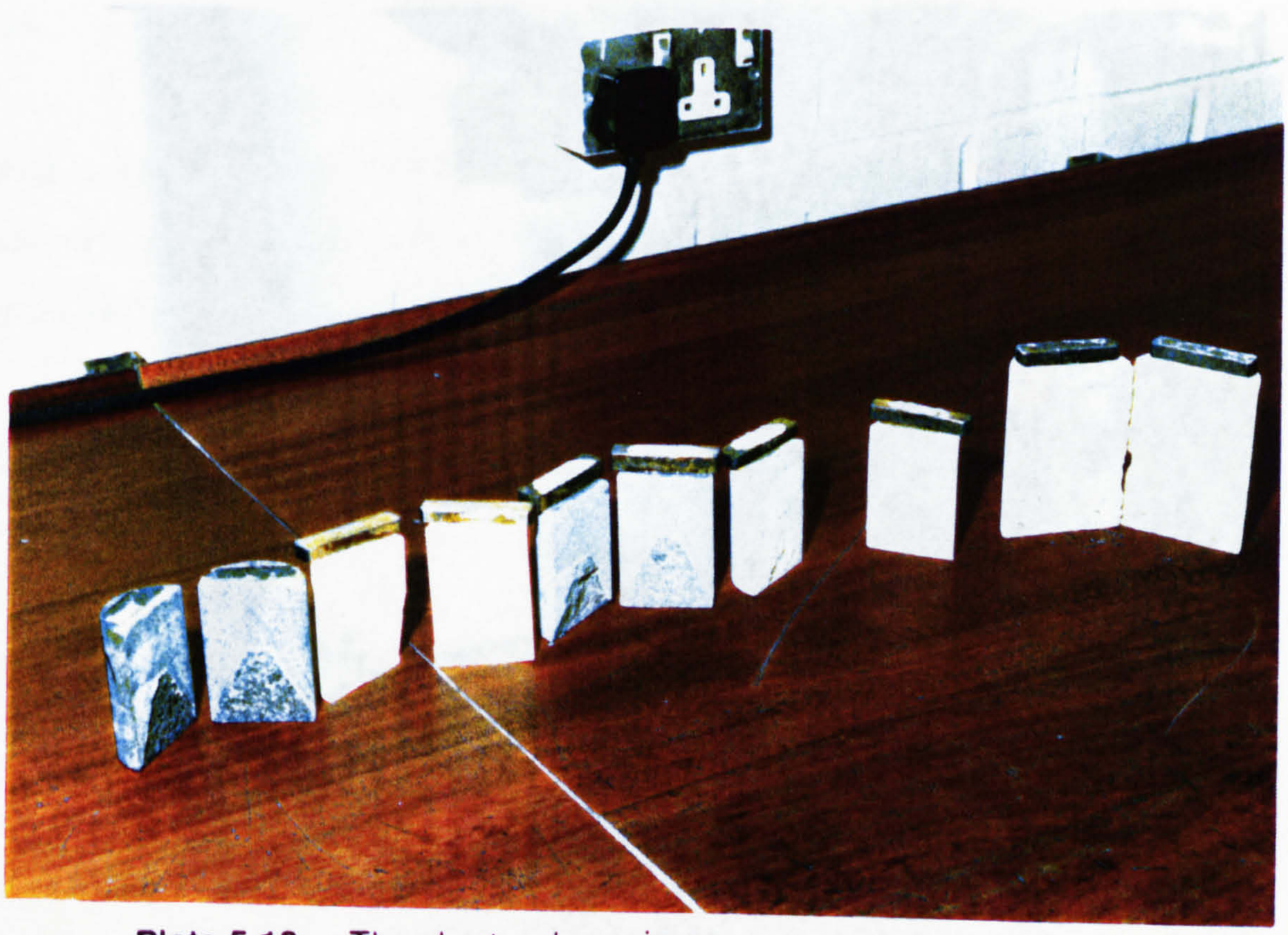

Plate 5.10 The short rod specimen

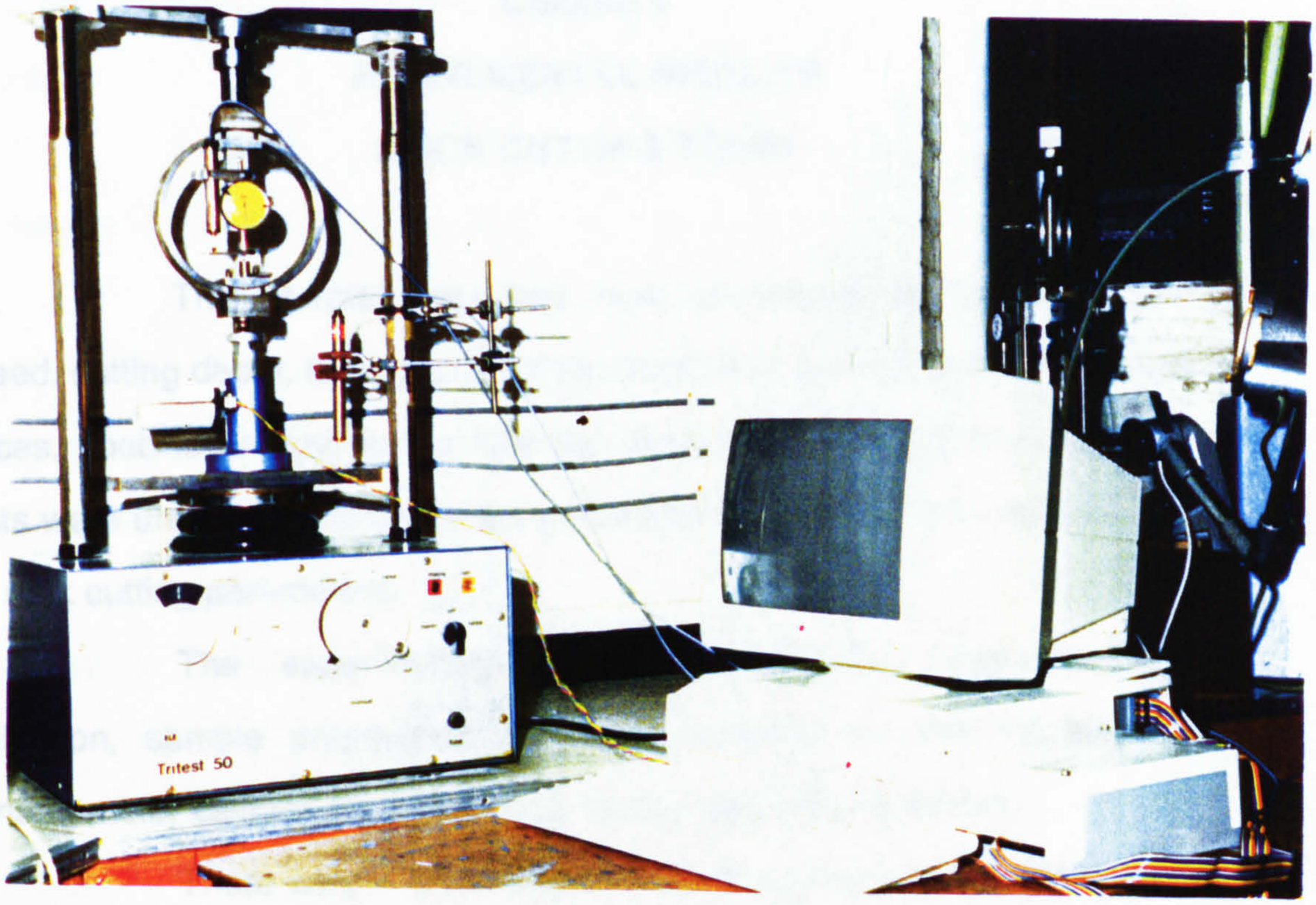

Plate 5.11 Setup for short rod fracture test

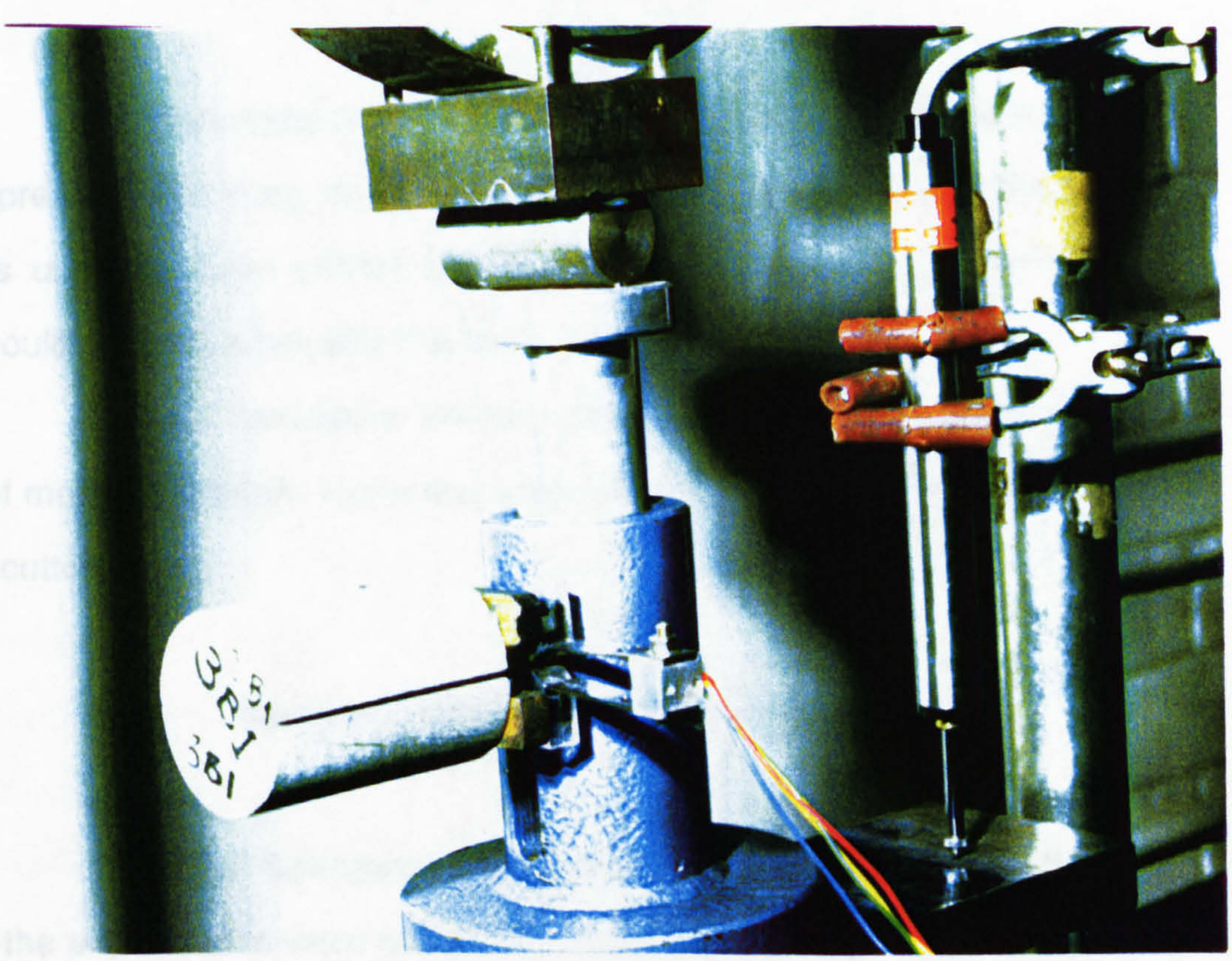

Plate 5.12 The load-displacement arrangements for short rod specimen

Chapter 6

EXPERIMENTAL RESULTS

ROCK CUTTING TESTS

This chapter describes how operational parameters (cutting speed, cutting depth, tool spacing) may affect rock cutting parameters (cutting forces, specific energy) in the fully saturated state. Furthermore, laboratory tests were undertaken to investigated the effect of presence of discontinuities on rock cutting parameters.

The experimental procedures followed involved sample collection, sample preparation, attaching samples on the machine bed, dynamometer calibration, mechanical cutting and data collection.

There was a need to test rocks specimens ranging from strong to weak, in an attempt to verify the validity of the conclusions reached in this work.

Pennant sandstone and Teesdale Whinstone were selected as being representitive strong rocks, while at the same time they were the same materials used by Zhao (1989) for fracture mechanics tests, therefore his results could be compared with this work.

Matlock limestone, Welton chalk and Springwell sandstone are typical of medium strength rocks and were also used by Jamalbastami (1990) for rock cutting tests.

6.1 Sample collection and preparation

Because Springwell sandstone is a locally available material most of the experiments were conducted using this type of rock. Large blocks were reduced with saw machines to 75 mm x 150 mm x 200 mm, bringing

them to the right size for a desiccator which was used for the water saturation.

For core grooving tests, cylindrical specimens of 75 mm diameter and 250 mm length were chosen.

For Springwell sandstone three moisture content states were chosen : dry, ambient and saturated. For the other rock materials (Pennant sandstone, Matlock limestone, Welton chalk) because of the lack of available material only ambient and saturated states were examined.

Most of the rock cutting experiments conducted by previous investigators dealt with intact materials, despite the importance of discontinuities and their effects on cutting parameters. Furthermore very limited research have been conducted in cutting jointed rocks under saturated conditions.

Under in situ conditions, moisture is present in geological layers, therefore there is a need to investigate cutting parameters under such conditions and to compare with dry and ambient moisture content to see the extent of the effect.

6.2 Core grooving of discontinuous rock

Specimens were water saturated by placing them in a desiccator for three hours. The test were done in different states as follows :

1-intact

2-with a single discontinuity (discontinuity angle 30° to core axis)

3-with a single discontinuity (discontinuity angle 45° to core axis)

4-with a single discontinuity (discontinuity angle 60° to core axis)

5-with a single discontinuity (discontinuity angle 75° to core axis)

6-with a single discontinuity (discontinuity angle 90° to core axis)

7-with a two parallel discontinuities (discontinuities angle 90° core axis)

8-with three parallel discontinuities (discontinuities angle 90° to core axis)

For all cases the above tests were conducted under dry, ambient, and saturated conditions. For each case a favourable reduction was observed in MCF from dry to ambient and from ambient to saturated condition. In addition the effect of angle was investigated. After observing no relationship between MCF and the relative angle of discontinuity, it was assumed that there may have been an interaction between the influence of angle of discontinuity and spacing of the discontinuity. To investigate the influence of the angle of discontinuity it was decided to conduct some tests with constant discontinuity spacing. However it was not possible to derive any meaningful relationship concerning the investigated parameters.

It was possible to show from the results that there is a reduction in specific energy for the joint spacing:

1-dry specimens:all the forces and SE were reduced proportionally as a function of the frequency of spacing.

2-ambient : there was no difference for yield and coarseness index between intact specimen and specimen containing a single discontinuity but there was a reduction of specific energy for two discontinuities.

3-saturated : MCF,MNF decreased from intact specimen to specimen containing a single discontinuity and again to two discontinuities, but PCF and PNF increased from intact to single discontinuity and further decreased for double discontinuity.

SE increased from intact to single discontinuity then decreased from single discontinuity to double discontinuity.

Comparison of the results of intact specimens with discontinuities show that there was a small increase in SE from intact specimen to specimen with one discontinuity. However there was a decrease in SE when examined the result of specimen with single discontinuity in comparison with specimen containing two discontinuities (see results in Appendix 2.1).

The general conclusions for the three states (dry, ambient, saturated) discontinuity in the rock specimens reduces the strength and the number of discontnuities is not important. This means when spacing is large enough (above 50 mm) rock behaves as intact rock.

6.2.1 Effect of angle of discontinuity for cuttability of rock

1-dry : if the SE results are examined for the intact specimen and as the angle of the discontinuity ranges from 75° to 30°, it can be seen that the best results, concerning specific energy, correspond to the angle of 75° and the worst to 30°. This is very important because SE was found in this position to be more than the SE of intact rock.

2-ambient : similarly there appears to be a reduction as the angles range from 75° to 30° and the best angle concerning SE is 30°.

3-saturated: with reference to the SE values it can be seen that the best angle is 60° and the worst is 45°.

Because the results showed that there is no trend between angle of discontinuities and cutting forces it was thought that tool spacing might affect the results. For this reason a series of tests were conducted with tool spacing held constant and also with discontinuity held constant. Again for

a discontinuity angle between 30°, 45° while the tool spacing was maintained constant, no significant influence on the cutting forcesr and SE was identified (Appendix 2.2).

6.2.2 Effect of spacing of discontinuities

To investigate the effect of the spacing of the discontinuities angle was kept constant while different spacings were examined.

When the discontinuity spacing was chosen to be very small, i.e 10 mm it was found that this spacing is advantageous (in terms of SE). Furthermore it appears that the discontinuum rock behaves as an intact rock if the spacing of discontinuities is greater than 10 mm. In this investigation for an angle of 45° a spacing of 50, 60, 85 and 95 mm was used and also for an angle of 30° a spacing 50 mm and 60 mm was adopted.

Aleman (1983) found that discontinuities spaced every 10 mm will dramatically increase cutting rate of mudstone.

6.2.3 Effect of type of intercalated geologic materials

Geological beds often are formed by different layers, for this reason it was decided to investigate the situation where different geological materials are in succession. It was decided to intercalate chalk and clay layers between sandstone (angle of discontinuity was 90°with respect to core axis).

When chalk was inserted between sandstone was placed all the forces increased except MCF which remained unchanged, the results are shown in (Table 6.1).

Table 6.1 Cutting Parameters of different types of specimen

Specimen Type	PNF kN	PCF kN	MNF kN	MCF kN
intact sandstone	2.70	3.54	1.69	1.73
sandstone with 1 discontinuity	2.12	3.00	1.41	1.31
composite sandstone containing chalk intercalation	2.43	3.17	1.47	1.31

For the next test China clay was used as filling material between three parts of sandstone with different thickness. The cutting forces decreased with clay intercalations, and also decreased with as the thickness of clay decreased.

It appears that 10 mm clay thickness results in the lowest forces and 25 mm to the largest forces, the relevant data are shown in Table 6.2 :

Table 6.2 Cutting Parameter of sandstone with intercalated clay

Specimen Type	MNF kN	PCF kN	PNF kN	MCF kN
sandstone without clay, with discontinuity	2.12	3.00	1.41	1.31
composite sandstone with 10 mm thickness clay	2.14	2.91	1.31	1.29
composite sandstone with 18 mm thickness clay	1.91	2.55	1.10	1.16
composite sandstone with 25 mm thickness clay	1.80	2.38	1.02	0.90

All the forces due to more compacting clay show favourable increase.

In another set of experiments where clay was intercalated between chalk the results showed that all the forces were reduced (Table 6.3):

Table 6.3 Cutting Parameter of chalk with intercalated clay

Specimen Type	PNF (kN)	PCF (kN)	MNF (kN)	MCF (kN)
chalk, one discontinuity	3.31	3.81	1.94	1.60
composite chalk with 10 mm , thickness clay between 3 parts of chalk	2.23	2.82	1.19	1.125

6.3 Effect of different degree of saturation

A total of 64 cutting experiments were carried out in Springwell sandstone for different saturation levels, from partial saturation to full saturation. The curves of the forces versus different degrees of saturation were drawn and as it can be seen water saturation had introduced a reduction of the cutting forces. Instead of using the actual water content the ratio between the moisture content of each sample and maximum saturation content (Ws/Wt) was used. The trend between water saturation and SE is very similar to that between water saturation and UCS of rock (Figs 6.1, 6.2, 6.3, 6.4) but for other materials such as chalk is not the same. this issue is discussed later.

6.3.1 Springwell sandstone

Springwell sandstone was used at three states of moisture content, dry ambient and saturated. Detailed results are given in Appendix (2) , and an summary of these results is given in Table 6.4.

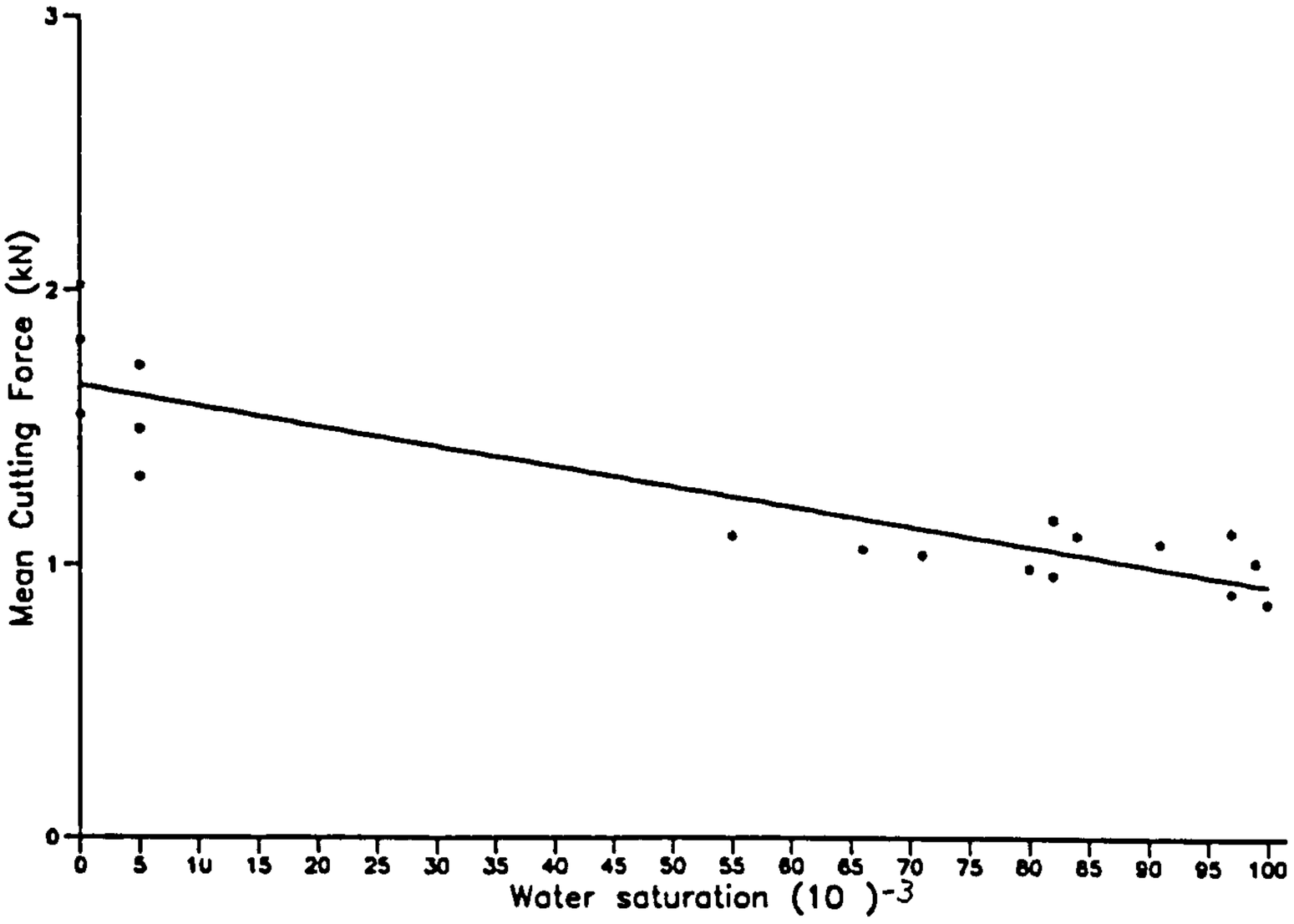

Fig 6.1 Mean cutting force v Water saturation

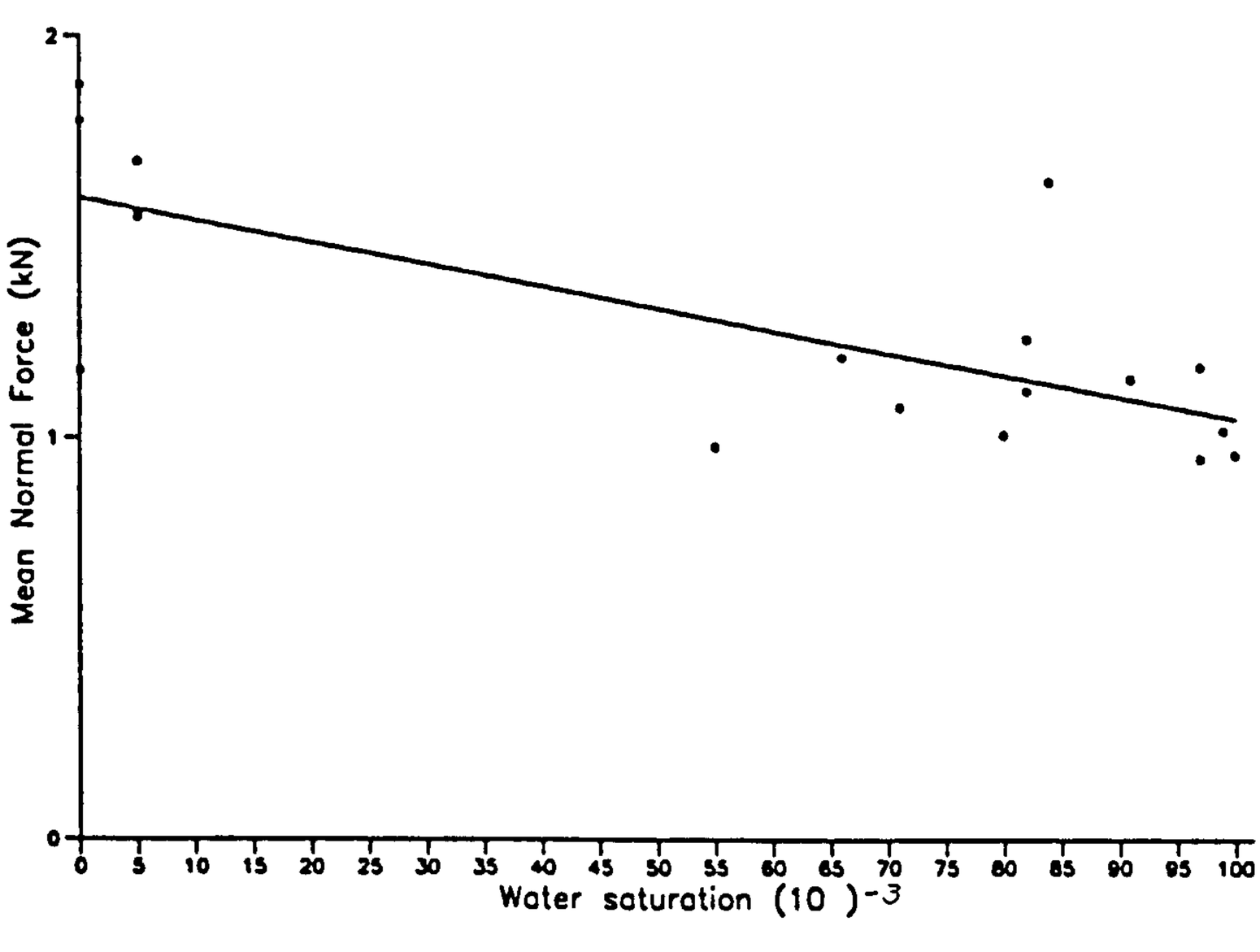

Fig 6.2 Mean normal force v Water saturation

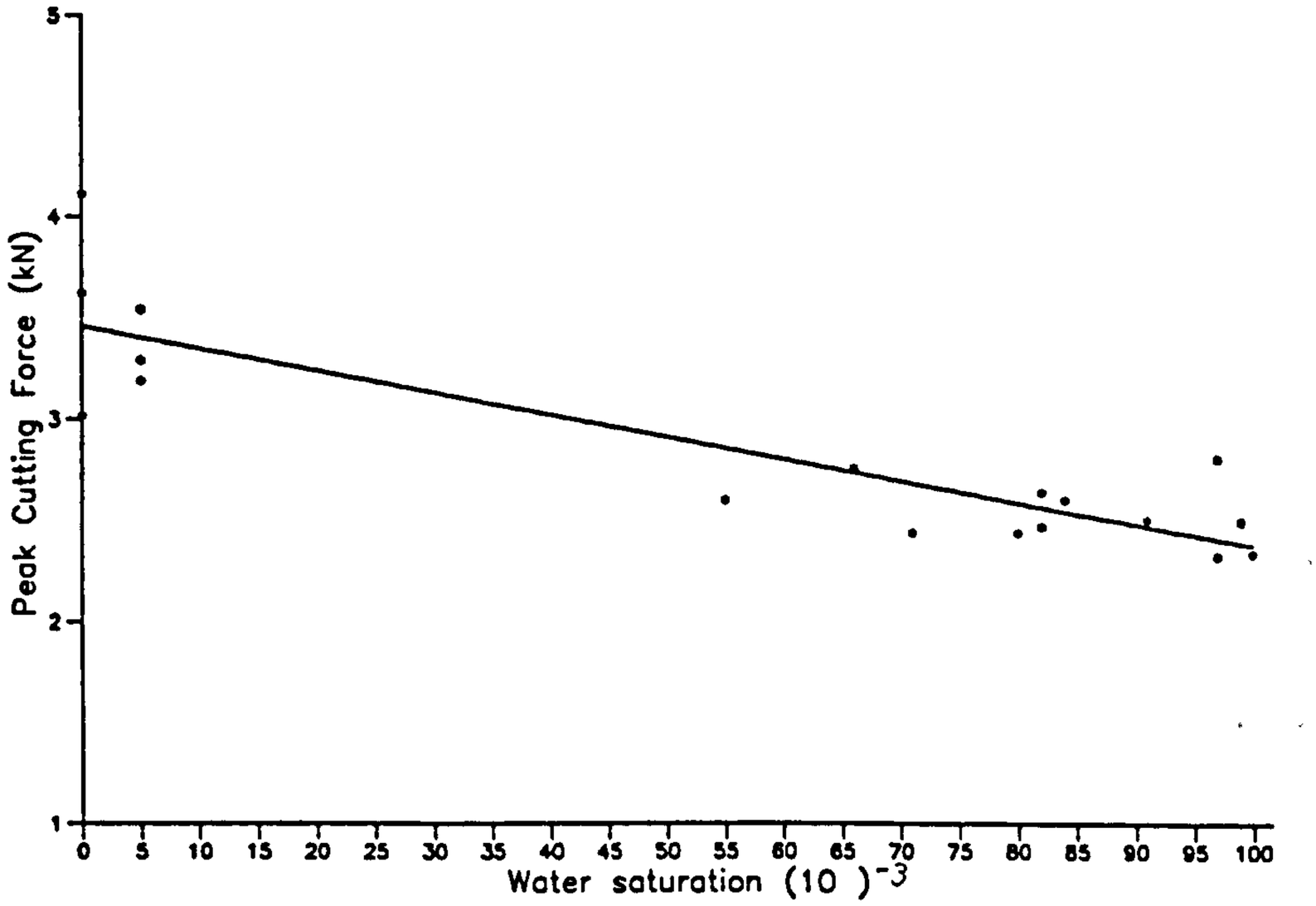

Fig 6.3 Peak cutting force v Water saturation

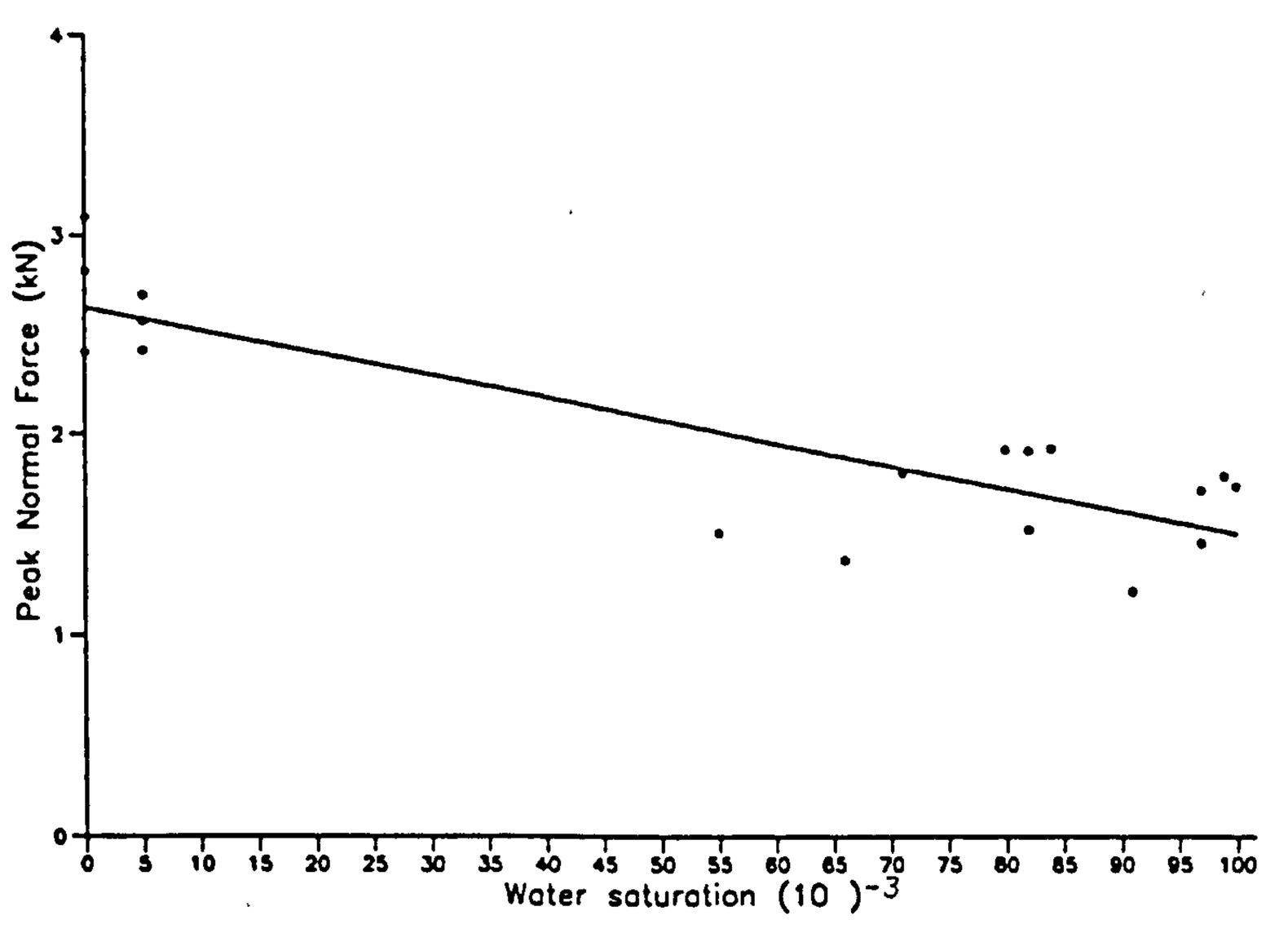

Fig 6.4 Peak normal force v Water saturation

Table 6.4 Effect of different moisture states on cutting parameters for Springwell sandstone

Rock condition	PNF	PCF kN	MNF kN	MCF kN	YIELD kN	SE m^3/m	Co.I MJ/m^3	%
dry		3.66	2.65	2.32	1.43	7.64	18.74	402
ambient		3.30	2.53	2.05	1.47	7.62	19.65	394
saturated		3.10	2.27	1.87	1.10	7.15	15.38	394

All the forces are reduced and the SE of saturated rock in comparison to dry and ambient is considerably reduced relative to dry and ambient. However the coarseness index did not change significantly.

Yield : the dry state produced more debris compared to other conditions. A phenomenon observed with the dry rock was that the chips were subjected to more kinetic energy, probably as a result of the higher strength rock material. Because dry rock is stronger than rock with ambient moisture content the bit produces more chips. If the ambient moisture content results are compared with the fully saturated state, there is a decrease of yield in the saturate state. Yield is directly proportional to break-out angle. The mechanism of breakage was different in each of the three moisture states. In the dry state the particles were large chips generated at high speed, in the ambient state the chips produced were slower, and in the saturated state they were much slower. The debris were deposited close to the specimen instead of being protected to a distance, furtheremore the chip size was more uniform.

6.3.2 Welton chalk

The samples of the tested chalk were without flint. Only two saturation content states were considered, ambient and fully saturated. This type of rock proved to be very different from Springwell sandstone. There were many natural microfractures in the rock specimen and for this reason some of the samples fractured before the traverse of the cutting tool was completed. A summary of results are as follows (Table 6.5):

Table 6.5 Effect of different moisture states on cutting parameters for Welton chalk

Rock Condition	PNF kN	PCF kN	MNF kN	MCF kN	YIELD m^3/m	SE MJ/m^3
ambient	3.97	2.4	1.78	1.14	11.37	10.86
saturated	4.44	3.11	2.65	1.53	8.00	19.10

In the saturated state all the forces and SE increased. Varley (1989) reported some tests on both saturated and dry chalk cores, without flint and with small flint inclusions. These tests provided laboratory SE values for air-dried sample of the order of 13 MJ/m^3, though saturation produced a drop in the UCS values from 50 MPa to 20 MPa the SE was similar to the mean value, 12 MJ/m^3 and 11 MJ/m^3 respectively.

The chalk used by Varley (1989) was exactly the same as that one used in this investigation.

From above it can be seen that there are no similarities between the effect of water content on UCS and SE. This response of Welton

chalk was also noted by Roxborough and Rispin (1973) during their work on the machineability characteristics of the Lower chalk in Kent. Chalk cores tested by them has shown increase for all of forces from ambient to saturated, and because yield decreased it resulted in an increase of the SE. The influence of water for chalk is different from sandstone, because sandstone is more porous than chalk.

6.3.3 Pennant sandstone

The results are as follows (Table 6.6):

Table 6.6 Effect of different moisture states on cutting parameters for Pennant sandstone

Rock Condition	PNF kN	PCF kN	MNF kN	MCF kN	YIELD m^3/m	SE MJ/m^3	Co.I %
ambient	11.46	6.55	6.73	3.63	6.20	59.6	439
saturated	9.35	5.72	5.6	3.00	6.76	45.68	439

It can be seen that all cutting forces, and the SE were reduced as the water content increased and only yield has increased. Coarseness Index did not change significantly.

6.3.4 Teesdale Whinstone

The results of the effect of water content are as follows (Table 6.7):

Table 6.7 Effect of different moisture states on cutting parameters for Teesdale Whinstone

Rock Condition	PNF kN	PCF kN	MNF kN	MCF kN	YIELD m^3/m	SE MJ/m^3	Co.I %
ambient	19.93	9.19	12.83	4.02	4.02	132.09	444
saturated	21.68	9.76	15.05	5.43	3.67	158.90	426

6.3.5 Matlock limestone

The results of the water content influence are as follows (Table 6.8):

Table 6.8 Effect of different moisture states on cutting parameters for Matlock limestone

Rock Condition	PNF kN	PCF kN	MNF kN	MCF kN	YIELD m^3/m	SE MJ/m^3	Co.I %
ambient	6.5	4.24	3.99	2.77	6.72	41.78	426
saturated	6.0	4.13	3.38	2.35	6.56	36.28	424

It can be seen that with the exception of coarseness index all the cutting forces, yield and specific energy decrease, as the water content increased from the ambient to the fully saturated state.

6.4 Effect of depth of cut and spacing

6.4.1 Effect of depth of cut

In the previous research, (Roxborough 1973), the depth of cut and spacing has been greatly considered. Consequently in this investigation three depths of cut were considered 4 mm, 6 mm and 8 mm , for Springwell sandstone in saturated condition. Up to a certain depth of cut, increasing of depth reduces SE, but as depth increases the wear will be higher. Consequently one can see from Figs 6.5 to 6.11 an optimum depth exists. There is a big reduction from 4 mm to 6 mm and hardly any difference between 6 mm and 8 mm. It can be concluded from the wear point of view that 6 mm is better than 8 mm, and 4 mm is the worst case because the specific energy is too high. The reason for this phenomenon may be attributed to the a rubbing movement instead of cutting resulting in an increase of all the forces MCF, PCF, MNF, PNF and the coarseness index and yield . The pick forces should not reduce below a certain depth of cut and excessive rubbing at shallow depths, often termed coring or grooving, generates heat which is not desirable.

6.4.2 Effect of tool spacing

The effect of different tool spacing on the cuttability of rocks was investigated for; medium rock (Springwell sandstone), and for both saturation states (air-dried and fully saturated).

Different depths of 4 mm, 6 mm and 8 mm for Springwell sandstone were tested and s/d ratios for each depth for Springwell sandstone are as follows:

d=4 mm	s/d=0.5,1,2,3,4
d=6 mm	s/d=0.5,1,2,3

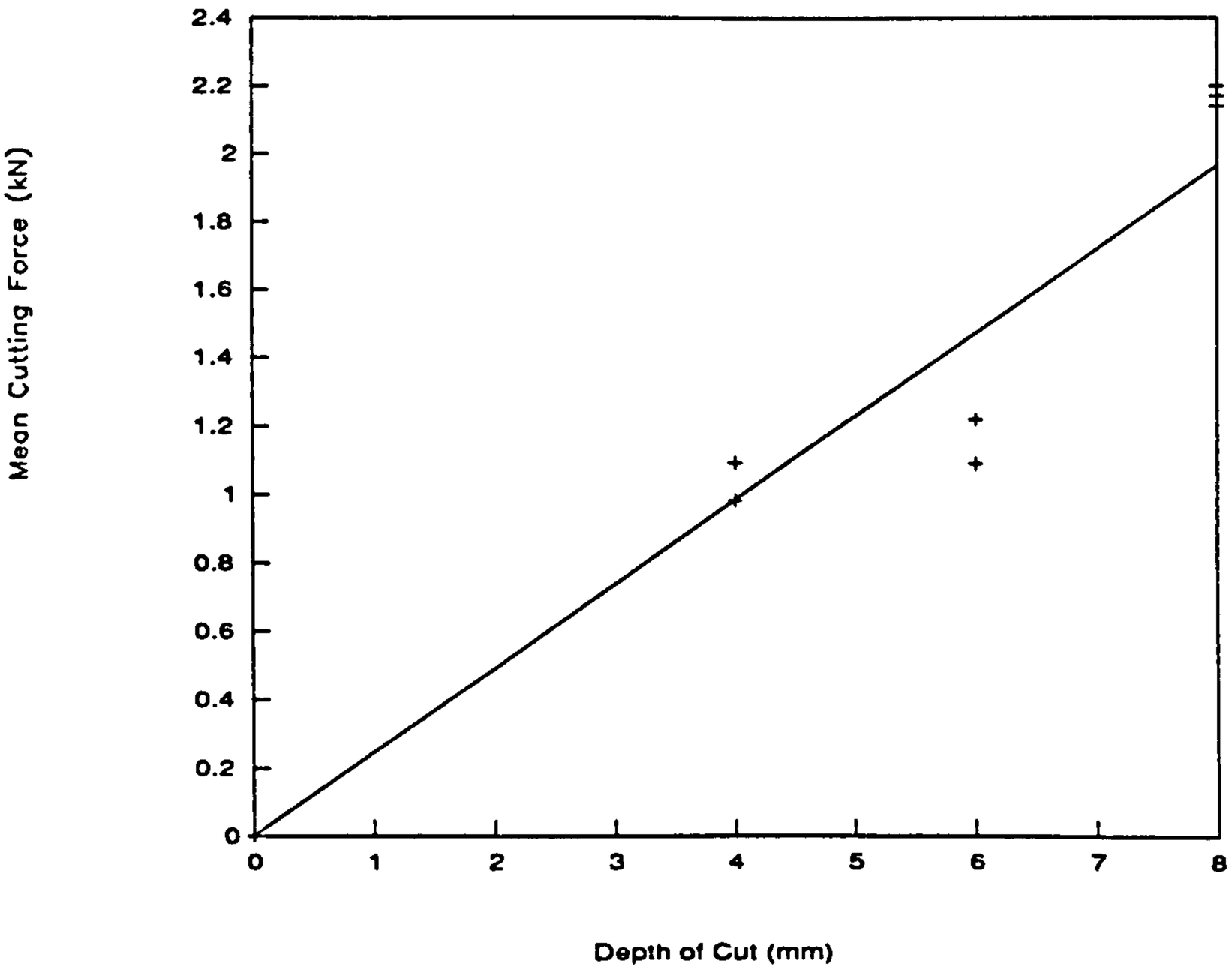

Fig 6.5 Mean cutting force v Depth of cut

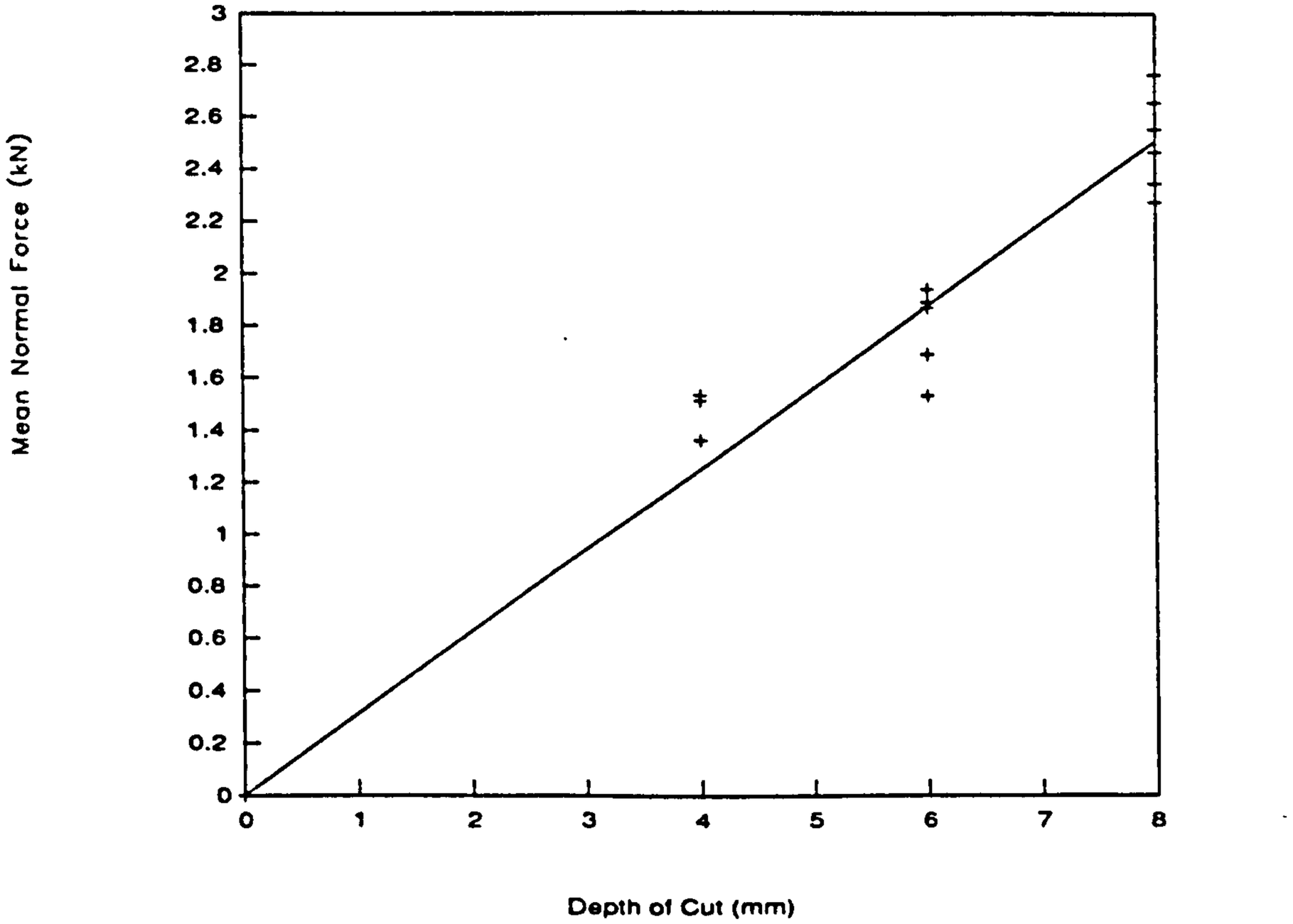

Fig 6.6 Mean normal force v Depth of cut

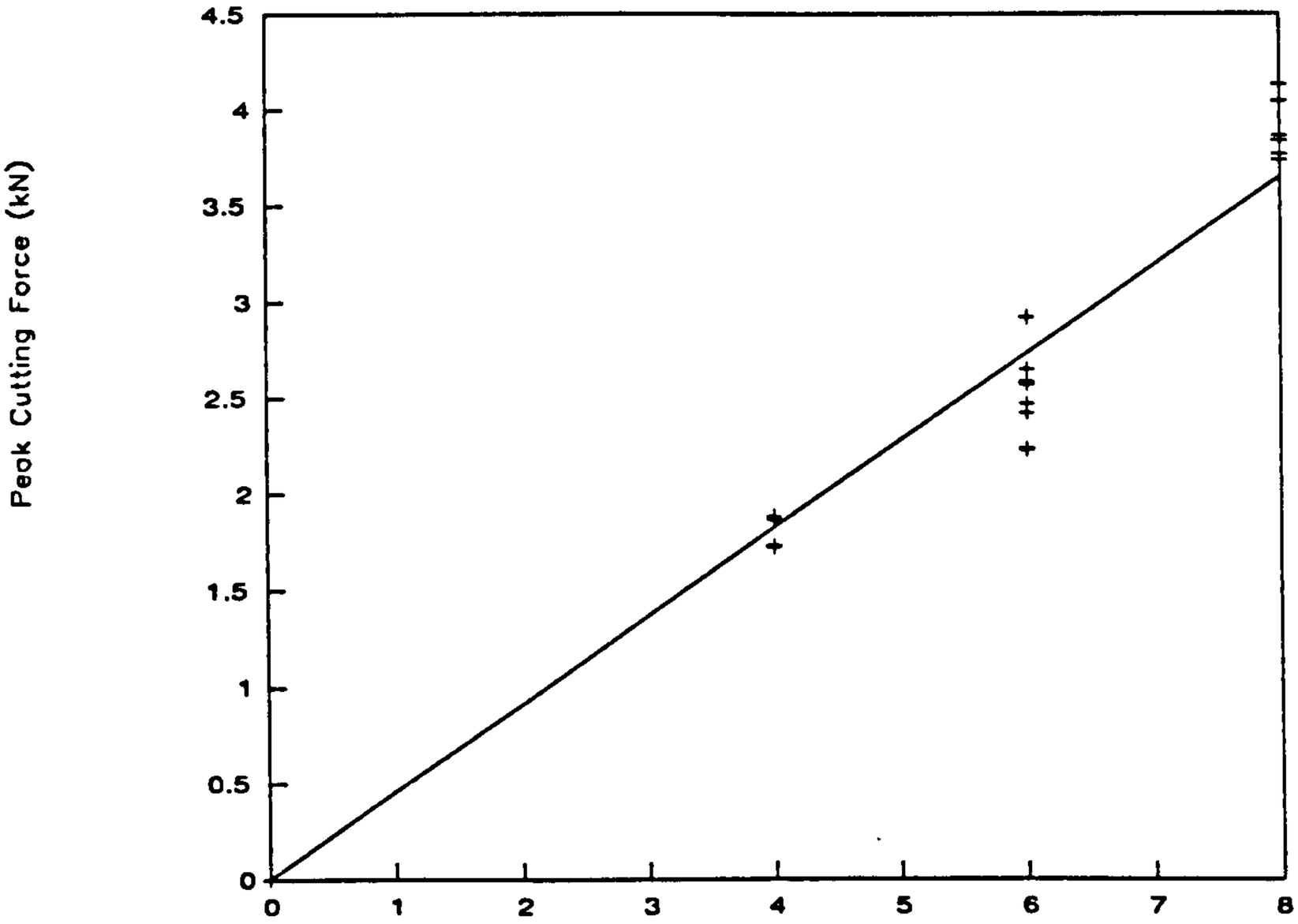

Fig 6.7 Peak cutting force v Depth of cut

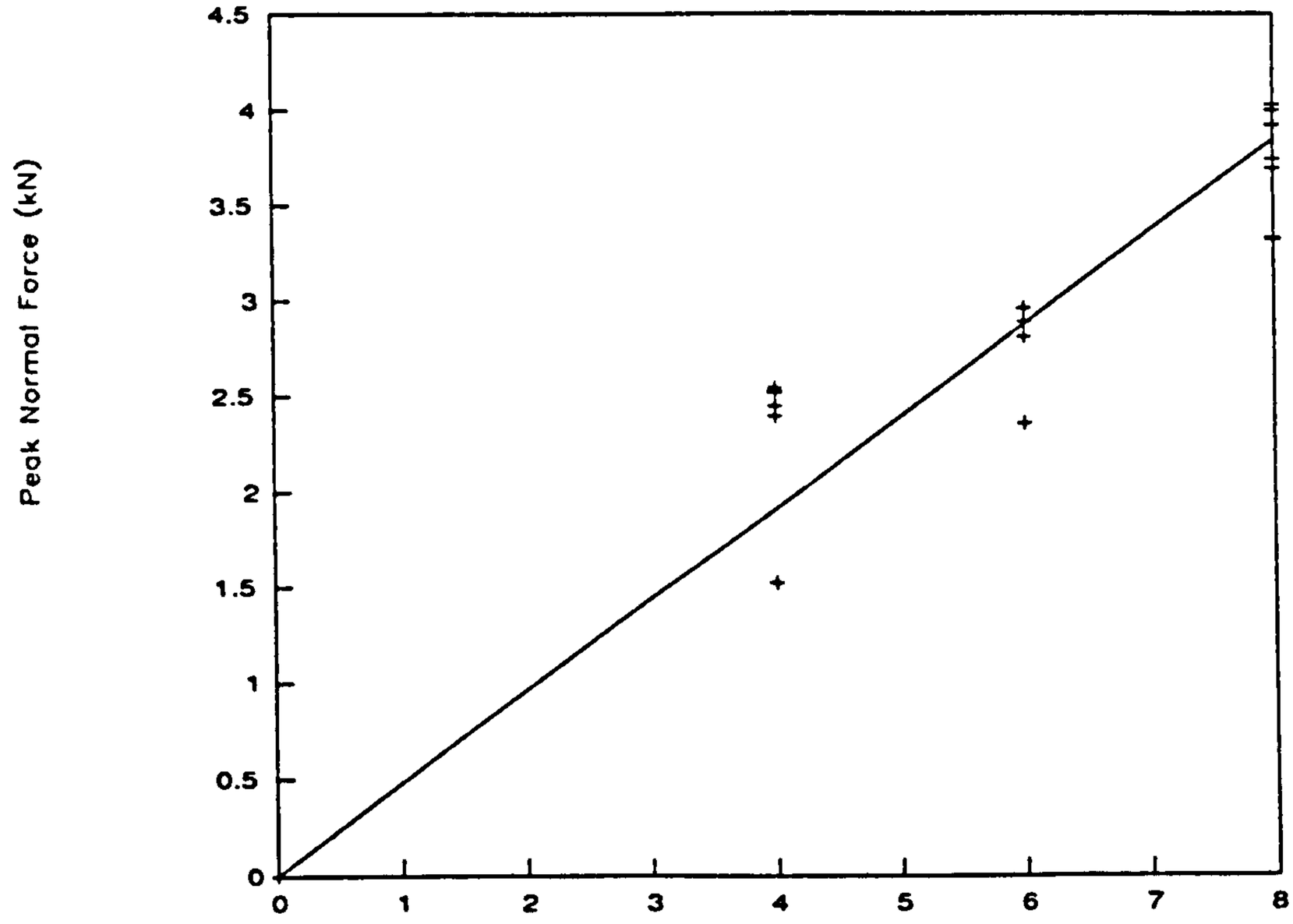

Fig 6.8 Peak normal force v Depth of cut

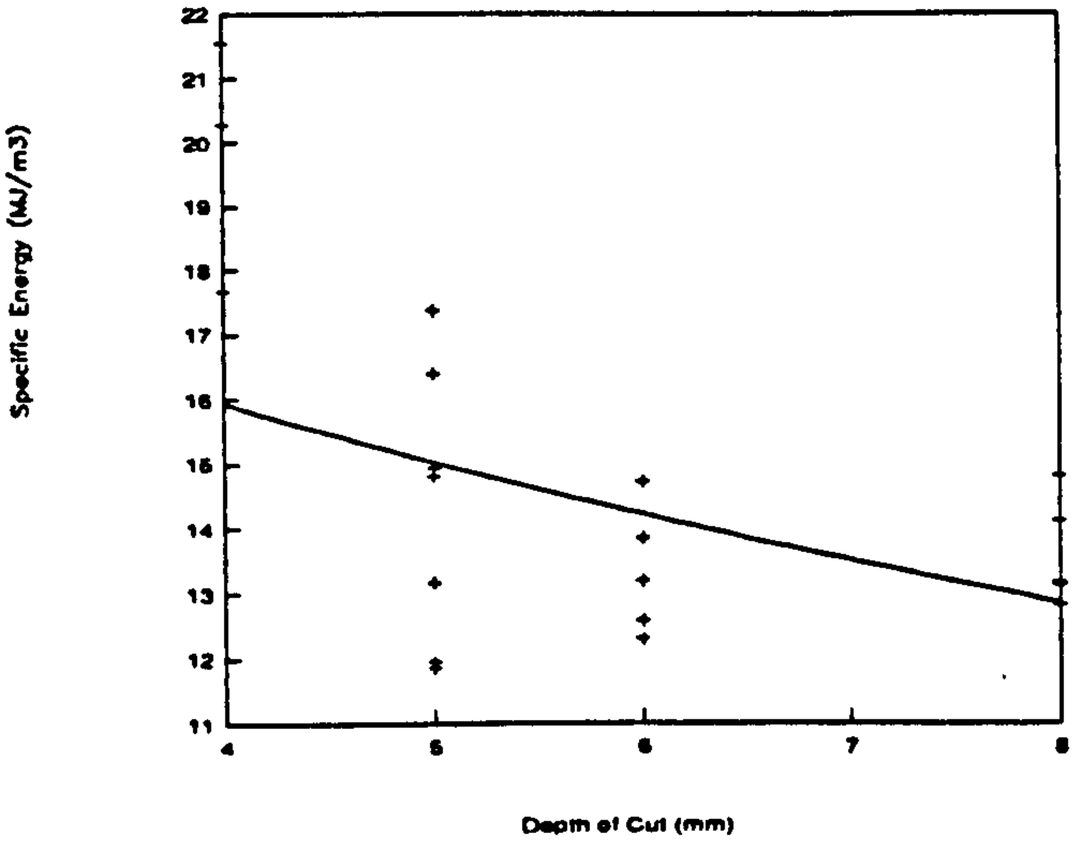

Fig 6.9 Specific Energy v Depth of Cut

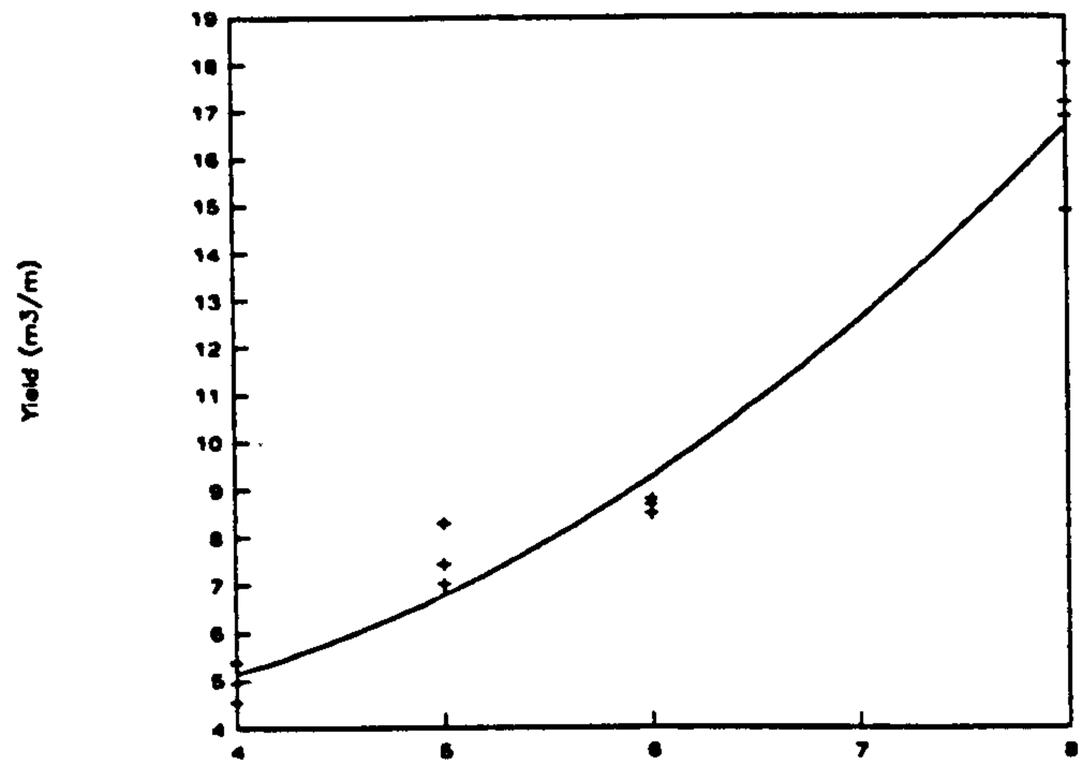

Fig 6.10 Yield v Depth of Cut

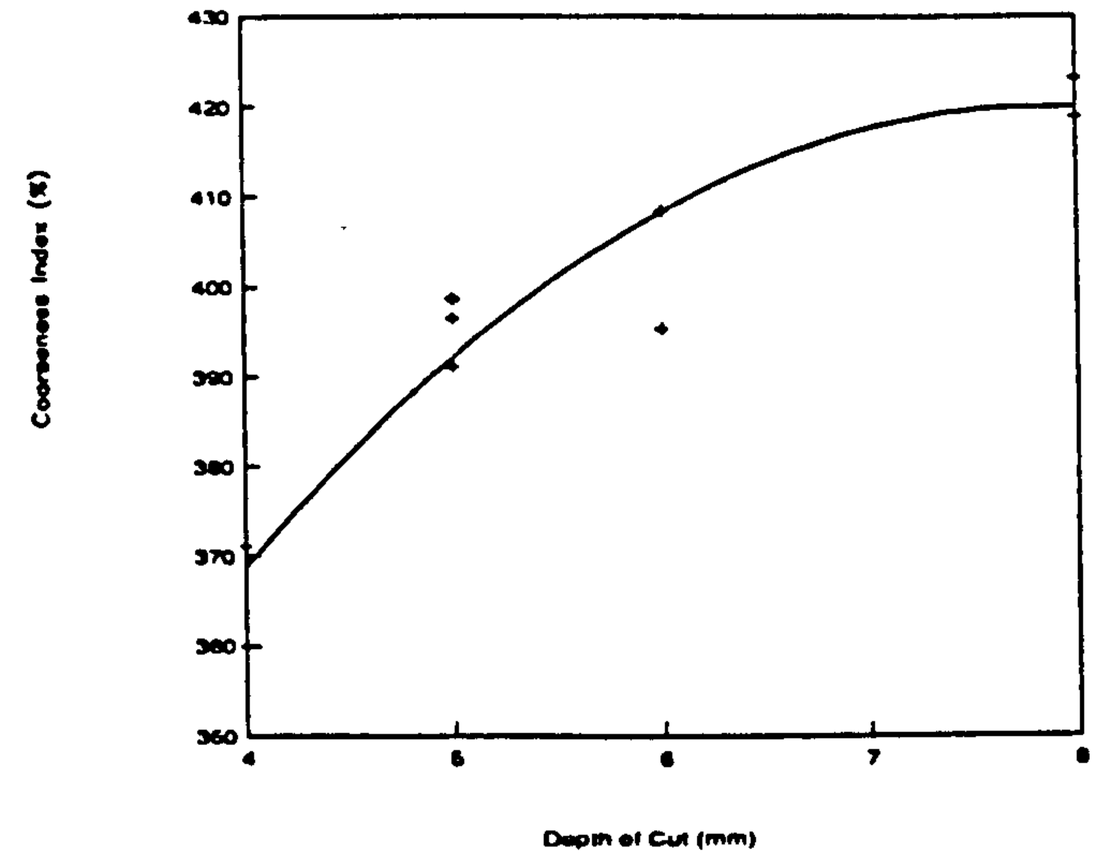

Fig 6.11 Coarseness Index v Depth of Cut

d=8 mm s/d=0.5,1,2,3

where s=spacing between tools

As indicated before, the width of block specimen for all the depths is constant because of limitation on the width of the desiccator, therefore for each depth of cut there is a different s/d.

The results for the different depths of cut (d) are as follows :.

a) d=4 mm

PNF : the lowest occurs when s/d=0.5,2

PCF : there is no trend and the minimum is when

s/d=0.5

MCF : there is no trend and the minimum is when

s/d=0.5, 2, 3

MNF : there is a trend and the minimum is when

s/d=0.5 and maximum when s/d=3

Yield : there is a trend and the maximum is when

s/d=2

coarseness index: there is no trend and the maximum

is when s/d=3

d=6 mm

PNF : the lowest value occurs when s/d=0.5

PCF : there is an increased trend and the lowest

value is taking place when s/d=0.5

MCF : the lowest one occurs when s/d=0.5

MNF : the lowest one occurs when s/d=0.5,2

Yield : there is a trend and the maximum one is when

s/d=2

coarseness index: there is no trend.

d=8 mm

PNF : there is a trend showing an increase and the

lowest one is when s/d=0.5,1

PCF : there is a trend and the lowest one is s/d=0.5

MCF : there is an increased trend and the lowest one is s/d=0.5

MNF : there is trend and the maximum is when s/d=2

yield : there is no trend and the maximum is when s/d=2 and

coarseness index: there is a trend and curve reaches s/d=1 and continues constantly.

The spacing beyond which there is no interaction between different cuts can be identified for different depths of cut and the results are as follows :

d=4 mm maximum spacing 40 mm

d=6 mm maximum spacing 65 mm

d=8 mm maximum spacing 74 mm

From the above results it is impossible to find any trend between s/d and cutting parameters, and may be because change in depth of cut with SE is not unique and contrary to the trend when rock is under the ambient state.

Pennant sandstone which is very hard rock was investigated with a cutting depth of 4 mm. It was difficult to work with 6 mm and 8 mm depths of cut, because of limitations in the stiffness of cutting machine. Cutting spacing was a maximum 32 mm (which was less than Springwell sandstone) and the production of debris was also less than Springwell sandstone.

Maximum spacing of limestone under saturated and ambient condition is 33 mm and 41 mm respectively. This agrees with yield for

saturated and ambient which is 6.56 m^3/m and 6.72 m^3/m respectively. Full detail of results are presented in Appendix 5.

6.5 Investigation of subsurface damage

In this work two types of rock, (medium rock strength) Springwell sandstone and Pennant sandstone (hard rock) were tested. The effect of subsurface damage and cut spacing were considered for both rocks.

6.5.1 Springwell sandstone

a- Effect of depth on trimmed surfaces

Springwell sandstone was investigated using different depths of cut (4mm, 6mm, 8mm). In the saturated state the sandstone was trimmed twice at the same depth as before, and some results show significant variation and scatter while others showed a good relationship. This can be judged from Figs (6.12 to 6.17), level 1 is representitive of intact rock. The trend of SE for depths of cut 4 mm and 8 mm indicate a reduction although the opposite behaviour is seen for the 6 mm cut. It is obvious that yield when 8 mm depth is used is more than that when a 4 mm depth is used. If certain limits of wear taken into consideration , the 8 mm depth of cut produces better results than 4 mm.

For 8 mm depth of cut the trend of SE and cutting forces indicated that a reduction exists when compared to intact rock. However for 4 mm or 6 mm there appears to be no such reduction. This is because the fractures are induced nearly continuously from stress concentrations below the base of the cutter. Therefore the chisel bit produces a damage zone beneath the bit which exceeds the depth of cut. The results show this damage zone is affected by the depth of cut. If depth of cut increases, cutting

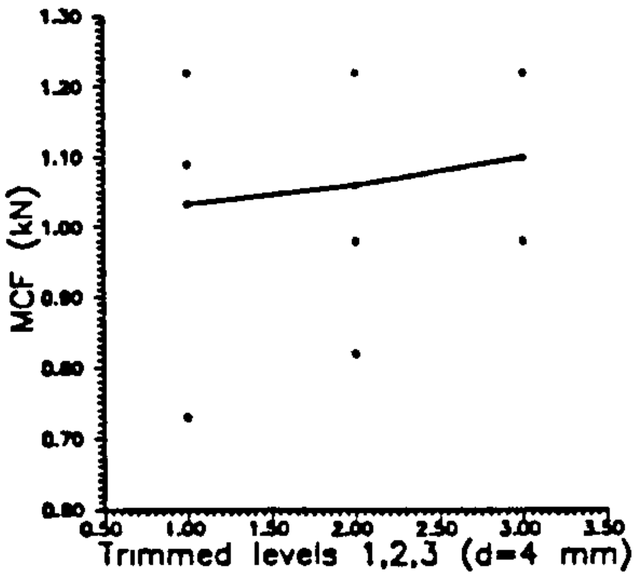

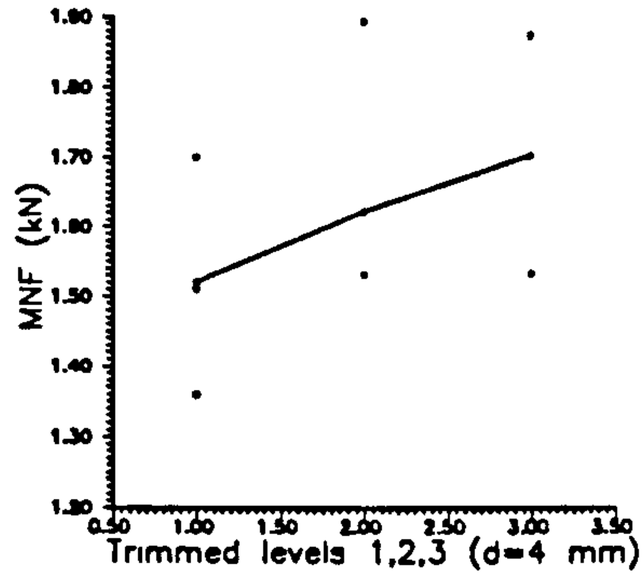

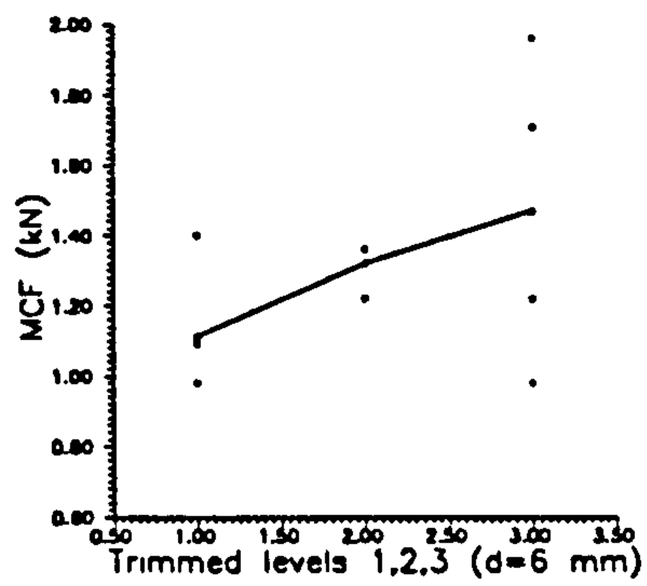

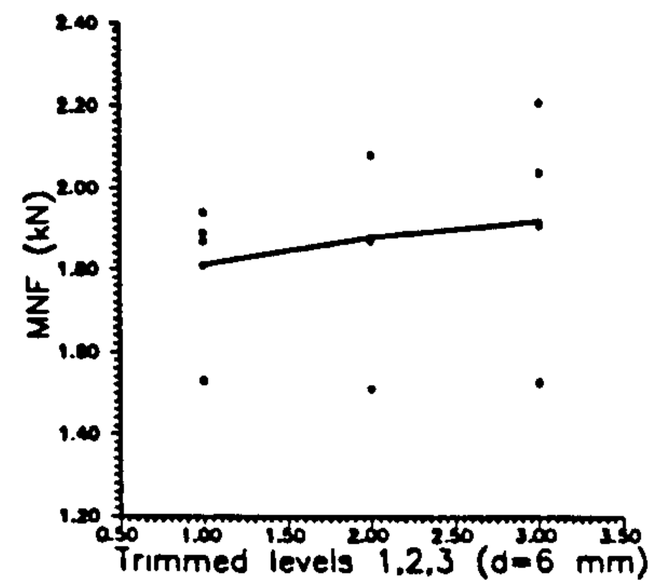

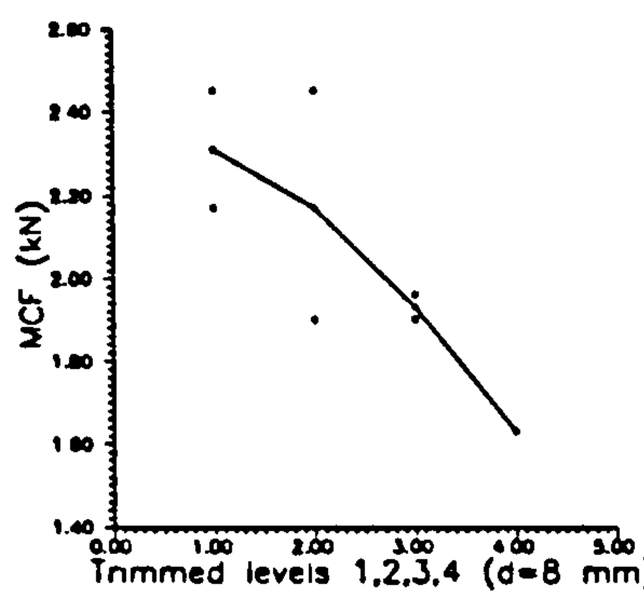

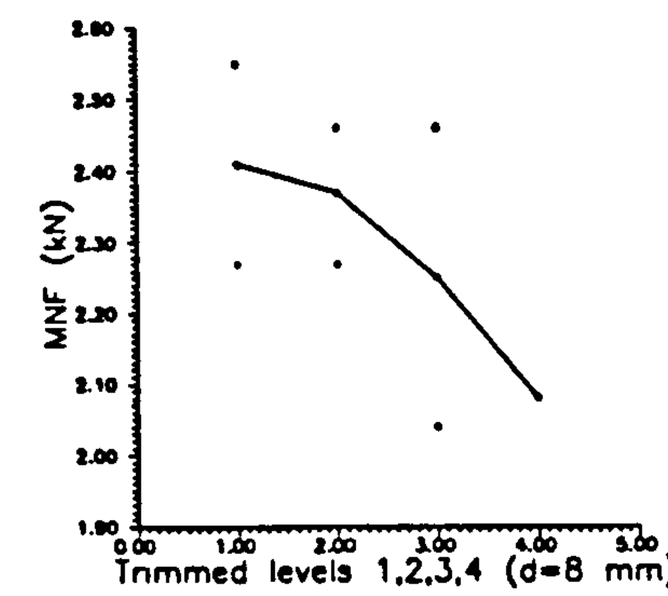

Fig 6.12 MCF and MNF v Trimmed levels

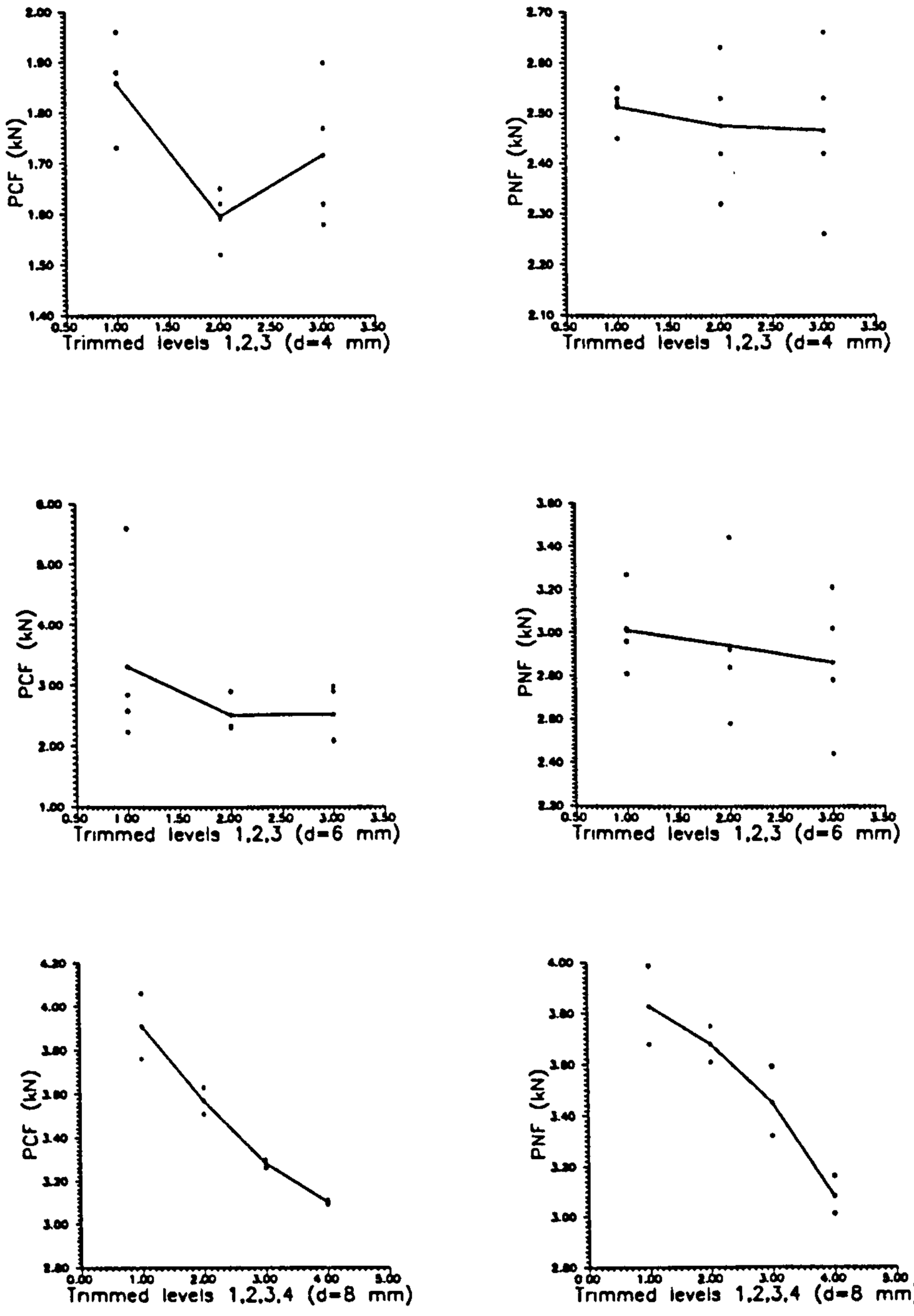

Fig 6.13 PCF and PNF v Trimmed levels

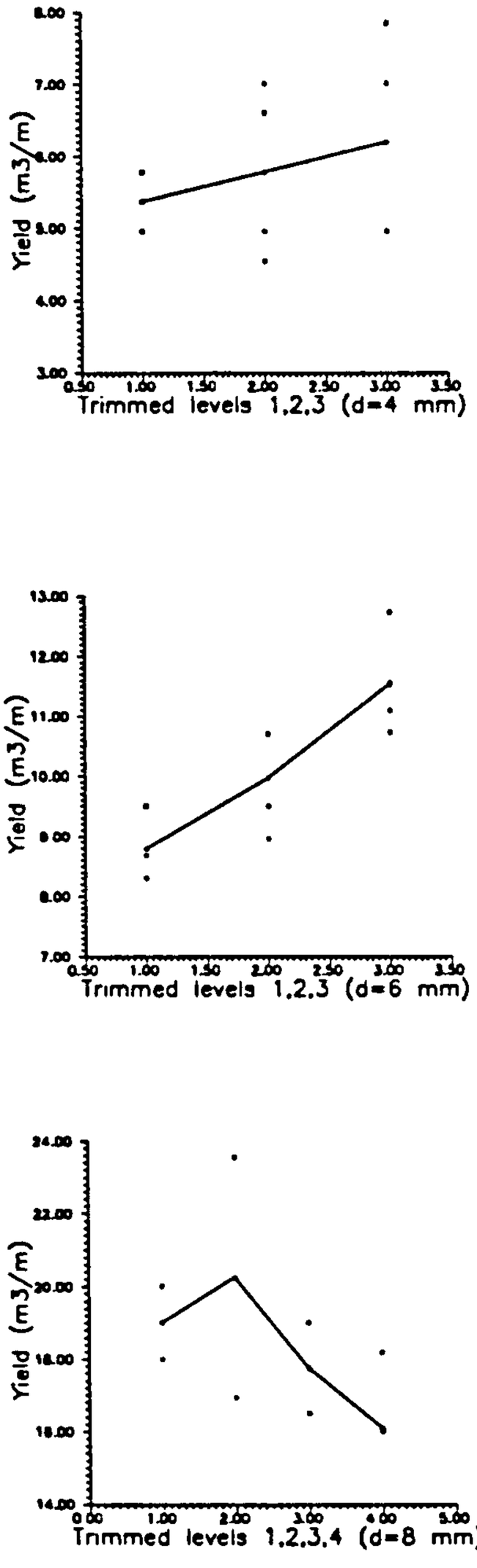

Fig 6.14 Yield and Specific energy v Trimmed levels

forces increase and eventually the damage zone and microcracks will propagated further. Perhaps this is the reason why for 4 mm, 6 mm, the damage zone is limited, and does not show any changes in forces and specific energy but for 8 mm there is a significant reduction.

b-Effect of different spacing on trimmed surfaces

In these tests only 4 mm and 6 mm depths of cut could be tested, because of limitation of thickness of specimen block. The comparison between the SE of trimmed surfaces shows that for 4 mm depth of cut SE has significantly increased and for 6 mm depth of cut with s/d=3 a considerable reduction exists for SE. The yield, and the coarseness index did not change significantly. The other forces show variations, but in s/d=3 there is good reduction. Thus between the 4 mm, and the 6 mm depth of cut, the later is more advantageous.

6.5.2 Pennant sandstone

The two states, ambient and saturated, were investigated employing a 4 mm depth of cut, (as was explained earlier the 6 mm depth of cut was tried unsuccessfully), but a problem with the cutting machine at this depth of cut had emerged. This behaviour is very similar to Springwell sandstone in saturated state. All specific energy results showed an increase in trimmed surface, but for ambient moisture content there was a reduction.

6.6 Effect of axial loading on the cutting characteristics of Springwell sandstone

To investigate the effect of compressive loading on the cutting characteristics of Sprigwell sandstone a series of rock cutting tests were conducted with specimens subjected to uniaxial compressive loading.

To conduct rock cutting test when rock is loaded in compression, there is a need to find out at what stress rock will break. For this reason UCS tests according to ISRM, were conducted (see chapter 4). The UCS results have been used to determine the percentage that was applied to the direction of cutting. Different uniaxial compressive stresses a 22.56, 29.33, 38.33 and 40.62 MPa were applied during rock cutting tests. To apply the uniaxial compressive stress, a specially modified pressure cell was used to allow the bit to move freely to the end of specimen. A hydraulic pump was used to apply the axial load during the cutting of rock. A pressure transducer was used in association with a hydraulic system to monitor the applied pressure. Any displacement in axial loading was recorded by an LVDT and also monitored by data logger. Details of equipment are presented in chapter 5.

Dunn (1977), also conducted cutting tests with compression loaded rock blocks.

Results of SE between unstressed and stressed at 90 % of UCS shows little changes and it is not significant. The cutting forces (MCF, MNF, PCF, PNF) have also been affected little. Full detailed results are presented in Appendix 6, and the summary of results is given in Table 6.9 :

Table 6.9 Effect of uniaxial loading on rock cutting

Applied load as % of UCS	MCF kN	MNF kN	PCF kN	PNF kN	YIELD m^3/m	SE MJ/m^3
group 0	1.47	1.47	3.30	2.53	7.62	19.65
group 50	1.62	1.90	3.64	2.87	8.04	20.22
group 65	1.73	1.95	3.35	2.78	7.51	23.10
group 85	1.43	1.65	3.10	2.68	7.52	19.10
group 90	1.42	1.80	3.05	2.61	7.81	18.11

6.7 Effect of rake angle

This parameter is very important in rock cutting, because with changes in rake angles rock cutting parameters also change. In this test, the effect of different rake angles in a saturated condition was investigated. The rake angles were made in the University's workshop, and for comparison, a negative -10°, a positive 16° and 0° angle were chosen. With reference to SE the results (Appendix 3) showed that a positive angle is advantageous by resulting in a SE of 6.89 MJ/m^3. As for the angles of 0° and -10° the resulting SE was close to 9.21 MJ/m^3 , and 10.6 MJ/m^3 respectively. The problem for the positive rake angle is strength, also, in the long term, the effect of wear is another parameter which affects one's choice of rake angle.

As the rake angle varies From +16° to 0° and -10° all the cutting forces increased. Yield for a rake angle of +16° , -10° is nearly the same, however for 0° rake angle these appear to be a reduction. Coarseness index does not seem to be affected at all by changes in the rake angle.

The two cutting theories, Nishimatsu (1972) and Evans (1962) are complementary and may be used in conjunction to determine the conditions for which a cutting action would be predominantly tensile or predominantly shear. For a rock with the properties shown in Fig (6.18), when the pick angle exceeds the range of 15-20°tensile failure will occur. For this reason an angle of 16° was chosen and the results were found to be consistent with Evans'theory.

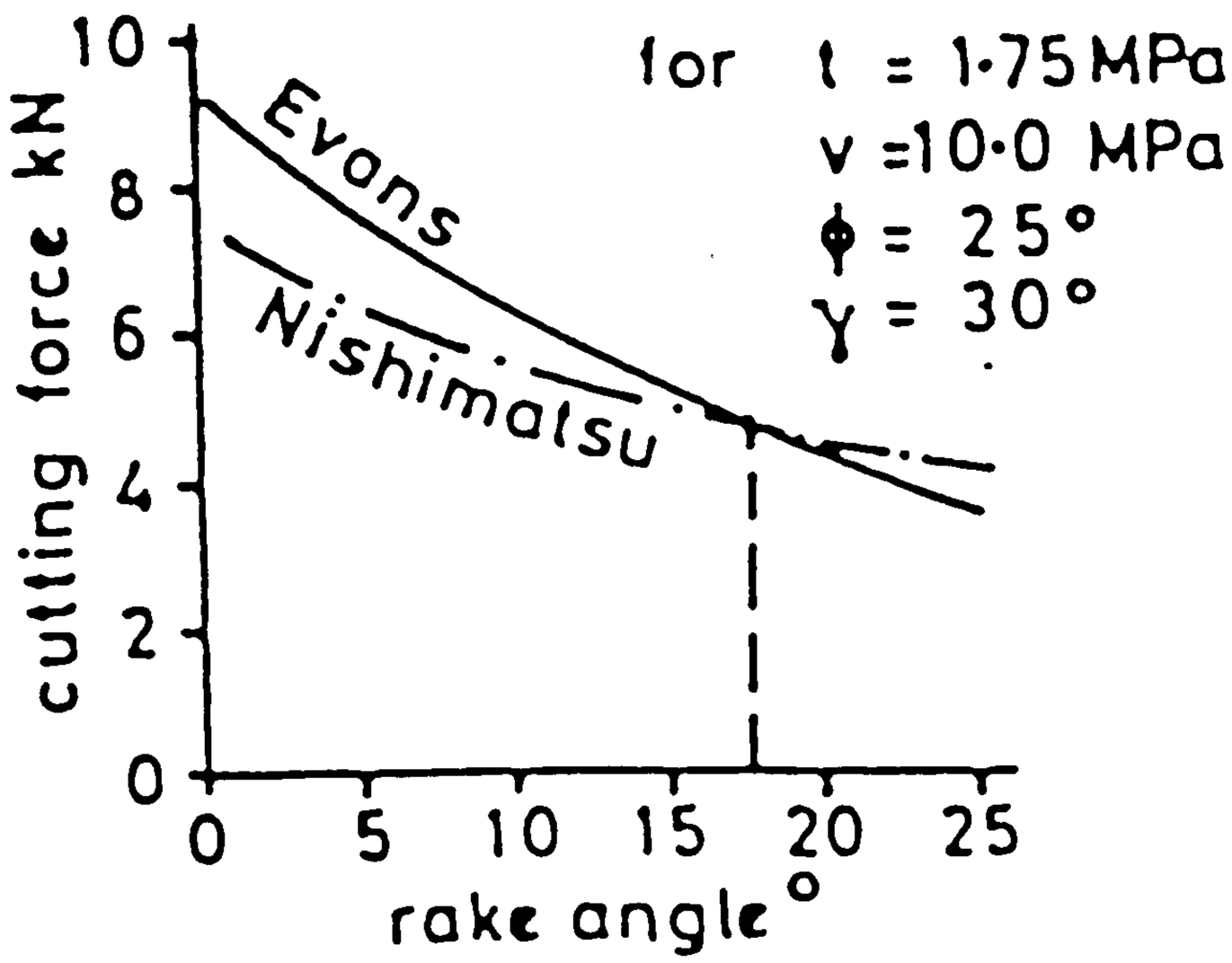

Fig 6.18 Cutting force v rake angle (after Roxborough, 1985)

6.8 Effect of speed of cutting tool

Cutting speed is another factor which affects the rock cutting parameters. Only the saturated state was investigated to investigated whether there is significant difference between various speeds. In these experiments a 5 mm depth of cut was constant for all the tests. It was found there is little difference for the saturated state, most of other parameters. Detail of results are represented in Appendix 4 and summary of the results as follows :

SPEED	PNF	PCF	MNF	MCF	YIELD	SE
m/s	kN	kN	kN	kN	m^3/m	MJ/m^3
0.10	2.72	3.12	1.67	1.90	15.14	12.69
0.125	3.87	3.94	2.54	2.22	16.19	13.87

Specific energy increased only 9%.

6.9 Wear

Wear is an important factor in determining the usefulness a rock cutting machine. The loss of weight after the termination of cutting can be shown as an indication of wear for a given travel distance. If wear exceeds a certain limit in very hard material, drag bit may not be suitable.

Before the cutting tests, the tip was weighed on an Oerling R20 electric balance that recorded the weight to an accuracy of 0.1 mg. This procedure was done as a standard test for all of the materials for different rake angles and for both water content conditions: nearly air-dried and saturated.

The results show a positive relationship between saturated and ambient as expected. There is a great reduction of wear, which is advantageous to rock cutting.

For different rake angles wear in -10° shows to be less than in 0° and 16°, which is more suitable than others.

Only the 0° angle and 16° have much difference (Table 6.10 and Table 6.11).

Table 6.10 Wear (mg/m)
ambient/saturated
Springwell sandstone
0.43/0.38
Welton chalk
0.35/——
Matlock limestone
1.16/0.49
Pennant sandstone
0.48/0.27
Teesdale Whinstone
0.74/0.50

Table 6.11 wear on saturated springwell sandstone with different rake angle			
rake angle	0°	1.88	(mg/m)
rake angle	-10°	0.83	(mg/m)
rake angle	16°	1.60	(mg/m)

6.10 Finite element modelling of rock cutting experiments

PAFEC-FE was used to model the stress distribution of rock during cutting. This can be useful in determining the extend of the damage zone beneath the drag bit and the dominant type of failure, i.e. tensile failure (Evans' theory) or shear failure (Nishimatsu theory).

In this investigation a real rock cutting situation was modelled in a special way because the cutting action of the bit depends in the first instance on the penetration of the tool into rock which must be superimposed on the load comparison to the cutting face. This finite element analysis assess the stress state of rock near the bit and the possible failure process under plane-strain conditions. Two types of materials in this investigation were used, tungsten carbide (drag bit) and Springwell sandstone (rock). Material properties used included Young's modulus, Poisson's ratio and density. The sign of stresses as produced by PAFEC-FE were based on mathematic sign convention.

Material	Young's modulus GPa	Poisson's ratio ————	density (kg/m^3)
tungsten carbide	600	0.25	14400
Sprimgwell sandstone	15	0.25	2210.6

The type of elements used were 8-noded isoparametric plate elements. For the particular mesh used the number of elements, number of nodes and degrees of freedom were :

number of nodes 34

degrees of freedom 88

The goemetry of the bit was chosen as a standard geometry (rake angle -5°, clearance angle 5°), and depth of cut applied 5 mm. At the early stages of the analysis the finite element mesh used was very coarse and the density of the mesh was not adequate (see Fig 6.15), therefore a

re-discretization of the finite element mesh was implemented especially in the area of interest which was near the bit. The improved finite element mesh is shown in Fig 6.16, where one can see that care was taken to ensure that contact between the bit and the rock was achieved.

Various configurations were implemented, at the first stage the cutting force and normal force (which were measured in rock cutting tests) were applied when there was only contact between flat surface of Springwell sanstone and the bit. However it was found that no failure was taking place in any elements, implying that the application of static load combined with simple contact between rock and bit did not cause any high stresses. In a second phase it was decided to lower the bit into the rock surface by 0.05 mm which was the same as Zuech et al (1983), but once more there was no failure and the FE mesh was in an elastic state. This can be varified by Figs 6.17 and 6.18 where one can observe that the stress concentration once more is at very low level . In a third phase, not only a vertical penetration of 0.05 mm was introduced, but the bit was moved by 7 mm (guided by Zuech et al, 1983) in the horizontal direction (direction of movement of drag bit). In this third phase it was found that tensile failure occured beneath the bit and also there was shear stress at the front face of the bit (details of distribution are shown in Figs 6.19 and 6.20 corresponding to major principal stress and minor principal stress respectively). As was expected the damage zone was located beneath the drag bit. The area of interest where failure conditions were assessed was an area of 24 mm x 12 mm around the bit (12 mm is distance from contact point between the bit and the rock to base of the rock specimen)

The failure criterion used to calculate the extent of the failure of rock was Mohr-Coulomb criterion with a maximum tensile stress cutt-off extension. Assuming that the rock is isotropic, the failure of rock can be expressed in twerms of principal stress using,

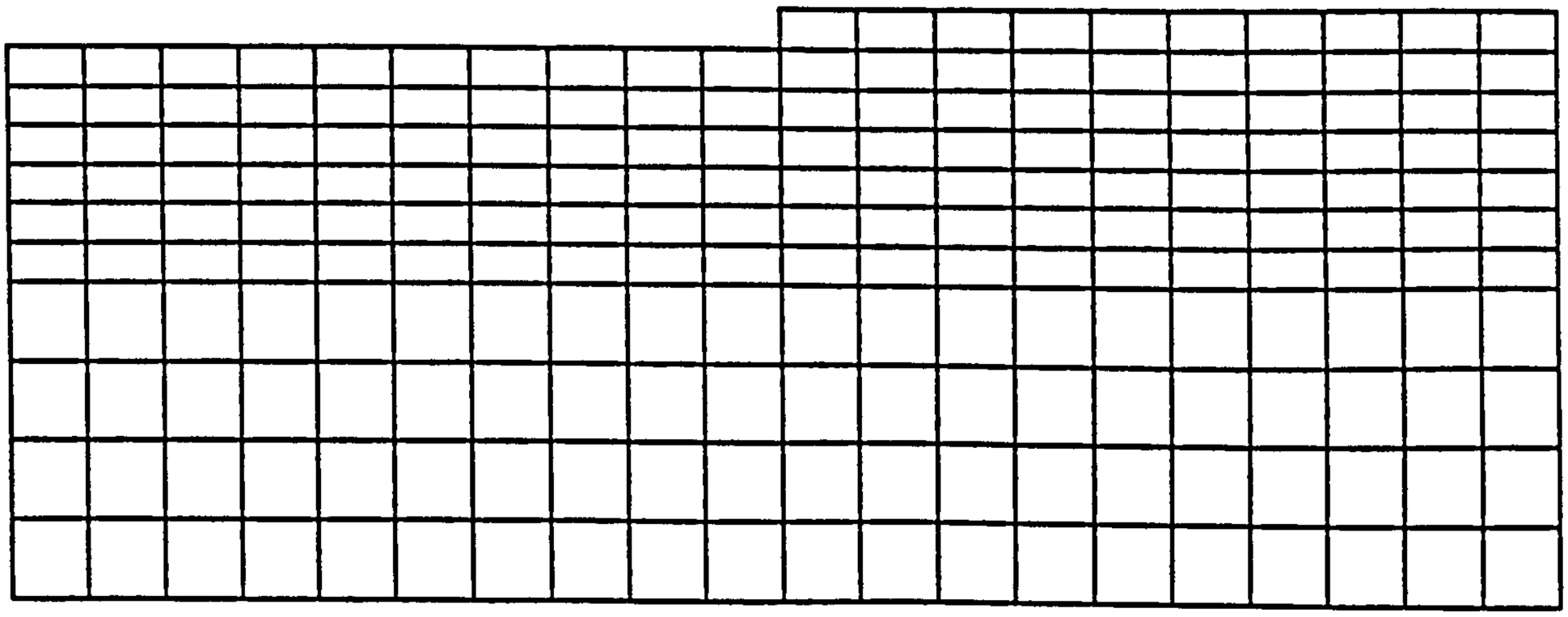

Fig 6.15 Finite element mesh early stage

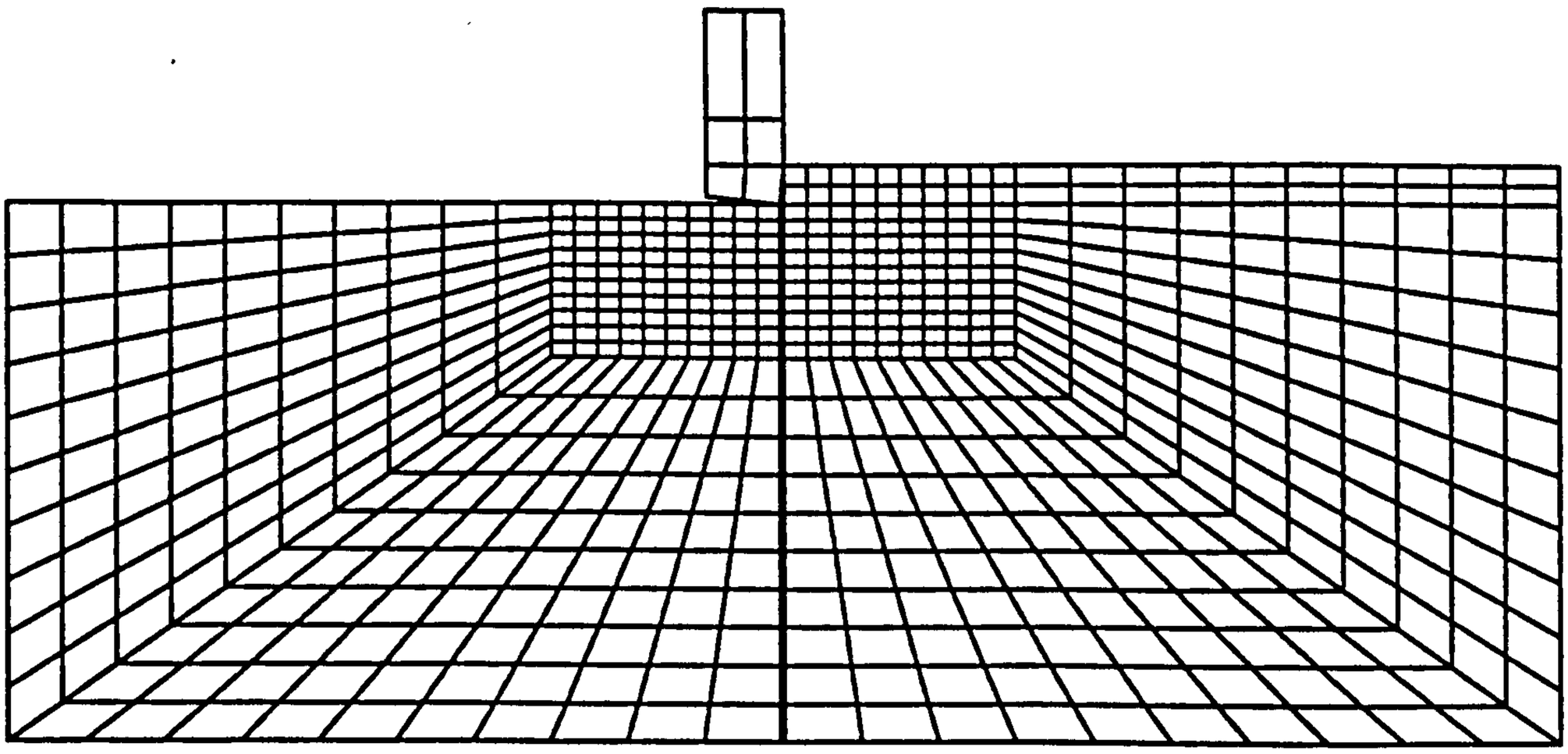

Fig 6.16 Finite element mesh improved

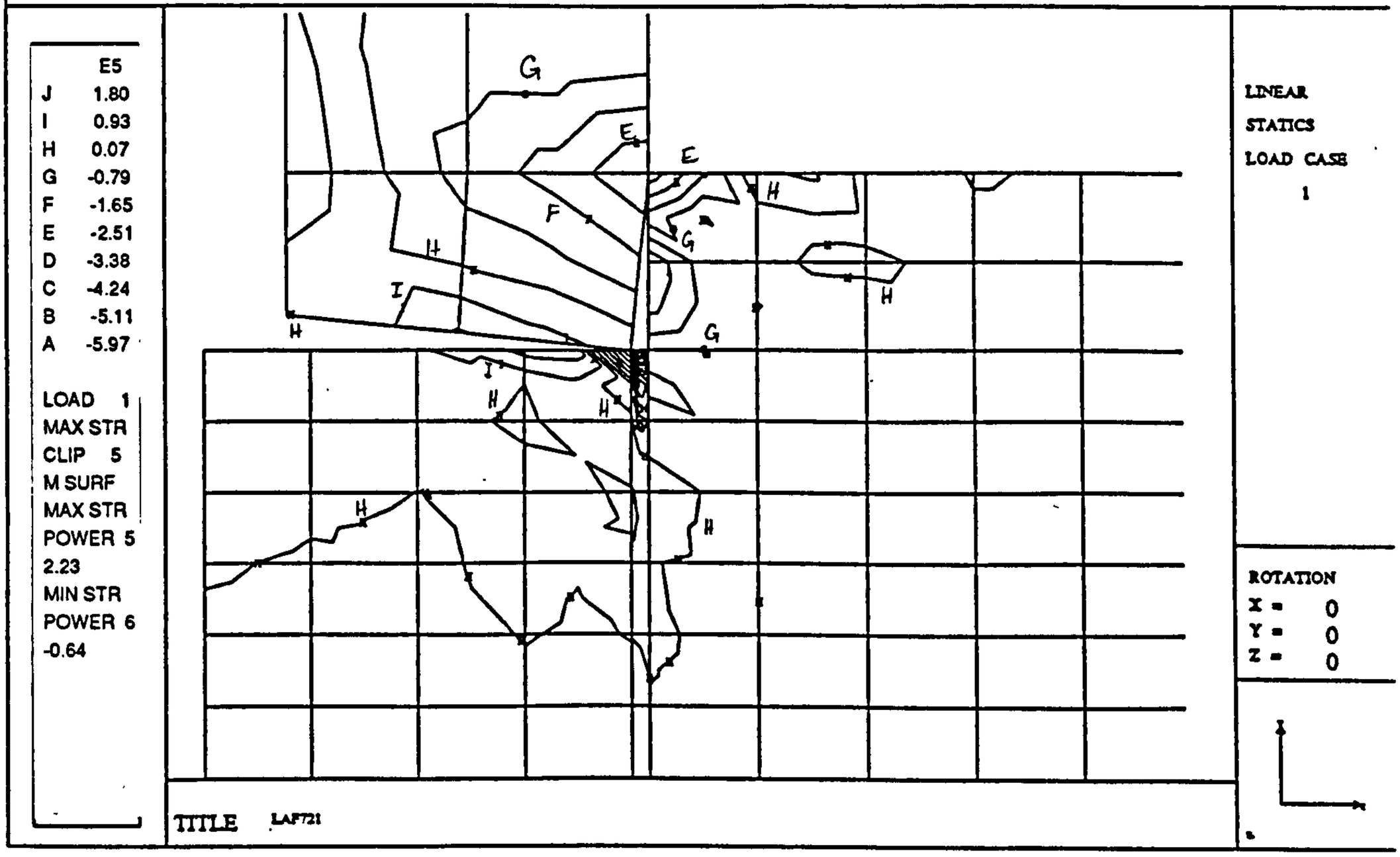

Fig 6.17 Major principal stress simply for contact

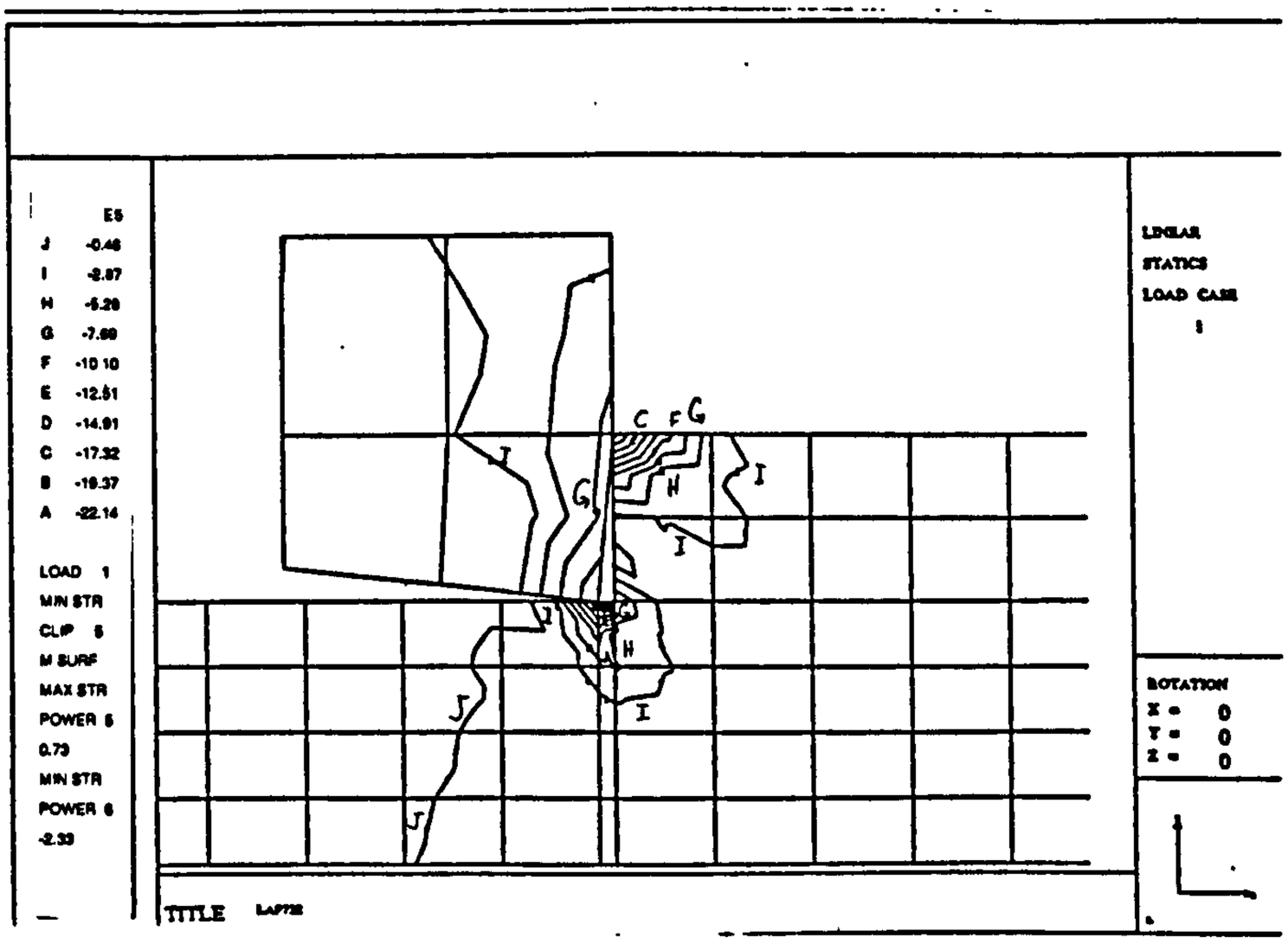

Fig 6.18 Minor principal stress simply for contact

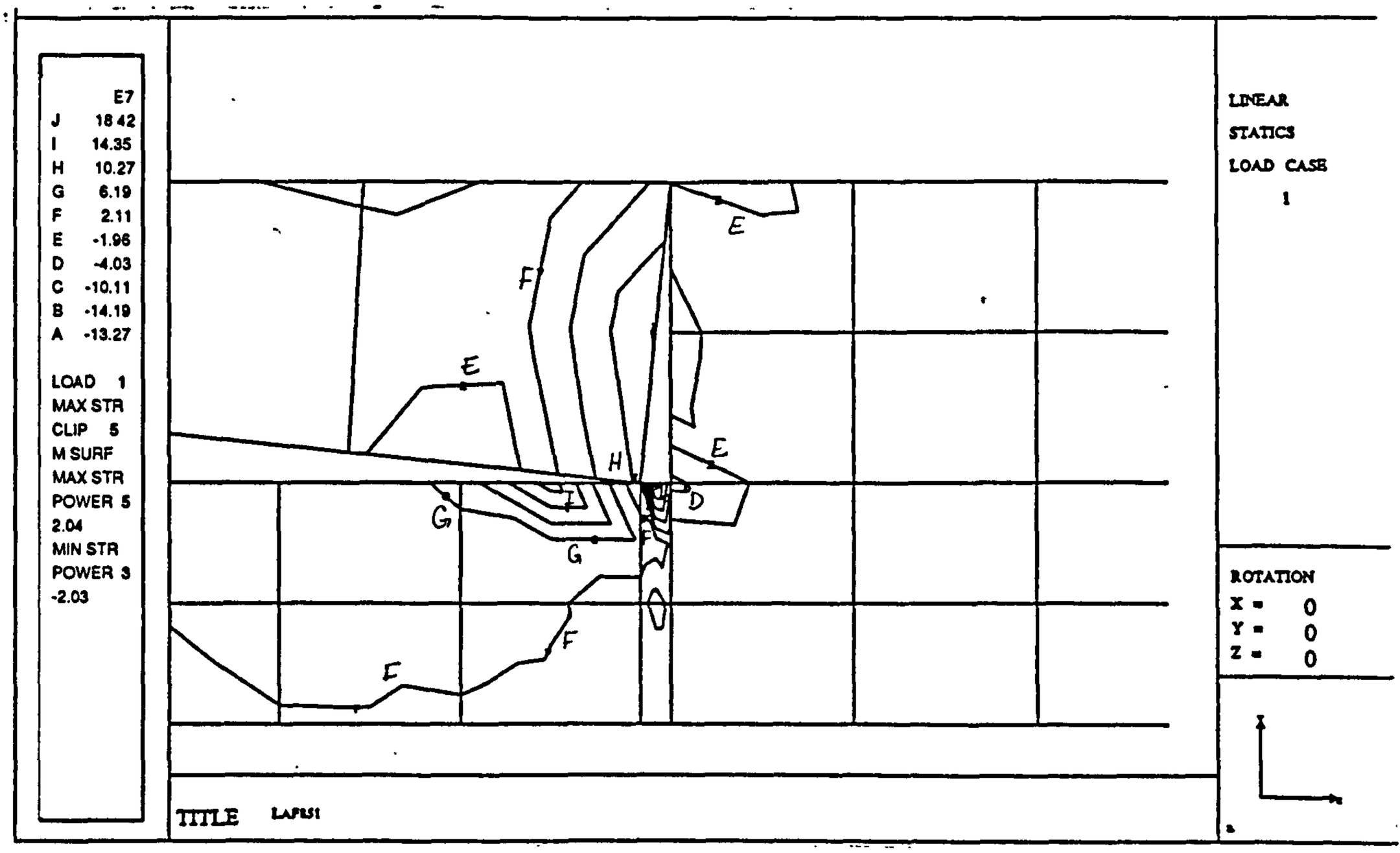

Fig 6.19 Major principal stress, 0.05 mm vertical penetration and 7 mm horizontal movement

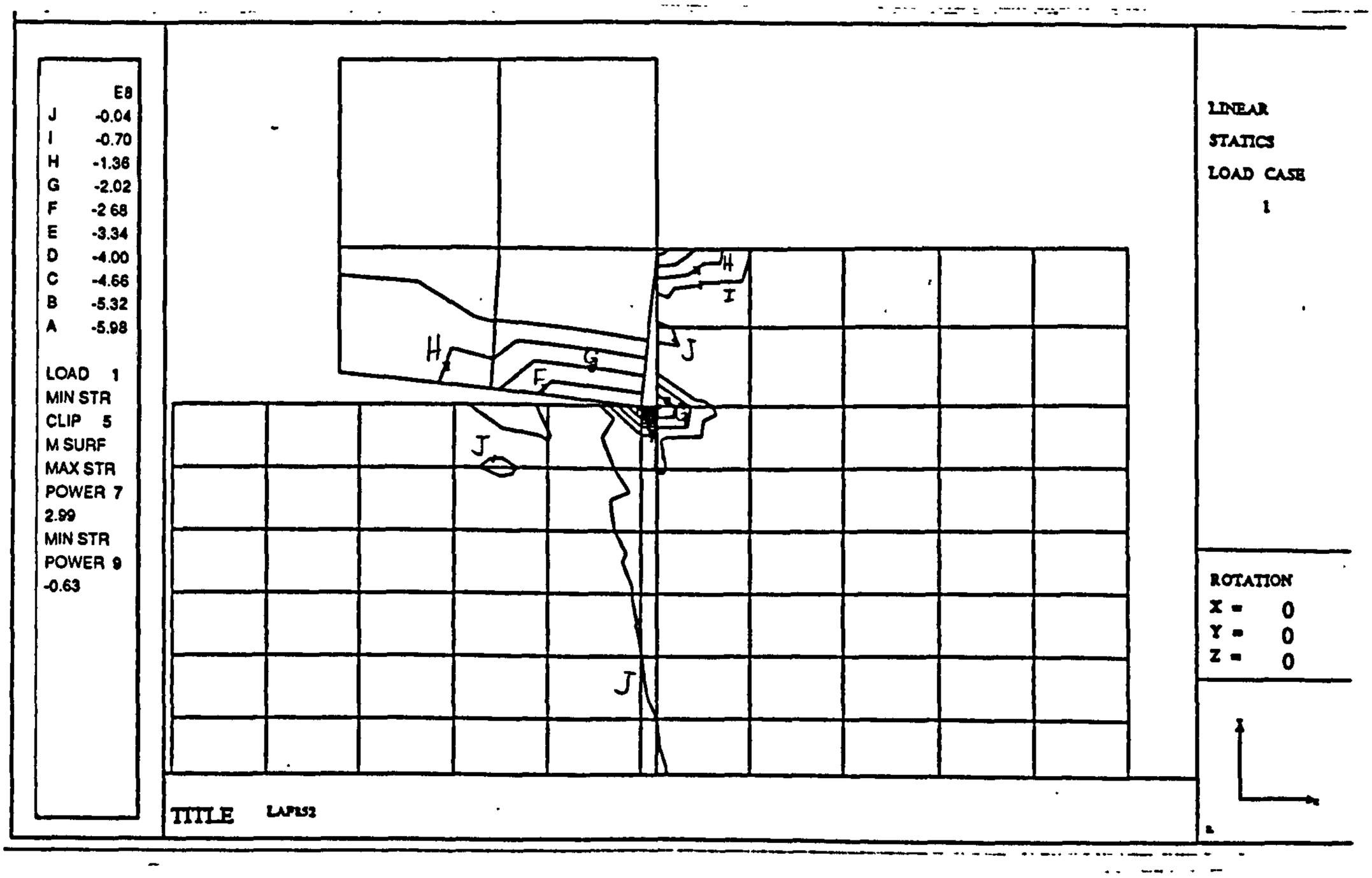

Fig 6.20 Minor principal stress, 0.05 mm penetration and 7 mm horizontal movement

$$\sigma_1=\tan(\psi)\,\sigma_2+\sigma_c \quad \text{for shear fracture and when } \sigma_2=\sigma_t$$

$$\text{where } \tan(\psi)=\frac{1+\sin\phi}{1-\sin\phi}$$

$\phi=37.3^{\circ}$=internal friction angle

σ_c=43.9 MPa=uniaxial compressive strength and σ_t=3.77 MPa=uniaxial tensile strength

From above equation for each element σ_{1f} (σ_1 at failure) according to σ_2 Factor of Safety of each element can be calculated.

$$\text{Factor of Safety=F.O.S}=\frac{\sigma_{1f}-\sigma_2}{\sigma_1-\sigma_2}$$

and in the tensile state Factor of Safety is $\frac{\sigma_t}{\sigma_2}$

The elements which are shown in Fig 6.21 having a Factor of Safety less than 1 indicate that failure has occurred. Furtheremore, in Fig 6.21 it can be seen the area where failure has taken place is located beneath the drag bit and it is tensile in nature. This finite element describes the state of stress induced into the rock by a drag bit and it was shown that the dominant type of failure is tensile which supports Evan's theory. However Evans (1972) caused by cutting of the coal along a curve is of a circular arc shape. Based on this assumption, he gave a solution for the cutting force on the wedge. This method may be not ideal because the stress distribution in the rock is unknown. Secondly it was found from this finite element analysis subsurface damage exists and this can be justified by experimental results.

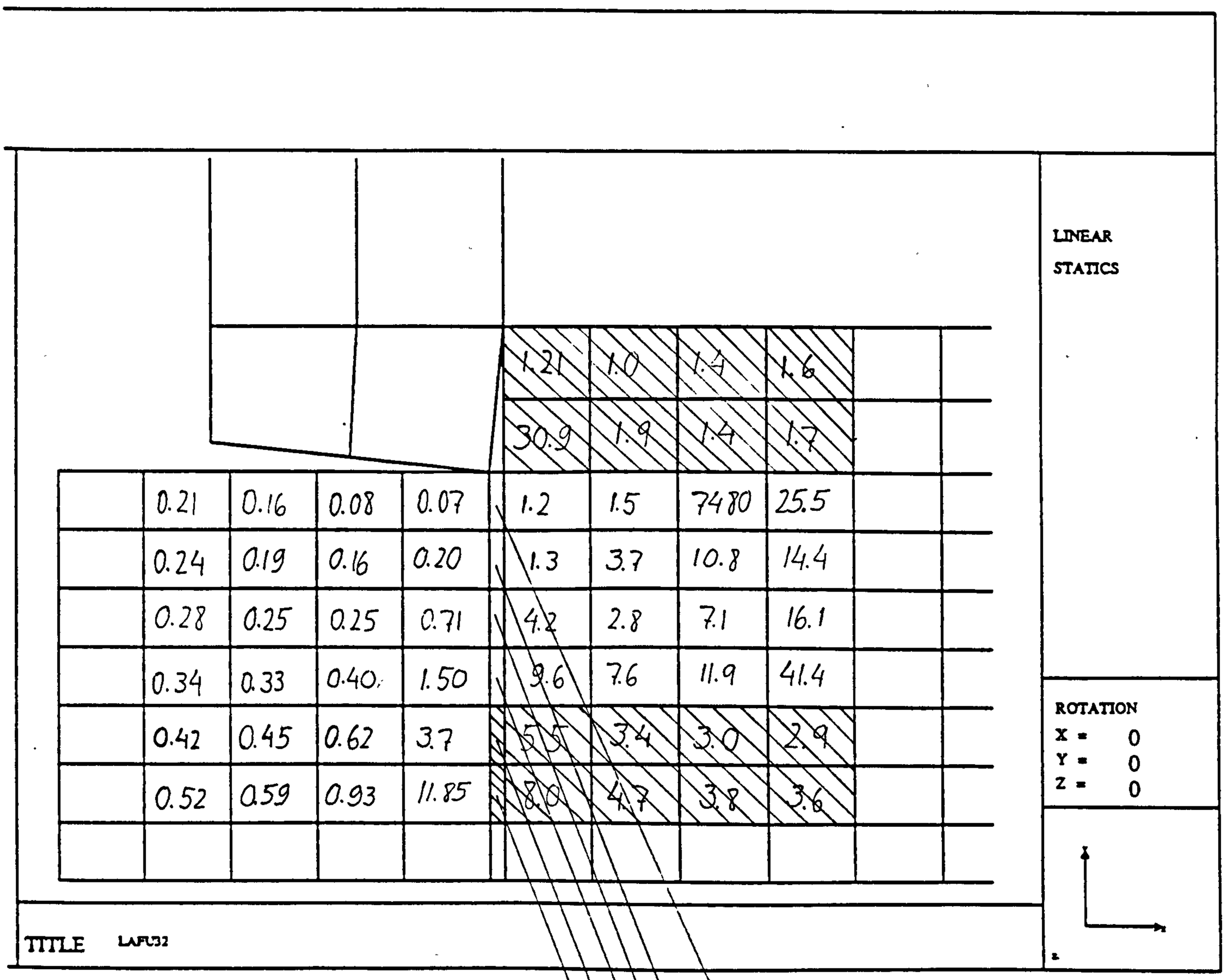

Fig 6.21 Failure area beneath the bit

The previous modelling attempts were not suitable for stress calculation corresponding to cutting operation. The models for rock cutting operation used modulus of elasticity derived from static loading tests. However during rock cutting operations the selection of this modulus would be inappropriately low and a higher value may be necessary. For this reason it was decided to increase Young's modulus by ten times. This is the opposite to the commonly adopted approach whereby the modulus is reduced by ten times when we move from laboratory to in-situ conditions. Use of increased Young's modulus resulted in tensile failure in the model located in the rock material below the cutting bit (Figs 6.22 and 6.23 major principal stress and minor principal stress coressponding to failure condition). This new analysis has shown that successful modelling can be applied to the rock cutting operation by the use of the FE Techniques provided that appropriate material constants are adopted.

6.11 Conclusions

Rocks with discontinuities subjected to cutting forces SE, reduce in three states compared to intact rock (dry, ambient, saturated) but two or three vertical discontinuities on the core axis behave the same as a single discontinuity.

During cutting with simultaneous axial stressing, no axial displacement was recorded at any loading level, this indicates that there is no change in the structure of the rock and the rock behaves the same as intact rock. The results of cutting parameters show only little changes when axial loading is near the yield limit (90 % UCS).

For rock specimens containing a discontinuity, at ambient moisture content, cutting forces and SE reduce for the various discontinuities

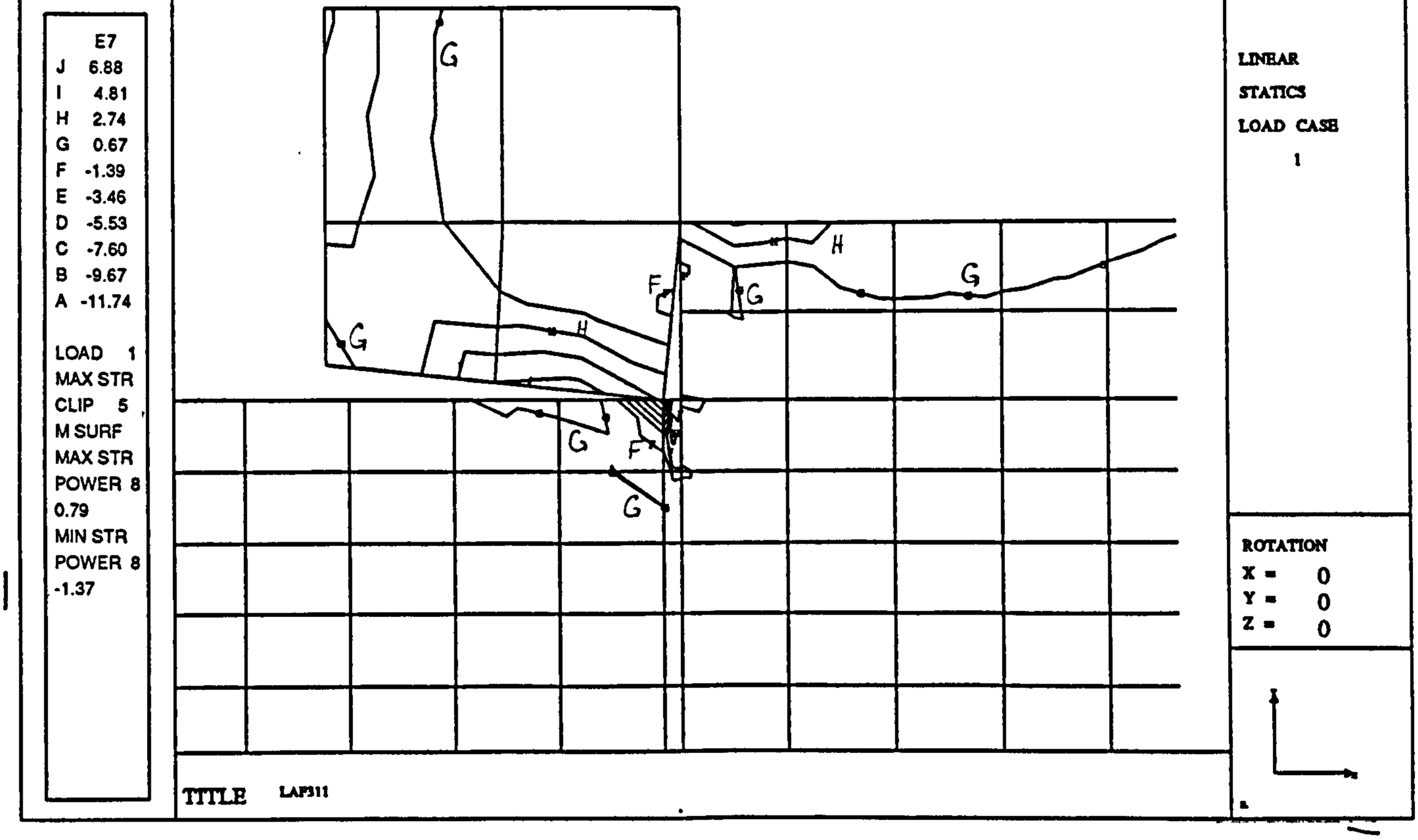

Fig 6.22 Major principal stress with coressponding to high Young's modulus

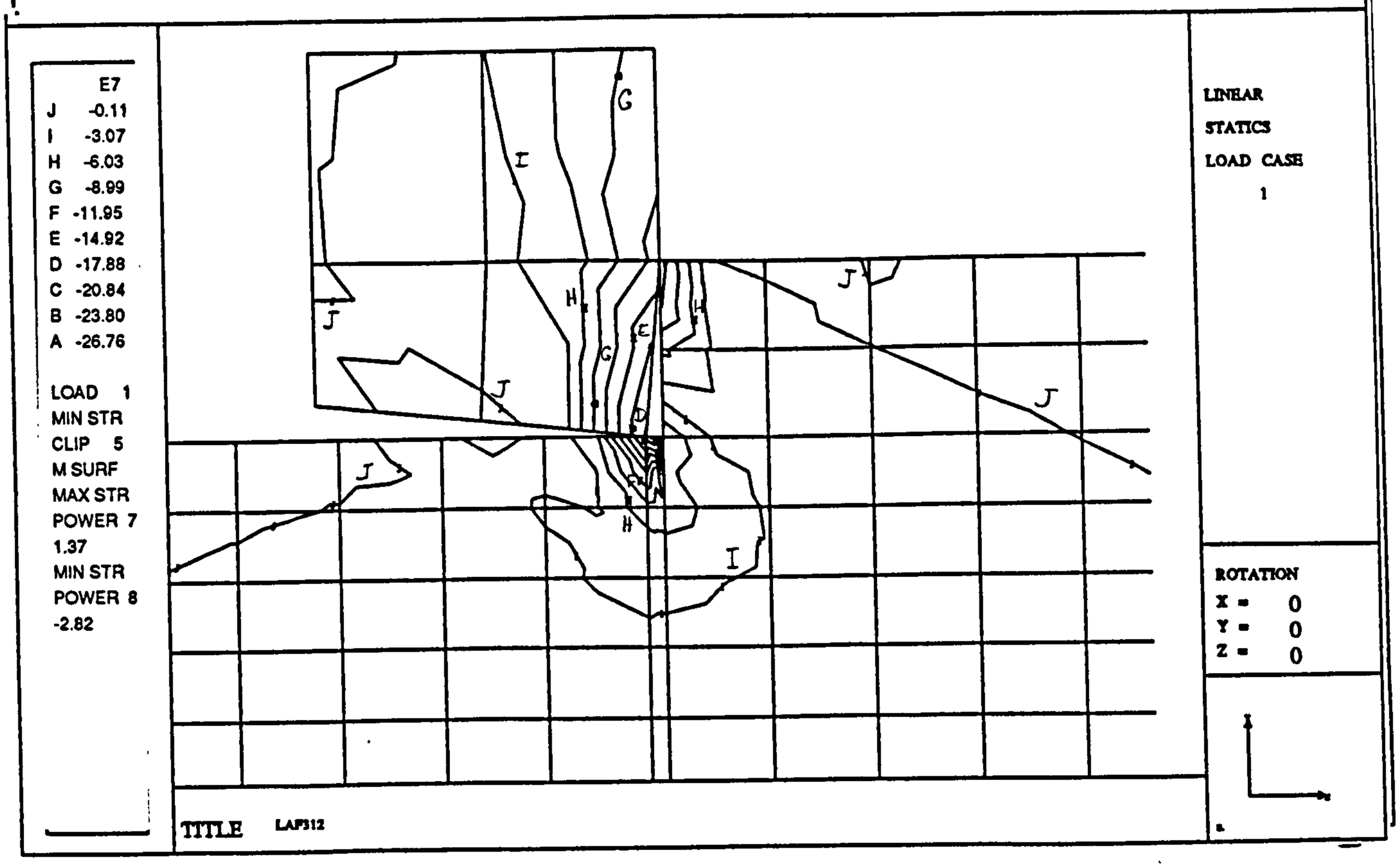

Fig 6.23 Minor principal stress with coressponding to high Young's modulus

and different angles when compared to intact rock. This reduction does not appear to be function of the angle of the discontinuities. In the dry state, (with the exception of the discontinuity angle of the discontinuity angle of 30°), all the forces and SE reduce but for both dry and saturated it is not possible to find any trend between results.

When the discontinuity spacing was chosen very small, e.g 50 mm, it was found this spacing is worthful, and it may be concluded that the rock behaves as an intact rock.

In Springwell sandstone discontinuities with more than 50 mm discontinuities spacing give results similar to intact rock. This supports the idea that discontinuities may affect rock cuttability.

The results with composite specimens of China clay, Springwell sandstone and Welton chalk, showed that the effect of the inclusions is greater than the discontinuity itself.

When clay is intercalated between rock layers, it makes the layer weaker and sometimes there is no need to use much energy to cut the rock. It is easy to ripp off the rock from the surface. It was found that when the thickness of clay was reduced, the specific energy was considerably reduced. This means that if the thichness of the clay is around 10 mm we use less SE than when the thickness is 25 mm. In this investigation the depth of cut was constant at 6 mm, while other parameters were retain constant (rake angle, speed), and the only parameter changed was the thichness of the clay.

Chalk insertions cause cutting forces to increase and clay insertions decreased the cutting forces when they were intercalated with Springwell sandstone specimens.

In general cutting forces in general reduce when the moisture condition changes from partial to saturated condition and there was evidence of a trend between cutting forces and different degrees of water saturation.

Water helps cutting efficiency, and cutting forces are reduced as we move from dry to ambient and from ambient to saturated conditions.

If we divide the five types of rock into three groups according to porosity, Springwell sandstone is porous, Welton chalk and Matlock limestone are less porous, while Pennant sandstone and Teesdale Whinstone are have very low porosity. We shall address the questions of whether there are any changes in rock cutting parameters (cutting forces, SE) when rock is saturated, whether it is the same for all rocks and whether is possible to find out any reason for this phenomenon. In springwell sandstone, which is more porous than other rocks, water reduces the strength of the sandstone therefore we can see a reduction in cutting forces and also in specific energy. However, for Pennant sandstone and Teesdale Whinstone which are very strong, and have low porosity, water gets trapped between the tool and the rock during cutting causing pore pressure increase, resulting in an increase in cutting forces. Welton chalk and Matlock limestone, which are less porous and not very strong are not affected very much by water.

The relationship between depth of cut and specific energy is very similar to the previous research results but it was found that the difference between 4 mm and 6 mm is more significant than 6 mm and 8 mm spacing.

The optimum spacing for saturated Springwell sandstone was found at s/d=7.5. Furthermore the break-out angle may be used to calculate the optimum spacing (according to Roxborough 1973).

There is a reduction on cutting parameters in depths 4 mm, 8 mm and the 6 mm depth of cut in s/d=3 showing a desirable reduction of the required SE.

It was found that between rake angle -10°, 0°, 16°, the specific energy for 16° value is less than others for the fully saturated condition.

Tests were carried out for different cutting speeds between 0.100 m/s and 0.125 m/s in the saturated state. There is no change in rock cutting parameters.

Wear for all materials used in the experimental work showed reduction for fully saturated state. Also, different angles were examined in saturated condition, and it was found that between -10°, 0°, 16°, rake angles the - 10° value results in less wear than the others.

Chapter 7

FRACTURE MECHANICS TESTS

Traditionally UCS and tensile strength were correlated with rock cutting parameters (cutting forces, specific energy). However recent trends in rock cutting research show that there is a need to assess whether fracture toughness can be correlated to rock cutting parameters.

Fracture mechanics tests have recently emèrged as an important tool in rock mechanics. It is believed that an understanding of the mechanics of rock fracture is a key element in solving a great many engineering problems involving geothechnical structures. Fracture mechanics has been applied widely, in the modelling of rock fragmentation, excavation by dynamic and hydraulic fracturing techniques, tunnelling and drilling. Fracture properties have been taken into account in the series of rock bursts, (Fairhurst et al, 1981), geothermal reservoirs, (Takahashi, 1989), formation of rock joints (Kemeny et al, 1985) and stability of rock slopes (Tharp et al, 1985). Since the ISRM suggested testing (1988,1989), relies on linear elastic fracture mechanics (LEFM), a simplified description of the use of LEFM to geomaterials is included below. A much more detailed insight into fracture mechanics theory may be found in works such as Atkinson (1987) and Rossamanith (1983).

The theory of LEFM is concerned with predicting the onset of crack propagation in a linear elastic material from a pre-existing flaw. To this end, two basic approaches are employed which are based upon consideration of the energy of the system or the stress intensity around the crack tip.

Griffith (1921) concluded the first successful analysis of a fracture dominant problem with a consideration of the propagation of brittle cracks in glass.

As a result of his work, Griffith put forward the concept that a crack will propagate if thereby the total energy of the system will be lowered. This idea suggested an energy balance between the decrease in strain energy in the continuum as the crack extends counteracted by the energy needed to create new crack surfaces.

The energy release rate or crack driving force, G, was put as the parameter characterizing crack propagation and was defined as the elastic energy per unit crack surface area available for infinitesimal crack extension. The crack initiation was assumed upon G reaching some critical value G_C.

The stress intensity approach to fracture problems was suggested by Irwin (1957). Irwin showed that, for certain simple fracture problems, the stress field in the vicinity of the crack tip was characterized by a parameter termed the stress intensity factor (SIF) which could be used to determine the onset of crack propagation. In addition it was concluded that, for LEFM, this quantity was directly related to the energy release rate. Thus the essence of the stress intensity approach to fracture is that crack propagation is controlled by the stress field which is responsible for the energy state at the crack tip. The general form of SIF is $K=\sigma\sqrt{a}$

where

a is crack length (m);

K is in $MPa\sqrt{m}$;

σ is in MPa

And the relationship between fracture energy and SIF as follows:

$$G=\frac{K^2(1-\nu^2)}{E}$$

where

K is in MPa$\sqrt{m}$;

G is in kN/m

E is Young's modulus in GPa;

ν= is Poisson's ratio;

The general state of deformation at the crack tip may be described in terms of three Modes which are summarised in Fig (7.1). Mode I characterises the crack face opening, Mode II the sliding of the crack faces relative to each other and Mode III the tearing type of deformation. Any general fracture analysis must take into account all three Modes of deformation and the crack tip stress field (K_I, K_{II}, K_{III}). The ISRM suggested method is based on Mode I fracture.

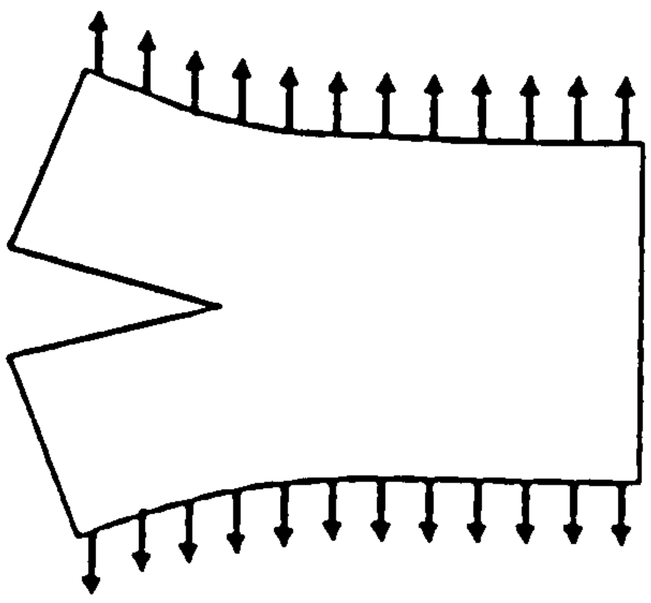

Mode I. Crack opening

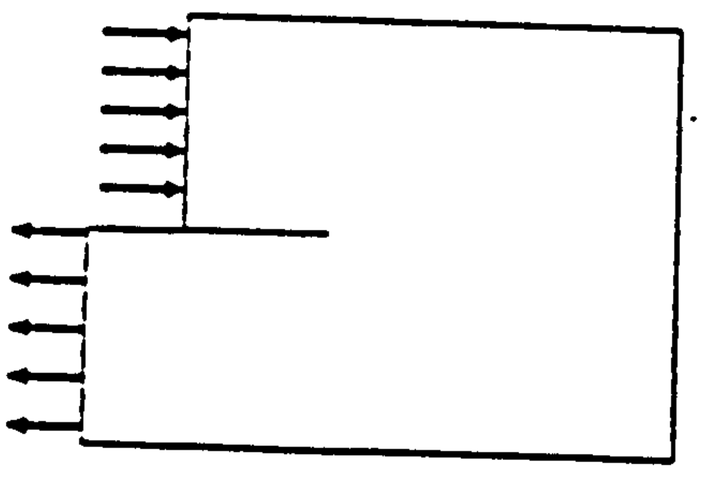

Mode II. Crack sliding

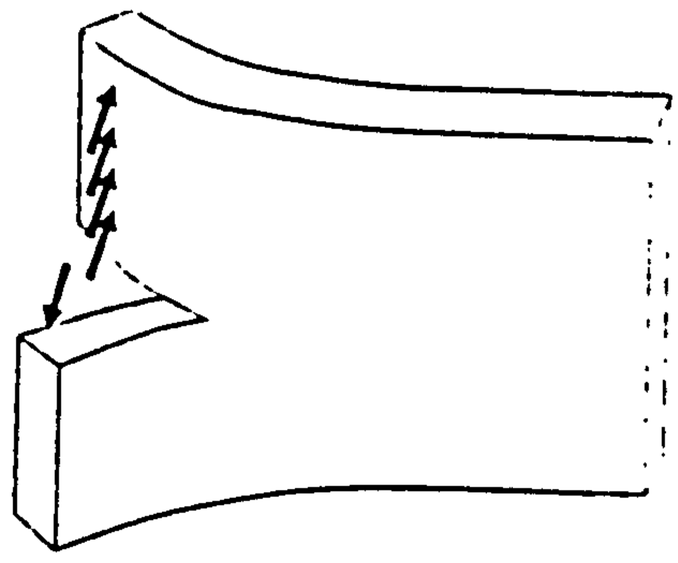

Mode III. Crack tearing

Fig 7.1 Three Modes of crack opening

Rock is an inherently variable material and often anisotropic. Most rocks contain planar anisotropies, which may affect fracture energy or toughness measurements (the critical state of K value is known as the fracture toughness, Rossamanith 1983) ; the most obvious are:

1) primary bedding and lamination

2) metamorphic banding and foliation due to compositional differences and the flattening of grains and alignment of platy minerals

3) microjoints sets and planar microcrack sets

Examples of such materials containing planar anisotropies are shale (Schmidth, 1977), sandstone, (Hoagland. et al, 1977), limestone (Schmidth, 1976) and granite, (Sun and Ouchterlony, 1986).

The test environment can affect values of fractures toughness. Water may affect crack propagation in rock chemically, by reacting with material at the crack tip and/or mechanically by reducing friction in the zone corresponding to the crack propagation. Fracture energy or toughness in the presence of water has been reported to be 10% lower than that measured in air in the Anvils Point Oil shale, (Schmidth, 1977), 33% lower in Berea sandstone, 34% lower in Salem limestone, (Hoagland et al, 1973) and 5% lower in granite, (Meredith , 1983). Temperature also can affect fracture energy and toughness measurements, (Hoagland, 1973).

Results of load versus load point displacement, load versus horizontal displacement, and load versus crack open displacement from the short rod with Teesdale Whinstone are shown in Figs 7.2, 7.3.

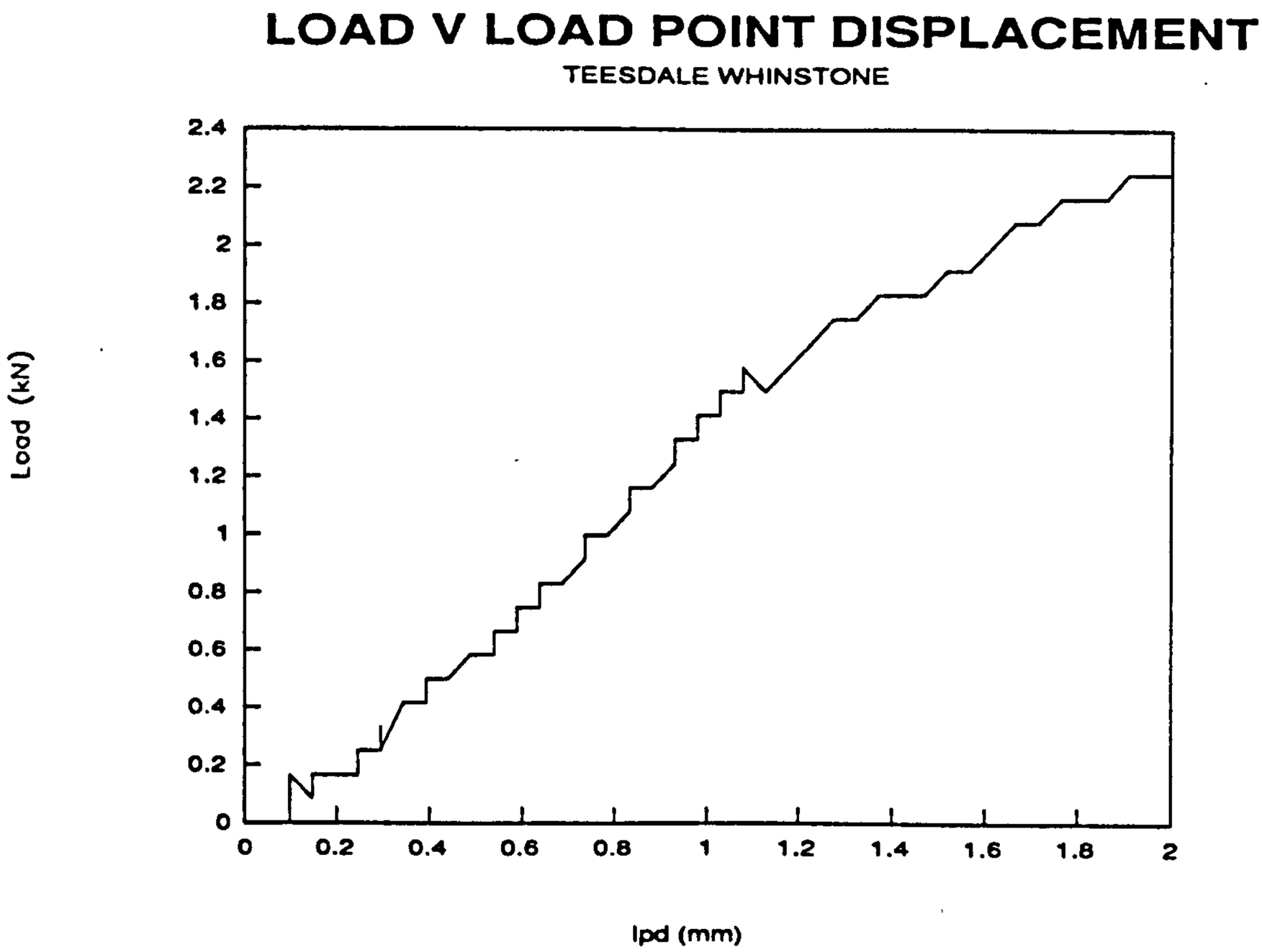

Fig 7.2 Load v Load point displacement

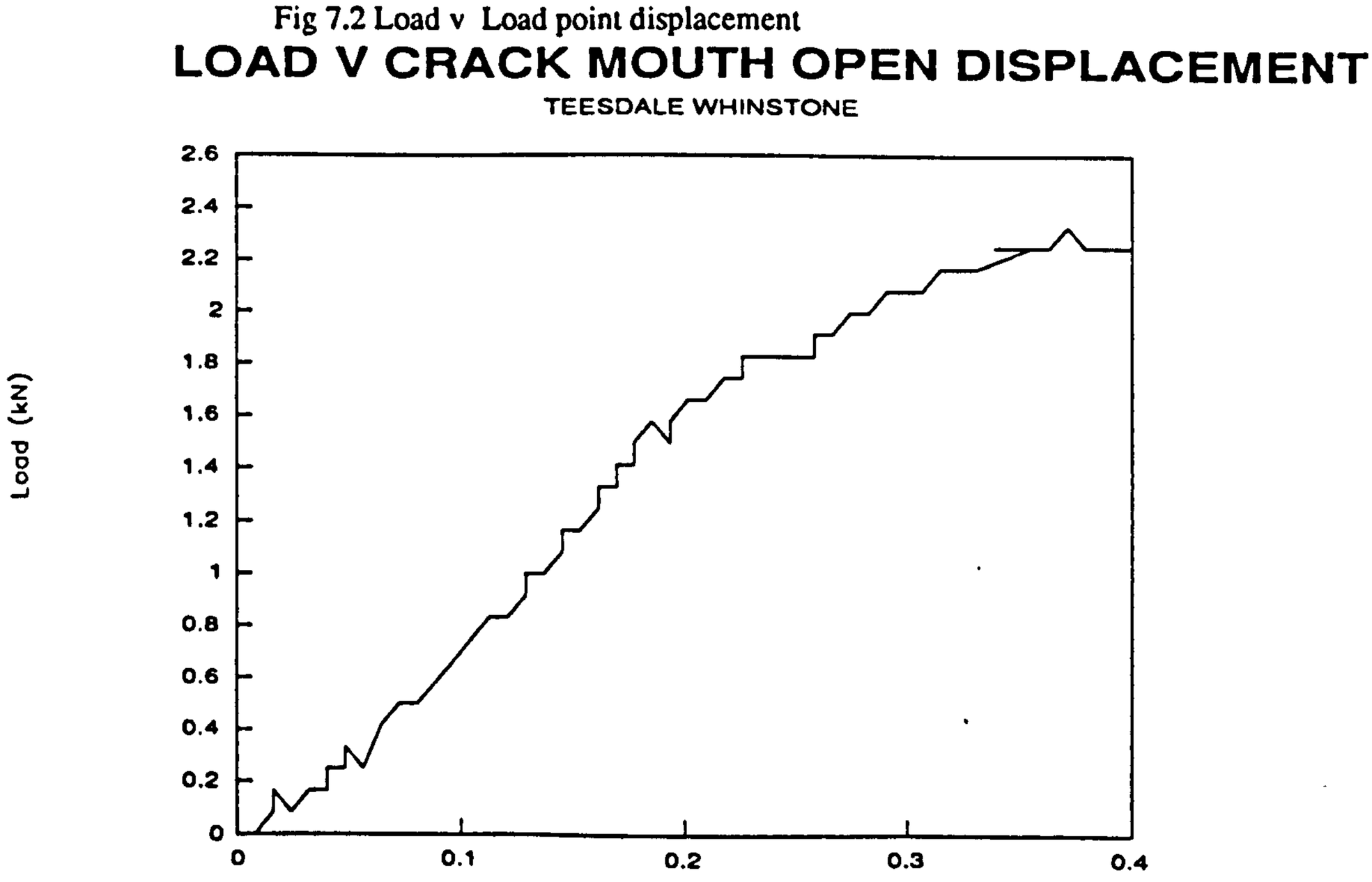

Fig 7.3 Load v Crack mouth open displacement

For level I testing of chevron bend specimen, the fracture toughness of all the specimens is calculated by the following formula (ISRM 1989, Newman 1984):

$$K_{Ic}= A_{min}F_{max}/D^{1.5}$$

where

$$A_{min}= [1.835+7.15\ a_o/D+9.85(a_o/D)^2]S/D$$

F_{max}=maximum load failure (kN);

D= specimen diameter(0.01m)

a_o=chevron tip position

K_{Ic}= fracture toughness (MPa)

For level I testing of short rod specimen, the fracture toughness of the specimen can be calculated by the following formula (Barker 1977, ISRM 1989):

$$K_{Ic}=24.0F_{max}/D^{1.5}$$

where :

K_{Ic}-mode I fracture toughness ($MN/m^{1.5}$);

Fmax-maximum failure load (kN)

D-the SR specimen diameter (0.01 m)

Care should be taken when this formula is used and should take into consideration the following correction factor :

$$Ck=(1-0.6Dw/D+1.4\ Da_o/D-0.01D\ \theta) \qquad (7.1)$$

The symbols Dw, Da_o,and $D\theta$ denote the differences between measured values and the nominal ones, e.g.Dw/D=W/D-1.45 etc. Otherwise the fracture toughness value shall be calculated from :

$$K_{Ic}= Ck\ 24.0\ F_{max}/D^{1.5}$$

The results of fracture tests are as follows:(Tabie 7.1).

Table 7.1

Short rod test	Chevron bend test
ambient/saturated	ambient/saturated
Springwell sandstone	springwell sandstone
0.86/0.43	0.50/0.28
0.65/1.08	0.50/0.22
0.86/0.43	0.62/0.28
0.65/0.43	mean 0.50/0.26
0.65/0.65	
——/0.65	
mean 0.73/0.61	
Pennant sandstone1	
1.08/1.08	2.08/2.36
2.38/1.95	2.13/1.96
3.24/2.16	1.85/2.08
2.59/2.16	2.02/2.13
2.81/1.51	2.24/2.02
3.03/1.73	—— /1.85
2.16/——	mean 2.06/2.07
2.38/——	
2.38/——	
mean 2.45/1.76	
Teesdale Whinstone	
2.12/4.11	2.36/1.85
3.46/3.89	2.99/2.69
3.46/3.89	2.66/2.75
3.46/——	mean 2.67/2.43
mean 3.12/3.96	

Table 7.1 (continued)

Matlock	limestone	
	2.59/1.30	1.01/1.01
	2.16/1.51	0.90/0.90
	2.16/1.30	0.95/0.84
	2.38/1.51	mean 0.95/0.92
mean	2.32/1.40	
Welton	chalk	
	1.08/0.65	
	0.65/0.86	
	0.65/1.08	
	1.30/0.65	
	0.86/———	
mean 0.91/0.81		

In this research it was found that with accurate measurements equation (7.1) is valid without the need to employ a correction factor.

There are two differences between these methods. To set up the CB method is time consuming while short rod is very simple. Another factor is choosing the method is the number of specimens available. One specimen in the three point test is equivalent to two in the short rod, as appeared from the ISRM's suggestion that after three point the specimen can be used for short rod testing as well. It appears therefore that use of short rod test is a better option, when limited quantity of material is available for investigations.

Chapter 8

ANALYSIS OF RESULTS

Full details of experimental results of rock cutting have been presented in chapter 6. It was shown that the moisture content of different rocks can affect rock cutting parameters. For some rocks this effect is very large (Springwell sandstone) and for others (Teesdale Whinstone and Pennant sandstone) is less significant. The influence of moisture content was found to be related to the porosity of rock materials.

It was found there is no correlation for discontinuity angle and small spacing in 90° (with respect to core axis). On the other hand discontinuity angle has an effect on rock cutting parameters provided the discontinuity spacing is less than 50 mm. Above this spacing, rock behaves the same as intact material.

The speed of the cutting tool in Springwell sandstone was examined in saturated state. It was found that there is not much difference in rock cutting parameters as the speed changed.

Wear is directly related to moisture condition and for each rock type wear in the saturated state is less than in the ambient state and between two rocks, in fact the rock which has more moisture content normally has less wear.

Even though a rake angle of 16°results in a smaller SE (in comparison with - 10°) the strength of the bit is reduced, consequently the rake angle of - 10° is still the optimum solution.

8.1 Numerical modelling of chevron bend specimen (CB)

Numerical analysis can be used to justify experimental testing and size requirement for rock fracture toughness testing. The method suggested by ISRM uses two types of cylindrical specimens with chevron cracks,i.e,short rod specimens (SR) and three point bend specimens (CB). In order to determine fracture toughness, a distribution of the SIF along the front edge of the chevron crack must be evaluated beforehand. For SR specimens, the SIF has already been evaluated by FEM and BEM analyses. However, for the CB specimens, these have not been attempted very much,and the SIF obtained experimentally by the so-called compliance method does not provide the information on the distribution of the stress intensity factor.

Yashi et al (1989) have reported the compliance of a CB specimen evaluated by the BEM analyses, and, the SIF determined experimentally agrees well with that determined from the compliance evaluated by the BEM analyses. However, this value of the SIF is considerably larger than the front edge that are evaluated directly by the BEM analyses. The discrepancy is more than 8 %.

Grestle (1991) has found the crack front compliances from the boundary element analyses are consistently larger than the experimentally obtained CF (compliance factor) compliances. This is because the experimental compliances are a measure of only the relative displacements between the crack front and the top of the round bar directly over the reaction points while the boundary element results reflect the difference in displacements between the crack front and the reaction points themselves. The evaluation of SIF have been calculated by BEASY programme (BEASY Manual). There are a number of ways of calculating the SIFs. BEASY-IMS uses the equations presented by Irwin (1957) which express the SIFs in terms of the displacements and stress components at a point near the crack

tip. The equations consider a coordinate system local to the crack, in which the crack may be considered on the left hand side (Fig 8.1) where r is the distance of a point near the crack tip, and θ ιs the angle as shown in the following figure.

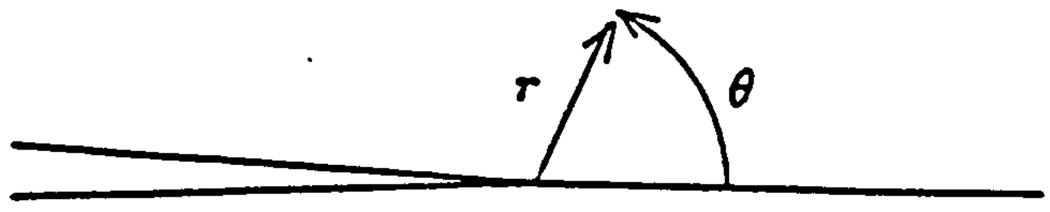

Fig 8.1 Local coordinate system around crack tip

BEASY uses the results at the boundary and at internal points to calculate the SIFs, according to the user's requirements. The equation for determinig K_I from displacements is :

$$\upsilon = \frac{K_I}{4\mu}\sqrt{\frac{r}{2\pi}}\left\{(2k+1)\sin\frac{\theta}{2} - \sin\frac{3\theta}{2}\right\}$$

where k is (3-4ν) for plane strain or (3-ν)/(1+ν) for plane stress, and μ is the shear modulus. The angle θ is equal to π for straight line cracks and ν is the Poisson's ratio of the material. The term on the left hand side ,υ is the displacement, in a direction normal to the line of the crack, at the point near the crack for which r and θ are evaluated.

Accurate SIF are found by evaluating at the least mesh point on the first element on the crack surface (Fig 8.2).

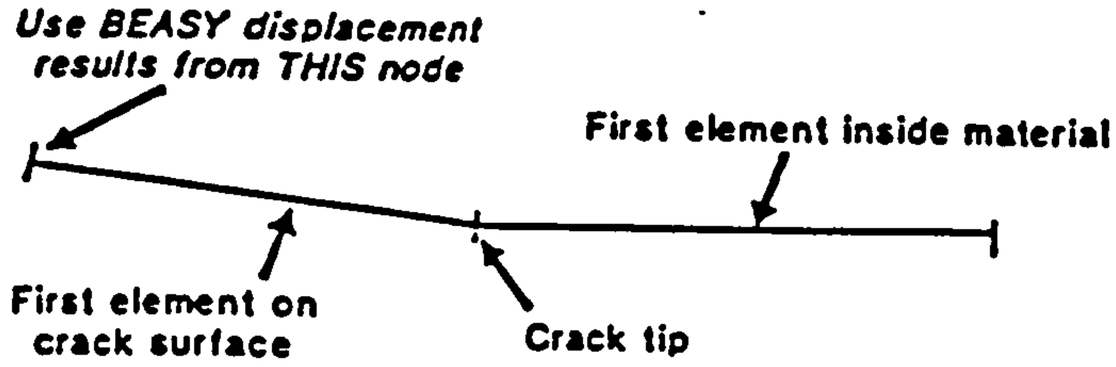

Fig 8.2 Crack tip mesh point fracture calibration

In modelling the crack tip behaviour with high stress concentration, the elements near the crack tip must be very small. In BEASY this can be done by element grading.

In this work it was found that for 2D boundary element, SIF is larger than experimental test, 0.45 MPa compare to 0.41 MPa for Springwell sandstone.

It was found that Poisson's ratio is more important than Young's modulus. Typical examples of 2D and 3D boundary element are presented, Figs (8.3 to 8.5)

8.2 Rock cutting related to fracture tests

Rock fracture toughness is an important rock property, which indicates a measure of cuttability. The results show that the cutting forces increase as rock fracture toughness increases. Correlations between the rock

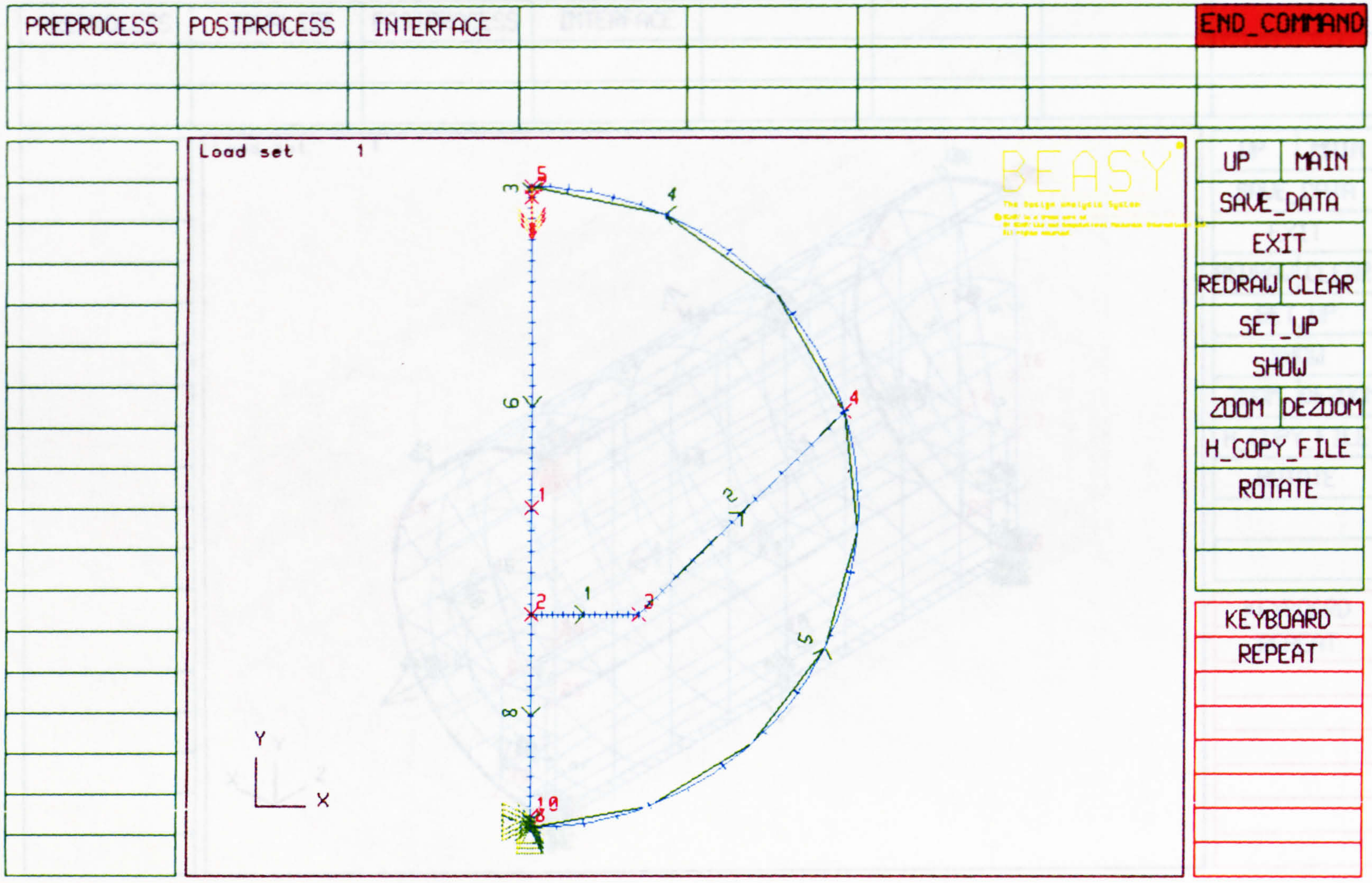

Fig 8.3 2D Boundary Element

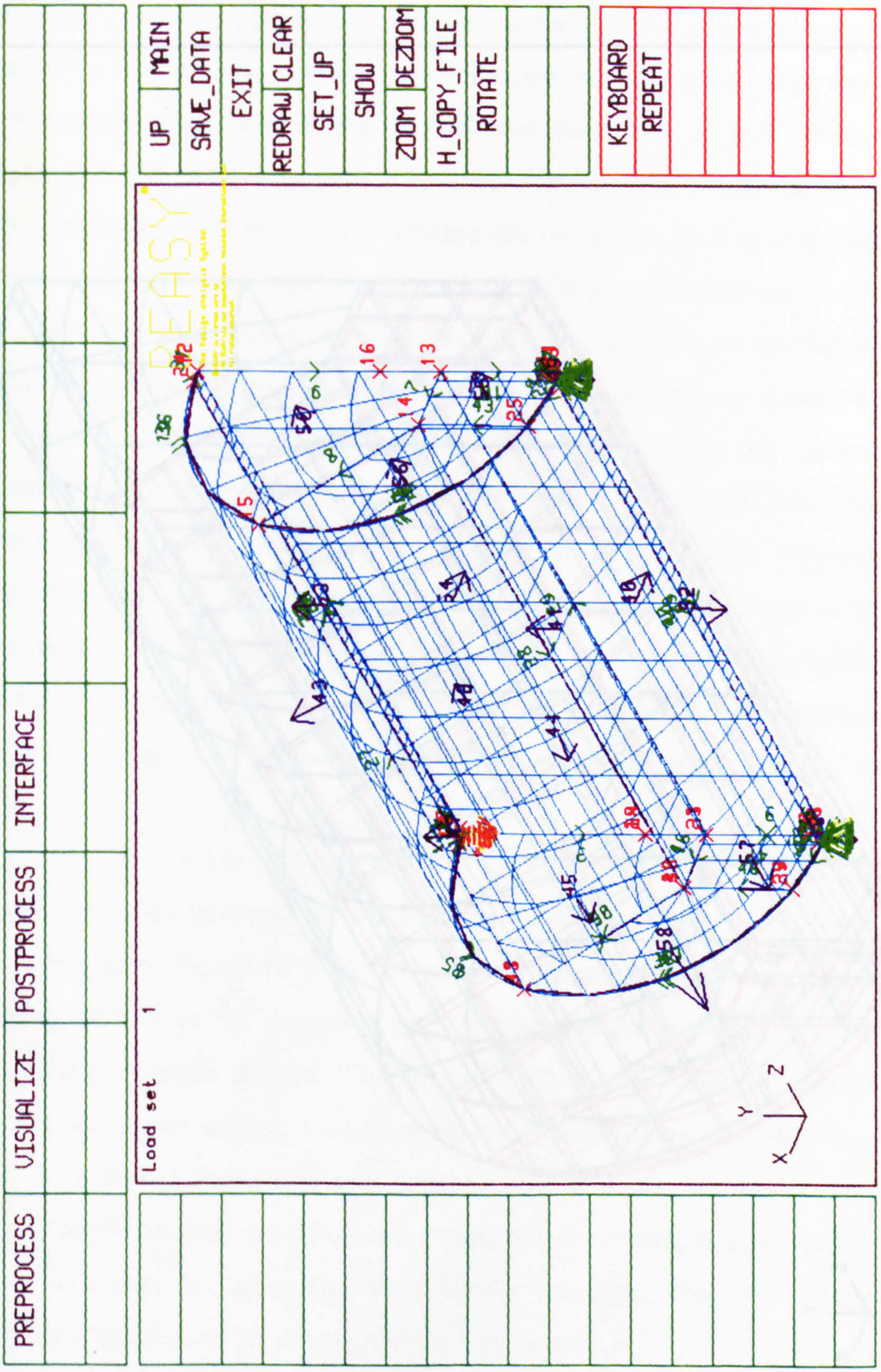

Fig 8.4 3D Boundary Element

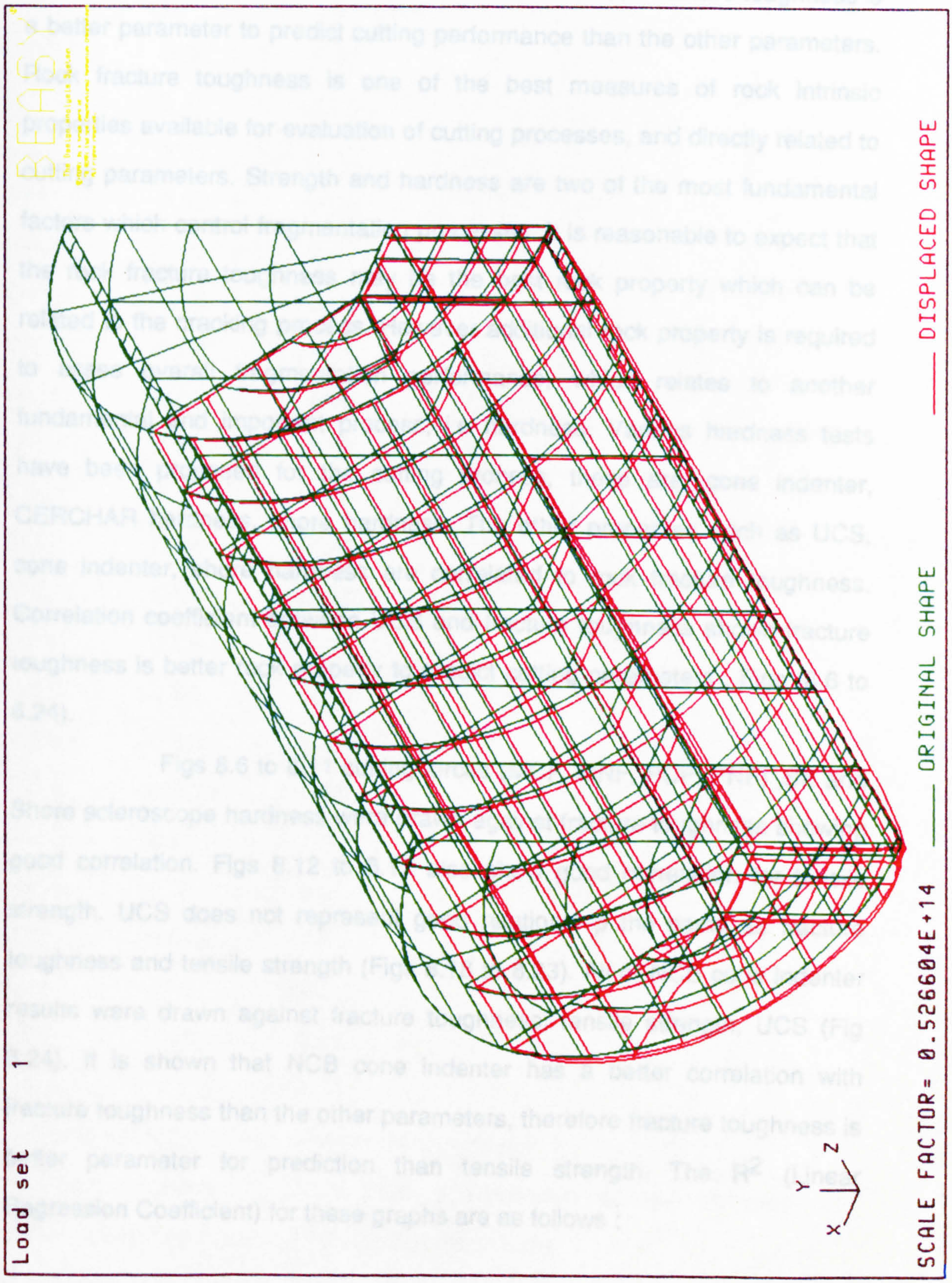

Fig 8.5 Deformed shape of 3D Boundary Element

fracture toughness and the cutting forces show that rock fracture toughness is a better parameter to predict cutting performance than the other parameters. Rock fracture toughness is one of the best measures of rock intrinsic properties available for evaluation of cutting processes, and directly related to cutting parameters. Strength and hardness are two of the most fundamental factors which control fragmentation processes. It is reasonable to expect that the rock fracture toughness may be the best rock property which can be related to the cracking process. However additional rock property is required to asses overall fragmentation performance, which relates to another fundamental and important process, i.e hardness. Various hardness tests have been proposed for the cutting process, these are: cone indenter, CERCHAR hardness, shore hardness. The other properties such as UCS, cone indenter, shore hardness are correlated to rock fracture toughness. Correlation coefficient between UCS and fracture toughness shows fracture toughness is better rock property to predict cutting parameters , Figs (8.6 to 8.24).

Figs 8.6 to 8.11 cutting forces (MCF, MNF, PCF, PNF) ,SE and Shore scleroscope hardness were drawn against fracture toughness showing good correlation. Figs 8.12 to 8.17 also show good correlation for tensile strength. UCS does not represent good relationship the same as fracture toughness and tensile strength (Figs 8.18 to 8.23). All of NCB cone indenter results were drawn against fracture toughness, tensile strength, UCS (Fig 8.24). It is shown that NCB cone indenter has a better correlation with fracture toughness than the other parameters, therefore fracture toughness is better parameter for prediction than tensile strength. The R^2 (Linear Regression Coefficient) for these graphs are as follows :

	R^2	coefficient
TSE	0.90	6.32
KSE	0.80	28.95
USE	0.52	0.45
TPCF	0.85	0.54
KPCF	0.90	2.81
UPCF	0.68	0.046
TPNF	0.98	1.01
KPNF	0.92	4.98
UPNF	0.59	0.08
TMCF	0.77	0.29
KMCF	0.84	1.65
UMCF	0.84	0.028
TMNF	0.63	1.04
KMNF	0.89	3.16
UMNF	0.55	0.05
TNCB	-35.29	0.75
KNCB	0.77	1.20
UNCB	0.48	0.02
TSH	0.099	5.1
KSH	0.38	29.15
USH	0.49	0.08

where :

T=tensile strength	K=fracture toughness	U=UCS
SH=shore hardness	NCB=NCB cone indenter	SE=specific energy
PCF=peak cutting force	PNF=peak normal force	
MCF=mean cutting force	MNF=mean normal force	

Rock cutting machinery requires capital investment, especially for large scale machines such as roadheader. Production is depends highly

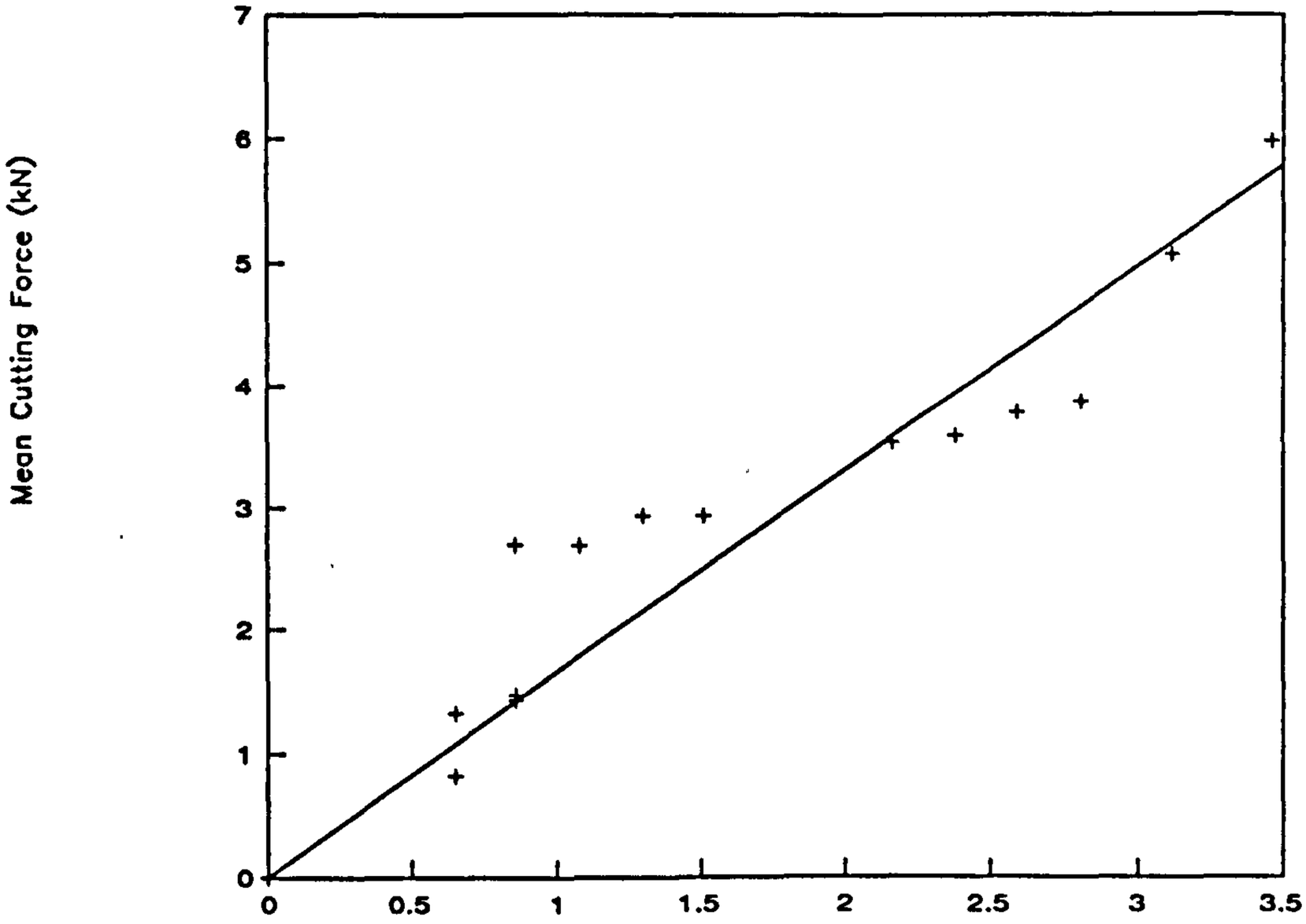

Fig 8.6 Mean cutting force v Fracture toughness

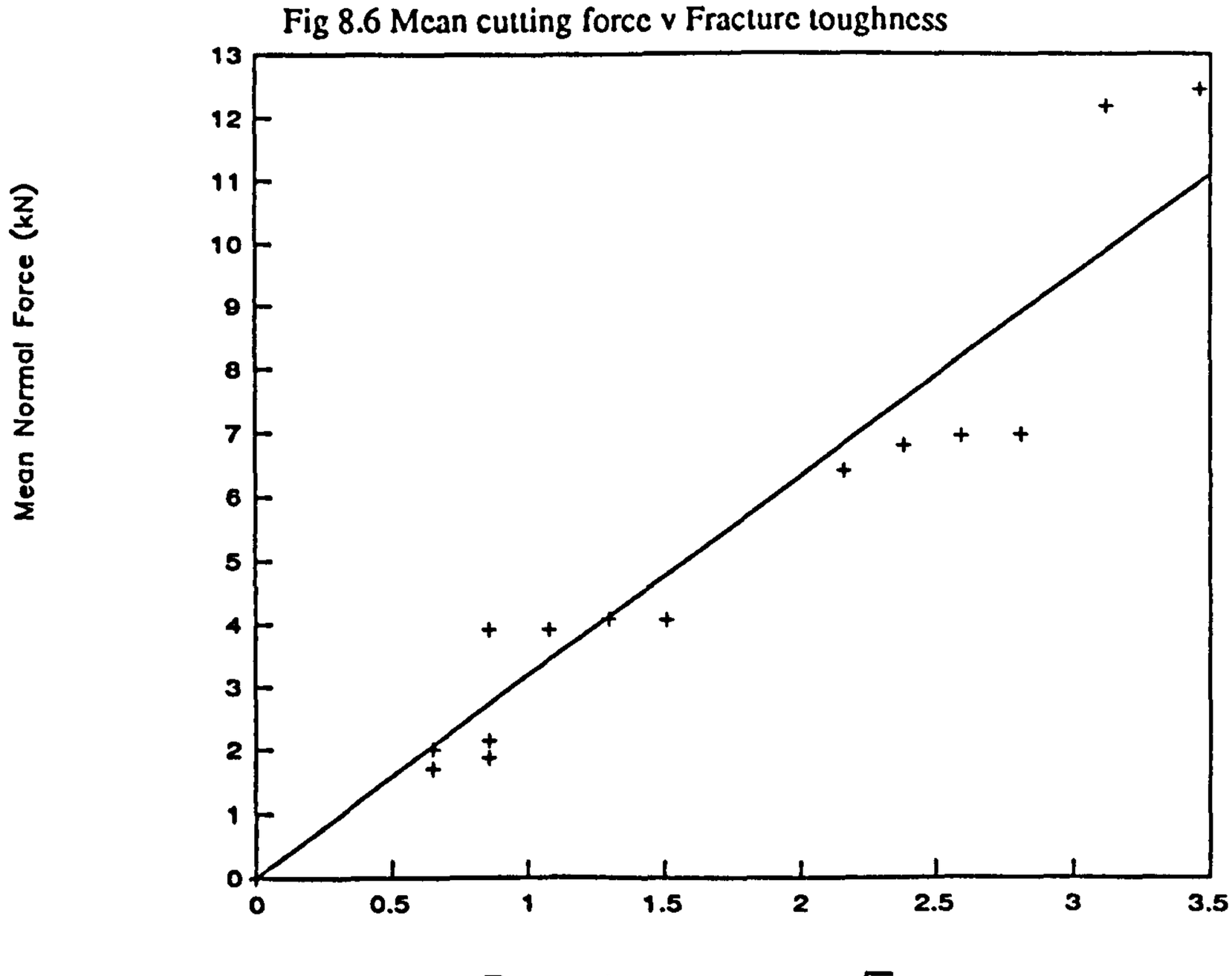

Fig 8.7 Mean normal force v Fracture toughness

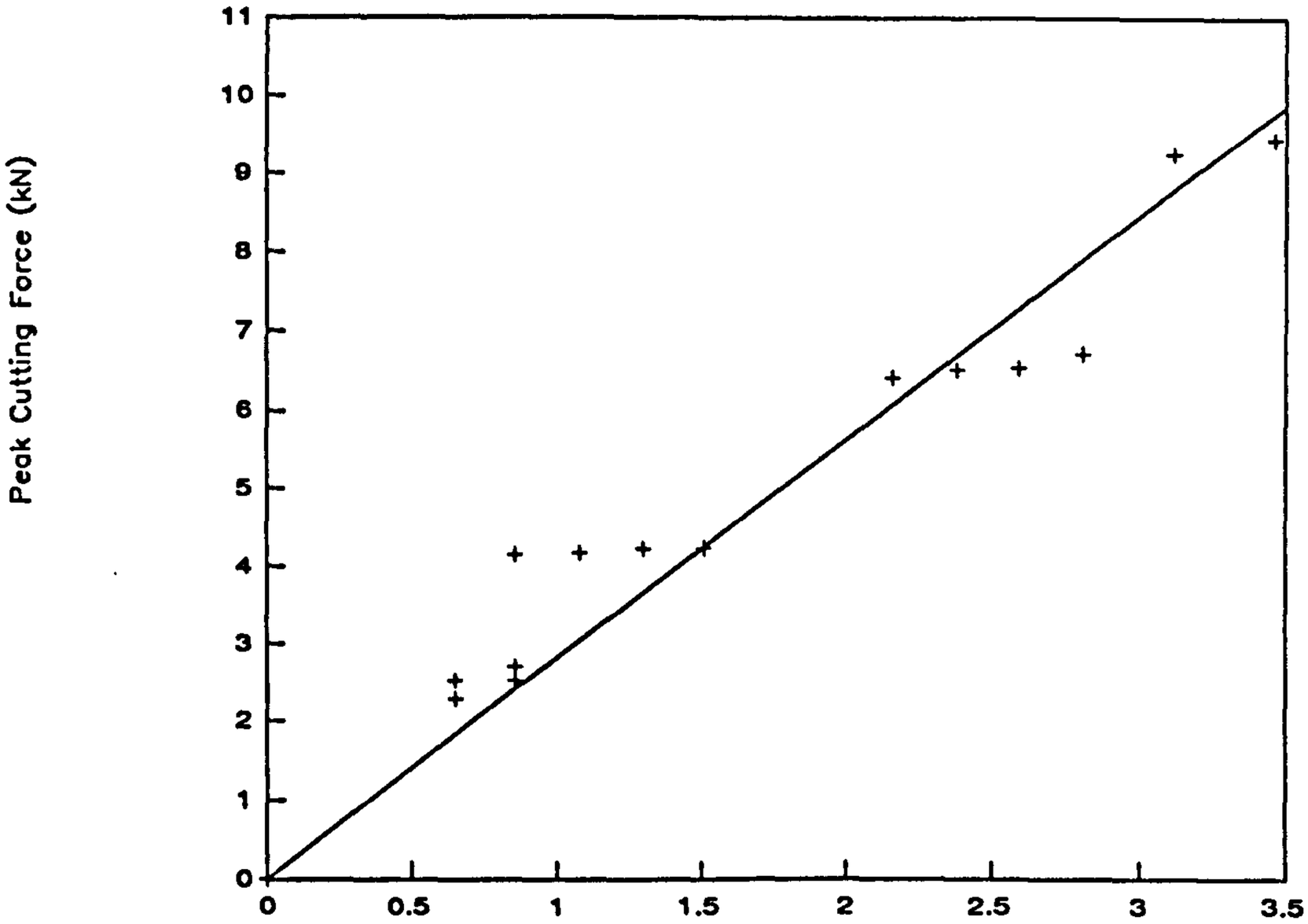

Fig 8.8 Peak cutting force v Fracture toughness

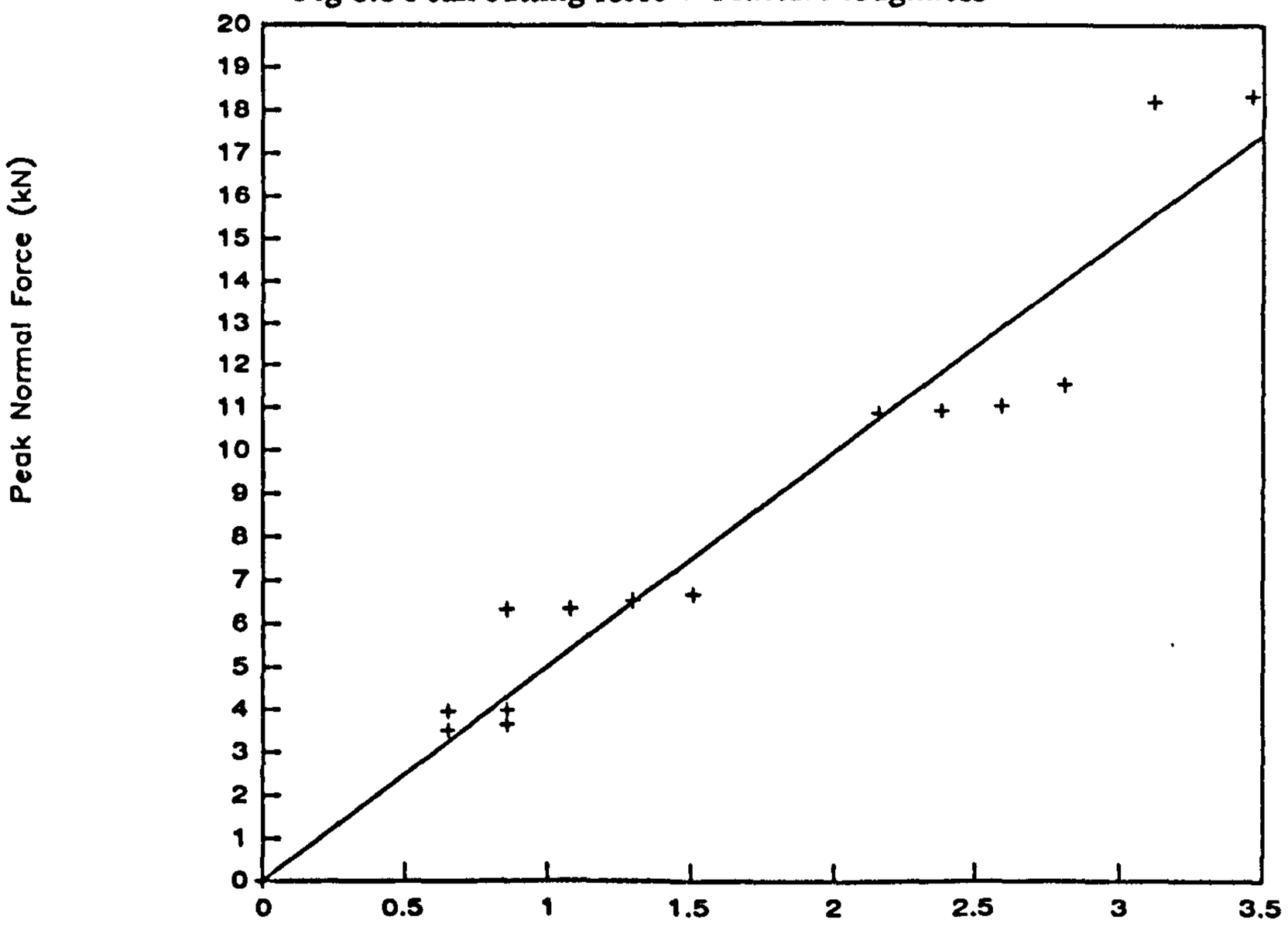

Fig 8.9 Peak normal force fracture toughness

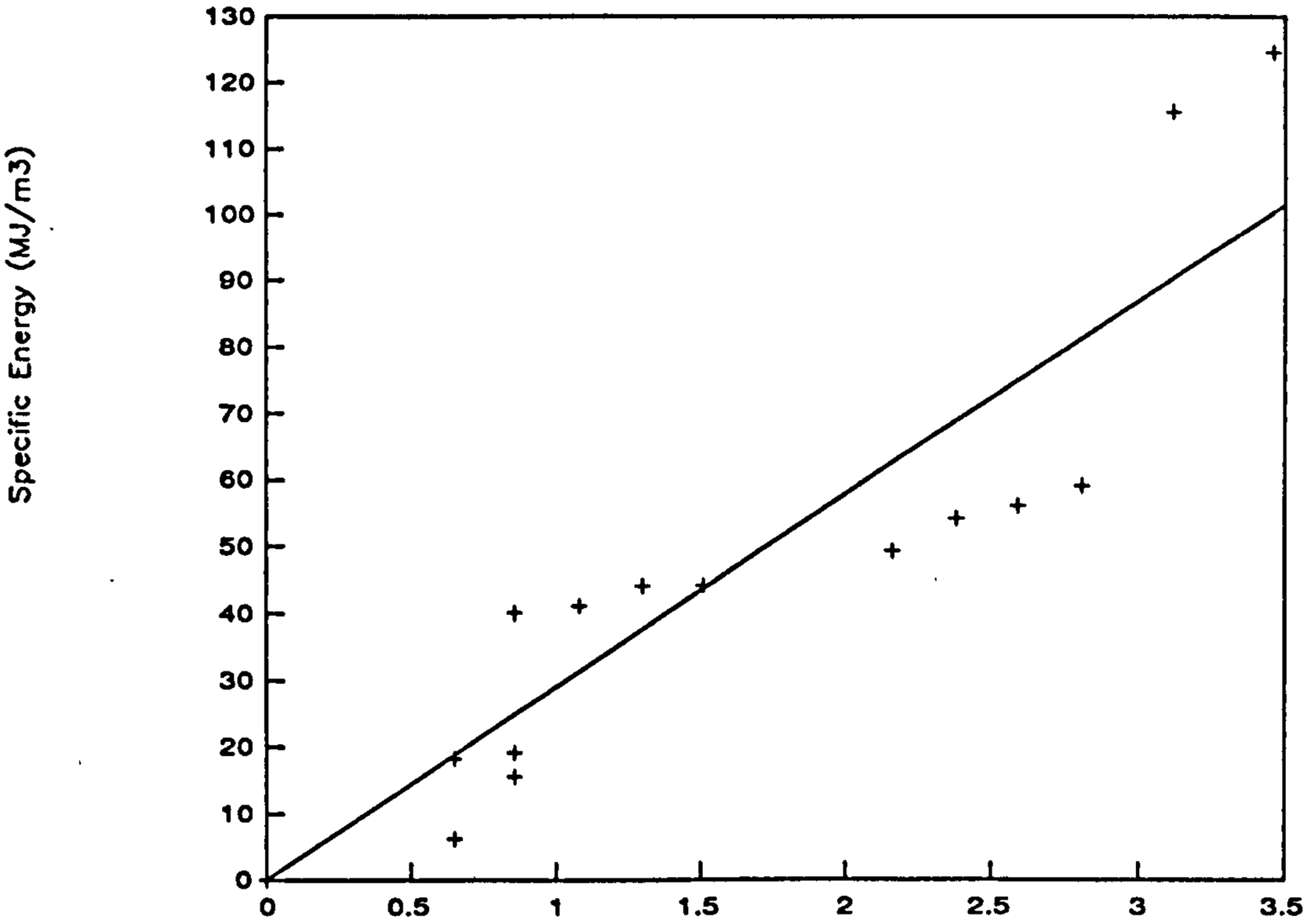

Fig 8.10 Specific Energy v Fracture toughness

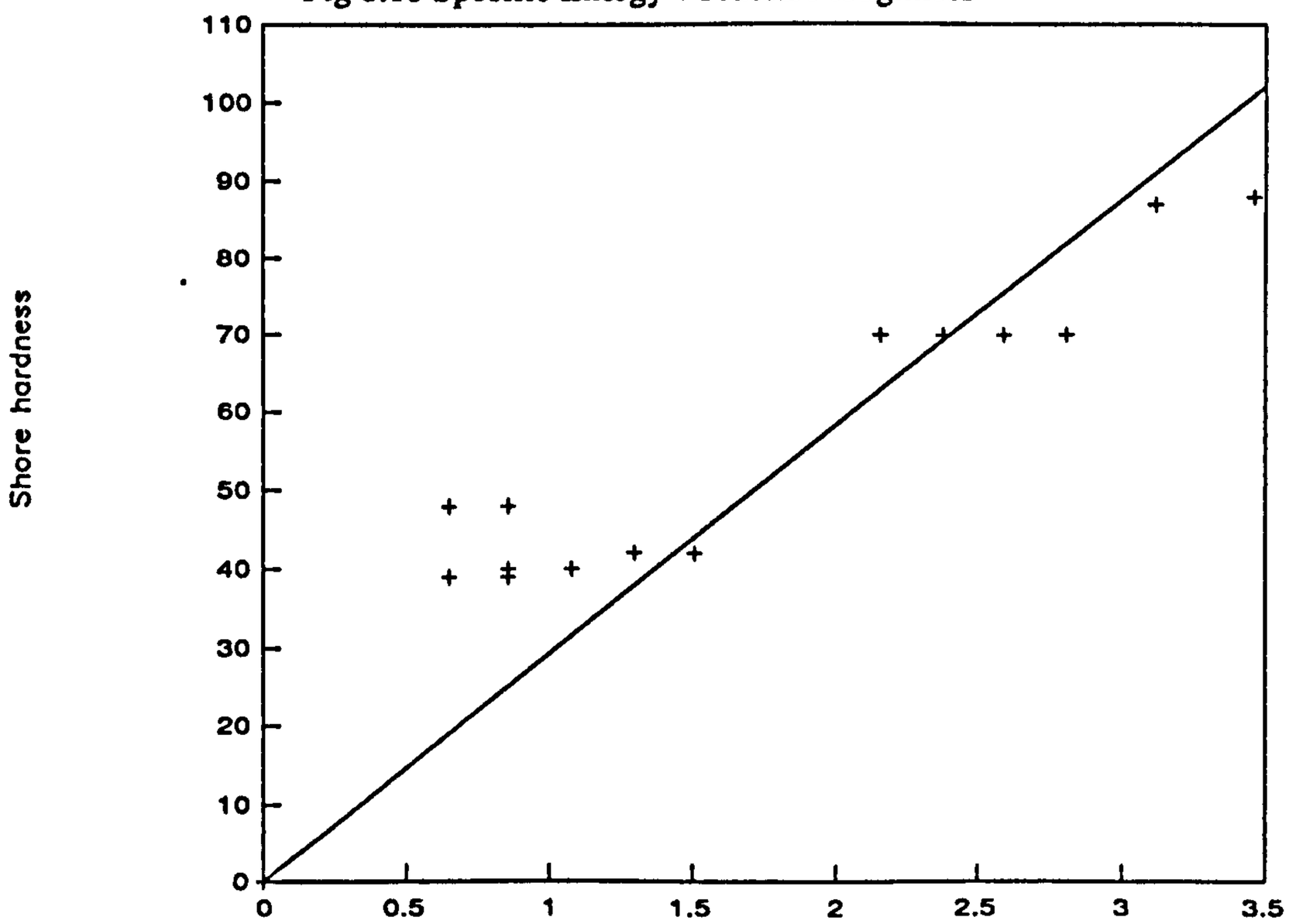

Fig 8.11 Shore hardness v Fracture toughness

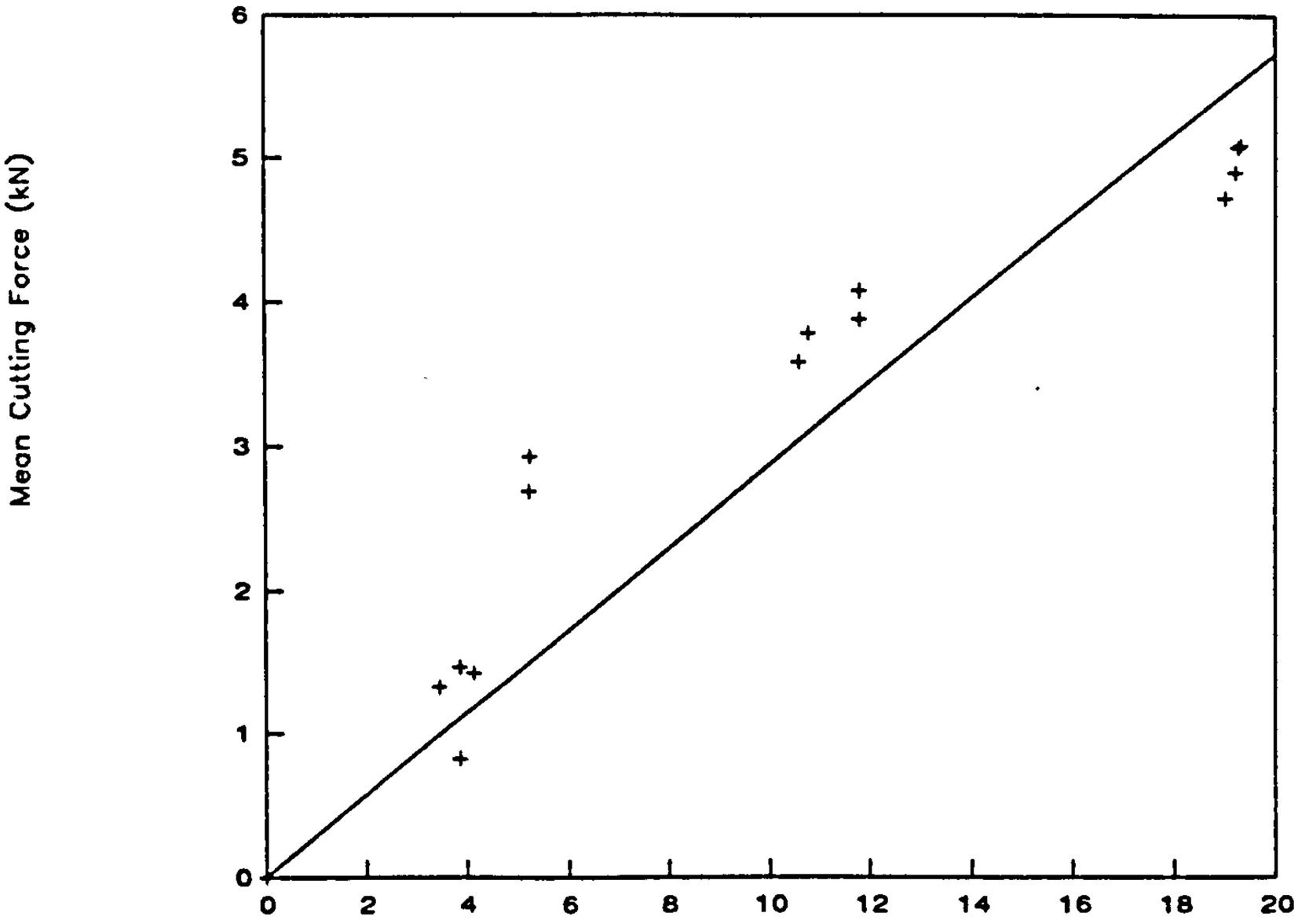

Fig 8.12 Mean cutting force v Tensile strength

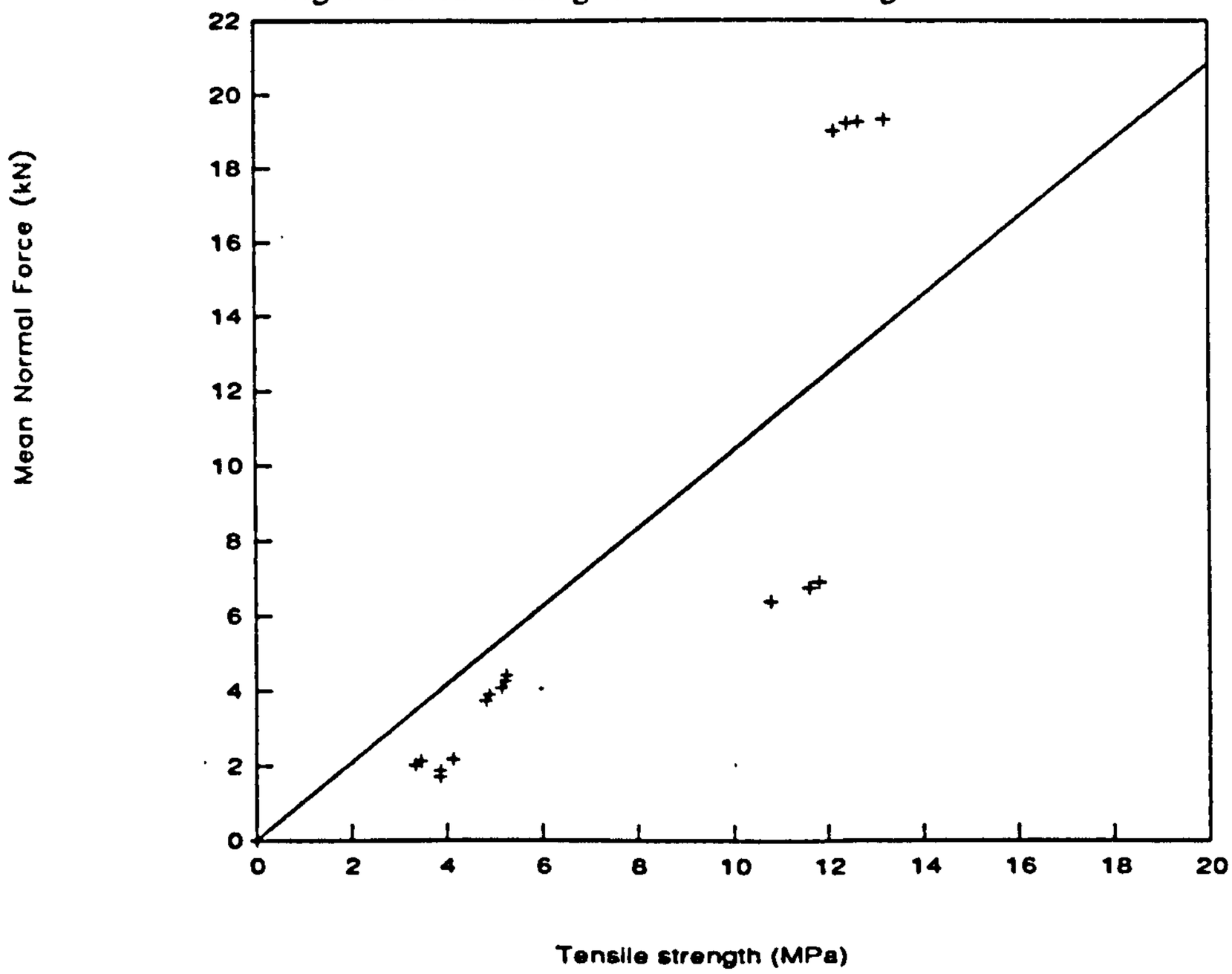

Fig 8.13 Mean normal force v Tensile strength

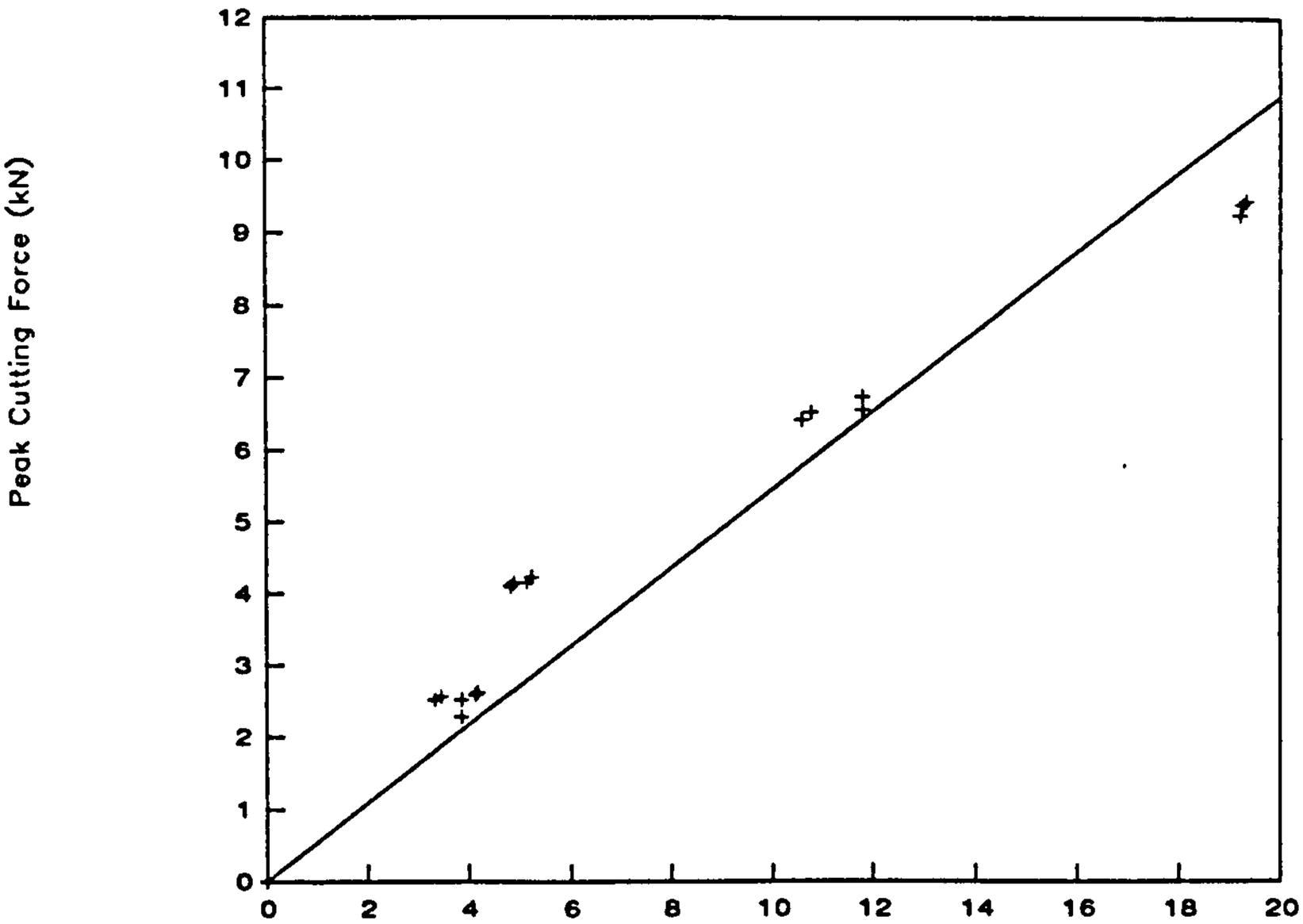

Fig 8.14 Peak cutting force v Tensile strength

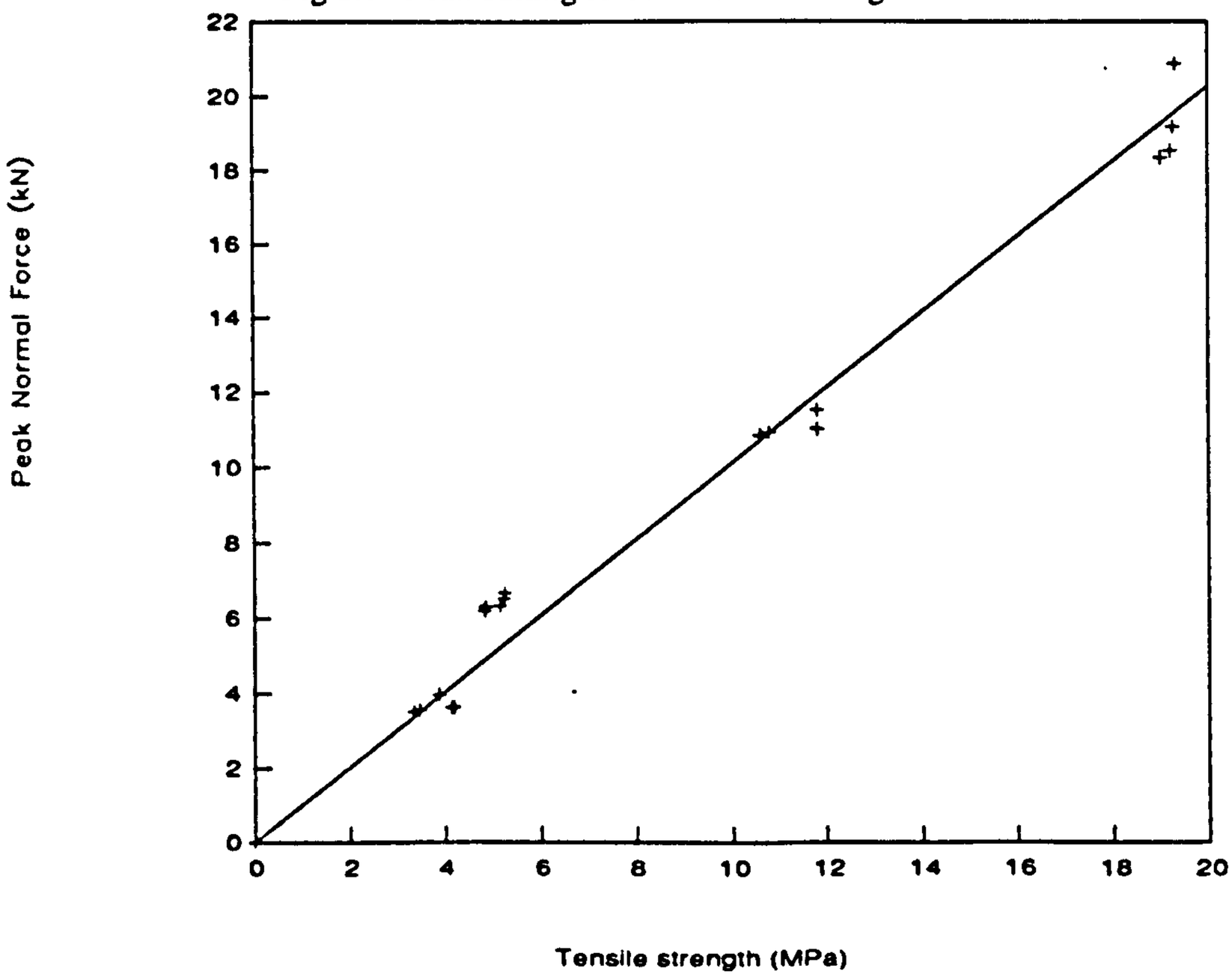

Fig 8.15 Peak normal force v Tensile strength

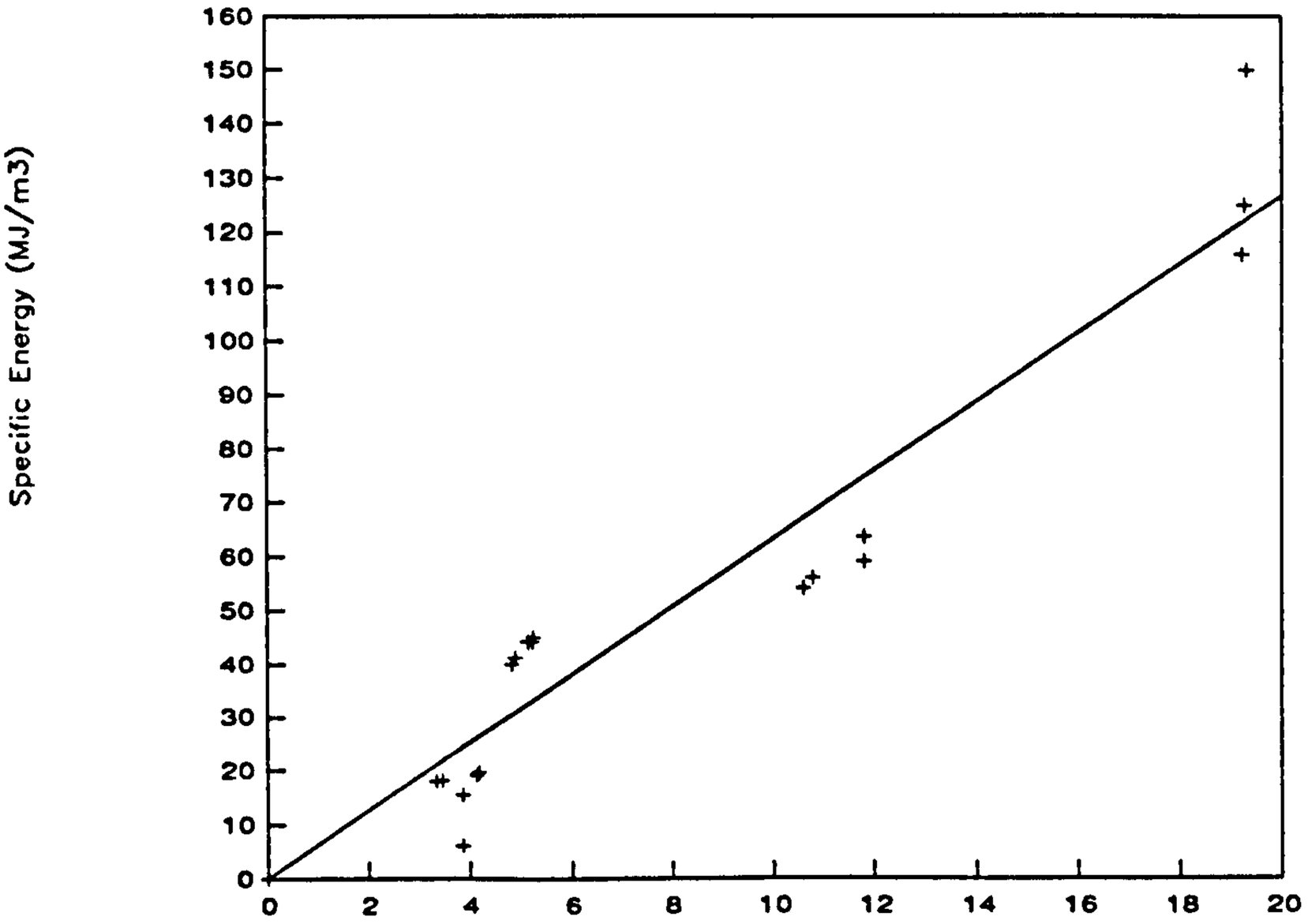

Fig 8.16 Specific Energy v Tensile strength

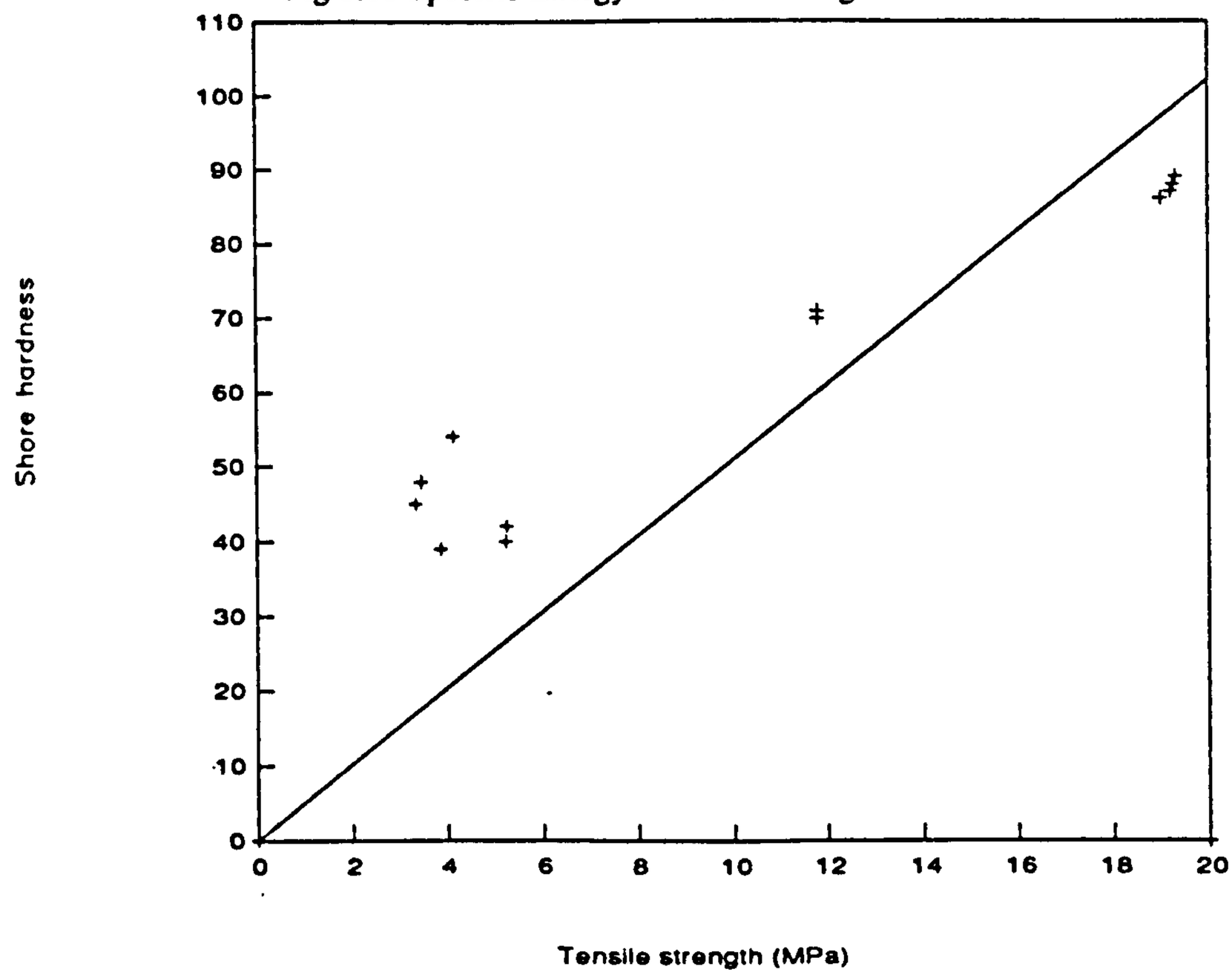

Fig 8.17 Shore hardness v Tensile strength

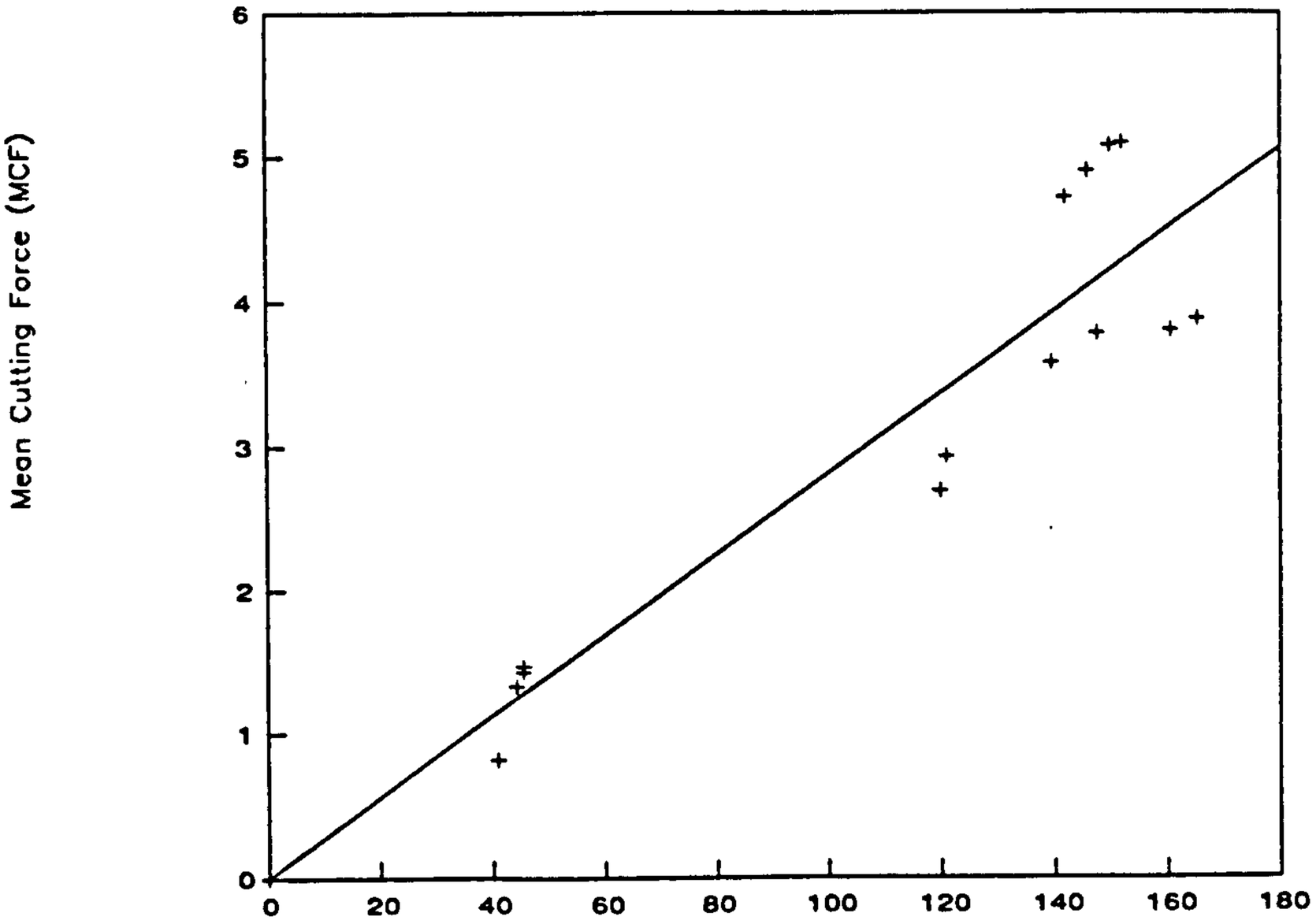

Fig 8.18 Mean cutting force v Uniaxial compressive strength

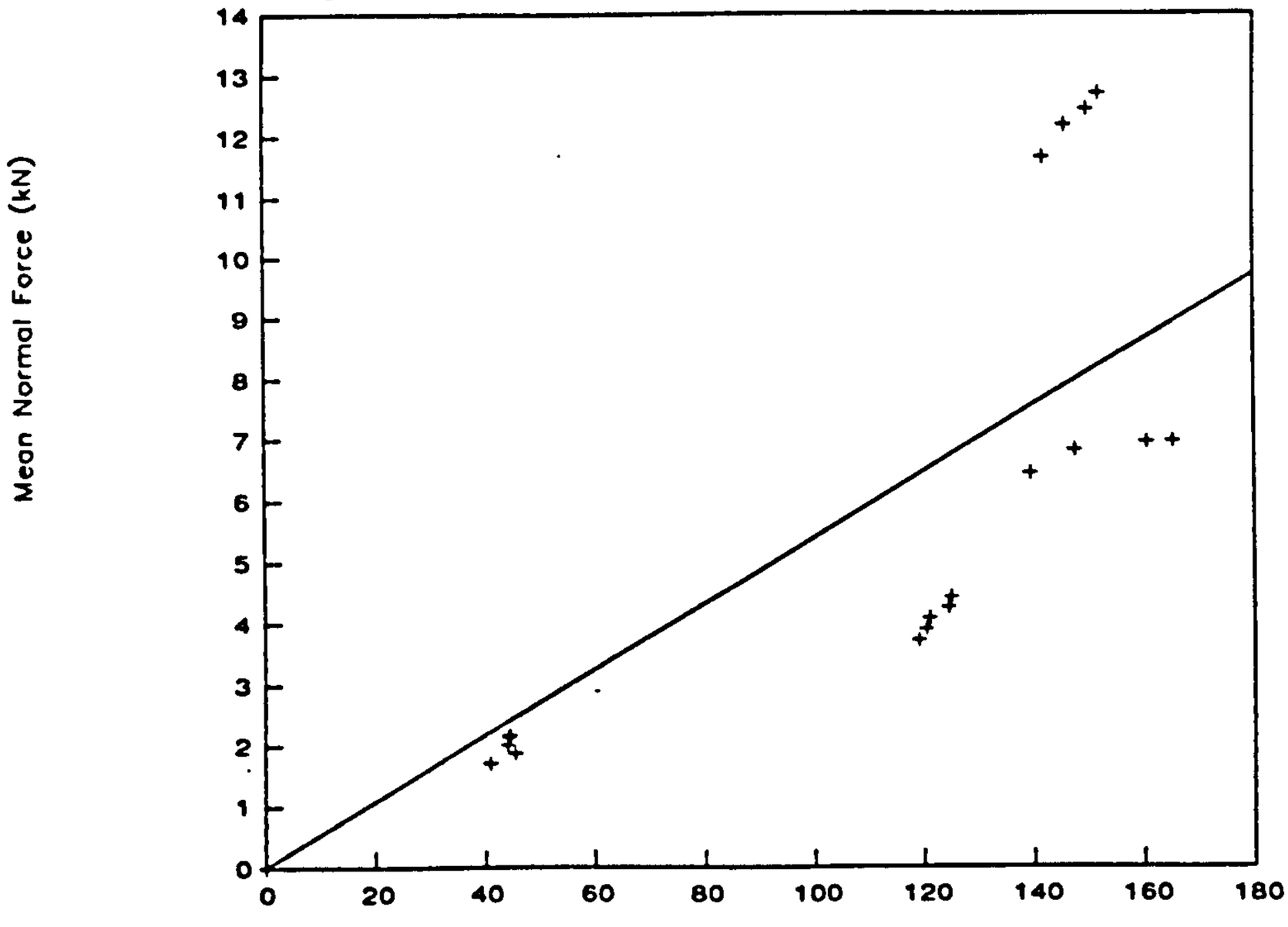

Fig 8.19 Mean normal force v Uniaxial compressive strength

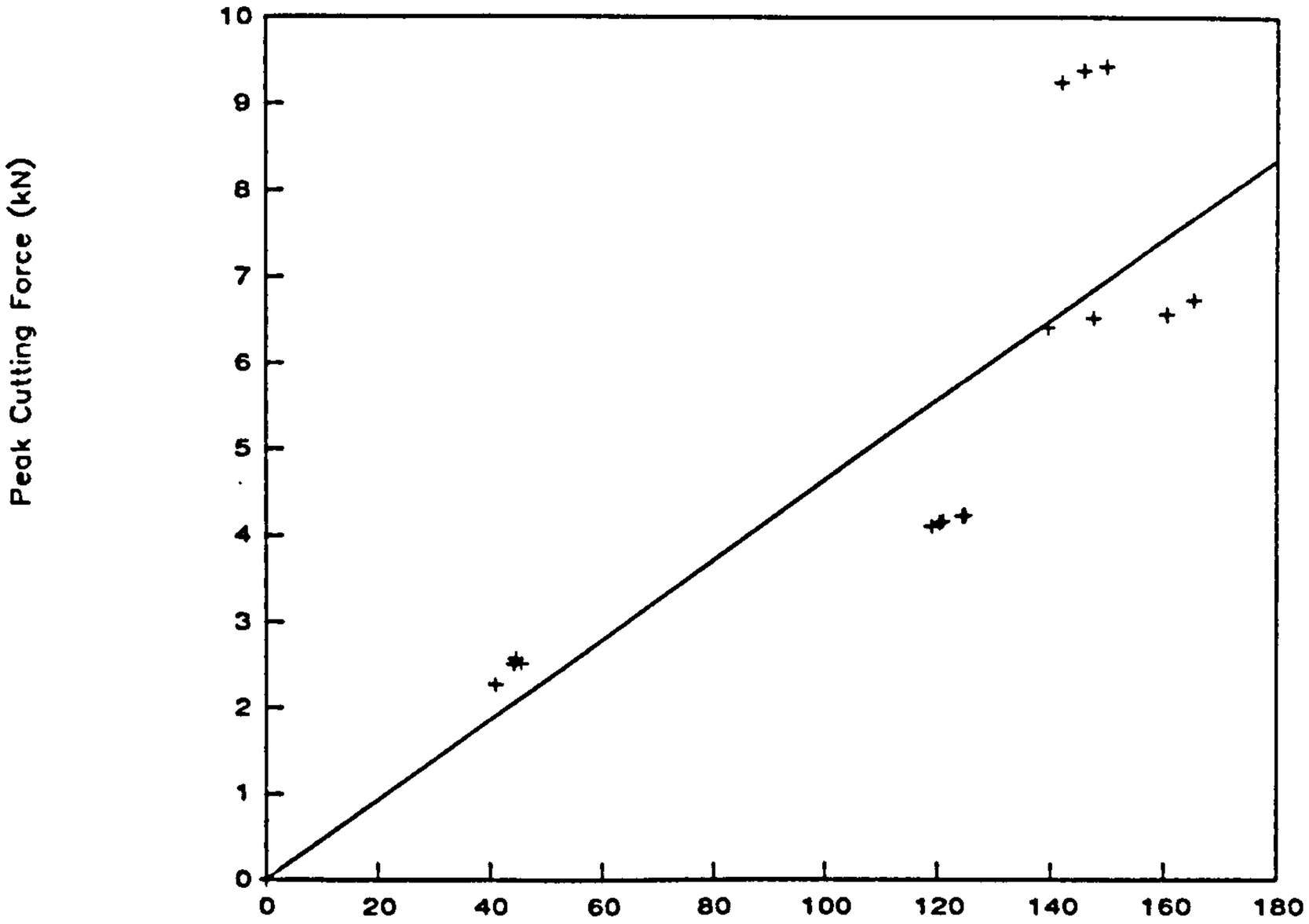

Fig 8.20 Peak cutting force v Uniaxial compressive strength

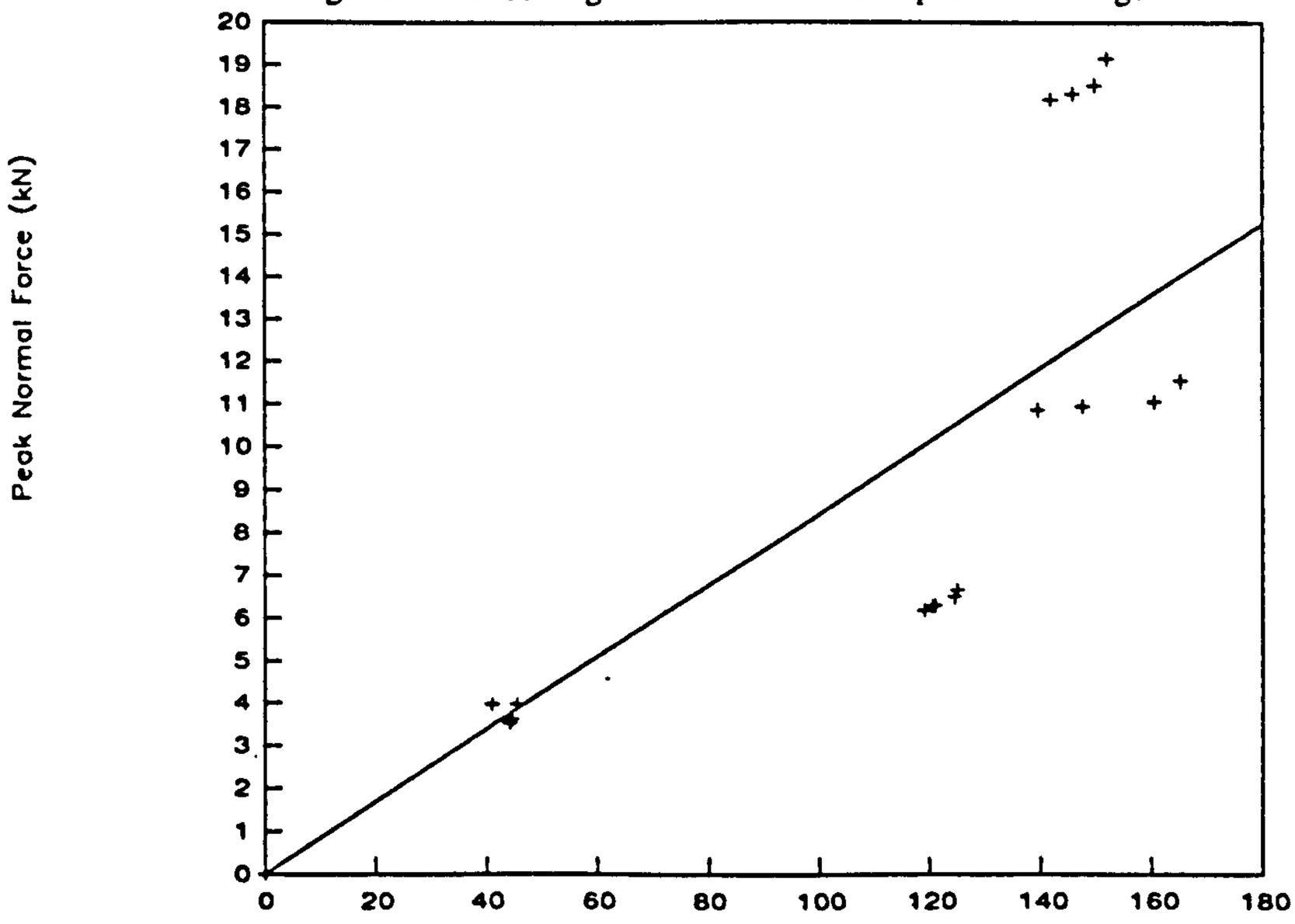

Fig 8.21 Peak normal force v Uniaxial compressive strength

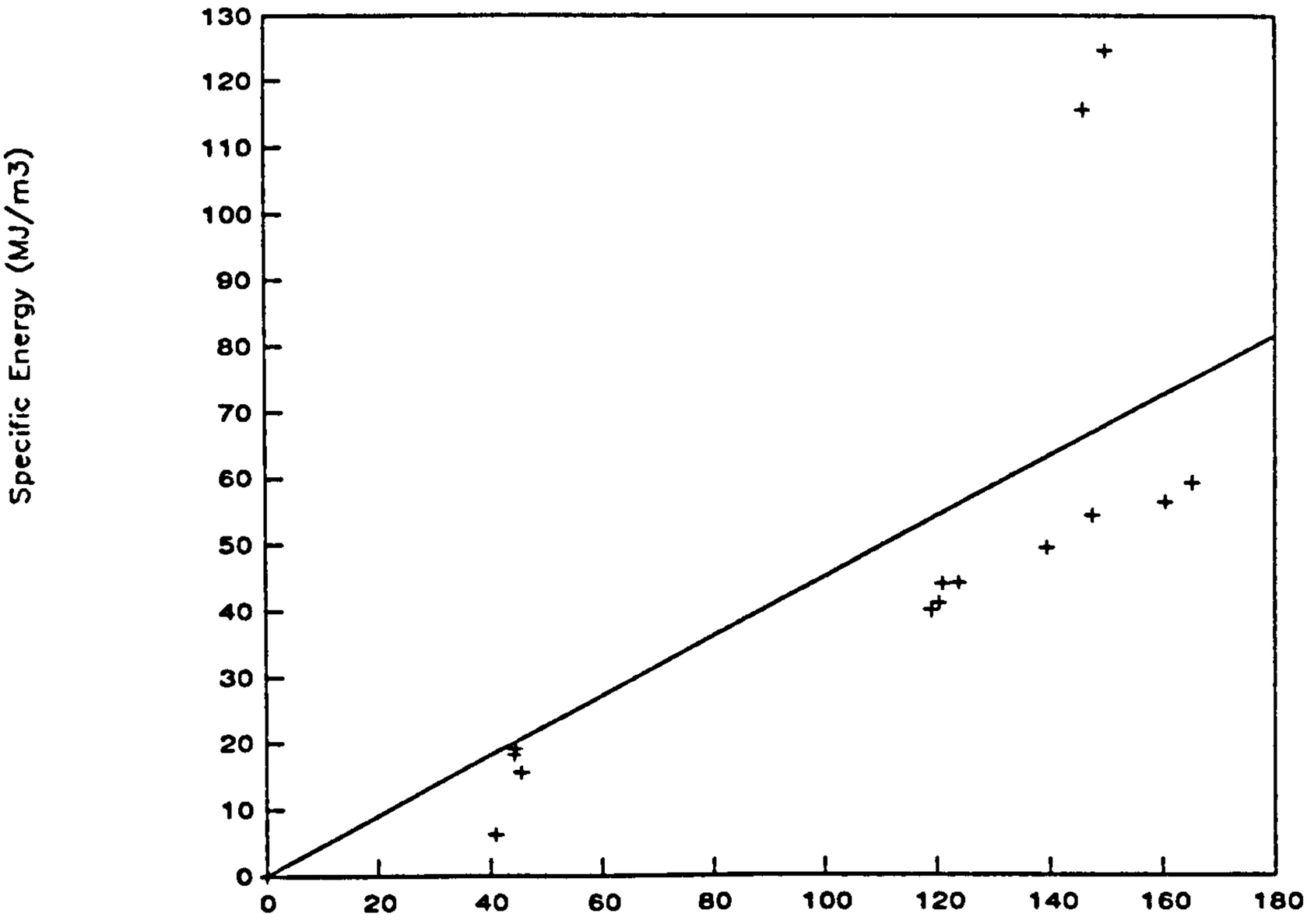

Fig 8.22 Specific Energy v Uniaxial compressive strength

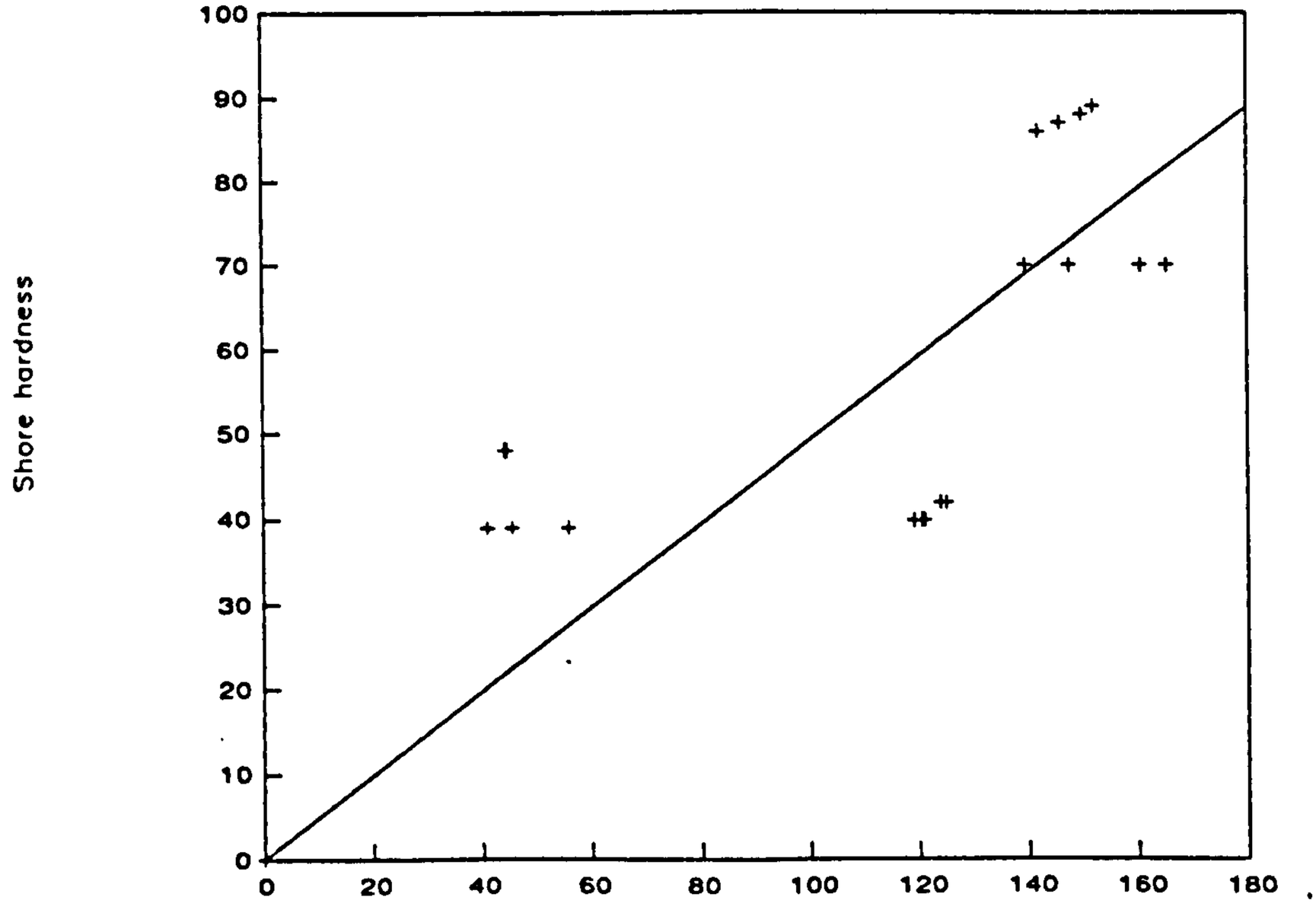

Fig 8.23 Shore hardness v Uniaxial compressive strength

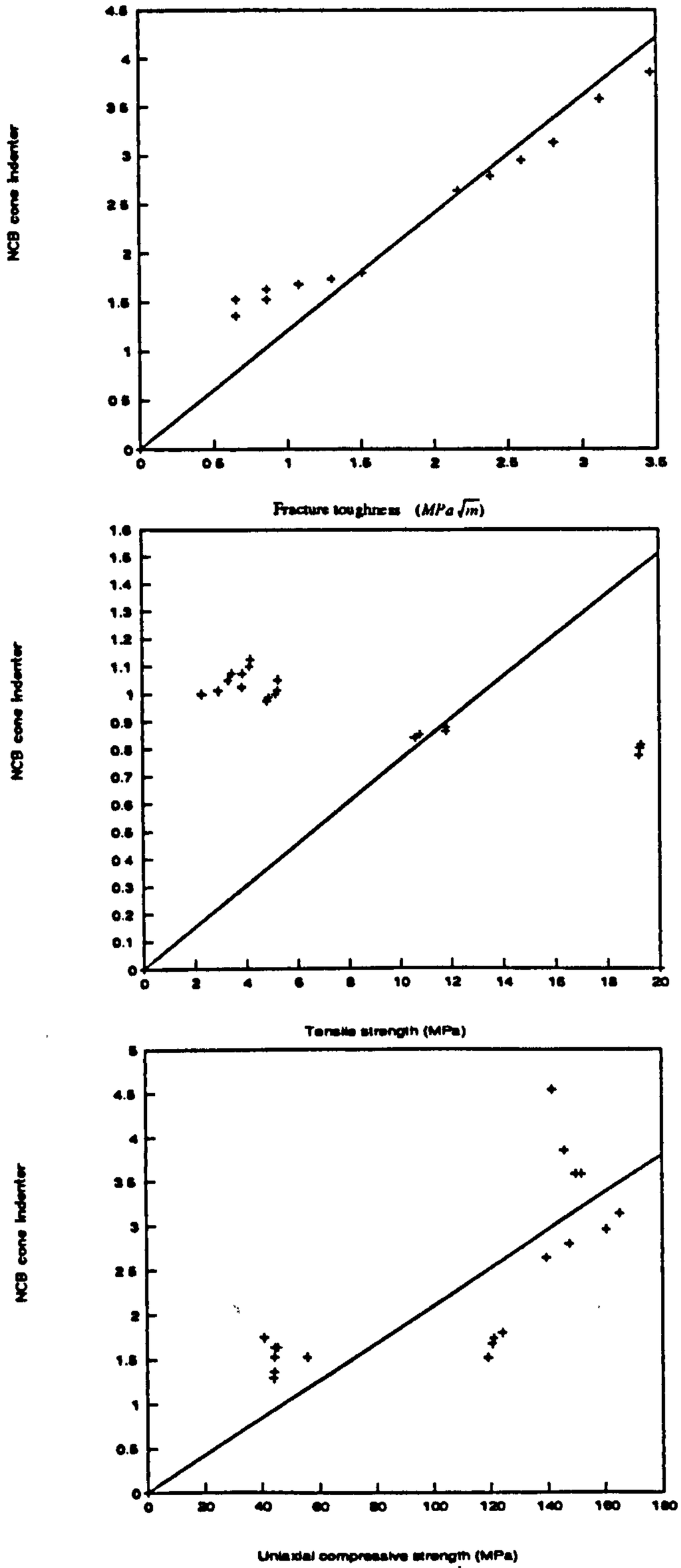

Fig 8.24 NCB cone indenter v Fracture toughness, uniaxial compressive strength, tensile strength

on performance and stability of the system. It is therefore very important to determine the most suitable cutting machine, and to assess the performance of the machine for particular rocks. An excavating process is influenced by many factors such as rock properties, machine operating parameter, i.e. thrust, torque, RPM etc. Prediction or assessment of cutting performance of rock cutting machine should be based on these factors.

In searching for a suitable measure of rock properties to assess rock cutting performance of rock cutting, many methods have been proposed, UCS being the most widely used parameter.

SE, is proposed by Teale (1965) as a parameter to measure the relative efficiency of various cutting tools, machines and cutting processes. Furthermore, SE has been used by many investigators to assess the relative resistance of various rocks for a given cutting tool or machine. A number of indentation tools have also been proposed, which normally involve an indenter with a some kind of configuration being forced into the surface of the rock, (NCB 1977). Rock cutting, such as drag bits, involves a rock response, i.e., as the tool penetrate into the rock, the rock around the tool is crushed. As the penetration continues, the cracks are developed. The propagation of these cracks result in rock fragments, which are removed by further movement of the cutting tool. This fracture mechanism suggests that rock cutting performance should be linked to rock fracture properties, i.e, rock fracture toughness.

Nelson et al (1985) correlated TBMs performance and the rock fracture parameters, such as fracture toughness K_{Ic} or strain energy release rate, G_{Ic}.

To rock machineability prediction using small samples has led to extensive research in this University in investigating the correlation of rock properties and tunnelling machine performance. (McFeat-Smith 1975; Fowell and Pyrecroft 1980).

In this work, rock fracture toughness which was presented in chapter 7, correlated with specific energy and cutting forces. It is shown among strength tests, UCS, Brazil tensile strength and point load index, fracture toughness has the least variation associated with it, and therefore may be a useful rock property to consider, Gunsallus and Kulhawy (1984).

As noted before fracture toughness, K_{IC}, is a material property of the intact rock and a measure of the stress intensity require to initiate crack propagation. G_{IC}, critical energy release rate induces rock strength and stiffness. Nelson et al (1985) could not find any relationship between field penetration index, R_f, fracture toughness, K_{IC}, but on the contrary they found a linear relation of increasing field penetration index with increasing G_{IC} (R^2 =0.92). The linear regression analysis of the relationship between specific energy and fracture toughness (for a line passing through origin) showed that it is no much difference from calculated R^2 for fracture toughness and critical energy release rate.

In the case of chisel bit, specific energy is an important factor which plays a major role in identifying cuttability of rock materials.

McFeat-Smith (1977) used multiple step-wise regression analysis to predict SE. An attempt was also made to predict SE by adding fracture toughness to this method. In investigations associated with previous research it was found there is good relationship between SE and fracture toughness.

$$SE=3.53\ (K_{IC})^3+19.3$$

(correlation coefficient =94.38)

On the base of fracture toughness, two theories exist for drag bit cutting : Cherapanove (1986), and Deliac (1988). The Cherapanov theory explains rock cutting force on the basis of fracture toughness Mode II. The ISRM suggested method is based on Mode I fracture toughness and two

levels (level1, level2). It is impossible to correlate our data with this theory, the theory suggests that cutting force is proportional to normal force, but in our case the forces are independent.

Deliac (1988) used indentation equations for his calculations, and later he found that this could be useful for the point attack tool, however the chisel pick is completely different from the point attack tool. Therefore our aim, was to find out whether any useful theories existed in the literature. By this we refer to theories which are close to our work and could be adapted to fit the saturated condition. The results showed that for Springwell sandstone Evan's theory was consistent.

Rock fracture toughness was measured as a rock property and this property has similarities with the tensile strength. In fact the measurements show a very similar relationship between SE, tensile strength and fracture toughness. Thus it can be hypothesized that tensile strength could be replaced in Evan's formula by fracture toughness.

Chapter 9

CONCLUSIONS AND RECOMMENDATIONS FOR FUTURE WORK

9.1 Conlusions

In this work the relationship of various rock properties with different parameters was investigated . Discontinuities angle and spacing are often thought to be important and in geological layers since most of the time the machine is excavating rock with discontinuities. However it was found for Springwell sandstone that the discontinuity angle is only important for joint angle which is 90°. For other angles; 30°, 45°, 60°, 75°, 90°, it was found that the orientation does not influence rock cutting parameters very much. Different spacings for right angle degree (90°) were investigated and it was found the spacing more than 50 mm rock behaves as an intact rock.

In real life in underground excavation most of the time rock is not dry but is under the influence of moisture conditions. Therefore it was felt reasonable to investigate the effect of saturated state in rock cutting parameter. Different states (dry, ambient, saturated) were chosen to investigate. A specific reduction in the values of the various cutting parametrs was found from dry to ambient and from ambient to fully saturated. This suggests that the machine spends less energy to excavate rock in fully saturated condition. In the same way that moisture content reduces the UCS of rock, it was also found that moisture content reduces the rock cutting parameters. Where in the case of joint filling, it was found that they affect the overall cutting performance more so than the presence of discontinuities.

Subsurface damage which is made by the drag bit can change the structure of the rock. It was found that for 8 mm depth of cut subsurface damage is very sensitive and is very useful because there is reduction in all

rock cutting parameters. However 4 mm and 6 mm did not show any important effect.

Rock cutting experiments were carried out when rock was subjected to uniaxial compressive stress. It was found there was little reduction of the rock cutting parameters when a stress less than 90% of UCS was used.

Rake angle is an important factor which can change rock cutting parameters. With rake angle of 18° Nishimatsu's theory and Evans ' theory have the same implication. A rake angle of 16°, which is very close to 18° was chosen to investigate which theory can satisfy the results for fully saturated samples. For Springwell sandstone Evans' theory is better than Nishimatsu's theory.

Speed is another factor which needs more investigation. Perhaps determination of the optimum speed is desirable, but wear after critical speed can be increased very much. With given limitations on the availability of high speed machines, it was found that for the range of 0.100 m/min and 0.125 m/min there is no significant change in rock cutting forces.

Wear is very important in drag bit cutting specially for abrasive rocks and very hard material. Up to certain limit the choice of mechanical excavation tool can be used. For this reason, on some occasions, choice of specific rock cutting machine may be based on tool consumption criteria.

Because the major part of the work was investigating the effect of water on rock cutting parameter, it was found that water is useful in reducing the amount of wear, and can be thought of as cooling factor that reduces the temperature (Cook 1984).

The finite element stress analysis was used to investigate which clamping device geometry is advantageous for rock cutting laboratory tests. With analysis of stress distribution by PAFEC-FE program it was found that block specimens are more useful than a core with shaped jaws. For different

depth of cut -4mm, 6 mm, 8 mm- where the core was hold by jaws the finite element analysis showed that the stress concentration were located around the tool tip.

Finite element analysis was also used to simulate the rock cutting operations. Because the Young's modulus determination by static loading is unsuitable for rock cutting operations, it was found necessary to increase the Young's modulus by ten times. The modelling was successful and it was found that FE can be applied satisfactory for simulation of rock cutting operations.

The stress vector plots revealed that cutting depth of mechanical tool has a strong influence on the area. At deeper depths more force is needed to initiate and propagate the fracture of the rock and hence the stressed area increases with increasing tool depth.

Fracture mechanics is a new approach in rock cutting which needs further investigation. Short rod and the three point bend specimens (CB) were used and a good relationship was found between fracture toughness and rock cutting parameters.

9.2 Recommendations for future work

Prediction of SE energy and rock cutting parameters on the basis of fracture mechanics approach needs further investigation. The number of rocks which were used was not very large compared to the results obtained by McFeat-Smith (1977), therefore it would be worth working with more rocks. In this investigation five types of rock were used. It is recommended that more rock types should be used to predict better for cutting performance. All results were based on Mode I fracture mechanics, but future research should perhaps be based on Mode II. In rock fracture

tests, special concern should be given to work with soft rock materials. It may be useful to investigate the wear of different bits with different metallurgy in water saturated state not only in 5 mm depth of cut but for different depths of cut. Fracture Mechanics of boundary element analysis of chevron specimen should be made a topic of future work.

REFERENCES

ALEMAN, V.P. (1981) A strata index for boom roadheader.Tunnels and Tunnelling, pp 52-55

ALEMAN, V.P. (1983) Prediction of cutting rates for boom type roadheaders. Tunnels and Tunnelling, pp 23-25.

ALEMAN, V.P. (1982) Characterization of strata with particular reference to the Performance of Roadway Drivage Machines, PhD thesis, University of Nottingham

ASTM E399 (1978) Standard Test Methods for Plane-Strain Fracture Toughness of Metal, ASTM Testing Standard.

ATKINSON, B.K. (1987) Fracture Mechanics of Rock, Academic Press Geology Series.

BARKER, L.M. (1977) A simplified method for measuring plane strain fracture toughness.Eng Fract. Mechanics. 9, 361-369.

BAZANT P, OHTSUBO H and AOH K. (1979) Stability and Post-critical growth of a system of cooling or shrinkage cracks. International Journal of Fracture, Vol.15, No.5, pp 443-456.

BEASY. (1991) Boundary Element Analysis System Package

BILGIN, N. (1977) Investigation into the mechanical cutting characteristics of some medium and high strength rocks, PhD thesis, University of Newcastle upon Tyne.

BROCH, E. (1979) The influence of water on some rock properties. 4th ISRM Conference , Montreax.

BROOK, N. and OJO,.O (1990) The effect of moisture on some mechanical properties of rock. Mining Science and Technology, pp 145-156.

BROWN, E.T. (1981) Rock characterisation testing and monitoring, ISRM Suggested methods, Pergamon Press, London.

CHERAPANOV, G.P. (1986) K Teorii Rezaiya Gornykh. Prod (theory of rock cutting) Part 8, pp 94-102.

COLBACK, P.S.B and WIDD B.L. (1965). The influence of moisture content on the compressive strength of rocks. Proc 3rd Rock Mech.Symposium. pp 65-83.

COOK, G.W.N. (1984) Wear on drag bits in hard rock. Mechanical Excavation,14th Canadian Rock Mechanics Symposium, pp 39-43.

DELIAC, E.P. (1986) Optimasation des machines d' abattage a'pics. Doctoral dissertation, Univ. of Paris VI, ed. by ENSMP/CMI, Paris/Fontainebeau, 501 P.

DELIAC, E.P. (1988) Theoretical and practical investigations of improved hard rock cutting systems. 29th U.S symposium, University of Minnesota. pp 553-562.

DUNN, P. (1975) An investigation into the mechanical cutting of hard rock materials in relation to the design of effective tunnelling system. PhD thesis, University of Newcastle upon Tyne.

EVANS, I. and POMEROY, M.J. (1962) The strength, fracture and workability of coal, Pergamon Press.

EVANS, I. (1972) Line spacing of picks for effective cutting. Int.J.Rock Mech. Min.Sci&Geomech. Abstr. Vol. 9, pp 355-361.

EVANS, I. (1982) Optimum line spacing for cutting picks. The Mining Engineer. pp 433-434.

EVENDEN, M.P and EDWARDS, J.S. (1985) Cutting theory and coal seam assessment techniques and their application to shearer design. Mining Science and Technology, pp 253-270.

FARMER, I. (1986) Mechanical Excavation of Rock. CIRIA Project PR 351.

FARMER, I. (1986) Energy based rock characterization. Procs of Symp held at SME-AME Annual Meeting New Orleans, Louisana, pp 17-23.

FAIRHURST, C. and CORNET, F H. (1981) Rock Fracture and Fragmentation. Rock Mechanics from Research to Applications, 22nd U.S. Symp.Rock Mech., Massachussetts Institute of Technology.

FOWELL, R.J.and JOHNSON, S.T. (1982) Rock classification and rapid excavation.Proc.Symp.Strata Mech, University of Newcastle Upon Tyne, pp 241-244

FOWELL, R.J.and JOHNSON, S.T. (1984) Boom tunnelling studies for improved excavation performance. Design and Performance of Underground Excavation, Cambridge U.K, pp 305-311.

FOWELL, R.J.and JOHNSON, S.T. (1985) A rational approach to practical performance assessment for rapid excavation using Boom-Type Tunnelling Machines. 25th U.S Symposium, pp 759-766.

FOWELL, R.J.and McFEAT-SMITH,I. (1976) Factors influencing the cutting performance of a selective tunnelling machine. Tunnelling 76, IMM, Ed. M.J.Jones, pp 1-11.

FOWELL, R.J.and PYCROFT, A.S. (1980) Rock machineability studies for the assessment of selective tunnelling machine performance. 21th U.S Symposium on Rock Mechanics

GEORGE, D.L. (1975) Some characteristics of cutting jointed rock. MSc thesis, University of Newcastle upon Tyne.

GOODMAN, R.E. (1989) Introduction to Rock Mechanics. pp 42-54

GRIFFITH, A.A. (1921) The phenomena of rupture and flow in solids. Proc. Trans. Royal Soc. A221, pp 163-198.

GRESTLE, W.H and INGRAFFEA, A.R. (1991) Compliance and stress intensity factor calibration of the CENRBB specimen using boundary element method. Int. J. Rock Mech. Min Sci & Geomech. Abs vol 28, No.1, pp 85-92.

GUO, H, STANDISH, P, SCHMIDTH, L C and AZIZ, N.I. (1988) A method of mechanical efficiency analysis for rotary drag bits, second international conference on mining machinery. Brisbane, Australia. pp 322-326.

GUNSALLUS, K.L and KULHAWY, F.H. (1984) A comprarative evaluation of rock strength measures. Int. J. Rock Mech.Min. Sci & Geomech. Abstr. Vol. 21, No. 5, pp 233-248

HAYASHI, K., ONO, A. and ABE, H. (1989) BEM Analysis of a cylindrical three point bend specimen with a chevron crack for fracture toughness test of rock. JSME International Journal, pp 427-431.

HEKIMOGLU, O.Z. (1984) Studies in the excavation of selected rock materials with mechanical tools. PhD thesis, University of Newcastle upon Tyne.

HOAGLAND, R.G, HAHN G.T. and ROSENFIELD, A.R. (1973) Influence of microstructure on fracture propagation in rock. Rock Mechanics Vol 5, pp 77-106.

HOOD M, TUTLUOGLU, L. and BARTON, C. (1983) An investigation of the Mechanisms of water jet assisted on the rock cutting process. 24th U.S Symposium on Rock Mechanics pp 743-749.

HOWARTH, D.F, ADAMSON, W.R. and BERNDT, J.R. (1986) Correlation of model tunnel boring and drilling machine performances with rock properties. Int J. Rock Mech. Min Sci & Geomech Abstr. Vol 23 No.2, pp 171-175.

IRWIN, G.R. (1957) Analysis of stress abd strain near the end of a crack traversing a plate. J. Appl. Mechanics, Vol 24, pp 361-364.

INRAFFEA, A.R. and BEECH, J.F. (1982) Three dimensional finite element calibration of the short rod specimen, International Journal of Fracture. Vol 18, No.3, pp 217-229.

IP, C.K.(1986) Laboratory water jet assisted drag tool rock cutting studies at high traverse speeds. PhD thesis, University of Newcastle upon Tyne.

ISRM (1988) Suggested method for determining the fracture toughness of rock. Int. J. Rock Mech. Min Sci & Geomech Abstr. Vol 25, No. 2, pp 73-96.

ISRM (1989) On the background to the formulae and accuracy of rock fracture toughness measurements using ISRM standard core specimens. Int. J. Rock Mech. Min. Sci. & Geomech Abstr. Vol 26, No.1, pp. 13-23.

JAMALBASTAMI, M. (1989) The effect of induced discontinuities on the mechanical and hybrid cutting of rocks. PhD thesis, University of Newcastle upon Tyne.

KEMENY, J and COOK, N.G.W. (1985) Formation and stability of steeply dipping joint sets. 26th U.S symposium on Rock Mechanics, pp 471-479.

KENNY, P. and JOHNSON, S.N. (1976) The effect of wear on the performance of minerals cutting tools, Colliery Guardian, Vol 24, No. 6, pp 246-253.

MATSUKI, K. (1989) Size effect and size requirement in fracture toughness evaluation of rock. International Workshop on fracture toughness and fracture energy, SENDAI, pp 287-303.

McFEAT-SMITH, I. (1975) Correlation of rock properties and tunnelling machine performance in selected sedimentary rocks. PhD thesis, University of Newcastle upon Tyne.

McFEAT-SMITH, I. (1977) Rock property testing for the assessment of tunnelling machine performance. Tunnels and Tunnelling, pp 29-33.

McFEAT-SMITH, I. (1982) Survey of rock tunnelling machines available for mining projects. Trans. Inst Min & Metall, 91, A23-A31.

MEREDITH, P.G. (1983) A fracture mechanics study of experimentally performed crushed rocks. PhD Thesis, University of London.

MERCHANT, M.E. (1944) Basic mechanics of metal cutting process, J. Appl Mech. Vol 11, pp A168-A175.

MICHALOPOULOS, A P. and TRIANDAFILIDIS G E. (1976) Influence of water on hardness strength and compressibility of rock. Bull Ass Engng Geology, Vol 13, PT1, pp 1-22.

MUIRHEAD, I.R. (1984) A challenge for tomorrow. mechanical excavation in mining. 14th Canadian Rock Mechanics Symposium, pp 68-75.

NCB (1977) NCB cone indenter handbook.

NELSON, P.P., INGRAFFEA, A.R. and O'ROURKE, T.D. (1985) TBM performance prediction using rock fracture parameters, Int J Rock Mech Min. & Geomech Abstr. Vol 22, No 3, pp 189-192.

NEWMAN, Jr. J.C (1984) A review of chevron-notched fracture specimens. chevron-notched specimens : Testing and Stress Analysis, ASTM STP 855.

NISHIMATSU, Y. (1972) The mechanics of rock cutting. Int J Rock Mech. Min Sci. Vol 9, pp 261-270.

NISHIMATSU, Y. (1979) On the effect of tool velocity in the rock cutting, International Conference on Mining and Machinery, Brisbane Australia, pp 314-319.

OBERT, L.and DUVALL, W.I. (1967) Rock mechanics and the design of structures in rock.

O'DOGHTERTY, M.J. and BURNEY, A.C. (1963) A laboratory study of the effect of cutting speed on the performance of two coal cutter picks. Colliery Engineering, pp 111-114.

OUCHTERLONY, F. and SUN, F. (1986) Fracture Toughness of Stripa granite cores. Int J Rock Mech. Min. Sci & Geomech. Abstr. Vol. 23 No.6 pp 399-409.

OUCHTERLONY, F. (1989) Fracture toughness testing of rock with core standard. The development of an ISRM standard, fracture toughness and fracture energy, pp 231-251.

PAFEC-FE (6.1) Pafec manual

PHILLIPS, H.R. (1975) The mechanical cutting characteristics and properties of selected rock formations, report to the Transport and Road Research Laboratory, University of Newcastle upon Tyne.

RAMBANDA, P.M.H.G. (1984) An investigation in to the effect of moisture on cuttability of rocks, MSc thesis,
University of Newcastle upon Tyne.

ROXBOROUGH, F.F. (1969) rock cutting research for the design and operation of tunnelling machines. Tunnels and Tunnelling, 1, 3, 125.

ROXBOROUGH, F.F. (1973) Cutting rocks with picks, The Mining Engineer, pp 445-452.

ROXBOROUGH, F.F. and RISPIN, A. (1973) The mechanical cutting characteristics of the lower chalk. Tunnels and Tunnelling, Vol. 1, pp 45-67.

ROXBOROUGH, F.F. and PHILLIPS H.R. (1975) The mechanical properties and cutting characteristics of the Bunter sandstone, report to the Transport and Road Research Laboratory, University of Newcastle upon Tyne.

ROXBOROUGH, F.F. (1985) Research in mechanical rock excavation, progress and prospects, RETC, pp 225-244.

ROXBOROUGH, F.F. (1990) Personal Communication.

SANDBACK, L A. (1985) Roadheader drift excavation and geomechanical rock classification at San Manuel, Arizona. RETC Proceedings, Volume 2.

SAUMA, VICTOR.E.and KLEINOSKY, MARY-LEE. (1984) Finite element simulation of rock cutting. A fracture mechanics approach, 25th U.S Symposium on Rock Mechanics, Northwestern University, pp 792-799.

SAUNDERS, T.W. and BROMLEY, J.C. (1987) Design, development and operation of a hardrock roadheader. Sixth Australian Tunnelling Conference, Melborne, pp 239-247.

SCHMIDTH, R. A. (1976) Fracture toughness of limestone. Expl Mech, Vol 16, pp 161.167.

SCHMIDTH, R.A. (1977) Fracture mechanics of oil shale unconfined fracture toughness, stress corrosion cracking, and tension test results. Proc 18th U.S Symposium on Rock Mech, pp 1-6.

TAKAHASHI, H. (1989) Application of rock fracture mechanics to HDR geothermal reservoir design. Fracture toughness and fracture energy, pp 591-610.

TEALE, R. (1965) The concept of specific energy in rock drilling. Int. J. Rock Mech. Min. Sci & Geomech. Abstr. Vol. 2, pp 57-73.

TECEN, O. (1982) High pressure water jet assisted drag tool cutting of rock materials. PhD thesis, University of Newcastle upon Tyne.

THARP, T.M. and COFFIN D.T. (1985) Field application of fracture mechanics analysis to small rock slopes, 26th U.S symposium on rock mechanics, pp 667-674.

VARLEY, P.M. (1989) Proceedings of the international chalk symposium held at Brighton Polytechnic, pp 485-492.

VUTUKURI, V.S., LAMA, R.D.and SALUJA S.S. (1974) Handbook on mechanical properties of rocks, Vol 1, pp 50-56.

VUTUKURI, V.S. (1974) The effect of liquids on the tensile strength of limestone. Int. J. Rock Mech. Min. Sci & Geomech Abstr. Vol 11, pp 27-29.

WEST, G. (1989) Rock abrasiveness testing for tunnelling. Int. J. Rock Mech. Min. Sci & Geomech Abstr. Vol 26, No.2, pp 27-29.

XIANG, J and SAPERSTEIN, L.W (1988) Numerical analysis of rock failure during drag bit cutting. Miner. Resour. Engng, pt 3, pp 249-261.

ZUECH, D.H., SWENSON, D.V. and FINGERR, J.T. (1983) Subsurface damage development in rock during drag bit cutting : observations and model predictions. 24th U.S symposium on Rock Mech, pp 731-741.

ZHAO, X. (1989) A fracture mechanics study of unassisted and water jet assisted rock disc cutting, PhD thesis, University of Newcastle upon Tyne.

APPENDIX 1

CUTTING THEORIES

MERCHANT'S THEORY

Merchant's semi-empirical theory was first developed to describe the cutting process during metal machining (Merchant, 1944) and later was adopted for the cutting of rocks (Evans, 1973).

A force F is applied by a wedge shaped tool on a piece of rock, taking a cut of uniform depth d from the plane surface of the rock (Fig A1). The depth of cut is small compared with the width of tool and therefore a condition of plane strain is assumed. Rock fails in shear along the line AB at an angle q with the horizontal. The shear strength of the rock is C (cohesion) and the angle of friction between the tool and the rock chip is φ'. The cutting force is :

$$F_C = \frac{C\, d \sin(b+\varphi')}{\sin(\theta)\sin(b+\varphi'+\theta)}$$

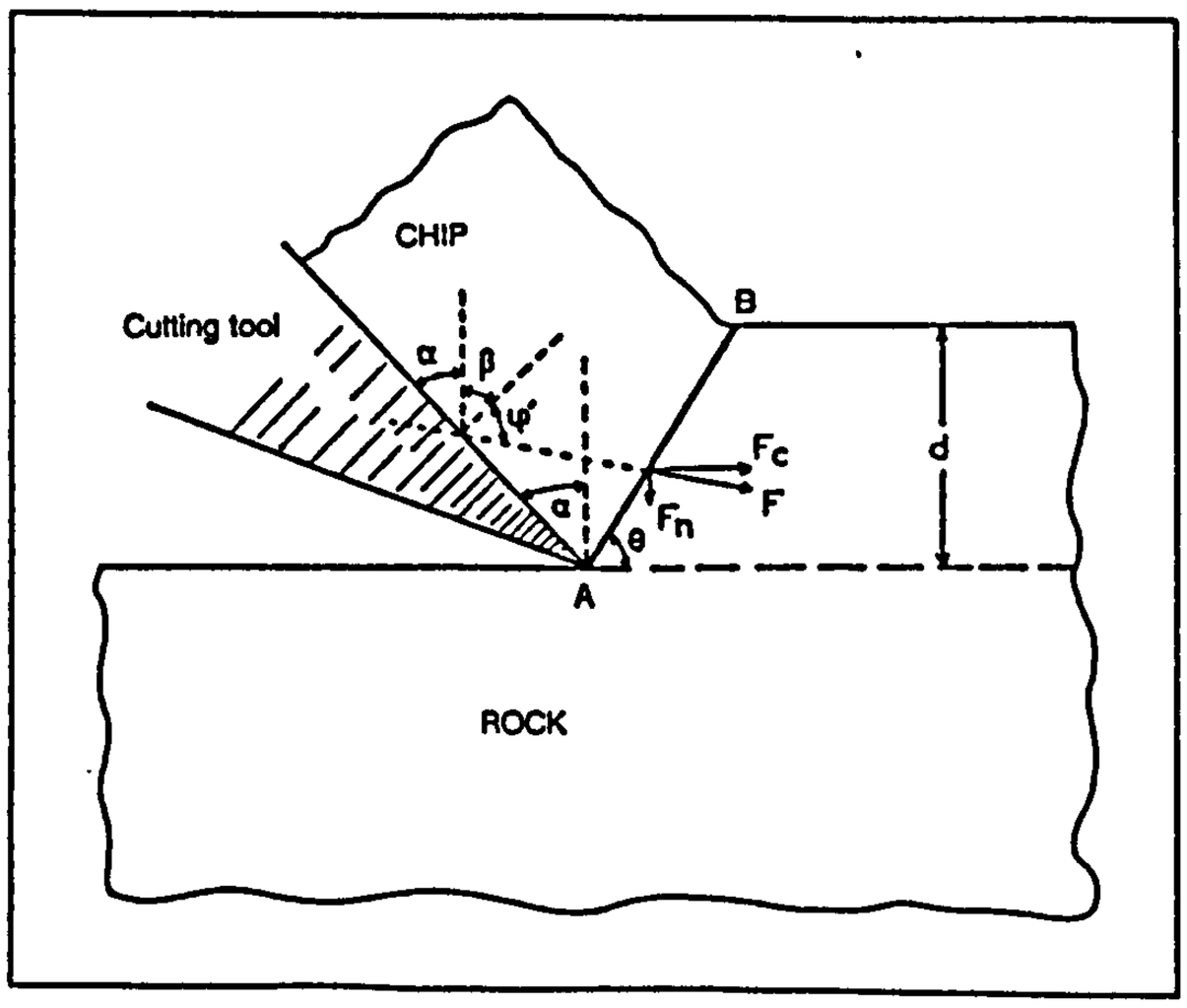

Fig A1 Schematic representation of cutting according to Merchant's theory

EVANS' THEORY

Evans, during coal cutting experiments using wedge shaped tools, noticed that brittle materials, like coal, when attacked by a symmetric wedge fail in tension along an arc which begins at the tip of the wedge and ends at the free surface of the buttock (Evans et al, 1973). In the original description of the theory, the initial wedge penetration into the coal before tensile failure begin was taken into consideration. If the depth of cut is selected to be such, so that the wedge penetration is small and can be neglected in comparison with the depth of cut, then the original theory can be simplified. This simplified version of Evans' tensile theory is presented here.

In Fig A2, a schematic representation of the cutting process according to Evans'theory is shown. The action of the wedge tends to prise away the rock and to rotate the chip separated about B. It is assumed that plain strain conditions exist and that tensile failure occurs along a circular arc AB of radius r, which makes horizontal tangent at the tip of the wedge A. The analysis also assumes that all forces are per unit width of cutting tool and that initially zero friction exists between the wedge and the rock.

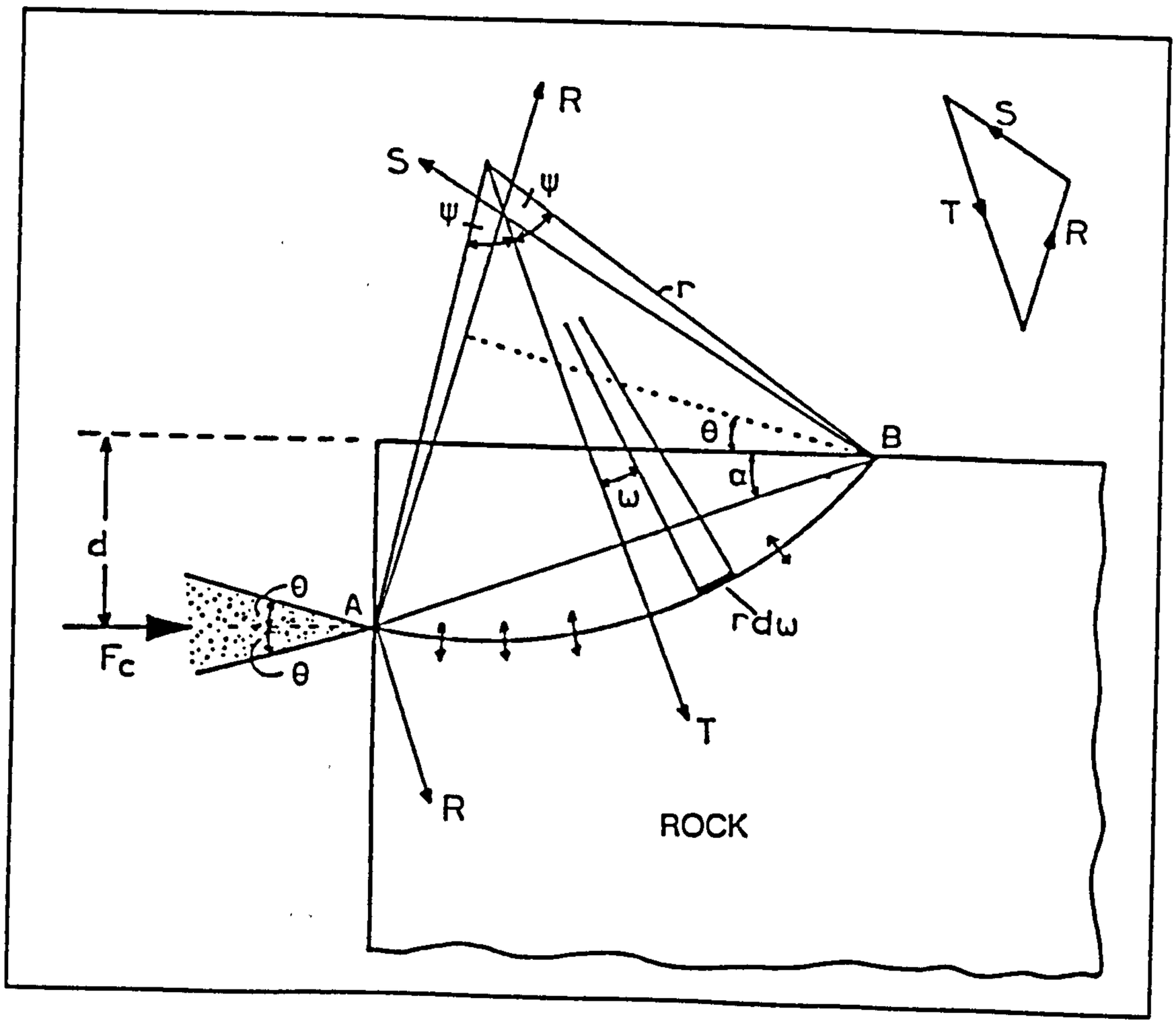

Fig A2 Schematic representation of cutting process according to Evan's theory

The cutting force is :

$$F_c = \frac{2\,\sigma_t\, d \sin(\theta+\varphi')}{1-\sin(\theta+\varphi')}$$

where :

F_c : cutting force per unit width of symmetric wedge

σ_t : tensile strength of rock

d : depth of cut

θ : halh wedge angle (symmetric wedge)

φ' : angle of friction between rock and wedge

for asymmetric wedge cutting force is :

$$F_C = \frac{2\,\sigma_t\, d \sin\left[1/2(\pi/2-\alpha)+\varphi'\right)]}{1-\sin[1/2(\pi/2-\alpha)+\varphi')]}$$

where :

F_C : cutting force per unit width of asymmetric wedge

σ_t : tensile strength of rock

d : depth of cut

α : wedge rake angle (asymmetric wedge)

φ' : angle of friction between rock and wedge

Roxborough (1973) conducting rock cutting experiments at Newcastle University, found that Evans'theory can be applied also to different rocks like anhydrite, limestone and sandstone. The following equation can be used :

$$F_C = \frac{2\,\sigma_t\, w\, d \sin 1/2(\pi/2-\alpha)}{1-\sin 1/2(\pi/2-\alpha)}$$

where :

F_C : cutting force at the instant of failure

σ_t : tensile strength of rock

w : width of wedge

d : depth of cut

α : wedge rake angle

NISHIMATSU'S THEORY

Based on observations of the rock cutting process and some simplifying assumptions, Nishimatsu (1972) developed his rock-cutting theory, using the Mohr-Coulomb criterion of failure during the formation of a chip. The observed process of rock cutting in a plane state of stress is schematically shown in Fig A3. As soon as the tool edge is pushed into the buttock, a crushed zone is generated about the tool edge. As the tool edge is pushed deeper into buttock, this crushed zone is forced against the rake face of the cutting tool, where it is recompacted and sticks on the tool (zone a in Fig A3). Thus, there appears a 'primary crushed zone'. The deeper the penetration of the tool edge, the greater the cutting force becomes. If a critical value of the depth of penetration generates a state of stress which allows the propagation of a macroscopic failure crack then the initiation and propagation of this failure crack results in the formation of a coarse cutting chip.

After the formation of a coarse chip, as the tool advances, a peak of rock remaining in the lower part of the initiation point of the macroscopic failure crack is crushed to a fine cutting chip (zone b in Fig A3). This crushed zone is named 'secondary crushed zone'. Following this step of the cutting process, the tool goes on into the overcutting zone (zone c in Fig A3) without any substantial resistance, until the tool edge is forced against the next buttock which is formed by the macroscopic failure crack mentioned above. Then, a new cycle of the rock cutting process starts again.

During this rock cutting cycle, the cutting force increases with depth of penetration of the tool tip to a maximum, at the initiation of the macroscopic failure crack, and decreases steeply after this maximum value has been reached. It should be noted that the macroscopic failure crack does not start from the lowest point of the primary crushed zone, but at a point near the upper limit of this zone (point A in Fig A3).

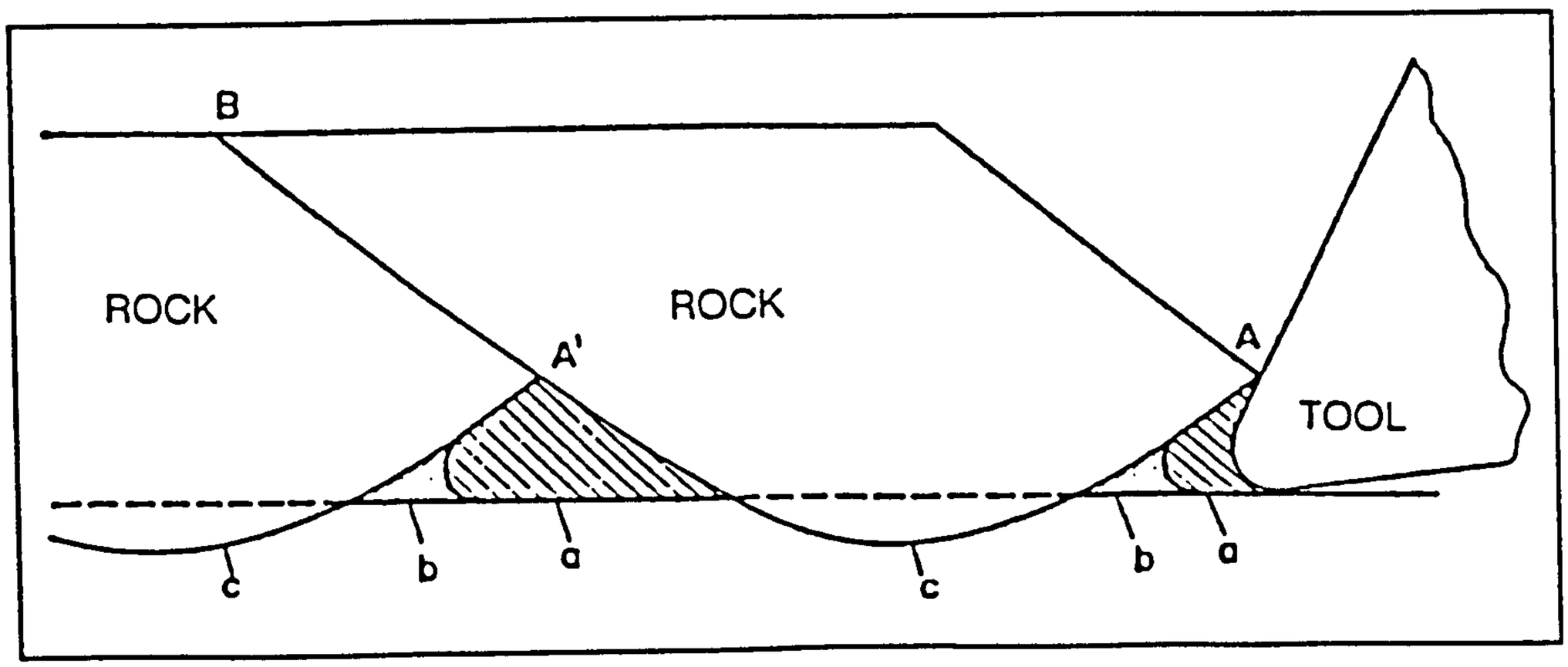

Fig A3 An illustration of the rock cutting process after Nishimatsu, (1972)

Fig A4 shows orthogonal rock cutting layout and cutting force will be as below :

$$Fc = \frac{2}{n+1} Ss \quad \sigma_t \quad \frac{\cos k}{1-\sin(k-\alpha+\phi)}$$

where :

S_s : shear strength

ϕ : angle of friction (the angle between the direction of the resultant cutting force and the normal to the face of the cutting tool)

k : angle of internal friction

α : rake angle

σ_t : tensile strength

n : stress distribution factor, constant determined from the state of stress

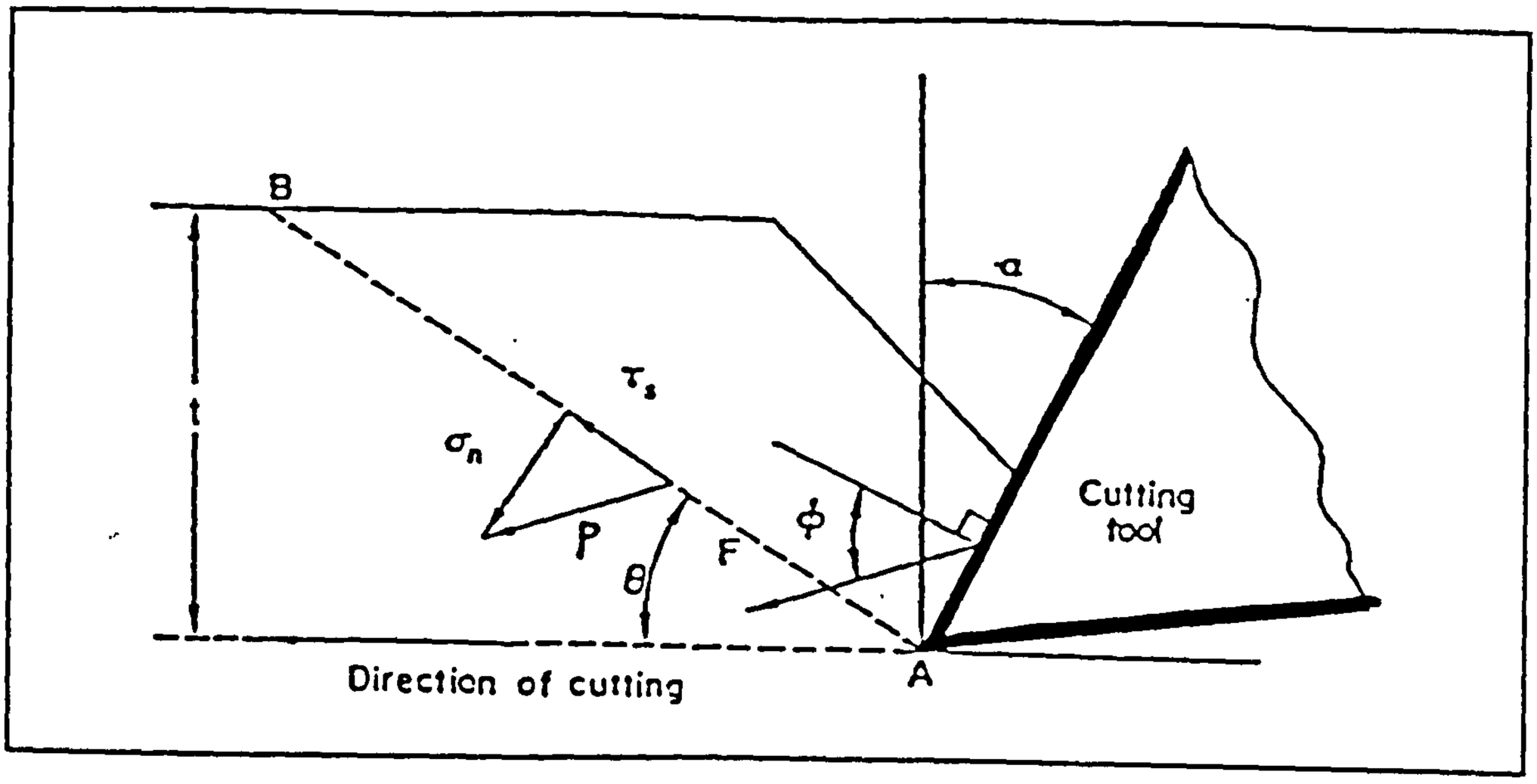

Fig A4 An illustration of the rock cutting process after Nishimatsu, 1972.

APPENDIX 2

CUTTING RESULTS

Springwell sandstone (dry)

Cut.No.	MPNF kN	MPCF kN	MNF kN	MCF kN	YIELD m^3/m	SE MJ/m^3
1						
2	3.08	2.33	1.85	1.33	8.80	15.12
3	3.53	2.66	1.87	1.22	7.41	16.47
4	3.49	2.64	2.16	1.33	7.41	17.95
5	3.69	2.48	2.41	1.43	7.41	19.30
6	3.96	2.87	2.47	1.56	7.87	19.82
7	3.76	2.81	2.47	1.56	7.41	21.06
8	4.09	2.89	2.78	1.56	7.41	21.06
9	3.70	2.50	2.55	1.43	7.41	19.30
Mean value :						
	3.66	2.65	2.32	1.43	7.6	18.8

Springwell sandstone (ambient moisture content)

Cut.No.	MPNF kN	MPCF kN	MNF kN	MCF kN	YIELD m^3/m	SE MJ/m^3
1	2.92	2.32	1.84	1.02	6.52	15.64
2	3.64	2.52	2.16	1.11	8.26	13.44
3	3.74	2.80	2.32	1.78	7.40	24.08
4	3.37	2.45	2.32	1.33	8.26	16.10
5	3.75	2.82	2.41	1.43	6.50	21.93
6	3.64	2.62	2.16	1.71	6.96	24.58
7	3.52	2.51	2.16	1.56	7.39	21.10
8	3.56	2.62	2.32	1.11	6.65	19.64
9	3.33	2.47	2.01	1.11	6.09	18.24
10	3.36	2.52	2.16	1.33	6.96	19.12
11	3.02	2.37	2.01	1.33	8.26	16.10
12	3.62	2.70	2.32	1.33	7.39	17.99
13	3.75	2.59	2.41	1.63	6.52	24.99
14	3.70	2.81	2.16	1.33	6.96	19.12
15	3.74	2.57	2.13	1.43	6.52	21.93
16	2.92	2.61	1.86	1.32	7.22	18.29
17	3.08	2.42	1.72	1.78	6.90	25.81
18	3.51	2.52	1.96	1.92	7.96	24.13
19	2.74	2.67	1.93	1.75	7.79	22.46
20	3.11	2.31	1.47	1.22	9.11	13.39
21	2.77	2.20	1.96	1.63	9.13	17.84
22	3.26	2.27	1.25	1.68	7.15	23.50
23	3.06	2.65	2.06	1.73	7.61	22.73
24	3.37	2.57	2.16	1.58	7.09	22.29
25	3.03	2.72	2.13	1.83	8.10	22.59
26	3.26	2.38	1.77	1.40	8.89	15.75
27	3.41	2.56	1.81	1.53	7.64	20.03
28	3.14	2.59	1.99	1.40	8.62	16.24
29	2.80	2.66	1.99	1.53	7.92	19.33
30	3.11	2.36	1.42	1.61	8.53	18.88
31	3.21	2.30	1.24	1.43	9.33	15.32
32	3.08	2.44	1.67	1.32	8.14	16.22
mean value :						
	3.30	2.53	2.05	1.47	7.62	19.65

Springwell sandstone (fully saturated)

Cut.No.	MPNF kN	MPCF kN	MNF kN	MCF kN	YIELD m^3/m	SE MJ/m^3
1						
2	3.23	2.34	1.94	1.05	7.02	14.95
3	2.99	2.22	1.53	0.98	8.26	11.86
4	3.05	2.14	1.70	0.98	6.61	14.82
5	3.11	2.21	1.87	0.98	6.61	14.82
6	3.36	2.36	2.04	1.22	7.02	17.37
7	2.77	2.10	1.54	0.89	7.44	11.96
8	3.02	2.05	1.87	0.98	6.60	11.86
9	3.05	2.24	2.21	1.47	5.78	25.41
10	2.82	2.25	1.85	1.33	7.02	18.93
11	3.28	2.30	2.04	1.22	7.44	16.40
12	3.15	2.77	2.04	1.22	7.44	16.40
13	3.41	———	2.04	———	8.26	———
14	3.07	2.32	1.70	0.98	7.44	13.17
Mean value :						
	3.1	2.22	1.87	1.09	7.23	15.60

Teesdale Whinstone (ambient moisture content)

Cut.No.	MPNF kN	MPCF kN	MNF kN	MCF kN	YIELD m^3/m	SE MJ/m^3
1	18.34	8.14	11.65	4.70	4.07	115.54
	18.54	8.29	11.55	5.07	4.07	124.64
	21.21	9.43	13.23	5.08	4.75	107.04
	18.20	9.38	12.44	5.08	3.38	149.86
	19.17	9.24	12.18	4.71	4.40	106.88
	23.15	9.96	16.08	5.98	3.73	160.37
	20.87	9.87	12.69	4.89	3.77	160.28
Mean value :						
	19.93	9.19	12.83	5.07	4.02	132.09

Teesdale Whinstone (fully saturated)

Cut.No.	MPNF kN	MPCF kN	MNF kN	MCF kN	YIELD m^3/m	SE MJ/m^3
1						
2	20.34	9.52	3.76	5.50	———	———
3	20.50	10.47	16.75	6.02	2.70	222.74
4	20.98	10.26	16.50	6.02	3.38	178.19
5	22.23	9.81	14.61	5.30	3.38	156.88
6	———	9.10	14.70	5.33	2.70	197.21
7	21.50	9.30	15.18	5.27	4.73	111.40
8	21.03	9.19	11.92	4.89	4.39	111.30
9	25.20	10.41	17.02	5.11	4.39	134.60
Mean vlue :						
	21.68	9.76	15.05	5.43	3.67	158.90

Pennant sandstone (ambient moisture content)

Cut.No.	MPNF kN	MPCF kN	MNF kN	MCF kN	YIELD m^3/m	SE MJ/m^3
1						
2	10.13	5.81	5.67	3.26	6.77	48.17
3	10.96	6.42	6.81	3.58	4.89	73.25
4	10.89	6.42	5.89	3.20	6.77	47.29
5	12.73	6.78	7.38	3.80	6.77	56.15
6	12.47	7.00	7.58	4.00	5.64	70.93
7	11.55	6.53	6.96	3.78	6.39	59.14
8	10.60	6.28	6.43	3.53	7.14	49.42
9	12.25	6.98	7.52	4.07	6.39	63.68
10	12.00	6.73	6.95	3.87	5.26	73.53
11	11.06	6.56	6.10	3.26	6.01	54.20
Mean value :						
	11.46	6.55	6.73	3.63	6.2	59.60

Pennant sandstone (fully saturated)

Cut.No.	MPNF kN	MPCF kN	MNF kN	MCF kN	YIELD m^3/m	SE MJ/m^3
1						
2	11.76	5.20	7.09	3.67	5.97	61.47
3	10.76	6.54	6.10	3.67	5.97	61.47
4	6.66	4.82	3.55	2.04	10.07	20.26
5	8.72	5.52	5.42	2.89	7.09	40.76
6	7.42	4.89	4.49	2.22	5.97	37.18
7	10.21	6.58	6.35	3.56	6.34	56.15
8	10.21	6.58	6.35	3.56	6.34	56.15
9	10.31	6.16	6.81	3.56	6.72	52.98
10	9.80	5.43	5.11	2.45	5.97	41.04
11	9.05	5.97	5.67	2.85	5.97	47.74
12	8.33	5.19	5.11	3.06	7.84	39.05
13	10.49	6.02	6.24	3.06	6.34	48.24
14	10.55	6.17	6.67	3.26	6.34	51.39
15	8.32	5.05	5.37	2.63	6.72	39.16
16	7.54	5.23	4.15	2.63	8.95	29.37
17	10.62	6.86	6.35	3.34	6.72	49.37
18	9.14	5.90	5.26	2.89	5.22	55.32
Mean value :						
	9.35	5.72	5.6	3.0	6.76	45.68

Matlock limestone (ambient moisture content)

Cut.No.	MPNF kN	MPCF kN	MNF kN	MCF kN	YIELD m^3/m	SE MJ/m^3
1	5.18	3.71	3.74	2.45	4.88	50.22
2	7.89	4.90	5.45	3.18	7.72	41.17
3	7.25	4.79	4.43	2.93	7.32	40.07
4	7.78	4.46	2.68	3.14	6.10	51.50
5	6.52	4.11	4.08	2.69	6.10	44.12
6	6.52	4.49	3.91	2.93	7.72	37.93
7	6.21	4.17	4.08	2.69	8.13	33.09
8	6.31	4.15	4.26	2.93	7.70	37.94
9	6.67	4.23	4.26	2.93	6.50	45.05
10	4.87	3.36	3.06	1.96	5.69	34.44
11	6.33	4.24	3.91	2.69	6.10	44.11
mean value :						
	6.50	4.24	3.99	2.77	6.72	41.78

Matlock limestone (fully saturated)

Cut.No.	MPNF kN	MPCF kN	MNF kN	MCF kN	YIELD m^3/m	SE MJ/m^3
1	6.94	5.00	3.83	2.45	5.95	41.16
2	5.94	4.14	3.06	1.96	5.95	32.93
3	6.70	4.59	3.87	2.67	6.75	39.58
4	5.69	4.01	2.94	2.22	6.75	32.91
5	5.40	3.62	3.59	2.17	5.55	39.06
6	6.33	4.64	3.74	2.45	8.70	28.06
7	6.12	3.47	3.06	1.96	5.55	35.28
8	6.21	3.90	3.23	2.45	6.75	36.32
9	5.41	4.27	3.40	2.89	7.94	36.41
10	5.24	3.54	3.09	2.22	5.16	43.03
11	6.10	4.28	3.40	2.45	7.14	34.30
mean value :	6.00	4.13	3.38	2.35	6.56	36.28

APPENDIX 2.1

DISCONTINUITY RESULTS

Springwell sandstone (dry)

	MPNF kN	MPCF kN	MNF kN	MCF kN	YIELD m^3/m	SE MJ/m^3
30° to core axis	3.27	4.14	2.05	2.27	8.96	25.33
45° to core axis	2.96	3.66	1.88	1.68	8.52	19.70
60° to core axis	3.10	3.89	1.88	1.91	8.89	21.50
75° to core axis	2.76	3.38	1.78	1.76	9.24	19.05
90° with a single discontinuity	2.72	3.73	1.52	1.65	9.33	17.70
90° with two parallel discontinuity	2.93	3.70	1.78	1.56	7.64	20.40
90° with three parallel discontinuity	2.88	3.62	1.60	1.52	8.33	18.30

Springwell sandstone (ambient moisture content)

	MPNF kN	MPCF kN	MNF kN	MCF kN	YIELD m^3/m	SE MJ/m^3
30° to core axis	2.58	3.15	1.59	1.60	9.73	16.44
45° to core axis	2.46	3.43	1.69	1.60	8.72	18.35
60° to core axis	2.73	3.35	1.79	1.57	8.49	18.49
75° to core axis	2.79	3.32	1.88	1.60	8.86	18.06
90° with a single discontinuity	2.51	3.33	1.54	1.68	8.17	20.60
90° with two parallel discontinuity	2.43	3.22	1.52	1.40	8.76	15.98
90° with three parallel discontinuity	2.59	3.34	1.61	1.65	8.33	19.81

Springwell sandstone (fully saturated)

	MPNF kN	MPCF kN	MNF kN	MCF kN	YIELD m^3/m	SE MJ/m^3
30° to core axis	2.28	3.02	1.28	1.23	8.96	13.78
45° to core axis	2.26	3.09	1.52	1.52	9.34	16.33
60° to core axis	1.98	2.51	1.11	1.12	10.06	11.13
75° to core axis	2.08	2.67	1.42	1.23	8.00	15.44
90° with a single discontinuity	2.44	3.12	1.43	1.30	9.00	14.44
90° with two parallel discontinuity	1.79	2.17	1.03	0.90	9.32	9.66
90° with three parallel discontinuity	1.97	2.59	1.28	1.23	10.01	12.34

APPENDIX 2.2

CUTTING RESULTS

Springwell sandstone (fully satuarted)

discontinuity angle = 45° spacing =52 mm

Cut.No.	MPNF kN	MPCF kN	MNF kN	MCF kN	YIELD m^3/m	SE MJ/m^3
1	2.14	2.65	2.42	1.41	21.4	14.55
2	1.83	1.98	1.17	1.23	23.5	11.56
3	2.38	2.81	1.64	1.54	21.1	16.14
4	2.18	2.26	1.25	1.10	23.1	10.57
5	2.13	2.76	1.64	1.85	21.5	19.02
6	2.29	2.33	1.46	1.37	20.1	15.07
7	2.00	2.19	1.62	1.41	21.4	14.57

Mean value :

2.13	2.42	1.60	1.41	21.73	14.50

discontinuity angle = 45° spacing =61 mm

Cut.No.	MPNF kN	MPCF kN	MNF kN	MCF kN	YIELD m^3/m	SE MJ/m^3
1	2.42	2.77	1.67	1.37	20.4	14.85
2	2.52	2.79	1.46	1.37	20.3	14.92
3	1.89	2.16	1.25	1.10	23.6	10.30
4	1.28	2.52	1.41	1.23	25.4	10.70

mean value :

2.03	2.56	1.45	1.27	22.4	12.69

discontinuity angle = 45° spacing =86 mm

Cut.No.	MPNF kN	MPCF kN	MNF kN	MCF kN	YIELD m^3/m	SE MJ/m^3
1	2.21	2.68	1.50	1.23	21.6	12.59
2	2.13	2.46	1.17	1.23	20.0	13.59
3	2.43	2.73	1.69	1.23	———	———
4	2.21	2.62	1.31	1.48	19.3	16.95

mean value :

2.24	2.62	1.42	1.29	20.3	14.38

discontinuity angle = 45° spacing =94 mm

Cut.No.	MPNF kN	MPCF kN	MNF kN	MCF kN	YIELD m^3/m	SE MJ/m^3
1	2.23	2.53	1.50	1.23	21.0	12.95
2	2.29	2.77	1.46	1.64	20.2	17.95
3	2.30	2.76	1.88	1.48	21.3	15.36
4	2.00	2.66	1.37	1.57	19.7	17.62

mean value :

2.20	2.68	1.55	1.48	20.0	15.97

discontinuity angle = 30° spacing =51 mm

Cut.No.	MPNF kN	MPCF kN	MNF kN	MCF kN	YIELD m^3/m	SE MJ/m^3
1	2.24	2.74	1.57	1.23	21.2	12.83
2	1.42	2.66	2.54	1.23	20.6	13.20
3	2.19	2.58	1.57	1.23	21.1	12.89
4	1.96	2.27	1.88	1.64	22.1	16.40
mean value :						
	1.95	2.56	1.89	1.33	21.2	13.83

discontinuity angle = 30° spacing =61 mm

Cut.No.	MPNF kN	MPCF kN	MNF kN	MCF kN	YIELD m^3/m	SE MJ/m^3
1	2.21	2.76	1.64	1.54	21.1	16.13
2	2.31	2.74	1.61	1.76	21.0	18.53
3	2.16	2.42	1.88	1.41	21.4	14.57
4	1.22	2.61	1.34	1.41	23.7	13.15
mean value :						
	1.97	2.63	1.62	1.53	21.8	15.59

APPENDIX 3
RAKE ANGLE RESULTS

Rake angle 0°, saturated, depth=5 mm

Cut.No.	MPNF kN	MPCF kN	MNF kN	MCF kN	YIELD m^3/m	SE MJ/m^3
1	1.12	2.10	0.74	0.64	6.20	10.32
2	1.15	1.84	0.74	0.61	6.60	9.23
3	1.14	2.63	0.61	0.76	6.60	11.49
4	1.00	2.25	0.49	0.76	7.02	10.82
5	1.15	2.37	0.74	0.76	9.09	8.36
6	1.09	2.37	0.67	0.69	9.09	7.59
7	1.00	1.95	0.54	0.56	8.26	6.78
Mean value	1.11	2.21	0.65	0.68	7.55	9.21

Rake angle -10°, saturated, depth=5 mm

Cut.No.	MPNF kN	MPCF kN	MNF kN	MCF kN	YIELD m^3/m	SE MJ/m^3
1	1.63	2.74	0.74	0.89	8.30	10.77
2	1.58	2.48	0.74	0.64	9.09	7.04
3	1.35	2.51	0.74	0.89	9.09	9.79
4	1.40	2.53	0.67	0.83	7.80	10.57
5	1.49	2.64	0.94	0.97	8.68	11.18
6	1.47	2.59	0.74	0.76	7.80	9.68
7	1.61	2.81	0.94	0.97	8.70	11.18
8	1.45	2.43	0.86	0.89	8.30	10.77
9	1.85	3.10	0.94	1.11	8.30	13.43
10	1.59	2.83	0.98	1.02	8.70	11.75
11	1.28	2.44	0.74	1.02	9.92	10.28
12	1.61	2.81	0.88	1.07	——	——
Mean value :	1.53	2.66	0.82	0.92	8.58	10.60

Rake angle 16°, saturated, depth=5 mm

Cut.No.	MPNF kN	MPCF kN	MNF kN	MCF kN	YIELD m3/m	SE MJ/m^3
1	0.93	2.28	0.67	0.69	8.70	7.95
2	0.93	1.96	0.49	0.51	7.80	6.49
3	0.84	1.74	0.67	0.69	12.40	5.57
4	1.13	1.94	0.67	0.69	8.70	7.95
5	0.71	1.77	0.37	0.57	8.30	6.90
6	0.83	1.16	0.59	0.76	9.09	8.36
7	0.77	1.64	0.49	0.51	7.80	6.50
8	1.03	1.77	0.74	0.61	9.90	6.15
9	1.04	2.00	0.74	0.76	8.70	8.67
10	1.06	2.00	0.67	0.56	9.50	5.89
11	1.16	1.93	0.80	0.41	9.09	4.51
12	1.06	1.93	0.74	0.51	8.68	5.88
13	1.06	1.84	0.74	0.64	8.30	7.74
14	0.99	1.64	0.61	0.51	9.09	5.61
15	1.04	1.97	0.79	0.71	7.80	9.04
Mean value	0.97	1.84	0.65	0.61	8.93	6.89

APPENDIX 4
CUTTING SPEED RESULTS

speed=0.100 m/s depth of cut=8 mm

Cut.No.	MPNF kN	MPCF kN	MNF kN	MCF kN	YIELD m^3/m	SE MJ/m^3
1	3.31	3.05	2.34	2.14	19.00	11.26
2	2.82	4.13	1.53	1.96	14.88	13.17
3	4.02	3.73	2.46	1.90	14.46	13.14
4	3.32	4.54	1.89	2.17	12.80	16.94
5	4.86	4.44	3.40	2.45	14.05	17.44
6	4.28	3.86	2.98	2.45	16.53	14.82
7	4.47	3.83	3.16	2.45	17.35	14.12
8	4.02	3.57	2.76	2.14	13.20	16.18
9	3.99	4.06	2.55	2.45	18.00	13.17
10	3.68	3.76	2.27	2.17	20.00	11.00
11	3.91	4.04	2.55	2.20	17.18	12.38
12	3.73	4.23	2.65	2.17	16.90	12.81

Mean value :

	3.87	3.94	2.54	2.22	16.19	13.47

speed=0.125 m/s depth of cut=8 mm

Cut No.	MPNF kN	MPCF kN	MNF kN	MCF kN	YIELD m^3/m	SE MJ/m^3
1	2.60	3.52	———	———	15.18	———
2	2.52	2.50	1.36	1.47	9.95	14.80
3	2.71	3.19	1.70	1.90	15.40	12.30
4	3.49	3.39	1.87	1.96	15.4	12.73
5	2.42	3.09	1.70	1.90	———	———
6	2.79	3.28	1.86	2.71	18.60	14.60
7	2.50	2.86	1.53	1.47	16.30	9.02

Mean value :

	2.72	3.12	1.67	1.90	15.14	12.69

APPENDIX 5

Effect of spacing on rock cutting parameter

The results of spacing in Springwell sandstone fully saturated are presentated, trimmed surfaces are shown in previous chapters, here only the results of interaction as follows with different spacing (s=spacimg in mm) and also with different depth :

d=4 mm

Cut No.	MPNF (kN)	MPNF (kN)	MNF (kN)	MCF (kN)	YIELD (m^3/m)	SE (MJ/m^3)	
1	1.94	1.62	1.19	0.73	4.54	16.06	
2	1.81	1.67	1.02	0.73	4.96	14.72	s=2
3	1.87	1.53	1.19	0.73	4.54	16.06	s=4
4	1.69	1.62	1.02	0.49	4.54	10.78	s=8
5	1.92	1.71	1.02	0.73	4.96	14.72	s=12
6	1.82	1.77	1.24	0.89	4.54	19.58	s=16

Cut No.	MPNF (kN)	MPNF (kN)	MNF (kN)	MCF (kN)	YIELD (m^3/m)	SE (MJ/m^3)	
1	1.53	1.72	1.02	0.98	4.54	21.56	
2	1.50	1.39	1.02	0.49	4.54	10.78	s=2
3	1.56	1.69	1.02	0.73	4.96	14.72	s=4
4	1.79	1.77	1.08	0.89	4.96	17.95	s=8
5	1.77	1.71	1.19	0.73	4.54	16.06	s=12
6	1.63	1.66	1.19	1.22	4.13	29.52	s=16

Cut No.	MPNF (kN)	MPNF (kN)	MNF (kN)	MCF (kN)	YIELD (m^3/m)	SE (MJ/m^3)	
1	2.40	1.62	1.53	0.73	4.13	17.67	
2	----	----	----	----	4.13	---	s=2
3	2.44	1.65	1.46	0.70	4.54	15.40	s=4
4	2.64	1.66	1.70	0.92	3.72	24.74	s=8
5	2.44	1.48	1.49	0.92	3.72	24.74	s=12
6	2.48	1.57	1.70	0.82	3.30	24.80	s=16

Cut No.	MPNF (kN)	MPNF (kN)	MNF (kN)	MCF (kN)	YIELD (m^3/m)	SE (MJ/m^3)	
1	2.98	2.04	1.89	1.36	5.40	25.32	
2	3.03	1.94	1.89	1.36	6.20	21.94	s=2
3	3.39	2.24	1.70	2.45	6.61	37.06	s=4
4	2.69	2.11	1.89	1.36	8.68	15.67	s=8
5	3.33	2.45	2.13	1.22	8.30	13.32	s=12
6	3.17	2.45	1.51	1.36	9.26	14.69	s=16

The results of trimmed surfaces as follows :

Cut No.	MPNF (kN)	MPNF (kN)	MNF (kN)	MCF (kN)	YIELD (m^3/m)	SE (MJ/m^3)	
1	2.28	1.94	1.91	1.22	4.54	26.84	
2	2.78	1.75	1.89	1.09	4.54	23.98	s=2
3	2.70	1.70	1.91	0.91	5.37	16.94	s=4
4	2.72	1.65	1.94	1.05	4.96	21.17	s=8
5	2.56	1.68	1.91	0.61	5.78	10.54	s=12
6	2.66	1.64	1.70	1.22	4.13	29.52	s=16

Cut No.	MPNF (kN)	MPNF (kN)	MNF (kN)	MCF (kN)	YIELD (m^3/m)	SE (MJ/m^3)	
1	3.01	1.82	1.89	2.71	5.78	46.84	
2	2.84	1.55	1.70	2.45	6.19	39.53	s=2
3	2.60	1.58	1.70	2.45	6.60	37.06	s=4
4	2.90	1.78	1.89	2.71	5.37	50.45	s=8
5	2.73	1.84	1.70	2.45	4.54	53.90	s=12
6	2.69	1.66	1.87	2.70	4.13	65.34	s=16

mean value :

Cut No.	MPNF (kN)	MPNF (kN)	MNF (kN)	MCF (kN)	YIELD (m^3/m)	SE (MJ/m^3)	
1	2.21	1.75	1.41	0.95	4.65	20.15	
2	2.11	1.67	1.31	0.86	4.96	15.81	s=2
3	2.31	2.37	1.34	1.15	5.16	20.81	s=4
4	2.20	1.79	1.42	0.91	5.47	17.28	s=8
5	2.36	1.84	1.46	0.90	5.38	17.21	s=12
6	2.27	1.86	1.41	1.07	5.31	22.14	s=16

Cut No.	MPNF (kN)	MPNF (kN)	MNF (kN)	MCF (kN)	YIELD (m^3/m)	SE (MJ/m^3)	
1	2.91	1.88	1.90	1.96	5.16	37.84	
2	2.81	1.65	1.79	1.77	5.36	31.75	s=2
3	2.65	1.64	1.80	1.68	5.89	27.00	s=4
4	2.81	1.71	1.91	1.88	5.16	35.81	s=8
5	2.64	1.76	1.80	1.53	5.16	32.22	s=12
6	2.67	1.65	1.78	1.96	4.13	47.43	s=16

d=6 mm

Cut No.	MPNF (kN)	MPNF (kN)	MNF (kN)	MCF (kN)	YIELD (m^3/m)	SE (MJ/m^3)	
1	2.08	2.42	1.02	1.22	9.92	12.30	
2	1.63	1.79	0.95	0.82	7.80	10.44	s=3
3	1.73	1.99	0.85	0.98	8.68	11.29	s=6
4	1.79	2.04	0.85	0.91	11.57	7.86	s=12
5	1.87	2.59	1.36	1.22	9.92	12.30	s=18

Cut No.	MPNF (kN)	MPNF (kN)	MNF (kN)	MCF (kN)	YIELD (m^3/m)	SE (MJ/m^3)	
1	2.36	2.58	1.19	1.22	10.33	11.81	
2	2.04	1.93	1.13	1.09	8.68	12.56	s=3
3	2.16	2.14	1.36	1.22	9.5	12.84	s=6
4	2.08	2.20	1.08	1.11	12.40	8.95	s=12
5	2.26	2.40	1.32	1.09	9.50	11.47	s=18

Cut No.	MPNF (kN)	MPNF (kN)	MNF (kN)	MCF (kN)	YIELD (m^3/m)	SE (MJ/m^3)	
1	2.11	1.24	1.28	0.61	7.40	8.20	s=3
2	2.64	1.87	1.70	0.91	11.16	8.16	s=6
3	2.74	2.33	1.70	1.09	12.81	8.51	s=12
4	2.63	2.18	1.70	1.71	11.98	14.27	s=18

Cut No.	MPNF (kN)	MPNF (kN)	MNF (kN)	MCF (kN)	YIELD (m^3/m)	SE (MJ/m^3)	
1	3.10	2.65	2.27	1.63	9.50	17.15	
2	2.21	1.82	1.53	1.22	8.26	14.76	s=3
3	2.52	2.09	1.87	1.47	9.09	16.17	s=6
4	2.69	2.42	1.51	1.36	13.22	10.28	s=12
5	2.57	2.34	2.04	1.47	9.90	14.82	s=18

Cut No.	MPNF (kN)	MPNF (kN)	MNF (kN)	MCF (kN)	YIELD (m^3/m)	SE (MJ/m^3)	
1	2.89	2.24	2.04	1.22	8.80	13.86	
2	2.10	1.37	1.36	0.49	8.30	5.93	s=3
3	2.68	1.96	1.87	1.22	6.19	19.68	s=6
4	2.68	2.21	1.70	1.22	9.09	13.42	s=12
5	2.76	2.09	1.87	0.98	8.30	11.86	s=18

trimmed surfaces

Cut No.	MPNF (kN)	MPNF (kN)	MNF (kN)	MCF (kN)	YIELD (m^3/m)	SE (MJ/m^3)	
1	2.22	2.66	1.32	1.36	11.98	11.35	
2	1.48	1.58	102	0.73	6.20	11.78	s=3
3	1.81	2.07	1.19	0.98	9.50	10.31	s=6
4	2.34	2.58	1.19	1.22	11.57	10.54	s=12
5	1.99	2.35	2.10	1.09	11.98	9.10	s=18

Cut No.	MPNF (kN)	MPNF (kN)	MNF (kN)	MCF (kN)	YIELD (m^3/m)	SE (MJ/m^3)	
1	2.60	2.54	1.53	1.22	10.7	11.35	
2	2.28	1.97	1.36	1.22	11.52	14.06	s=3
3	2.11	1.73	1.19	0.98	8.68	11.29	s=6
4	2.53	2.57	1.42	0.82	12.81	6.40	s=12
5	2.28	2.27	1.70	0.92	11.57	7.95	s=18

Mean value :

Cut No.	MPNF (kN)	MPNF (kN)	MNF (kN)	MCF (kN)	YIELD (m^3/m)	SE (MJ/m^3)	
1	2.61	2.47	1.63	1.32	9.64	13.78	
2	2.52	1.63	1.25	0.85	8.09	10.38	s=3
3	2.35	2.01	1.53	1.16	8.92	13.63	s=6
4	2.40	2.24	1.37	1.14	11.82	9.80	s=12
5	2.42	2.32	1.66	1.29	9.92	12.94	s=18

mean value of trimmed results :

Cut No.	MPNF (kN)	MPNF (kN)	MNF (kN)	MCF (kN)	YIELD (m^3/m)	SE (MJ/m^3)	
1	2.41	2.60	1.42	1.29	11.34	11.35	
2	1.88	1.77	1.19	0.97	8.86	12.92	s=3
3	1.96	1.90	1.19	0.98	9.09	10.80	s=6
4	2.43	2.57	1.30	1.02	12.19	8.47	s=12
5	2.13	2.31	1.90	1.00	11.77	8.52	s=18

d=8 mm

Cut No.	MPNF (kN)	MPNF (kN)	MNF (kN)	MCF (kN)	YIELD (m^3/m)	SE (MJ/m^3)	
1	4.86	2.95	2.04	2.45	14.05	17.44	
2	3.82	2.95	2.04	1.71	14.05	12.17	s=4
3							s=8
4	4.20	4.44	2.92	2.45	16.11	15.20	s=16

Cut No.	MPNF (kN)	MPNF (kN)	MNF (kN)	MCF (kN)	YIELD (m^3/m)	SE (MJ/m^3)	
1	4.28	3.86	2.98	2.45	16.53	14.82	
2	3.27	2.77	1.91	0.91	9.50	9.57	s=4
3	3.51	2.75	1.91	1.53	15.29	10.01	s=8
4	3.77	3.38	2.55	1.83	13.64	13.42	s=16

Cut No.	MPNF (kN)	MPNF (kN)	MNF (kN)	MCF (kN)	YIELD (m^3/m)	SE (MJ/m^3)	
1	4.47	3.83	3.16	2.45	17.35	14.12	
2	2.87	2.30	1.70	1.09	9.09	11.99	s=4
3	3.57	2.98	2.27	1.63	12.81	12.72	s=8

Cut No.	MPNF (kN)	MPNF (kN)	MNF (kN)	MCF (kN)	YIELD (m^3/m)	SE (MJ/m^3)	
1	4.02	3.57	2.76	2.14	13.20	16.18	
2	2.86	2.43	1.94	1.40	10.74	13.03	s=4
3	4.33	3.89	2.68	2.09	18.59	11.24	s=8
4	4.58	4.32	2.98	2.45	15.30	16.02	s=16

Mean value :

Cut No.	MPNF (kN)	MPNF (kN)	MNF (kN)	MCF (kN)	YIELD (m^3/m)	SE (MJ/m^3)	
1	4.41	3.92	3.07	2.37	15.28	15.64	
2	3.20	2.61	1.90	1.28	10.84	11.69	s=4
3	3.80	3.21	2.29	1.75	15.56	11.32	s=8
4	3.14	4.05	2.82	2.24	15.02	11.16	s=16

APPENDIX 6
UNIAXIAL LOADING RESULTS

In conducting the experiments for the physical and mechanical properties of Springwell sandstone , it was decided to form five groups (according to uniaxial compression), each group consisting of three specimens and to conduct four cuts per specimen. The planned pattern of cuts is shown belw :

Group	(MPa)	Specimen Used	Number of Cuts
1	0	5	17
2	22.56	4	12
3	29.33	3	12
4	38.36	4	5
5	40.62	7	12

The results as follows:

group 1 is presented in Appendix 2 under ambient moisture condition.

Group2 :

Cut No.	MPCF (kN)	MPNF (kN)	MNF (kN)	MCF (kN)	YIELD (m^3/m)	SE (MJ/m^3)
1	3.83	3.01	1.28	1.53	6.63	23.09
2	3.56	2.90	1.22	1.53	7.37	20.75
3	3.75	2.96	1.20	1.75	9.00	19.44
4	4.20	3.09	1.23	1.83	8.51	21.50
5	3.68	2.63	1.08	1.63	8.21	19.85
6	3.94	2.87	1.16	1.68	8.95	18.78
7	3.67	2.99	1.14	1.88	8.40	22.37
8	3.38	2.73	1.27	1.43	7.03	20.36
9	3.32	2.68	1.03	1.53	7.20	21.26
10	2.81	2.62	1.43	1.31	7.57	17.31
11	3.62	2.87	1.12	1.68	8.83	19.02
12	3.86	3.08	1.17	1.68	8.83	19.03
Mean value :	3.64	2.87	1.93	1.62	8.04	20.23

Group3 :

Cut No.	MPCF (kN)	MPNF (kN)	MNF (kN)	MCF (kN)	YIELD (m^3/m)	SE (MJ/m^3)
1	3.95	2.66	2.15	1.99	9.23	21.55
2	4.10	2.76	2.11	1.96	9.27	21.15
3	3.19	2.80	1.77	1.63	6.92	23.57
4	3.38	2.65	1.81	1.48	7.16	20.66
5	3.26	2.66	1.96	1.63	6.64	24.56
6	3.74	2.76	2.11	1.78	7.44	23.94
7	3.61	3.10	1.96	1.73	6.84	25.28
8	3.39	2.75	1.77	1.58	6.70	23.60
9	3.63	2.81	1.96	1.68	7.09	23.68
10	3.99	2.95	2.01	2.04	9.36	21.80
11	3.29	2.75	1.88	1.65	6.67	24.75
12	3.13	2.70	1.86	1.56	6.86	22.74
Mean value :	3.55	2.78	1.95	1.73	7.51	23.11

Group4 :

Cut No.	MPCF (kN)	MPNF (kN)	MNF (kN)	MCF (kN)	YIELD (m^3/m)	SE (MJ/m^3)
1	2.89	2.53	1.62	1.27	7.31	17.37
2	3.59	2.96	2.12	1.47	8.00	18.37
3	2.84	2.71	1.67	1.38	7.16	19.26
4	2.68	2.56	1.81	1.28	7.79	16.44
5	3.49	2.42	1.63	1.77	7.35	24.08
Mean value :	3.10	2.62	1.77	1.43	7.5	19.10

Group5 :

Cut No.	MPCF (kN)	MPNF (kN)	MNF (kN)	MCF (kN)	YIELD (m^3/m)	SE (MJ/m^3)
1	2.56	2.00	1.81	1.40	8.45	16.56
2	2.39	2.20	1.22	1.41	7.93	17.77
3	3.05	2.73	2.10	1.59	7.24	21.95
4	2.66	2.57	1.72	1.12	7.45	15.04
5	3.46	3.02	1.86	1.59	8.09	19.64
6	2.73	2.47	1.59	1.22	8.15	14.73
7	2.96	2.64	1.83	1.59	7.66	20.77
8	3.02	2.76	1.81	1.31	7.53	17.39
9	2.97	2.42	1.57	1.22	7.46	16.36
10	3.80	3.00	1.77	1.43	7.93	18.03
11	3.67	2.83	2.31	1.66	7.76	21.38
12	3.39	2.73	1.84	1.44	8.11	17.76
Mean value :	3.05	2.61	1.79	1.42	7.81	18.11

APPENDIX 7

FINITE ELEMENT GRAPHICS OUTPUT

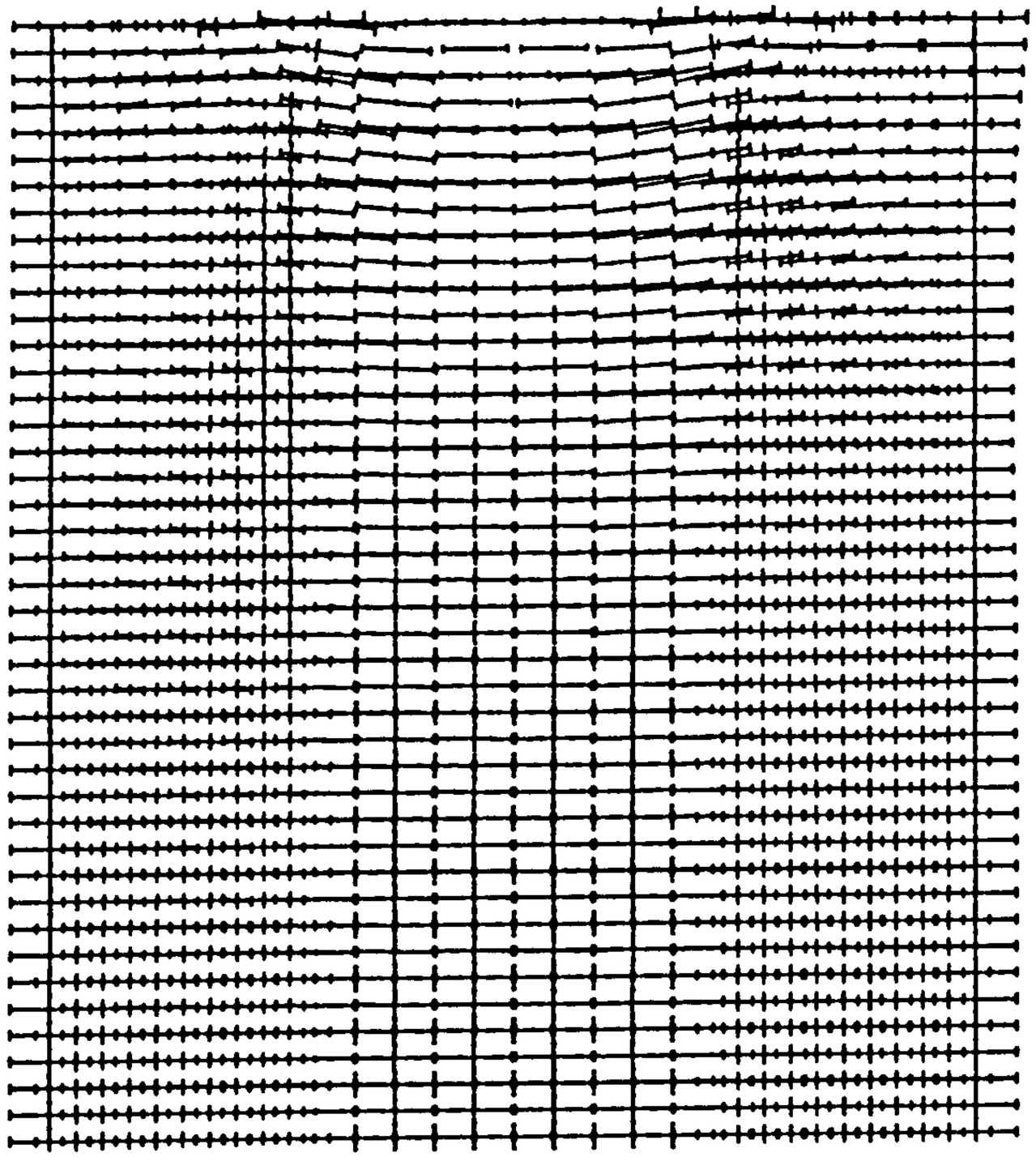

PAFEC

VIEW FROM X = 0.0000
Y = 0.0000
Z = 1.000 0

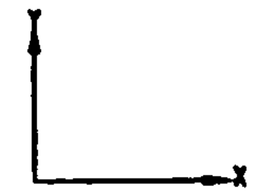

Z TOWARDS VIEWER

LOAD CASE = 1
SCALE OF VECTORS =
0. 3454E 6 UNITS/CM.
COMPRESSIVE STRESS VECTOR
SHOWN WITH END BARS.
VECTORS WITHIN 30 DEGREES OF
PAPER NORMAL DENOTED
BY TRIANGLES
(TENSILE POINT UPWARD

WHOLE STRUCTURE DRAWN
AS DEFINED IN FRONT. ORDER

DRAWING NO. 2

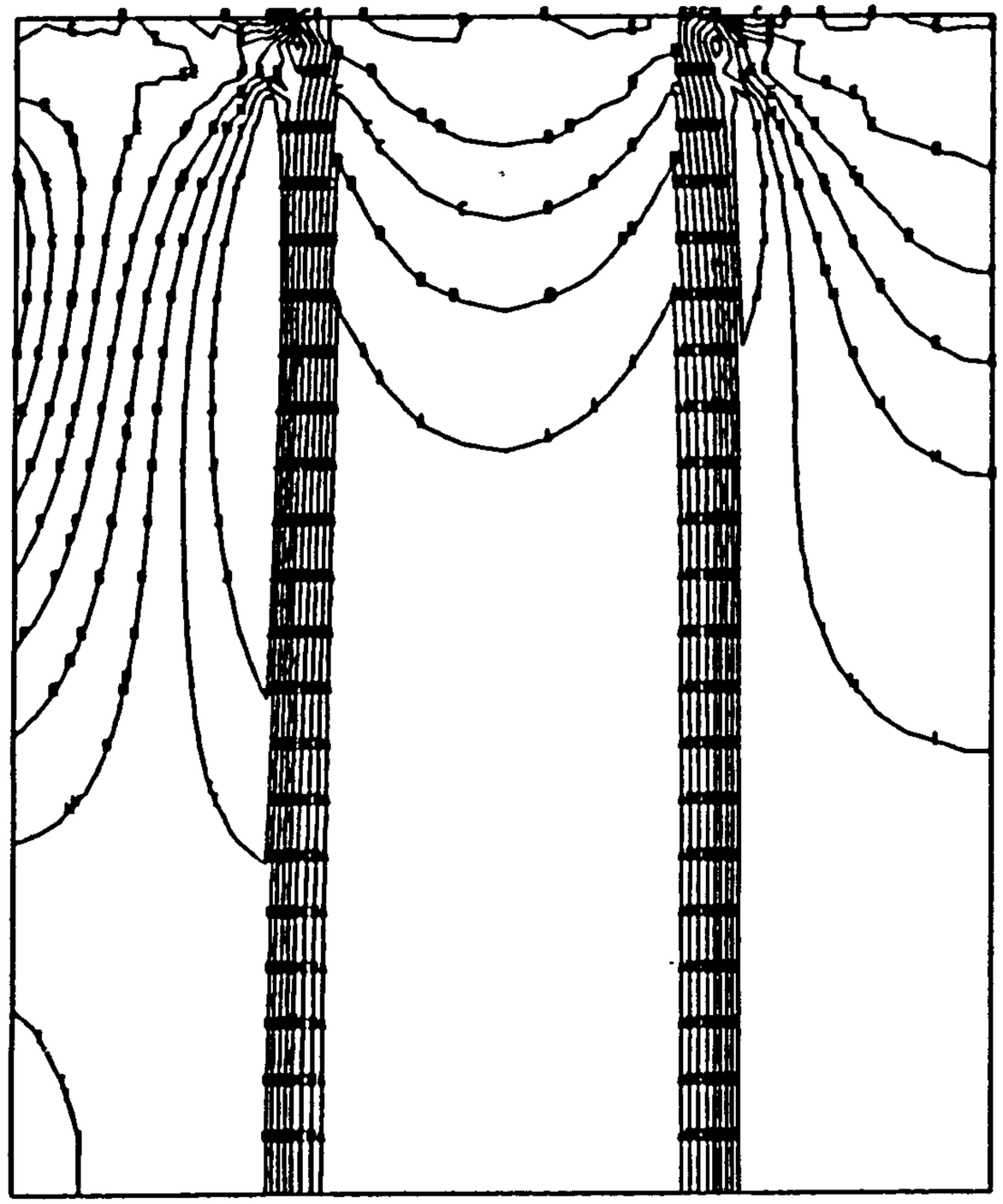

PAFEC

VIEW FROM X = 0.0000
Y = 0.0000
Z = 1.000

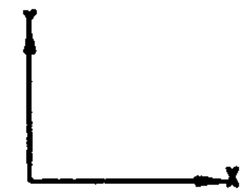

Z TOWARDS VIEWER

MAXIMUM
PRINCIPAL
(MOST
POSITIVE)
STRESS
(MIDDLE SURFACE)

-0.	7830E 5	A
-0.	5880E 5	B
-0.	3920E 5	C
-0.	1960E 5	D
	-115. 0	E
0.	1940E 5	F
0.	3900E 5	G
0.	5850E 5	H
0.	7810E 5	I
0.	9760E 5	J

LOAD CASE = 1

WHOLE STRUCTURE
AS DEFINED IN FRONT.

DRAWN
ORDER

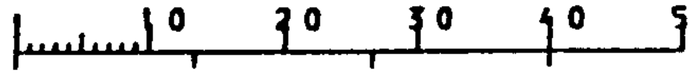

DRAWING NO. 3

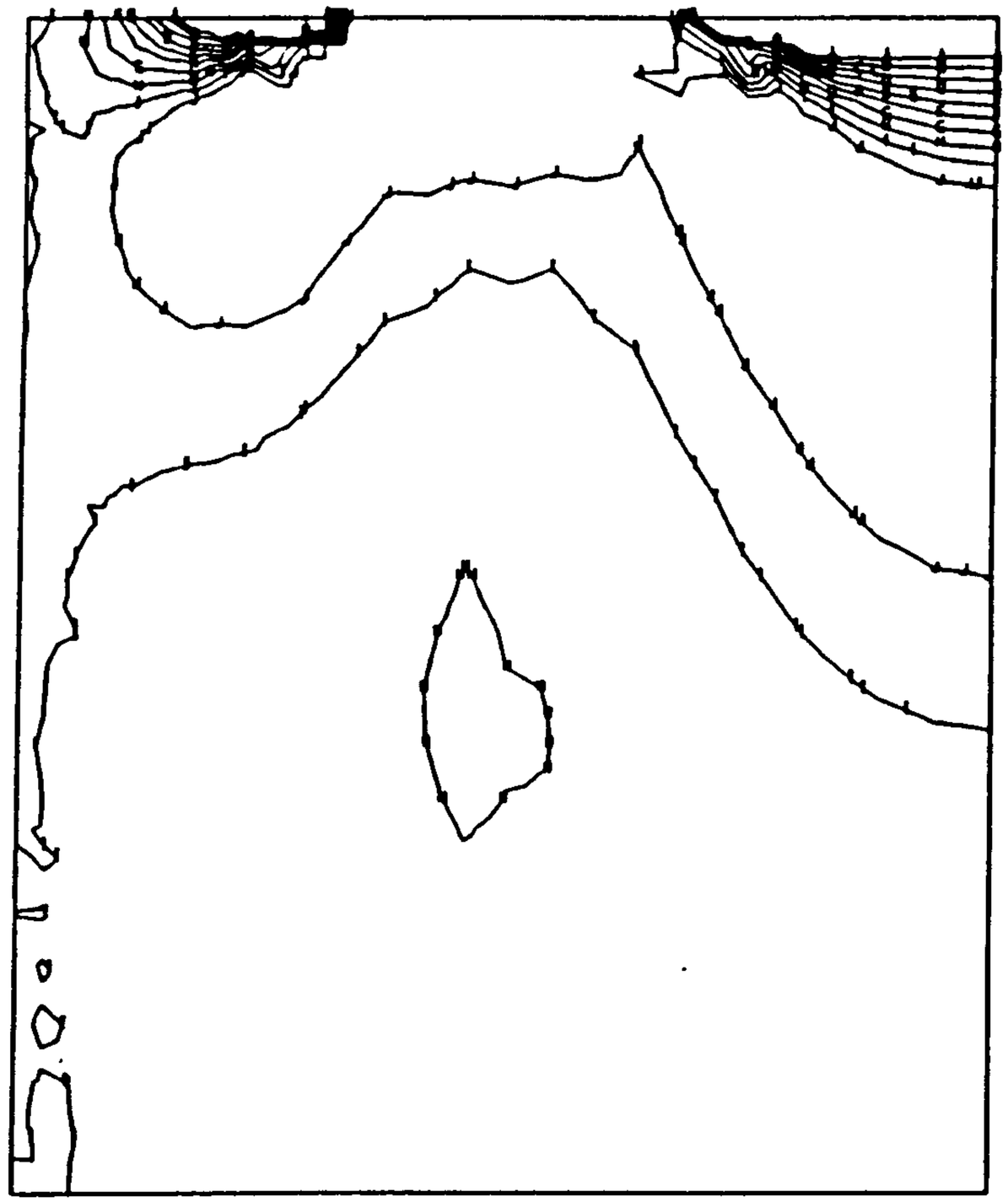

PAFEC

VIEW FROM X = 0.0000
Y = 0.0000
Z = 1.000

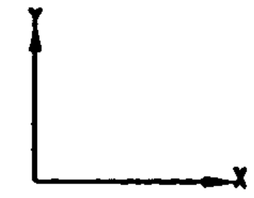

Z TOWARDS VIEWER

MINIMUM
PRINCIPAL
(MOST
NEGATIVE)
STRESS
(MIDDLE SURFACE)
MULTIPLY
BY 10^{6}

- 0. 4270
- 0. 4180
- 0. 4080
- 0. 3980
- 0. 3880
- 0. 3790
- 0. 3690
- 0. 3590
- 0. 3500
- 0. 3400

LOAD CASE = 1

WHOLE STRUCTURE
AS DEFINED IN FRONT.

DRAWN
ORDER

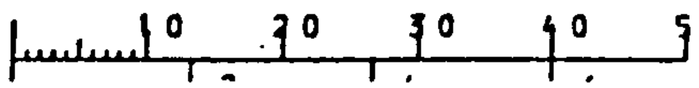

DRAWING NO. 4

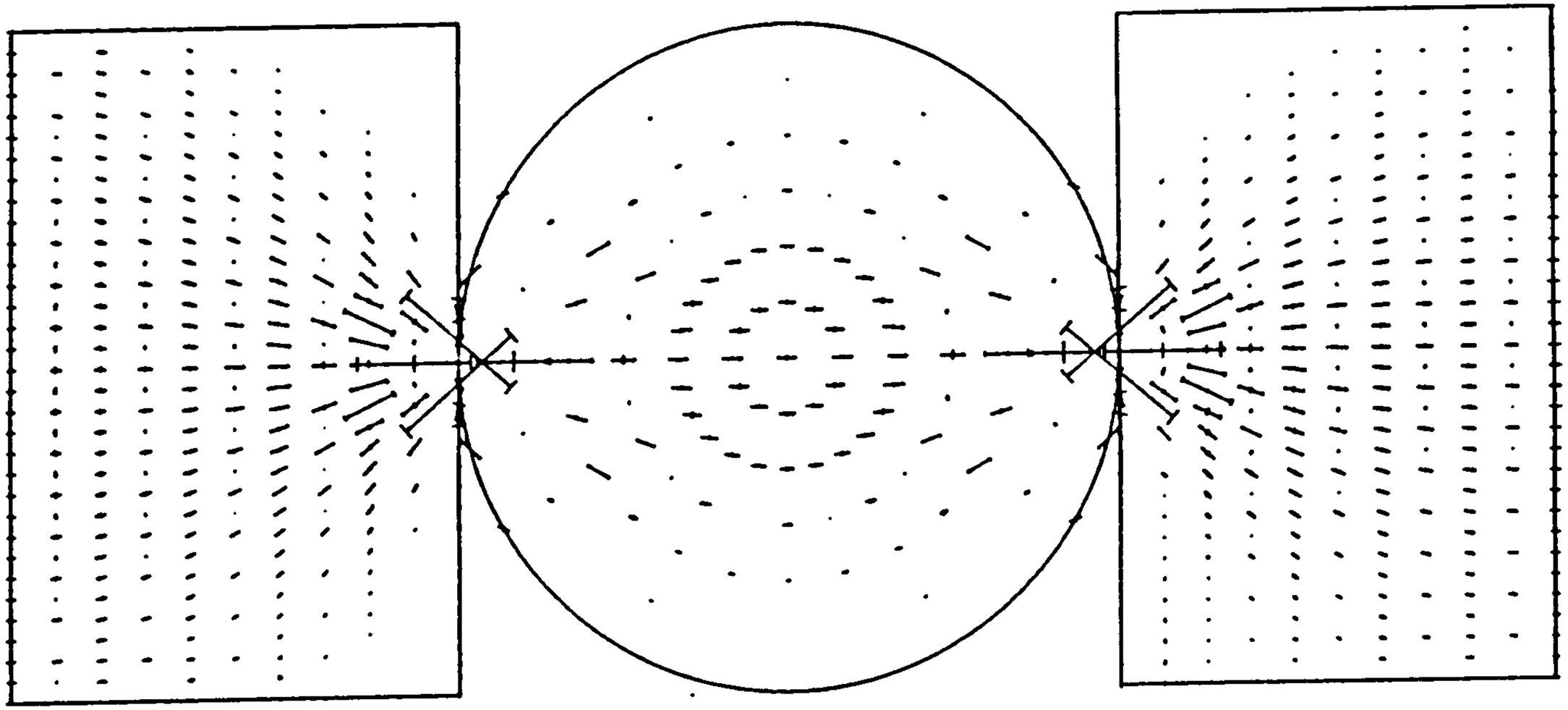

PAFEC

VIEW FROM X = 0.0000
Y = 0.0000
Z = 1.000

Z TOWARDS VIEWER

LOAD CASE = 1
SCALE OF VECTORS =
0. 2768E 7 UNITS/CM.
COMPRESSIVE STRESS VECTO
SHOWN WITH END BARS.
VECTORS WITHIN 30 DEGREES C
PAPER NORMAL DENOTED
BY TRIANGLES
(TENSILE POINT UPWARD)

WHOLE STRUCTURE DRAWN
AS DEFINED IN FRONT. ORD

DRAWING NO. 2

10 20 30 40 50 MM.

PAFEC

VIEW FROM X = 0.0000
Y = 0.0000
Z = 1.000

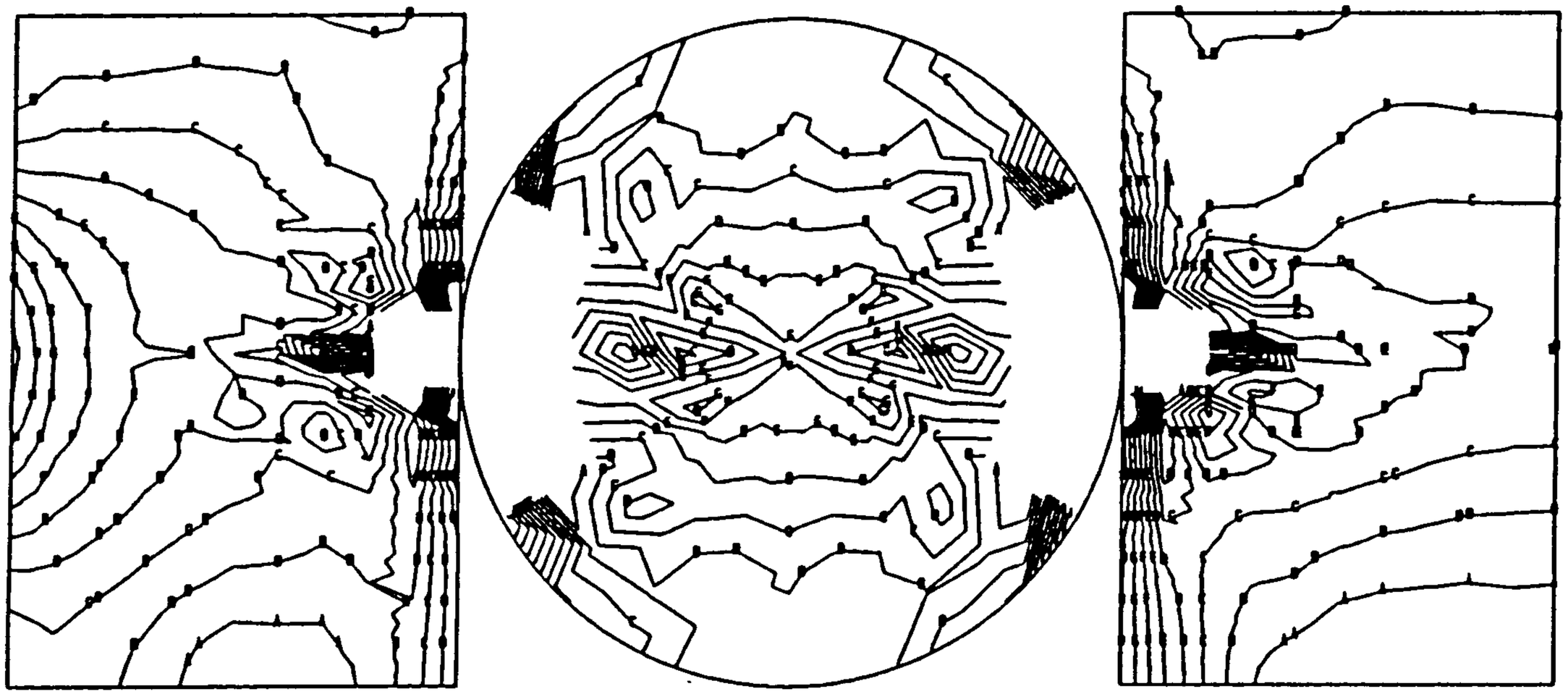

Z TOWARDS VIEWER

MAXIMUM PRINCIPAL (MOST POSITIVE) STRESS (MIDDLE SURFACE)
MULTIPLY BY 10^{4}

-0. 1890E-1	A
0. 3070E-1	B
0. 8040E-1	C
0. 1300	D
0. 1790	E
0. 2290	F
0. 2790	G
0. 3280	H
0. 3780	I
0. 4280	J

LOAD CASE = 1

WHOLE STRUCTURE AS DEFINED IN FRONT.

DRAWN ORDE

FOR SOME ELEMENTS IN THIS VIEW, COMPLETE AVERAGED STRESSES ARE NOT AVAILABLE.

10 20 30 40 50 MM.

DRAWING NO. 3

SCALE - 1 250

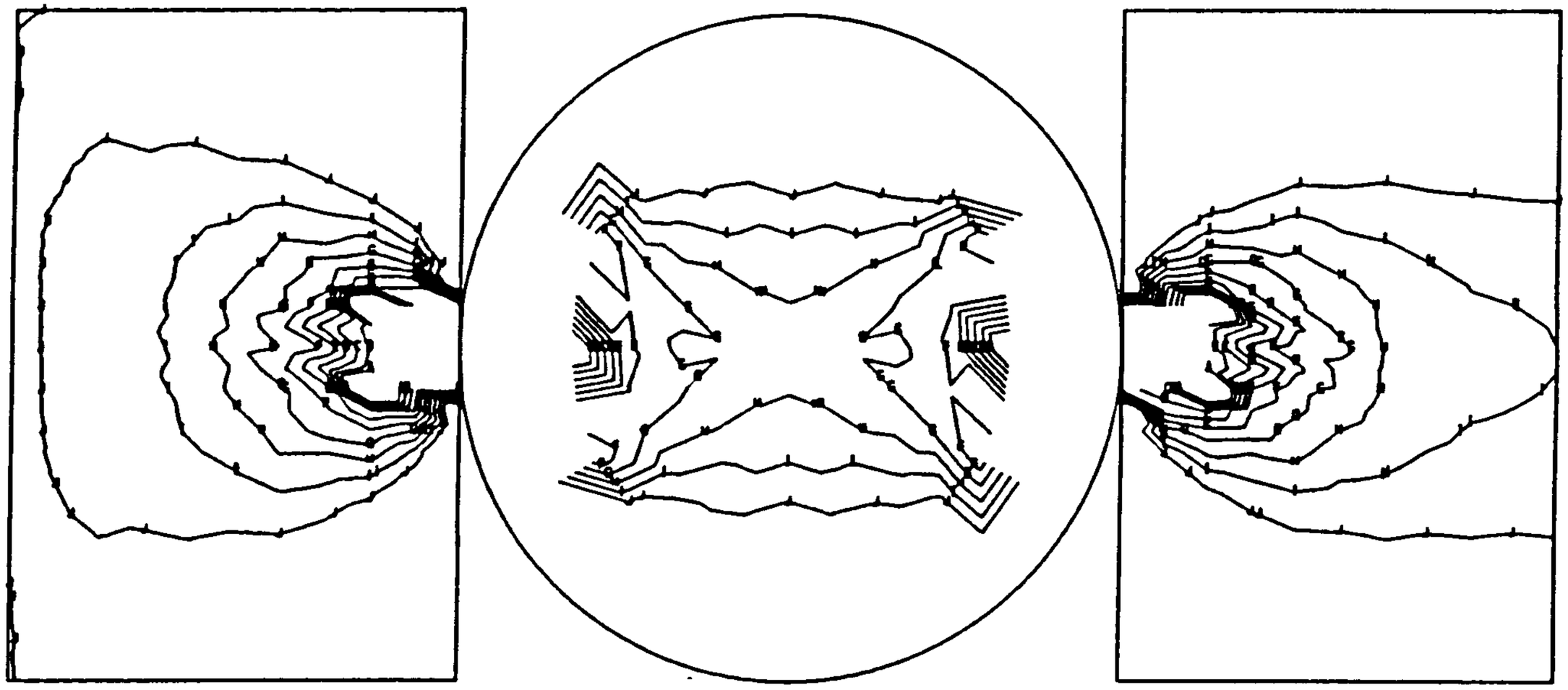

PAFEC

VIEW FROM X = 0.0000
Y = 0.0000
Z = 1.000

Z TOWARDS VIEWER

MINIMUM
PRINCIPAL
(MOST
NEGATIVE)
STRESS
(MIDDLE SURFACE)
MULTIPLY
BY 10^{4}

-1. 500	A
-1. 380	B
-1. 250	C
-1. 120	D
-0. 9980	E
-0. 8700	F
-0. 7420	G
-0. 6140	H
-0. 4870	I
-0. 3590	J

LOAD CASE = 1

WHOLE STRUCTURE DRAWN
AS DEFINED IN FRONT. ORDE

10 20 30 40 50 MM.

DRAWING NO. 4
SCALE - 1 250

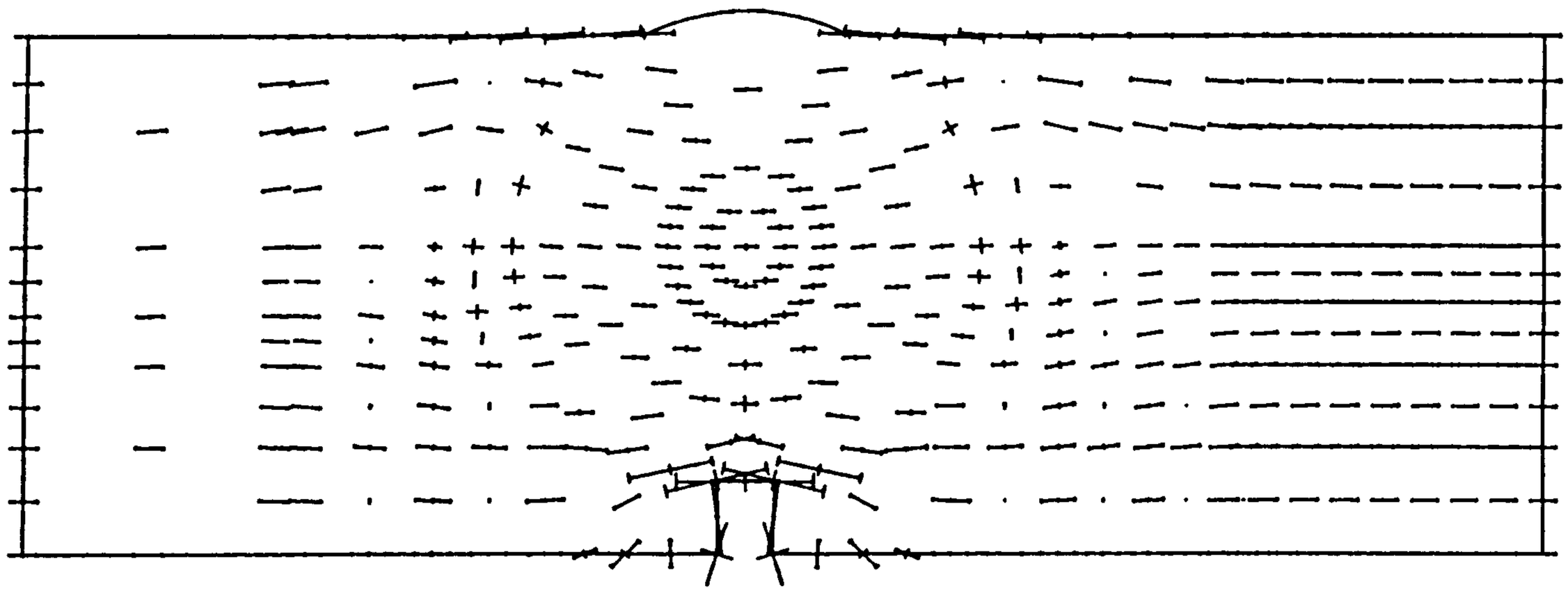

PAFEC

VIEW FROM X = 0.0000
Y = 0.0000
Z = 1.000

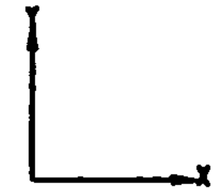

Z TOWARDS VIEWER

LOAD CASE = 1
SCALE OF VECTORS =
0. 8613E 6 UNITS/CM.
COMPRESSIVE STRESS VECTO
SHOWN WITH END BARS.
VECTORS WITHIN 30 DEGREES C
PAPER NORMAL DENOTED
BY TRIANGLES
(TENSILE POINT UPWARD

WHOLE STRUCTURE DRAWN
AS DEFINED IN FRONT. ORD

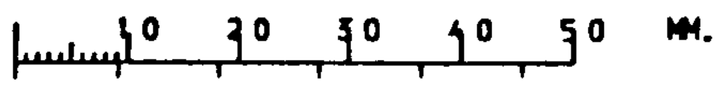

DRAWING NO. 2

PAFEC

VIEW FROM X = 0.0000
Y = 0.0000
Z = 1.000

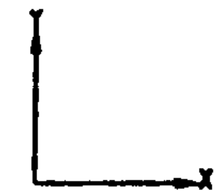

Z TOWARDS VIEWER

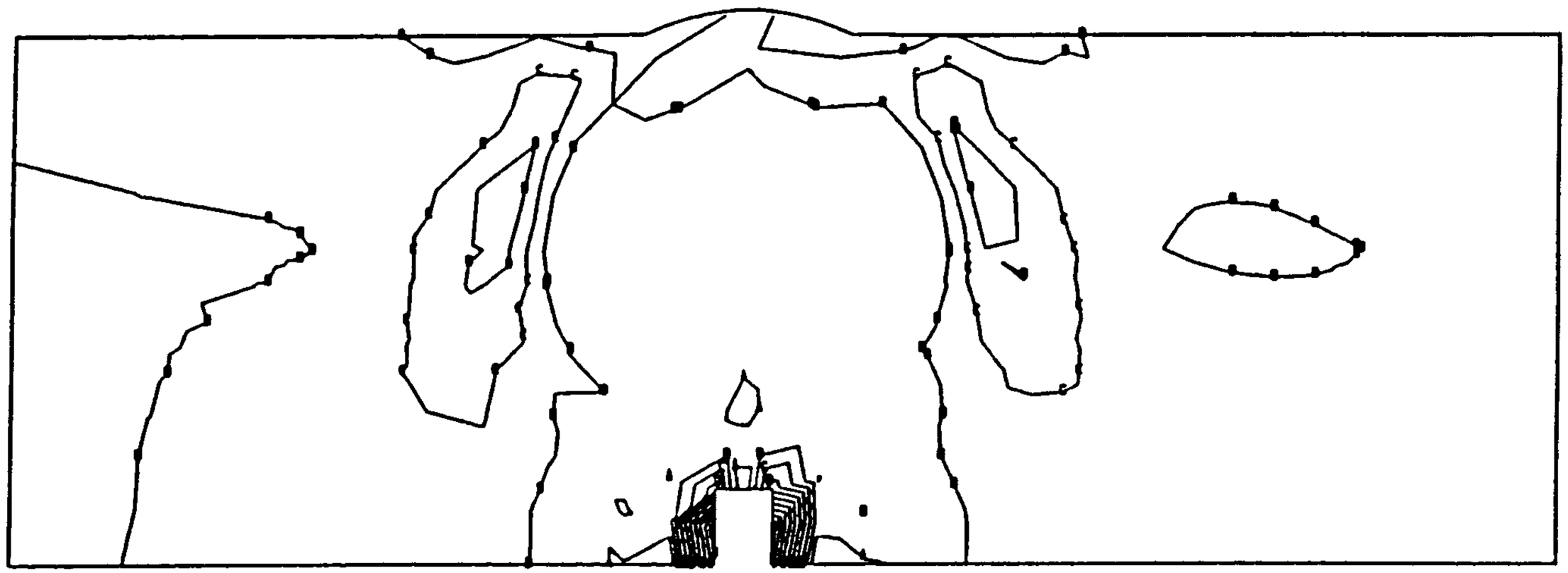

MAXIMUM
PRINCIPAL
(MOST
POSITIVE)
STRESS
(MIDDLE SURFACE)
MULTIPLY
BY 10^{4}

-0. 1300	A
-0. 2010E-1	B
0. 9000E-1	C
0. 2000	D
0. 3100	E
0. 4200	F
0. 5300	G
0. 6400	H
0. 7510	I
0. 8610	J

LOAD CASE = 1

WHOLE STRUCTURE DRAWN
AS DEFINED IN FRONT. ORDE

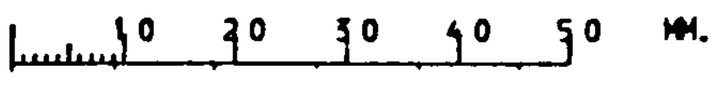

DRAWING NO. 3

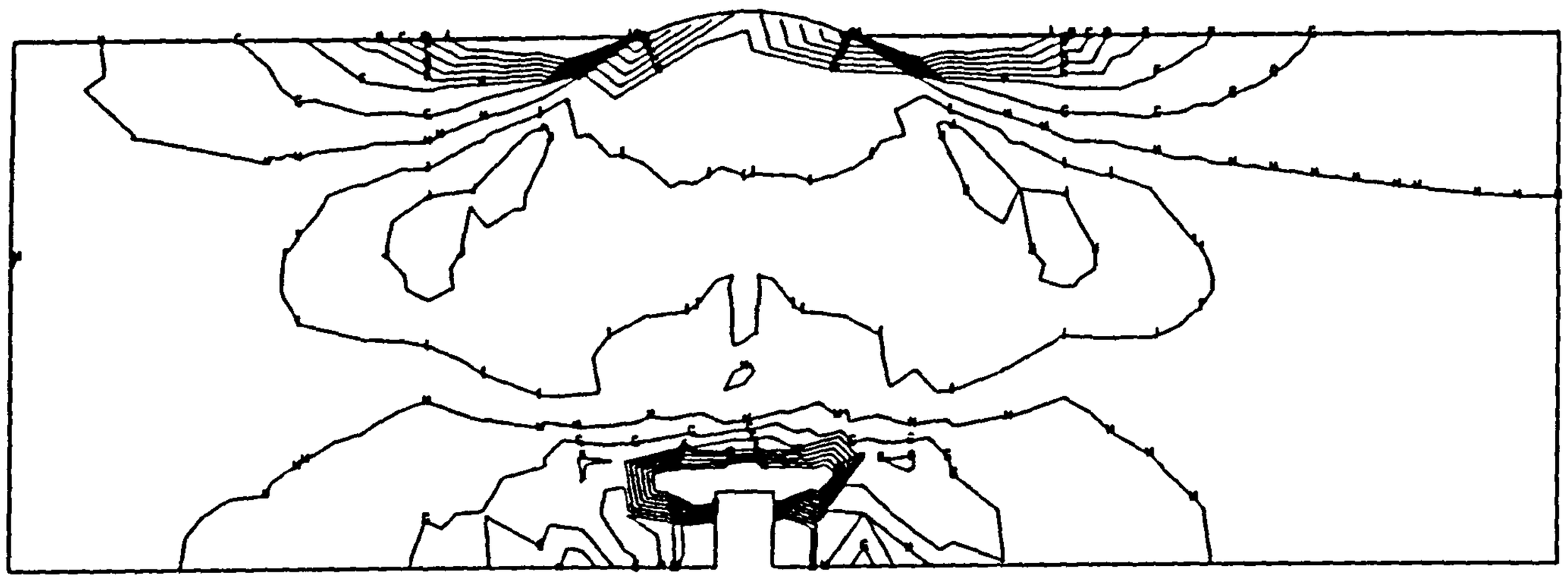

PAFEC

VIEW FROM X = 0.0000
Y = 0.0000
Z = 1.000

Z TOWARDS VIEWER

MINIMUM
PRINCIPAL
(MOST
NEGATIVE)
STRESS
(MIDDLE SURFACE)
MULTIPLY
BY 10 ^4

-0. 8640	A
-0. 7920	B
-0. 7210	C
-0. 6490	D
-0. 5780	E
-0. 5060	F
-0. 4340	G
-0. 3630	H
-0. 2910	I
-0. 2200	J

LOAD CASE = 1

WHOLE STRUCTURE DRAWN
AS DEFINED IN FRONT. ORDE

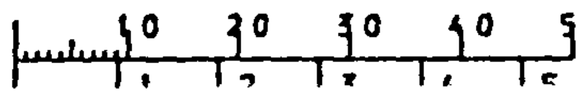

DRAWING NO. 4
SCALE = 0. 9100

PAFEC

VIEW FROM X = 0.0000
Y = 0.0000
Z = 1.000

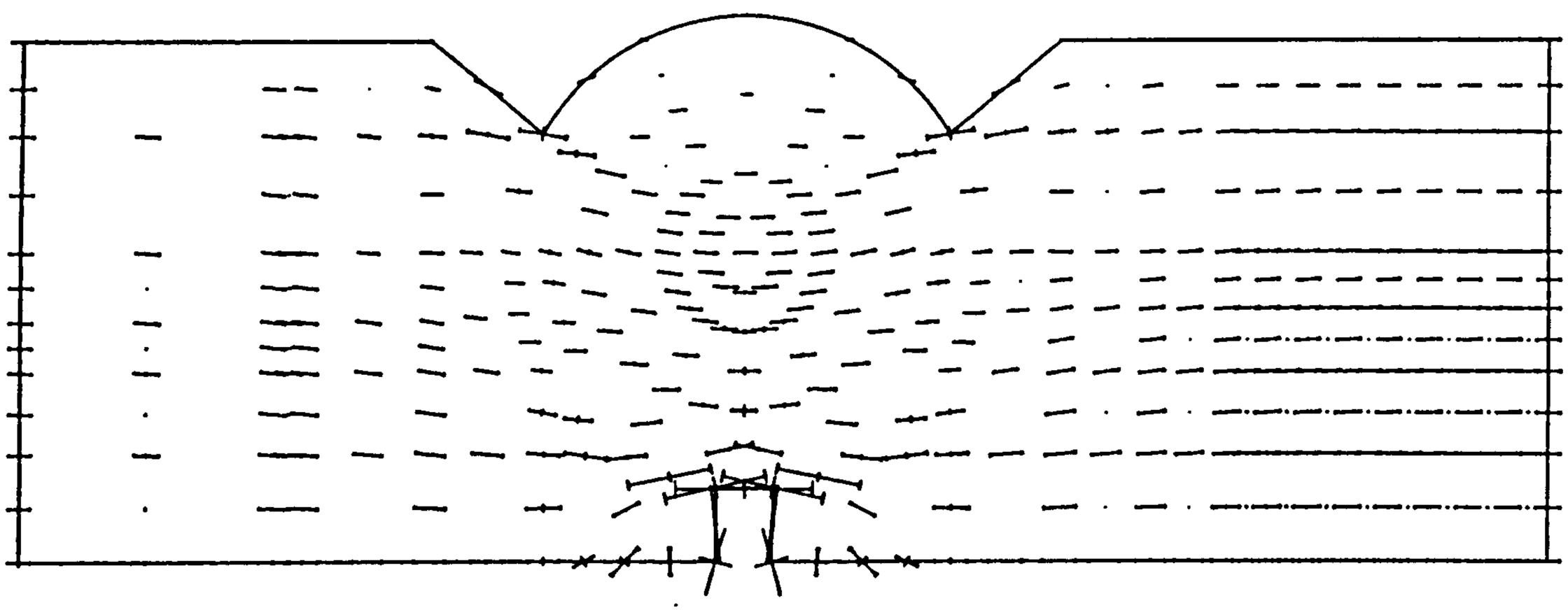

Z TOWARDS VIEWER

LOAD CASE = 1
SCALE OF VECTORS =
0. 1030E 7 UNITS/CM.
COMPRESSIVE STRESS VECTC
SHOWN WITH END BARS.
VECTORS WITHIN 30 DEGREES C
PAPER NORMAL DENOTED
BY TRIANGLES
(TENSILE POINT UPWARD

WHOLE STRUCTURE DRAWN
AS DEFINED IN FRONT. ORD

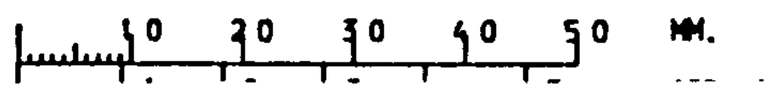

DRAWING NO. 2

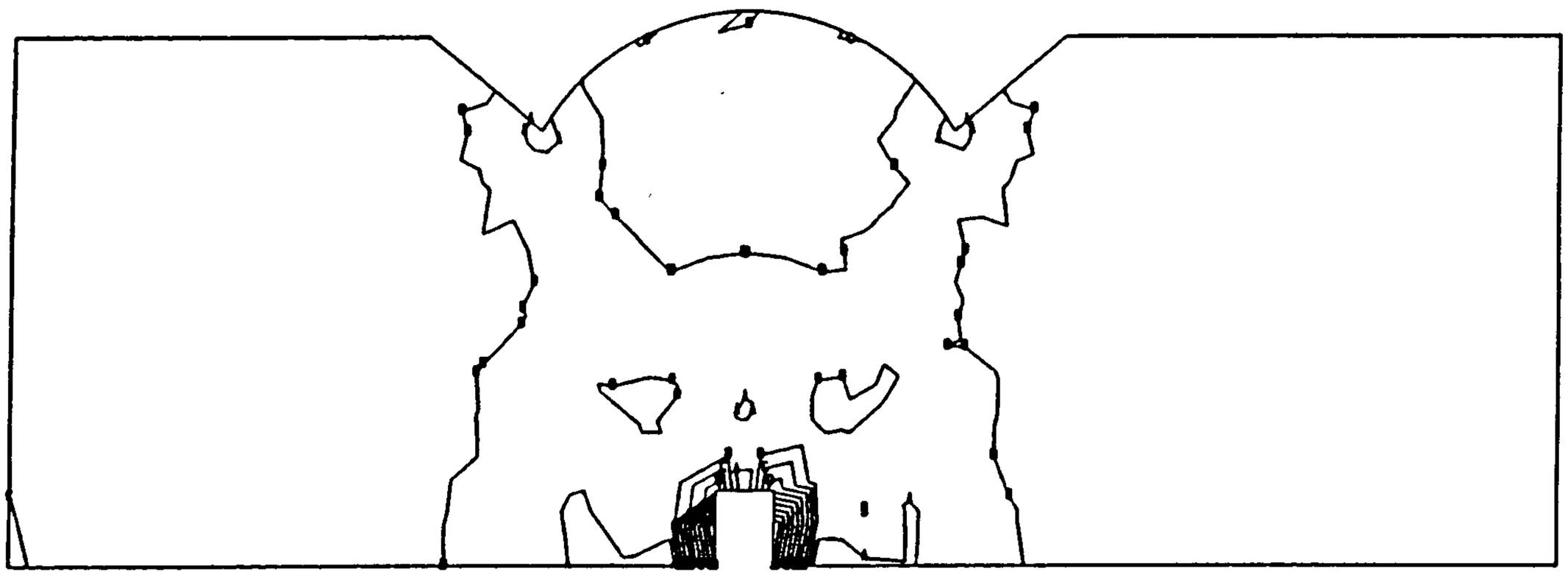

PAFEC

VIEW FROM X = 0.0000
Y = 0.0000
Z = 1.000

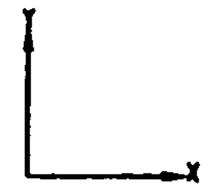

Z TOWARDS VIEWER

MAXIMUM
PRINCIPAL
(MOST
POSITIVE)
STRESS
(MIDDLE SURFACE)
MULTIPLY
BY 10^{4}

-0. 1500	A
-0. 1980E-1	B
0. 1110	C
0. 2420	D
0. 3730	E
0. 5040	F
0. 6360	G
0. 7670	H
0. 8980	I
1.020	J

LOAD CASE = 1

WHOLE STRUCTURE DRAWN
AS DEFINED IN FRONT. ORDE

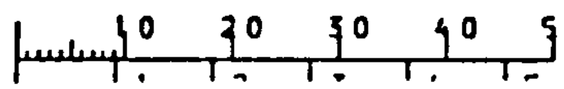

DRAWING NO. 3

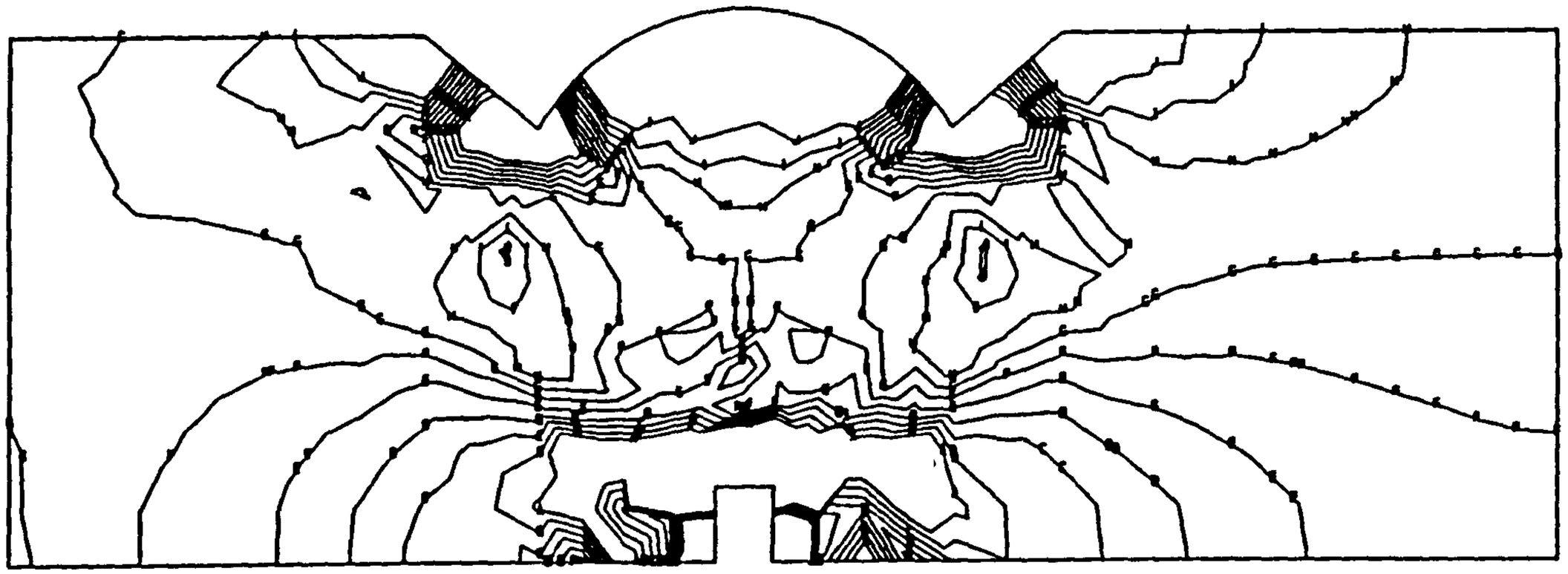

PAFEC

VIEW FROM X = 0.0000
Y = 0.0000
Z = 1.000

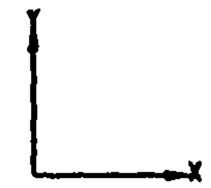

Z TOWARDS VIEWER

MINIMUM
PRINCIPAL
(MOST
NEGATIVE)
STRESS
(MIDDLE SURFACE)
MULTIPLY
BY 10^{4}

-0. 5140	A
-0. 4860	B
-0. 4570	C
-0. 4290	D
-0. 4000	E
-0. 3710	F
-0. 3430	G
-0. 3140	H
-0. 2860	I
-0. 2570	J

LOAD CASE = 1

WHOLE STRUCTURE
AS DEFINED IN FRONT.

DRAWN
ORD

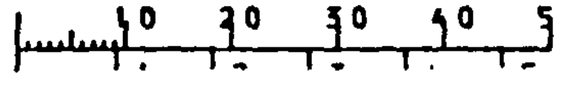

DRAWING NO. 4

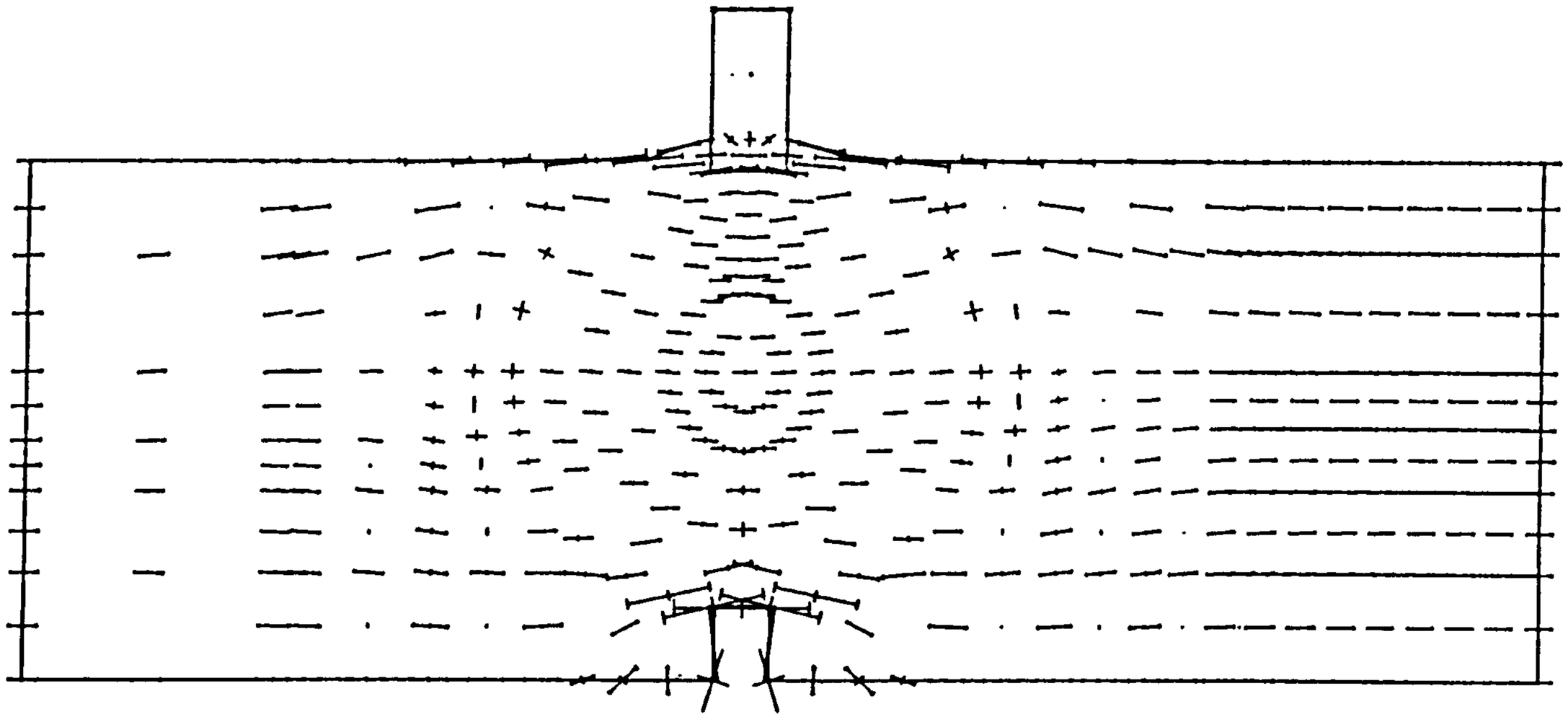

PAFEC

VIEW FROM X = 0.0000
Y = 0.0000
Z = 1.000

Y
X

Z TOWARDS VIEWER

LOAD CASE = 1
SCALE OF VECTORS =
0. 8495E 7 UNITS/CM.
COMPRESSIVE STRESS VECTO
SHOWN WITH END BARS.
VECTORS WITHIN 30 DEGREES O
PAPER NORMAL DENOTED
BY TRIANGLES
(TENSILE POINT UPWARD)

WHOLE STRUCTURE DRAWN
AS DEFINED IN FRONT. ORDE

10 20 30 40 50 MM.

DRAWING NO. 2

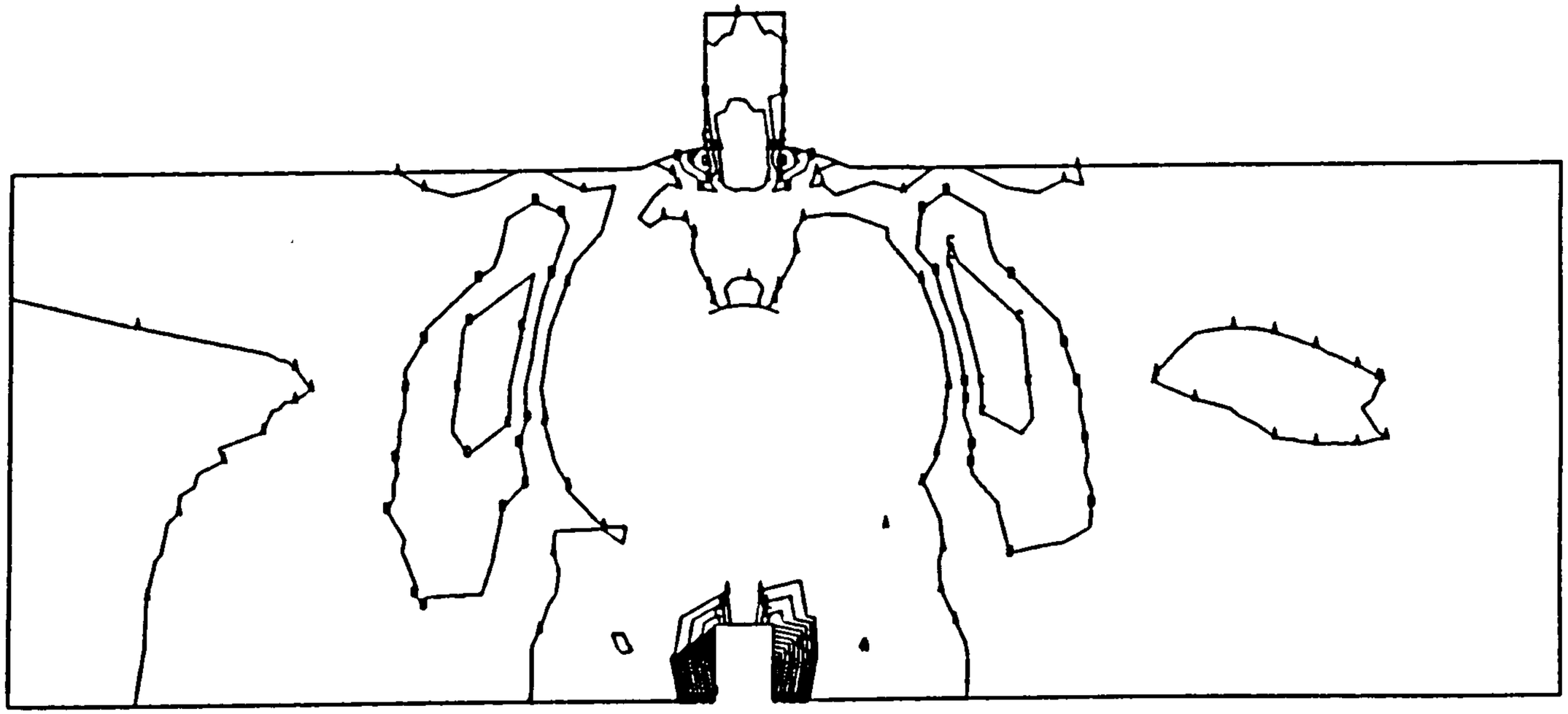

PAFEC

VIEW FROM X = 0.0000
Y = 0.0000
Z = 1.000

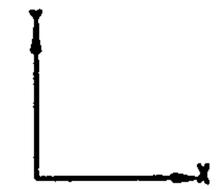

Z TOWARDS VIEWER

MAXIMUM
PRINCIPAL
(MOST
POSITIVE)
STRESS
(MIDDLE SURFACE)
MULTIPLY
BY 10^{4}

-0. 1970	A
0. 7680	B
1. 730	C
2. 690	D
3. 660	E
4. 630	F
5. 590	G
6. 560	H
7. 520	I
8. 490	J

LOAD CASE = 1

WHOLE STRUCTURE DRAWN
AS DEFINED IN FRONT. ORDE

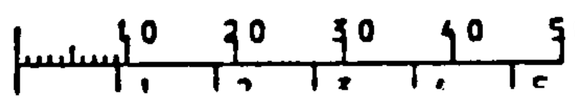

DRAWING NO. 3
SCALE = 0.9100

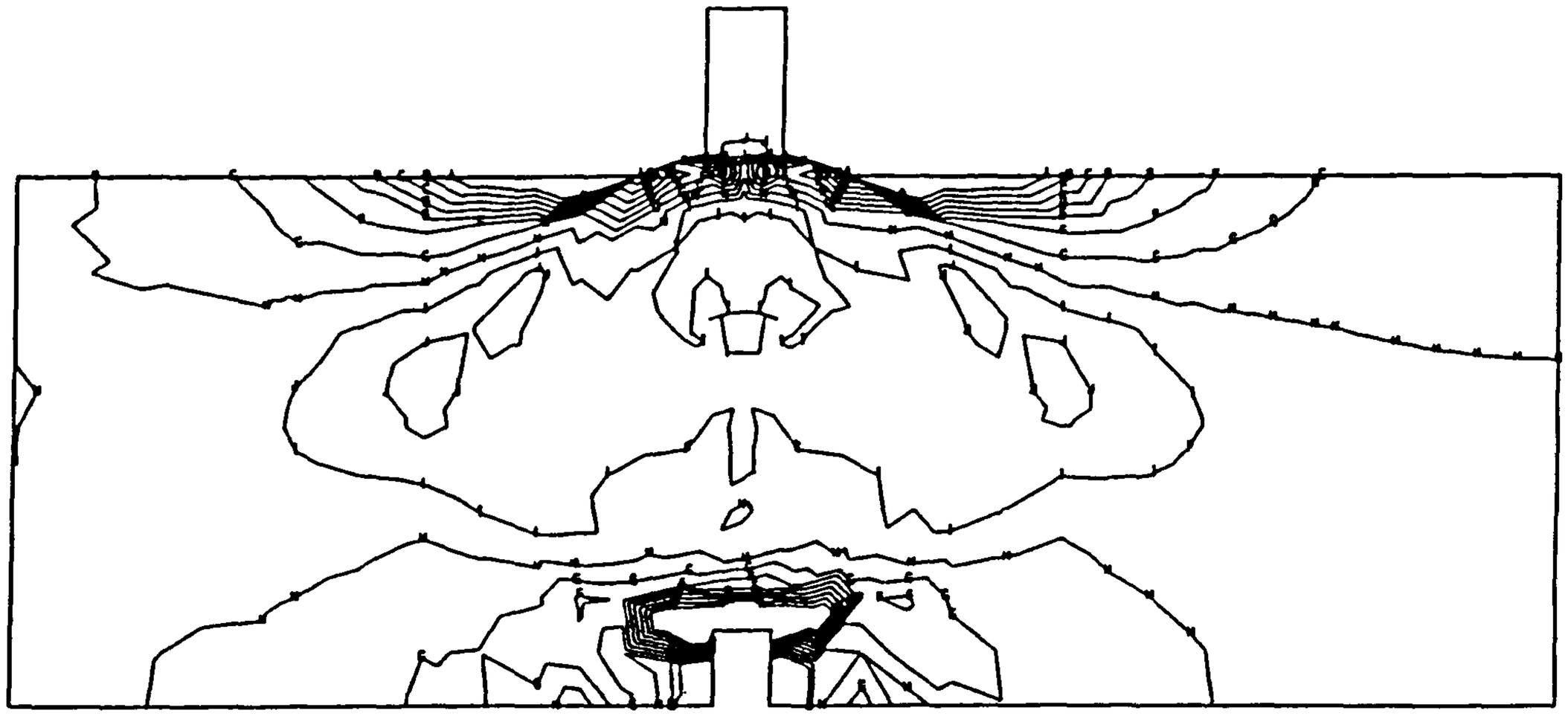

PAFEC

VIEW FROM X = 0.0000
Y = 0.0000
Z = 1.000

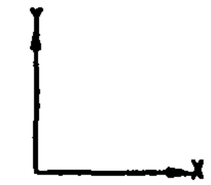

Z TOWARDS VIEWER

MINIMUM
PRINCIPAL
(MOST
NEGATIVE)
STRESS
(MIDDLE SURFACE)
MULTIPLY
BY 10^{4}

-8. 560
-7. 850
-7. 140
-6. 430
-5. 720
-5.0 10
-4. 300
-3. 590
-2. 880
-2. 170

LOAD CASE = 1

WHOLE STRUCTURE DRAWN
AS DEFINED IN FRONT. ORDE

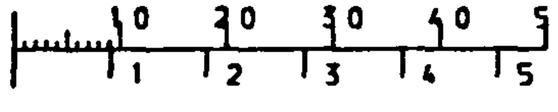

DRAWING NO. 4
SCALE = 0. 9100